ISSN 1854-6250

APEM journal

Advances in Production Engineering & Management

Volume 15 | Number 4 | December 2020

University of Maribor

Published by CPE
apem-journal.org

Advances in Production Engineering & Management

Identification Statement

ISSN 1854-6250 | Abbreviated key title: **Adv produc engineer manag** | Start year: 2006
ISSN 1855-6531 (on-line)

Published quarterly by **Chair of Production Engineering (CPE)**, **University of Maribor**
Smetanova ulica 17, SI – 2000 Maribor, Slovenia, European Union (EU)

Phone: 00386 2 2207522, Fax: 00386 2 2207990
Language of text: English

APEM homepage: apem-journal.org
University homepage: www.um.si

APEM Editorial

Subscription Rate: 120 EUR for 4 issues (worldwide postage included); 30 EUR for single copies (plus 10 EUR for postage); for details about payment please contact: info@apem-journal.org
Cover and interior design: Miran Brezocnik
Printed: Tiskarna Koštomaj, Celje, Slovenia
Subsidizer: The journal is subsidized by Slovenian Research Agency

Advances in Production Engineering & Management is indexed and abstracted in the **WEB OF SCIENCE** (maintained by **Clarivate Analytics**): **Science Citation Index Expanded**, **Journal Citation Reports** – Science Edition, **Current Contents** – Engineering, Computing and Technology • **Scopus** (maintained by **Elsevier**) • **Inspec** • **EBSCO**: Academic Search Alumni Edition, Academic Search Complete, Academic Search Elite, Academic Search Premier, Engineering Source, Sales & Marketing Source, TOC Premier • **ProQuest**: CSA Engineering Research Database – Cambridge Scientific Abstracts, Materials Business File, Materials Research Database, Mechanical & Transportation Engineering Abstracts, ProQuest SciTech Collection • **TEMA** (**DOMA**) • The journal is listed in **Ulrich's** Periodicals Directory and **Cabell's** Directory

University of Maribor
Chair of Production Engineering (CPE)

Advances in Production Engineering & Management

Volume 15 | Number 4 | December 2020 | pp 373–496

Contents

Journal homepage: apem-journal.org

ISSN 1854-6250 (print)
ISSN 1855-6531 (on-line)

Scope and topics

Advances in Production Engineering & Management (*APEM journal*) is an interdisciplinary refereed international academic journal published quarterly by the *Chair of Production Engineering* at the *University of Maribor*. The main goal of the *APEM journal* is to present original, high quality, theoretical and application-oriented research developments in all areas of production engineering and production management to a broad audience of academics and practitioners. In order to bridge the gap between theory and practice, applications based on advanced theory and case studies are particularly welcome. For theoretical papers, their originality and research contributions are the main factors in the evaluation process. General approaches, formalisms, algorithms or techniques should be illustrated with significant applications that demonstrate their applicability to real-world problems. Although the *APEM journal* main goal is to publish original research papers, review articles and professional papers are occasionally published.

Fields of interest include, but are not limited to:

Additive Manufacturing Processes
Advanced Production Technologies
Artificial Intelligence in Production
Assembly Systems
Automation
Big Data in Production
Computer-Integrated Manufacturing
Cutting and Forming Processes
Decision Support Systems
Deep Learning in Manufacturing
Discrete Systems and Methodology
e-Manufacturing
Evolutionary Computation in Production
Fuzzy Systems
Human Factor Engineering, Ergonomics
Industrial Engineering
Industrial Processes
Industrial Robotics
Intelligent Manufacturing Systems
Joining Processes
Knowledge Management
Logistics in Production
Machine Learning in Production
Machine Tools
Machining Systems
Manufacturing Systems
Materials Science, Multidisciplinary
Mechanical Engineering
Mechatronics
Metrology in Production
Modelling and Simulation
Numerical Techniques
Operations Research
Operations Planning, Scheduling and Control
Optimisation Techniques
Project Management
Quality Management
Risk and Uncertainty
Self-Organizing Systems
Statistical Methods
Supply Chain Management
Virtual Reality in Production

APEM journal
Advances in Production Engineering & Management
Volume 15 | Number 4 | December 2020 | pp 377–389
https://doi.org/10.14743/apem2020.4.372
ISSN 1854-6250
Journal home: apem-journal.org
Original scientific paper

A layered genetic algorithm with iterative diversification for optimization of flexible job shop scheduling problems

Amjad, M.K.[a,*], **Butt, S.I.**[a], **Anjum, N.**[a], **Chaudhry, I.A.**[b], **Faping, Z.**[c], **Khan, M.**[a]

[a]School of Mechanical and Manufacturing Engineering, National University of Sciences and Technology, Islamabad, Pakistan
[b]Department of Industrial Engineering, College of Engineering, University of Ha'il, Kingdom of Saudi Arabia
[c]School of Mechanical Engineering, Beijing Institute of Technology, Beijing, P.R. China

A B S T R A C T

Flexible job shop scheduling problem (FJSSP) is a further expansion of the classical job shop scheduling problem (JSSP). FJSSP is known to be NP-hard with regards to optimization and hence poses a challenge in finding acceptable solutions. Genetic algorithm (GA) has successfully been applied in this regard since last two decades. This paper provides an insight into the actual complexity of selected benchmark problems through quantitative evaluation of the search space owing to their NP-hard nature. A four-layered genetic algorithm is then proposed and implemented with adaptive parameters of population initialization and operator probabilities to manage intensification and diversification intelligently. The concept of reinitialization is introduced whenever the algorithm is trapped in local minima till predefined number of generations. Results are then compared with various other standalone evolutionary algorithms for selected benchmark problems. It is found that the proposed GA finds better solutions with this technique as compared to solutions produced without this technique. Moreover, the technique helps to overcome the local minima trap. Further comparison and analysis indicate that the proposed algorithm produces comparative and improved solutions with respect to other analogous methodologies owing to the diversification technique.

A R T I C L E I N F O

Keywords:
Scheduling;
Flexible job shop scheduling problem (FJSSP);
Complexity;
Diversity;
Combinatorial optimization;
Genetic algorithm

**Corresponding author:*
kamal.amjad@smme.edu.pk
(Amjad, M.K.)

Article history:
Received 19 May 2020
Revised 27 November 2020
Accepted 30 November 2020

1. Introduction

Modern manufacturing processes consist of several carefully planned sub-processes that require to be completed in a predefined manner to achieve the intended product [1]. With the continuously changing business flux and fluctuating product demand, it is imperative that manufacturing flexibility may be added to the shop floor so that a maximum variety of operations can be performed. Flexible manufacturing systems (FMS) can handle a great deal of product variety with reasonable volumes as they are capable of variable routing among different workstations. Modern concepts of group technology (GT) and cellular manufacturing have specifically been designed to incorporate flexibility in the manufacturing process [2]. The decision making regarding allocation of tasks or set of activities to available resources is termed as scheduling [1, 3]. Optimum utilization of resources is possible if the tasks are efficiently performed according to predefined criteria. Since many sequences can be executed for a said product, many schedules can be developed. Optimization of schedules is conventionally evaluated through benchmark problems against a predefined cost function. The cost function, in this case, is scheduling an objective that is used to assess the optimality of the generated schedule concerning the said objective.

Job shops are popular because they can handle a variety of processes in a single facility [4], thereby offering a significant advantage over classical product or process based layouts. They can handle the different sequences of operations on various fixed machines. The flexible job shop (FJS) offers flexibility in the job shop through the introduction of flexible machines whereby required operations may be performed on several alternative machines [5]. Therefore, the problem can be decomposed as an assignment and scheduling problem. Additionally, cases of partial and total flexibility are also formulated, whereby all operations can be performed on all machines in the case of total flexibility and only some operations can be performed on several machines in the case of partial flexibility [6]. Whereas this extension has provided effective resource utilization and added manufacturing flexibility, it also has increased the complexity of scheduling optimization manifold. Therefore, flexible job shop scheduling problem (FJSSP) has been studied in a dedicated and detailed manner owing to its NP-hard nature [7, 8] and complexity [9].

It has been reported that there are $(n!)^m$ possible sequences for generating a schedule for n jobs on m machines in case of a JSSP. Consequently, the computational resources either expire or become scarce when attempting large instances of problems. Where FJSSP offers more flexibility in terms of assignment, the problem becomes more complex as an additional layer of alternatives is available in this case. Thus, exact solution methods are seldom attempted [10, 11] and artificial intelligence-based approaches have gained extreme popularity. Although, various dedicated case studies of FJSSP have been reported in [12], traditionally, benchmark problems are used to test the developed algorithms [13, 14].

Schedules are developed keeping in view a certain objective. Thus, a schedule meant for optimum use of resources may not be applicable for optimum workload minimization. Many objectives have been addressed in literature with regards to FJSSP; however, makespan has been addressed the most [15], which is the maximum time required to complete all operations of the selected dataset.

FJSSP is one of the most challenging optimization problems [16]. To achieve optimum solutions in a reasonable time, meta-heuristic algorithms have gained tremendous popularity. Whereas, a lot of studies have been conducted using various algorithms; Genetic algorithm (GA) has gained outstanding attention in this regard [17]. In a comprehensive study considering various approaches for solving FJSSPs, it has been pointed out that GA is the most popular algorithm with publications amounting to 34 % [18]. It has also been pointed out that 26.4 % of studies performed on FJSSPs have been conducted using GA [19].

GA mimics the phenomena of human evolution based on the "survival of the fittest" rule [20]. It provides an effective mechanism to conduct a directed random search for finding optimal solutions and therefore it has used effectively for sequencing problems in flexible manufacturing systems, gaining exceptional popularity in the last decade [15]. An approach by localization along with benchmark problems of FJSSP with total flexibility was presented [21]. Goa *et al.* [22] addressed the FJSSP with multi-objective optimization and proposed GA for the solution of selected benchmarks. Similarly, Pezzella *et al.* [23] suggested a GA with various strategies for algorithm improvement. Gu *et al.* [24] presented an improved GA with a hybrid population initialization method.

Population diversity plays an extremely important role in solution quality. Traditionally, crossover and mutation operators have been used to introduce diversity within the principles. A cluster of population at a local minimum enforces the algorithm to converge prematurely. Alternatively, an extremely diverse population may not allow the algorithm to converge. Therefore, population diversity on one side provides solution quality, while on the other side; it may allow the algorithm to run for long periods. Research has thus been carried out in order to propose mechanisms to attain a balance between these two different ends. Wang *et al.* [25] have introduced a population diversity technique through the conservation of a single elitist solution. Xiong *et al.* [26] introduced a crowding distance measure to ensure population diversity. Teekeng *et al.* [27] proposed a modified version of mutation to ensure population diversity.

A pure GA based approach is presented in the current study to solve the FJSSP. The diversification and intensification regimes are used side-by-side to increase the capability of the algorithm to further explore the search space while conserving the best solutions and deferring premature convergence. When local minima are encountered after several iterations, re-initialization is invoked. The algorithm is then implemented and tested on selected standard benchmark problems of FJSSP. An in-depth analysis of the algorithm efficacy for FJSSP is then discussed and conclusions are presented.

2. Problem formulation and complexity

The FJSSP is formulated as a set of N jobs ($J = J_1, J_2, J_3,..., J_N$) to be processed on M machines ($M = M_1, M_2, M_3,..., M_M$). Each job J_i consists of predefined operations O_{ij} to be processed on any of the available machines, where O_{ij} is the operation j of job i. The processing time required for completion of operation O_{ij} on machine M_k is a known aspect termed as P_{ijk}. As number of operations for each job may differ, the total number of operations for all operations is as follows:

$$L = \sum_{i=1}^{N} J_{io} \tag{1}$$

where J_{io} is the total number of operations for a single job J_i. Accordingly, a sequence may be assigned to an operation O_{ij} such that:

$$n_{ij} = \sum_{x=1}^{i-1} J_{xo} + j \tag{2}$$

where n_{ij} is the sequence number for a said operation. The operations can be scheduled on any machine depending upon the condition that the previous operation is complete, and the machine is available at the said time. Other assumptions are formulated below [18].

i. All resources are available at time t = 0:

$$t_{ijk} \geq 0 \qquad O_{ijk} \epsilon N \tag{3}$$

$$r_{ijk} \geq 0 \qquad \forall\, O_{ijk} \epsilon N \tag{4}$$

ii. Only one operation can be performed on one machine at a provided time:

$$t_{ijk} - t_{i'j'k} \geq P_{i'j'k} \qquad \forall\big(O_{ij}, O_{i'j'}\big)\, \epsilon\, S_k \tag{5}$$

iii. Operations are performed in a predefined order:

$$t_{ijk} - t_{ij'k'} \geq P_{ij'k'} \qquad \forall\big(O_{ijk}, O_{ij'k'}\big)\, \epsilon\, J_{io} \tag{6}$$

iv. Operations are not interrupted once they are started, i.e. pre-emption or cancellation is not considered:

$$E_{ijk} - t_{ijk} = P_{ijk} \qquad \forall\, O_{ij} \epsilon J_{io}\ \&\ M_k\, \epsilon\, M \tag{7}$$

v. There is no free time between any two operations

$$t_{ijk} = \max\big(C_k, r_{ijk}\big) \tag{8}$$

Where, t_{ijk} is the start time of O_{ij} on machine M_k, r_{ijk} is the release time of O_{ij} on machine M_k, $t_{i'j'k}$ is the start time of the previous operation on machine M_k, $P_{i'j'k}$ is the processing time of the previous operation on machine M_k and E_{ijk} is the end time of O_{ij} on machine M_k. Additionally, all jobs have equal priorities and the setup times are either zero or considered in the operation time.

FJSSP is one of the most challenging combinatorial optimization problems. Even for the simpler JSSP, the computational effort increases in an exponential manner with the increase of problem size and computational time for an exact solution may rise to millions of years [28]. The actual depiction of problem complexity lies in the evaluation of search space. The size of the search space depends upon the chromosome length and level of flexibility U_{ij} of the problem. Henceforth, changing the length or definition affects the search space. In every gene, there is an upper bound U_{ij}, i.e. the number of machines on which a said operation can be performed. According to the chromosome definition of Zhang *et al*. [29], search space (SS) is the combination of all possible values of a gene. The same is formulated as Eq. 9.

$$SS = SS(MS) \cdot SS(OS) = \prod_{i=1}^{N} \prod_{j=1}^{J_{io}} U_{ij} \cdot \frac{L!}{\prod_{i=1}^{N} J_{io}!} \tag{9}$$

Where $SS(MS)$ and $SS(OS)$ are the search space for machine selection (MS) and operation selection (OS) parts of the chromosome respectively. For the MS part, SS is all possible valid combinations for all genes, i.e. product of U_{ij} for all operations. For the OS part, SS is the ratio of OS part chromosome length and product of all $J_{io}!$. The computations of search space for Fattahi [30] and Kacem [21] are presented in Table 1 and graphically shown in Fig. 1. Here, M, N, and L represent the total number of jobs, machines, and sequences, respectively. It is evident that the search space size increases manifold in an exponential manner. This depiction of problem complexity has not been attempted before.

Table 1 Search space for Kacem and Fattahi datasets

Instance	*N*	*M*	*L*	*SS*	Instance	*N*	*M*	*L*	*SS*
SFJS1	2	2	4	9.60E+01	MFJS3	6	7	18	4.67E+18
SFJS2	2	2	4	2.40E+01	MFJS4	7	7	21	1.12E+23
SFJS3	3	2	6	1.44E+03	MFJS5	7	7	21	7.45E+22
SFJS4	3	2	6	1.44E+03	MFJS6	8	7	24	1.81E+27
SFJS5	3	2	6	5.76E+03	MFJS7	8	7	32	3.00E+36
SFJS6	3	3	9	1.08E+05	MFJS8	9	8	36	2.82E+42
SFJS7	3	5	9	8.60E+05	MFJS9	11	8	44	1.35E+55
SFJS8	3	4	9	8.60E+05	MFJS10	12	8	48	6.28E+61
SFJS9	3	3	9	8.60E+05	Kacem 1	4	5	12	6.77E+13
SFJS10	4	5	12	9.46E+07	Kacem 2	10	7	29	1.41E+48
MFJS1	5	6	15	1.39E+13	Kacem 3	10	10	30	4.39E+54
MFJS2	5	7	15	2.12E+14	Kacem 4	15	10	56	2.03E+112

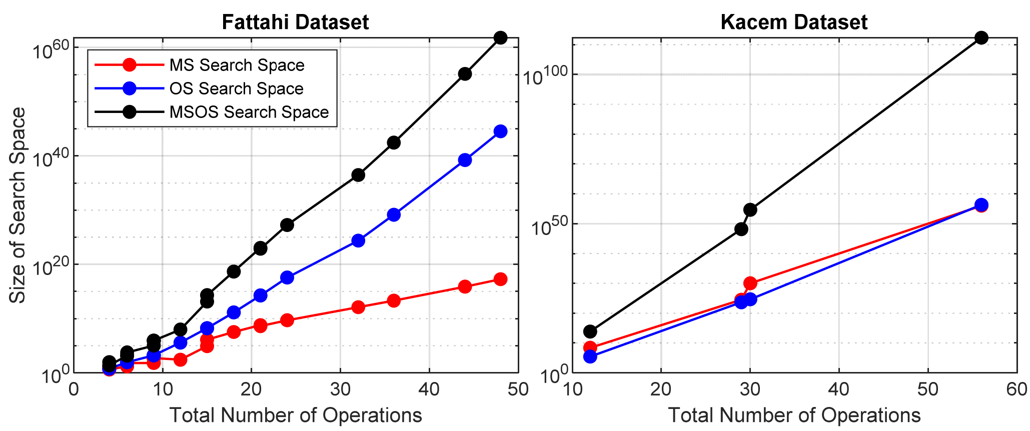

Fig. 1 Problem size vs. search space

3. Proposed algorithm

3.1 Methodology

To explore the problem search space sufficiently, crossover and mutation operators are introduced in GA [6]. These operators bring diversity in the population through exchanging information between individual chromosomes.

At the initialization phase of the algorithm, the population is fairly diverse as the algorithm generates initial chromosomes on a random basis. When convergence is achieved after certain generations in a GA routine, the population tends to have a large amount of better solutions and variance of the population therefore decreases. Where the convergence is an indication of the best solution, there is also a known tendency of GA to get trapped in local minima. Literature proposes to run the algorithm for extended generations [23] or employ local search techniques to overcome this issue [24]. Although both techniques have proven to be successful in obtaining acceptable solutions, they have their inherent drawbacks. Extended generations come at the cost of computational effort and time. Similarly, local search not only increases the algorithm complexity with regards to implementation but also increases the computational effort. This study proposes a Re-initialization based genetic algorithm (R-GA) to overcome these observations. Fig. 2 presents an overall information exchange four-layer scheme followed in R-GA. A detailed description of these layers is presented in subsequent sections.

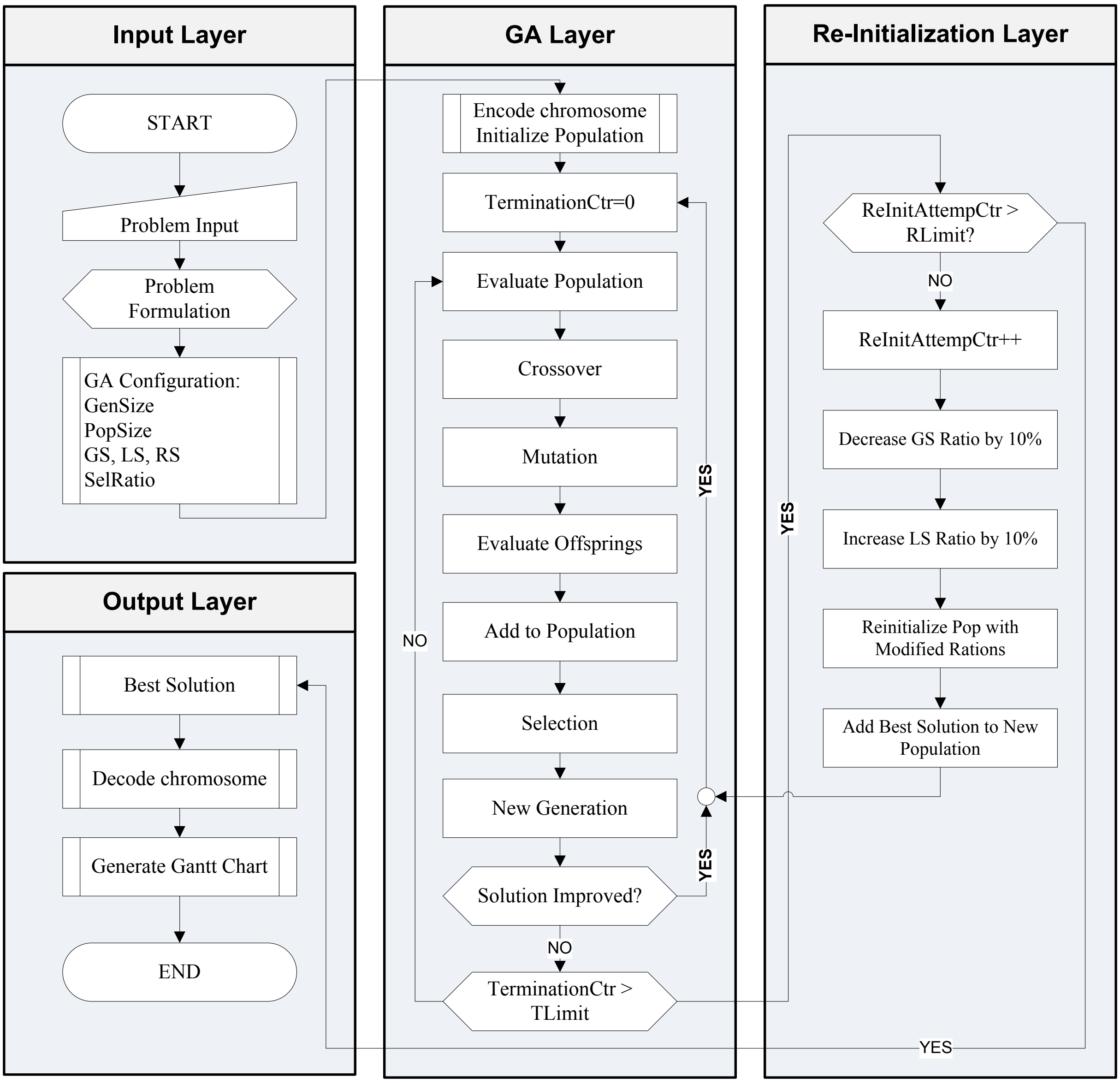

Fig. 2 Flowchart of proposed algorithm (R-GA)

3.2 Input layer

The input layer takes various pre-defined parameters from the user as input to GA. The values of parameters taken for the current implementation and testing is listed in Table 2. The adaptability of applicable parameters is explained in relevant sections.

Table 2 Input parameters for R-GA

Parameter	Description	Value
Population size	Total chromosomes in a population	1500
Generation size	Number of iterations in GA	250
Crossover probability	Likelihood for chromosome crossover	Adaptive
Mutation probability	Likelihood for chromosome mutation	Adaptive
Global selection ratio	Population initialization factor for global selection	Adaptive
Local selection ratio	Population initialization factor for local selection	Adaptive
Random selection ratio	Population initialization factor for random selection	Adaptive
Elitism ratio	Elite chromosome selection factor	20
Roulette wheel ratio	Factor for roulette wheel selection	80
Termination counter limit	Limit for GA before re-initialization	100
Re-initialization counter limit	Number of re-initialization attempts	4

3.3 GA layer

This layer contains the implementation of GA. The chromosome representation of machine selection (*MS*) and operation selection (*OS*) as proposed by Zhang *et al*. [29] is used in this study. This representation avoids generating infeasible chromosomes during the evolution process and used a single chromosome for handling the routing and scheduling aspects.

MS vector represents the machine number allocated for any operation O_{ij} out of all available machines. In *OS* vector, every operation is represented by its job number i and the schedule is decoded by the sequence of these numbers. Consider the problem presented in Table 3 consisting of 4 jobs that are to be scheduled on 4 machines. The candidate solution chromosome can be represented in MSOS format as shown in Fig. 3. The job, operation and machine routing have been color-coded to elaborate the representation, e.g. in the fifth gene of MS vector, O_{31} can be assigned on M_1, M_2 and M_4 however gene value 2 indicates that it has been assigned on 2nd machine from all available set of machines, i.e. M_2. Similarly, for OS vector, the first gene value 3 indicates that O_{31} will be scheduled first; second gene value 1 indicates that O_{11} will be scheduled second and so on.

The population initialization is important since it determines the quality of solutions in the search space. The global selection (*GS*), local selection (*LS*) and random selection (*RS*) are used in this study for the *MS* part [29]. Initially, *GS* is taken as 50, *LS* is taken as 20 and *RS* is taken as 30. For the OS part, the population is generated through random selection.

Table 3 A Sample FJSSP

Job	Operation	Machine			
		M_1	M_2	M_3	M_4
J_1	O_{11}	∞	10	∞	20
	O_{12}	25	30	10	∞
	O_{13}	15	60	15	10
J_2	O_{21}	15	∞	50	∞
J_3	O_{31}	80	10	∞	50
	O_{32}	∞	80	10	10
J_4	O_{41}	20	60	10	10
	O_{42}	20	∞	∞	∞

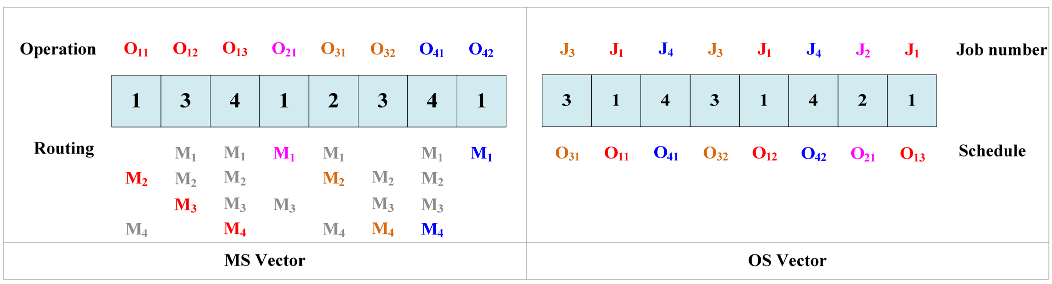

Fig. 3 An illustration of MSOS representation

Three different crossover methods have been used for the *MS* part. In the single point crossover (SPX) method [31], a random number r is generated in the range $[1, L]$ and offspring are then generated by swapping genes $[1, r]$ and $[r, L]$ of two parents. In the two point crossover (TPX) method [32], two random numbers are generated in the range $[1, L]$ and the *MS* chromosome is divided into three parts, i.e. $[1, r_1]$, $[r_1, r_2]$ and $[r_2, L]$. Offspring are then generated by swapping the resultant three parts. In uniform crossover (UX) method [29], even and odd number of genes of parent chromosomes is swapped to generate offspring.

The crossover of the OS vector is delicate due to its precedence order constraints. To avoid generating invalid chromosomes and preserving the scheduling constraints in OS vector, Improved precedence order crossover (iPOX) technique has been used [33] as shown in Fig. 4. This procedure generates two sets of jobs, i.e. J_{s1} and J_{s2} and then uses these sets to generate offspring from parent chromosomes. In this study, we generated job sets J_{s1} and J_{s2} by generating a random integer in the range $[1, n]$. Job sets are then generated as $J_{s1} = [1, r]$ and $J_{s2} = [r, n]$.

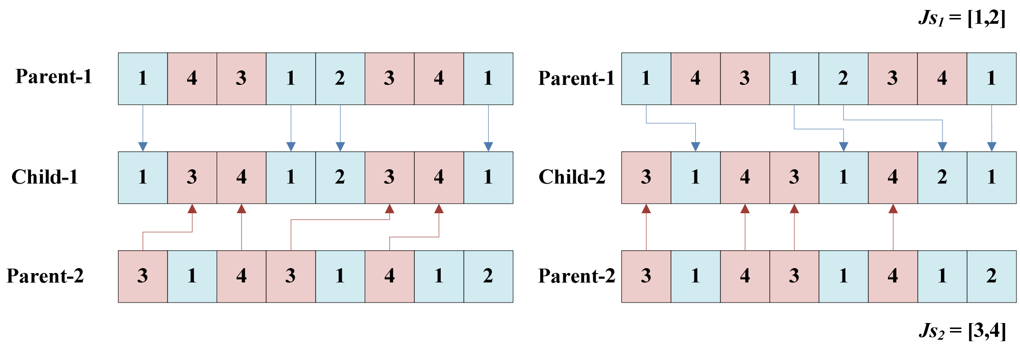

Fig. 4 Improved precedence order crossover

Conventionally, crossover probability (P_c) is kept at a predefined value, normally in the range of 0.8-0.9. In this study, P_c is adaptive in nature as formulated in Eq. 10. This increases the crossover probability as convergence is achieved, hence introducing the possibility for maximum diversification.

$$P_c = \frac{\overline{Ft}}{\max Ft} \tag{10}$$

Here, Ft and $\overline{Ft}$ is the overall and mean fitness of the entire population under consideration, respectively.

Random intelligent mutation has been used for the *MS* part. A random number r_1 is generated in the range $[1, L]$. A mutation is then performed at r_1 gene. To mutate r_1 gene, another random number generated in the range between one and the total number of machines on which operation at gene r_1 can be performed. The value of r_1 gene is then replaced with r_2. This procedure does not allow generation of infeasible chromosome and ensures generation of new child by restricting duplication of parent chromosomes. For the OS part, swap mutation has been used as proposed in [33]. Both procedures are presented in Fig. 5.

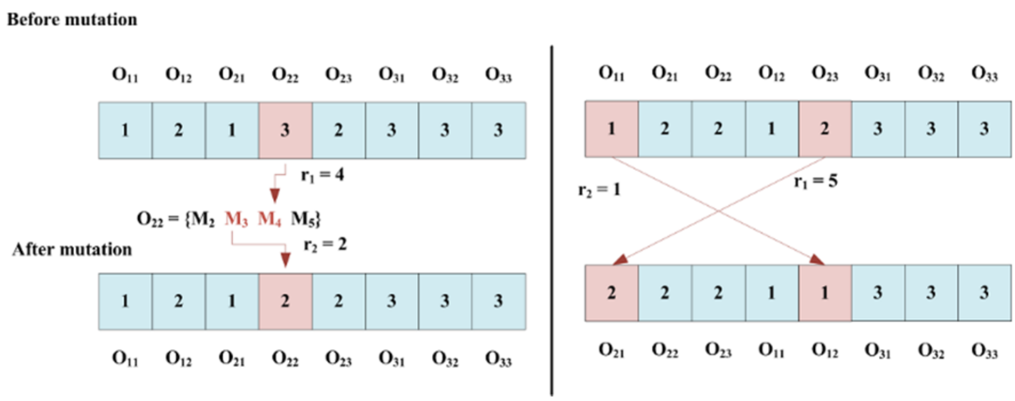

Fig. 5 Random intelligent mutation and swap mutation

Mutation probability (P_m) is generally kept at a lower side, ranging from 0.1-0.25. In this study, P_m is adaptive in nature as governed by Eq. 11. As the population is converged, P_m is increased as the values of minimum and maximum fitness comes close to each other. This further enhances the ability of the algorithm to achieve a diverse population.

$$P_m = \frac{\min Ft}{\max Ft} \tag{11}$$

Once crossover and mutation are carried out, offspring are generated and their fitness is evaluated with regards to makespan minimization. A combination of elite and roulette wheel selection is used to curtail the population down to population size. In this study, elitism ratio is kept at 20 % of the whole population. Chromosomes having improved fitness with respect to other competitor chromosomes are introduced into the population thereafter. GA routine is continued until improved solutions are found. The algorithm terminates if no improvement is found till 100 iterations consecutively and the final solution is fed into the re-initialization layer so that elite preservation is ensured.

3.4 Re-initialization layer

This layer receives the elite chromosomes and reinitializes the population to produce diversity for re-exploring the search space. During this process, GS and LS are decreased and increased by 10 % respectively. This approach enhances the generation of chromosomes by local search procedure and reduces global search in every re-initialization while preserving the elite solution. Thus, intensification around the best solution is carried out. Here, as the mutation probability is also adapted on the higher side to maximize the generation of new possible solutions. The new population is again returned to the GA layer until the re-initialization count limit is reached.

3.5 Output layer

This layer decodes the elite chromosome and generates the Gantt chart for the problem accordingly along with the best solution makespan.

4. Results and discussion

Before commencing with the large scale application, the parameters of R-GA were optimized such that algorithm efficiency was achieved. The algorithm was run on a Pentium Core i7 with 4GB RAM and experimental results are compared with known benchmark problems of Kacem [21] and Fattahi [30]. Since the proposed algorithm is pure GA, thus comparison is made either with pure GA based approaches or other standalone comparable evolutionary algorithms.

Fig. 4 shows the convergence pattern for MFJS8. R-GA initializes and generates a random population using the initialization procedures and starts to converge. The initial population is diverse and as convergence is achieved, it initially traps at local minima (922) at 120 generations and retains there for 100 iterations. As no improvement is observed until 100 generations, re-initialization is invoked to introduce diversity in population for search space evaluation. Additionally, the improved local selection in the new generation is also imposed for compensating diversification and intensification. The algorithm again starts to converge and just after re-initialization, attains 884 makespan. The algorithm then continues until termination criteria are met. It is remarkable that the similar algorithm without the proposed diversification technique does not perform to produce comparable results and retains trapped in local minima as obvious from Fig. 6. Similar behavior can be observed for MFJS2, MFJS 4, MFJS5 and MFJS6 as shown in Fig. 7 and Fig. 8. The algorithm, after initial convergence, reinitializes and attains a new minimum which is comparable to available benchmark problem solutions.

The proposed algorithm therefore successfully gets out of the local minima trap owing to the diversification methodology and produces comparable/better results as compared to other similar algorithms. In addition, the proposed scheme also minimizes the possibility of premature convergence as population diversity is initiated to check the local minima trap once the average fitness between generations becomes stable. However, the scheme requires more computational power accordingly owing to the additional features.

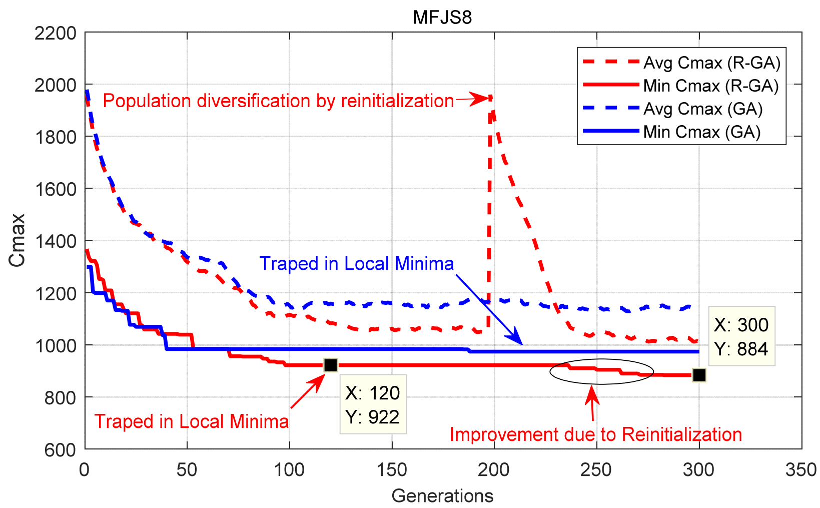

Fig. 6 Convergence pattern for MFJS8 and its comparison with GA

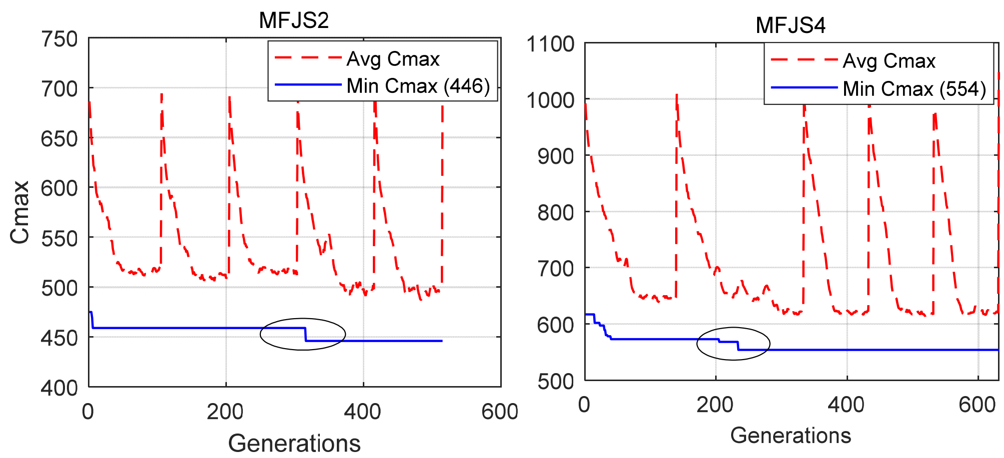

Fig. 7 Convergence pattern for MFJS2 and MFJS4

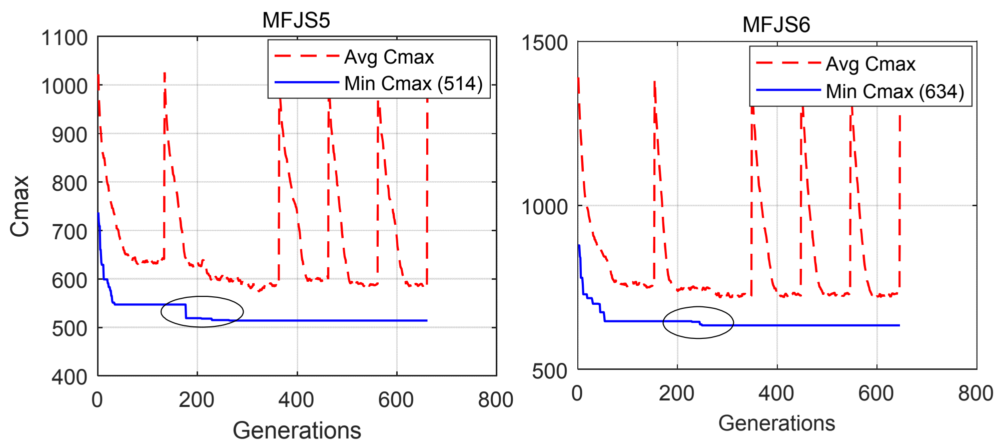

Fig. 8 Convergence pattern for MFJS5 and MFJS6

Table 4 presents the solutions of R-GA in contrast with other comparable algorithms. The algorithm results are compared with standalone optimization algorithms that have solved similar benchmarks. Notably, the algorithm outperforms other algorithms in various instances. Positive mean percentage deviation calculated from Eq. 12 shows that the algorithm performs competitively when tested against these benchmarks and even outperforms in some instances. Fig. 9 presents a final Gantt chart of MFJS8.

$$\%\Delta = \frac{Reference - Achieved}{Reference} \cdot 100 \quad (12)$$

Table 4 Comparison of R-GA with other similar approaches

Problem	R-GA	HTS/TS [30]		HTS/SA[30]		GA[34]		AIA[35]		CP[36]	
		C_{max}	%Δ	C_{max}	%Δ	C_{max}	%Δ	C_{max}	%Δ	C_{max}	%Δ
SFJS1	66	66	0	66	0	66	0	66	0	66	0
SFJS2	107	107	0	107	0	107	0	107	0	107	0
SFJS3	221	221	0	221	0	221	0	221	0	221	0
SFJS4	355	355	0	355	0	355	0	355	0	355	0
SFJS5	119	119	0	119	0	119	0	119	0	119	0
SFJS6	320	320	0	320	0	320	0	320	0	320	0
SFJS7	397	397	0	397	0	397	0	397	0	397	0
SFJS8	253	253	0	256	1.2	253	0	253	0	253	0
SFJS9	210	210	0	210	0	210	0	210	0	210	0
SFJS10	516	516	0	516	0	516	0	516	0	516	0
MFJS1	468	469	0.2	469	0.2	468	0	468	0	468	0
MFJS2	446	482	7.5	468	4.7	448	0.4	448	0.4	446	0
MFJS3	466	533	12.6	538	13.4	466	0	468	0.4	466	0
MFJS4	554	634	12.6	618	10.4	554	0	554	0	554	0
MFJS5	514	625	17.8	625	17.8	514	0	527	2.5	514	0
MFJS6	634	717	11.6	730	13.2	634	0	635	0.2	634	0
MFJS7	879	964	8.8	947	7.2	881	0.2	879	0	931	5.6
MFJS8	884	970	8.9	922	4.1	891	0.8	884	0	884	0
MFJS9	1091	1105	1.3	1105	1.3	1094	0.3	1088	-0.3	1070	-2
MFJS10	1238	1404	11.8	1384	10.5	1286	3.7	1267	2.3	1208	-2.5
Kacem1	11	-	-	-	-	-	-	-	-	11	0
Kacem2	11	-	-	-	-	-	-	-	-	11	0
Kacem3	7	-	-	-	-	-	-	-	-	7	0
Kacem4	12	-	-	-	-	-	-	-	-	12	0
Mean %Δ			4.7		4.2		0.3		0.3		0

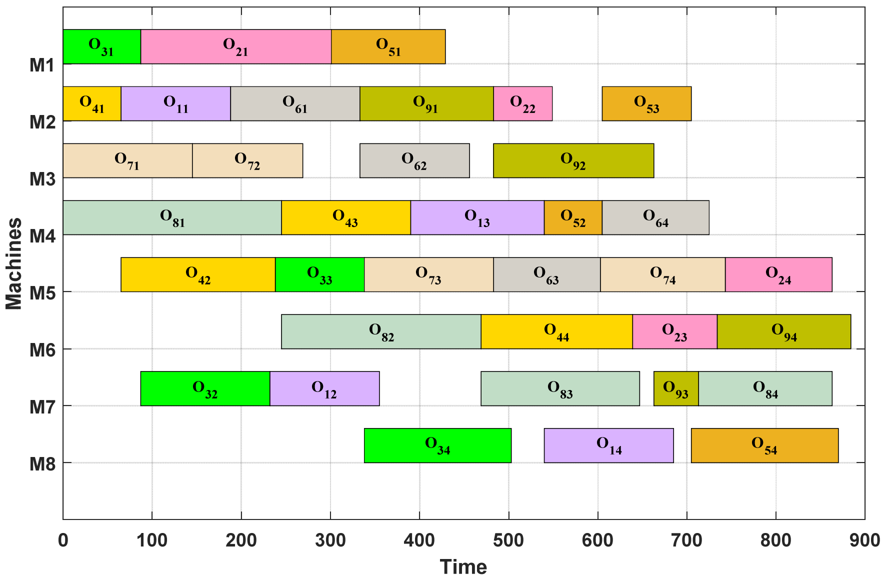

Fig. 9 Gantt chart for MFJS 8

Fig. 10 shows percentage deviation of R-GA from five different algorithms for ten problems, i.e. MFJS1 to MFJS10. Positive deviation indicates that R-GA performed better than reference algorithm while negative deviation indicates otherwise. It is notable that R-GA performs better than other algorithms for more complex problems e.g. MFJS10 etc. It is also evident that R-GA performs in a satisfactory manner as the problem complexity increases since significant positive deviation is achieved in nearly all problems as shown in Fig. 10. However, R-GA lagged for MJFS9 when compared with AIAA and CP and MFJS10 when compared with CP.

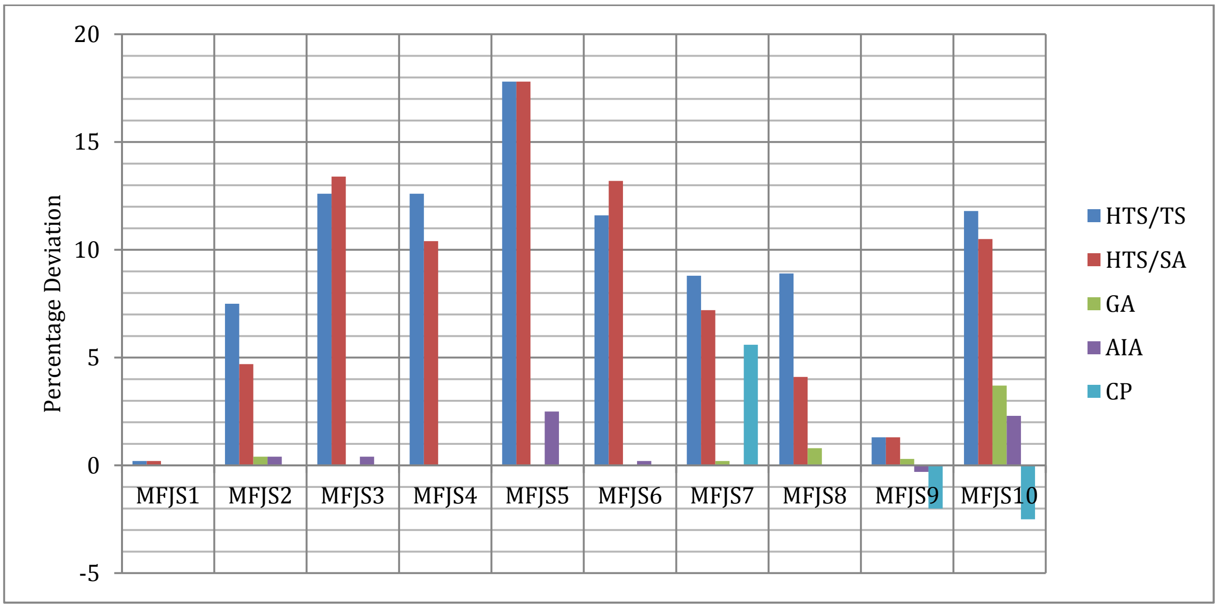

Fig. 10 Percentage deviation of R-GA from different algorithms

5. Conclusion

In this paper, the search space of well-known benchmark problems is addressed qualitatively by proposing a chromosome-based formulation and an insight into the actual problem complexity is presented owing to the NP-hard nature of the problem. A modified GA is then developed and implemented for solving the selected benchmark problems of FJSSP for makespan optimization. In this approach, GA is initialized based upon global, local and random selection techniques and adaptive reproductive operators are applied to intelligently evolve the algorithm. Adaptability has been incorporated in the parameters so that the algorithm may adhere to the current population diversity and acquire additional benefits out of the intensification and diversification regimes. The algorithm converges to a certain limit and traps in local minima while preserving the best available solution. To divulge the algorithm from this point, diversification methodology is employed with revised adaptive parameters and the algorithm converges until termination criteria are encountered. The algorithm is tested extensively on selected benchmarks and it is concluded that the proposed algorithm not only performs effectively for solving the FJSSP but also escapes out of local minima trap at various instances. The convergence patterns along with solution quality further endorse the algorithm efficacy. It is also identified that the proposed diversification methodology produces better results when integrated with the GA and surpasses most of the other standalone comparable approaches.

This work enhances the utility of GA through the effective use of various diversification techniques and provides a framework for effectively exploring the huge search space with an easy-to-program approach. A user-friendly software is developed in this work which requires minimum input from the user and can be used in other similar optimization applications. Future research involves the expansion of algorithm application on multi-objective problems and other objective functions.

Acknowledgement

The authors gratefully acknowledge the support of National University of Science and Technology, Islamabad, Pakistan for funding the studies

References

[1] Pinedo, M.L. (2012). *Scheduling: Theory, algorithms, and systems*, Springer, Boston, USA, doi: 10.1007/978-1-4614-2361-4.

[2] Jain, A., Jain, P.K., Chan, F.T.S., Singh, S. (2013). A review on manufacturing flexibility, *International Journal of Production Research*, Vol. 51, No. 19, 5946-5970, doi: 10.1080/00207543.2013.824627.

[3] Dauzère-Péres, S., Lasserre, J.-B. (2012). *An integrated approach in production planning and scheduling*, Springer-Verlag, Berlin, Germany, doi: 10.1007/978-3-642-46804-9.

[4] Groover, M.P. (2015). *Automation, production systems, and computer-integrated manufacturing*, 4th edition, Pearson Education, Delhi, India.

[5] Azzouz, A., Ennigrou, M., Said, L.B. (2017). A hybrid algorithm for flexible job-shop scheduling problem with setup times, *International Journal of Production Management and Engineering*, Vol. 5, No. 1, 23-30, doi: 10.4995/ijpme.2017.6618.

[6] Kacem, I. (2013). Genetic algorithms for solving flexible job shop scheduling problems, In: Jarboui, B., Siarry, P., Teghem, J. (eds.), *Metaheuristics for Production Scheduling*, John Wiley & Sons, New York, USA, 19-44, doi: 10.1002/9781118731598.ch2.

[7] Chaudhry, I.A., Usman, M. (2017). Integrated process planning and scheduling using genetic algorithms, *Tehnički Vjesnik – Technical Gazette,* Vol. 24, No. 5, 1401-1409, doi: 10.17559/TV-20151121212910.

[8] Cheng, T.C.E., Shafransky, Y., Ng, C.T. (2016). An alternative approach for proving the NP-hardness of optimization problems, *European Journal of Operational Research*, Vol. 248, No. 1, 52-58, doi: 10.1016/j.ejor.2015.06.076.

[9] Brucker, P., Sotskov, Y.N., Werner, F. (2007). Complexity of shop-scheduling problems with fixed number of jobs: A survey, *Mathematical Methods of Operations Research*, Vol. 65, No. 3, 461-481, doi: 10.1007/s00186-006-0127-8.

[10] Candan, G., Yazgan, H.R. (2015). Genetic algorithm parameter optimisation using Taguchi method for a flexible manufacturing system scheduling problem, *International Journal of Production Research*, Vol. 53, No. 3, 897-915, doi: 10.1080/00207543.2014.939244.

[11] Ojstersek, R., Lalic, D., Buchmeister, B. (2019). A new method for mathematical and simulation modelling interactivity: A case study in flexible job shop scheduling, *Advances in Production Engineering & Management*, Vol. 14, No. 4, 435-448, doi: 10.14743/apem2019.4.339.

[12] Borreguero-Sanchidrián, T., Pulido, R., García-Sánchez, Á., Ortega-Mier, M. (2018). Flexible job shop scheduling with operators in aeronautical manufacturing: A case study, *IEEE Access*, Vol. 6, 224-233, doi: 10.1109/ACCESS.2017.2761994.

[13] Nidhiry, N.M., Saravanan, R. (2014). Scheduling optimization of a flexible manufacturing system using a modified NSGA-II algorithm, *Advances in Production Engineering & Management*, Vol. 9, No. 3, 139-151, doi: 10.14743/apem2014.3.183.

[14] Hecker, F.T., Hussein, W.B., Paquet-Durand, O., Hussein, M.A., Becker, T. (2013). A case study on using evolutionary algorithms to optimize bakery production planning, *Expert Systems with Applications*, Vol. 40, No. 17, 6837-6847, doi: 10.1016/j.eswa.2013.06.038.

[15] Amjad, M.K., Butt, S.I., Kousar, R., Ahmad, R., Agha, M.H., Faping, Z., Anjum, N., Asgher, U. (2018). Recent research trends in genetic algorithm based flexible job shop scheduling problems, *Mathematical Problems in Engineering*, Vol. 2018, No. 32, Article ID 9270802, doi: 10.1155/2018/9270802.

[16] Zhang, J., Ding, G., Zou, Y., Qin, S., Fu, J. (2019). Review of job shop scheduling research and its new perspectives under Industry 4.0, *Journal of Intelligent Manufacturing*, Vol. 30, No. 4, 1809-1830, doi: 10.1007/s10845-017-1350-2.

[17] Janes, G., Perinic, M., Jurkovic, Z. (2017). An efficient genetic algorithm for job shop scheduling problems, *Tehnički Vjesnik – Technical Gazette,* Vol. 24, No. 4, 1243-1247, doi: 10.17559/TV-20150527133957.

[18] Chaudhry, I.A., Khan, A.A. (2016). A research survey: Review of flexible job shop scheduling techniques, *International Transactions in Operational Research*, Vol. 23, No. 3, 551-591, doi: 10.1111/itor12199.

[19] Çaliş, B., Bulkan, S. (2015). A research survey: Review of AI solution strategies of job shop scheduling problem, *Journal of Intelligent Manufacturing*, Vol. 26, No. 5, 961-973, doi: 10.1007/s10845-013-0837-8.

[20] Ida, K., Oka, K. (2011). Flexible job-shop scheduling problem by genetic algorithm, *Electrical Engineering in Japan*, Vol. 177, No. 3, 28-35, doi: 10.1002/eej.21194.

[21] Kacem, I., Hammadi, S., Borne, P. (2002). Approach by localization and multiobjective evolutionary optimization for flexible job-shop scheduling problems, *IEEE Transactions on Systems, Man, and Cybernetics, Part C (Applications and Reviews),* Vol. 32, No. 1, 1-13, doi: 10.1109/TSMCC.2002.1009117.

[22] Gao, J., Gen, M., Sun, L., Zhao, X. (2007). A hybrid of genetic algorithm and bottleneck shifting for multiobjective flexible job shop scheduling problems, *Computers & Industrial Engineering*, Vol. 53, No. 1, 149-162, doi: 10.1016/j.cie.2007.04.010.

[23] Pezzella, F., Morganti, G., Ciaschetti, G. (2008). A genetic algorithm for the flexible job-shop scheduling problem, *Computers & Operations Research*, Vol. 35, No. 10, 3202-3212, doi: 10.1016/j.cor.2007.02.014.

[24] Gu, X., Huang, M., Liang, X. (2019). An improved genetic algorithm with adaptive variable neighborhood search for FJSP, *Algorithms*, Vol. 12, No. 11, Article No. 243, doi: 10.3390/a12110243.

[25] Wang, L., Luo, C., Cai, J. (2017). A variable interval rescheduling strategy for dynamic flexible job shop scheduling problem by improved genetic algorithm, *Journal of Advanced Transportation*, Vol. 2017, Article ID 1527858, doi: 10.1155/2017/1527858.

[26] Xiong, J., Tan, X., Yang, K.-W., Xing, L.-N., Chen, Y.-W. (2012). A hybrid multiobjective evolutionary approach for flexible job-shop scheduling problems, *Mathematical Problems in Engineering*, Vol. 2012, Article ID 478981, doi: 10.1155/2012/478981.

[27] Teekeng, W., Thammano, A. (2012). Modified genetic algorithm for flexible job-shop scheduling problems, *Procedia Computer Science,* Vol. 12, 122-128, doi: 10.1016/j.procs.2012.09.041.

[28] Framinan, J.M., Leisten, R., García, R.R. (2014). *Manufacturing scheduling systems*, Springer-Verlag, London, United Kingdom, doi: 10.1007/978-1-4471-6272-8.

[29] Zhang, G., Gao, L., Shi, Y. (2011). An effective genetic algorithm for the flexible job-shop scheduling problem, *Expert Systems with Applications*, Vol. 38, No. 4, 3563-3573, doi: 10.1016/j.eswa.2010.08.145.

[30] Fattahi, P., Saidi Mehrabad, M., Jolai, F. (2007). Mathematical modeling and heuristic approaches to flexible job shop scheduling problems, *Journal of Intelligent Manufacturing*, Vol. 18, No. 3, 331-342, doi: 10.1007/s10845-007-0026-8.

[31] Song, W.J., Zhang, C.Y., Lin, W.W., Shao, X.Y. (2014). Flexible job-shop scheduling problem with maintenance activities considering energy consumption, *Applied Mechanics and Materials*, Vol. 521, 707-713, doi: 10.4028/www.scientific.net/AMM.521.707.

[32] De Giovanni, L., Pezzella, F. (2010). An improved genetic algorithm for the distributed and flexible job-shop scheduling problem, *European Journal of Operational Research,* Vol. 200, No. 2, 395-408, doi: 10.1016/j.ejor.2009.01.008.

[33] Nouri, H.E., Driss, O.B., Ghédira, K. (2017). Solving the flexible job shop problem by hybrid metaheuristics-based multiagent model, *Journal of Industrial Engineering International*, Vol. 14, 1-14, doi: 10.1007/s40092-017-0204-z.

[34] Zandieh, M., Mahdavi, I., Bagheri, A. (2008). Solving the flexible job-shop scheduling problem by a genetic algorithm, *Journal of Applied Sciences*, Vol. 8, No. 24, 4650-4655, doi: 10.3923/jas.2008.4650.4655.

[35] Bagheri, A., Zandieh, M., Mahdavi, I., Yazdani, M. (2010). An artificial immune algorithm for the flexible job-shop scheduling problem, *Future Generation Computer Systems*, Vol. 26, No. 4, 533-541, doi: 10.1016/j.future.2009.10.004.

[36] Behnke, D., Geiger, M.J. (2012). *Test instances for the flexible job shop scheduling problem with work centers*, Universitätsbibliothek der Helmut-Schmidt-Universität, Hamburg, Germany, from *https://d-nb.info/1023241773/34*, accessed May 2020.

APEM journal
Advances in Production Engineering & Management
Volume 15 | Number 4 | December 2020 | pp 390–402
https://doi.org/10.14743/apem2020.4.373
ISSN 1854-6250
Journal home: apem-journal.org
Original scientific paper

A review of production technologies and materials for manufacturing of cardiovascular stents

Polanec, B.[a], Kramberger, J.[a], Glodež, S.[a,*]

[a]University of Maribor, Faculty of Mechanical Engineering, Maribor, Slovenia

ABSTRACT

The purpose of this article is to give a general overview of the production technologies of stents with consideration of their design and materials. Since the beginning of the use of stents in medicine for atherosclerosis treatment, their development has changed rapidly. Various stents have also been developed with the development of materials science, treatment techniques and new manufacturing processes. In this way the development has shifted from the initial bare-metal stents (BMS), to drug-eluting stents (DES) and bio-resorbable stents (BRS), which are made of biodegradable polymers or metals. Various studies agree that it will be necessary to further review the experimentally obtained material properties with analytical and numerical studies. Here, the computational modelling (Finite element analysis – FEA and Computational fluid dynamics – CFD) was found as a valuable tool when evaluating stent mechanics and optimizing stent design. The development of the stent manufacturing technologies has also changed and been supplemented over the years. Nowadays, 3D printing could be an exciting manufacturing method to produce polymeric bio-materials, suitable for the latest generation of biodegradable stents applications.

ARTICLE INFO

Keywords:
Stent;
Bare-metal stent;
Drug-eluting stent;
Bio-resorbable stent;
Stent coatings;
Drug delivery;
Stent manufacturing;
Stent material;
Laser cutting;
Additive manufacturing (3D printing)

**Corresponding author:*
srecko.glodez@um.si
(Glodež, S.)

Article history:
Received 22 September 2020
Revised 8 December 2020
Accepted 12 December 2020

1. Introduction

A stent can be defined as an endovascular prosthesis. They are skeletal meshes made of metal, placed inside a clogged coronary artery. The stent is developed for the purpose of preventing complications which occur in atherosclerosis. The latter is a chronic disease caused by the accumulation of fatty deposits on the walls of blood vessels, which causes the blood vessels to constrict. In this case, the supply of tissues is insufficient, which may lead to a heart attack or stroke. The most important characteristics of a stent are corrosion resistance, low thrombosis rate, biocompatibility, radiopacity, easy positioning, flexibility, high radial strength, low elastic displacement, uniformity, minimum surface area, low pass profiles and low costs [1].

In 1977, the German physician Andreas Gruentzig performed the first coronary balloon angioplasty on a conscious man. Problems which occurred after such procedures were acute vascular closure, short-term elastic displacement and prolonged restenosis. Restenosis is the artery's response to severe damage, caused by balloon angioplasty. One of its characteristics is the increased proliferation of smooth muscle cells and deposition outside the cell matrix, leading to progressive luminal narrowing. This phenomenon was observed in 33 % of the patients [1].

In 1986, Siguart and Puel performed a technique with a self-expanding stainless-steel stent on a human. The technique involved the expansion and permanent installation of a mechanical support device. Since then, many improvements have been made in the fields of Design, Materials, Implementation technique, etc. All of this has helped to increase the use of stents. Furthermore, with the insertion of the stent, it was proven that the restenosis rate decreased compared with the balloon angioplasty. However, a new problem can arise, which is called in-stent restenosis (ISR). As a final product, a neointima formation appears, consisting of smooth muscle cells and components of the extracellular matrix. The process of neointima formation stabilises in the human body after about 3-6 months.

2. Basic characteristics of stents

2.1 Stent shape

The shape of a stent is usually cylindrical and has at least one structural element (Fig. 1). These elements are arranged so that the stent can be stretched and compressed radially. The structural elements can be splints, rods, fibres, wires, or threads. The platform of the stent must provide [2]:

- Mechanical characteristics which, in the process, means that it matches the curvature of the vessel easily after stretching and maintains sufficient radial strength to withstand the force of the load on the arterial wall.
- Radio impermeability, to prevent the transmission of X-rays or other ionising radiation due to any necessary interventions.
- An easily replaceable base, namely, the stent should have a narrow profile in a compressed state so that it can be placed easily and can pass through narrow veins, with stenoses, effortlessly.
- Biocompatibility, which means that the material of the stent should be compatible with the blood and the surrounding vascular wall.

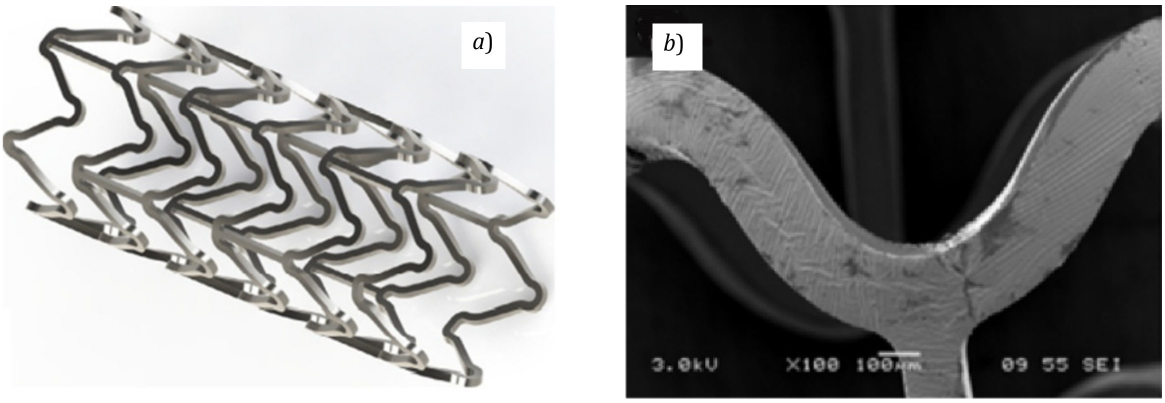

Fig. 1 a) Designed model of a cardiovascular stent, b) Scanning electron micrographs of a stent at 100× magnification with strut thickness of 150 μm [2]

2.2 Stent construction

The first stent implanted into humans was the Wallstent. It had a self-expanding platform that contained a stainless-steel metal structure. The Palmaz-Schatz stent introduced an alternative mechanism using an expandable balloon. Today, all stents are made from this principle. These stents have higher radial strength and better clinical outcome than the competing mesh and coil stent structures. Further platform developments have established a balance between coil flexibility and radial strength of stent models with mesh structures [3].

2.3 Stent geometry

The main attributes of a stent are its flexibility and radial strength. To achieve both, different geometric configurations must be made. Rogers and Edelman [4] showed that the geometry of the stent is an important factor in restenosis. If, at the same material and surface area, the number of junctions of the support struts increases, then the neointimal area increases proportionally. Other researches have proved that this condition is also necessary to reduce vascular damage [5, 6].

2.4 Stent strut thickness

Various clinical studies and researches have shown that the degree of restenosis depends on the thickness of the splint. The thinner the splint, the lower the rate of restenosis. Two stent brace thicknesses were compared in [7]. A 50 µm splint thickness caused 15 % restenosis, and a 140 µm caused 26 % restenosis. The thickness of the splint has more effect on restenosis than its geometry. Because of that, they started using metal splints with a minimum thickness (60-100 µm). The design and fabrication of the stent platform are two crucial factors in clinical success. Also, great attention is paid to the optimisation of materials and the design of the stent platform.

3. Materials for the stent's platform

The choice of materials for stents is very important (see Table 1). They must have several important characteristics, such as sufficient mechanical strength and ductility, they must be biocompatible and antibacterial. The material must also be flexible, and must have the ability to spread. Non-biocompatible material can trigger an immune response and lead to rapid cell proliferation via a stent, leading to a cytotoxic effect and chronic inflammation [8].

3.1 Bare-metal stents (BMS)

The first generation of stents were bare-metal stents (BMS), where 316L stainless steel was used as a base material. The main benefit characteristics of such stents were high durability, corrosion resistance and biocompatibility. However, these stents are poorly degradable, which may cause inflammation after some period of implementation.

Improvements in stent design have been made possible due to the development in the science of materials. Significant progress in this area is seen in the use of metal alloys that have higher mechanical strength (compared to 316L stainless steel). Greater strength is crucial for the possibility of using thinner splints. Those are more effective and reduce further health problems, which can occur later [9]. In recent years, the emphasis has been placed on research on the types of materials for stents, where the emphasis has primarily been on observing the mechanical properties and biocompatibility of materials [10, 11]. The greatest progress has been made in the use of alloys and representative materials for bare metals, such as nickel-titanium, cobalt-chromium, magnesium, platinum-iridium, etc. The best mechanical strength was shown by the cobalt-chromium alloy; thus, it is used mostly for the stent platform. The use of metal alloys reduced the thickness of the struts, improved performance, and maintained radial strength. The disadvantage of these stents is the occurrence of late restenosis which may be avoided with the use of drug-eluting stents.

3.2 Drug-eluting stents (DES)

A drug-eluting Stent (DES) can load and deliver medicine that is inserted into polymer coatings on the surface of bare-metal stents. Drug-eluting stents began to develop because of restenosis problems after implantation of the previous stents. They have been shown to reduce the rate of restenosis development [12]. DES presents a revolution in stent development. The first generation was Cypher DES (Cordis Corp., Johnson & Johnson). Problems with these stents manifested as thrombosis (clogging of the veins). Therefore, the researchers focused their development on improving DES.

In general, three key components contribute to overall stent safety and efficacy, namely the stent platform, the remedy, and the medicine coating technology. Hence, it can be argued that the design of a DES stent is a multidisciplinary process. For the development of DES it is necessary to intervene in the science of materials, in the field of engineering, advanced technology, for the use of medicine areas such as physiology, pharmacology and chemistry. Delivery engineering, pharmaceutical science, and, again, chemistry, are once more important for delivering a medicament to the required location. The performance of the stent depends on the optimisation of each of these aspects [13, 14]. Different generations of stents have always used the most advanced stent platform during their development. The first generation, which includes Cypher (Cordis Corp.) in Fig. 2A and Taxus (Boston Science) in Fig. 2B, used a stainless-steel platform with a splint thickness of 130-140 μm. Later generations such as Driver (Medtronic), Multi-Link vision (Abbot Vascular) shown in Fig. 2C and Omega (Boston Scientific) have thinner splints (80-90 μm). Newer platforms are biodegradable. To ensure sufficient radial strength, these splints had to be made thicker [15]. The shape of the splint has changed, with development from rectangular to round shapes and with the latest DES with rounded edges.

The DES design included optimising drug release based on the proposed drug action mechanisms. The first generation contained drug coatings to ensure long-term release within 90 days [16]. Computer models show that there are opportunities to optimise drug release further for existing and new drugs. To achieve the desired release profile, it is necessary to attach a biological agent to the surface of the stent. The possibilities of polymer-based and non-polymer-based systems are being investigated [16].

a) *b*) *c*)

Fig. 2 a) Cypher by Johnson & Johnson, b) Taxus by Boston Scientific, c) XienceV by Abbott [44]

Release of drugs with permanent polymers

A wide range of polymers has been investigated as a possible solution for stent coating [17]. The first two generations used durable polymer coatings containing the drug (paclitaxel) and a copolymer of poly (styrene-B-isobutylene B-styrene). Research has led to improvements in drug efficacy and the development of improved approaches for stent drug administration [18].

The first-generation of DES reported hypersensitive responses to polymers. Therefore, research efforts have evolved towards greater biocompatibility. The biomimetic polymer Phosphorylcholine (ChoP) was used in the Endeavor stent (Medtronic) [19]. Because this stent released drugs too quickly, they began developing the Endeavor Resolute DES, which released the drug slowly over the time. The difference was in the new BioLinx polymer blend, which contains Polyvinyl Pirolipon as a carrier layer for the drug, which is mostly released over two months [20]. To improve biocompatibility, poly (vinylidene fluoride - co - hexafluoropropylene) (PVDF-HFP) was used as the outer carrier layer for the drug (Everolimus). This combination is used in DES at Abbot Vascular and Promus Element Boston Scientific. Research [21] has shown that prolonged exposure to durable polymer coatings prolongs the healing time of blood vessels. As a solution, further research has gone into the use of degradable polymer coatings and polymer-free coatings.

Release of drugs with degradable polymers

The latest generation of DES includes several biocompatible polymers to alleviate the inflammation and thrombosis risk. Degradable polymers are lactide and glycolide. Degradation produces lactic and glycolic acid, which is metabolised to non-toxic products in the body. Stents coated with poly (lactide-co-glycolide) (PLGA) were considered in the study [22]. They produced different release profiles, and focused on changing the rate, duration of drug release by changing the number of layers, and the ratio of lactide and glycolide. In vivo, they discovered that the combination of paclitaxel and PLGA decelerates the formation of neointima in pigs. Similar results were obtained in vitro with the use of poly (d, 1,1-lactide - co - glycolide) when paclitaxel or sirolimus was released [23]. Poly (d, 1) lactide (PDLLA) is a polymer coating used in many stents, such as BioMatrix (Biosensors, International) and Nobori (Terumo) Biolimus A9. These stents were among the first to apply a polymer-drug coating only to the non-luminous side of the stent, which was an innovation. This resulted in better drug delivery to the artery tissue and faster endothelialisation. These stents have a relatively thick splint (120 μm). Stent Synergy (Boston Scientific), which uses a very thin layer of PLGA for the controlled release of Everolimus, has a platinum-chromium platform with a splint thickness of 74-81 μm. These splints have shown clinical benefits of use. Nevertheless, the second generation of DESs were fabricated on conventional bare-metal stent platforms and traditional coating application techniques. Some stents, however, have used alternative coating techniques (Cordis Corp.). Such platform designs allow precise loading of drug layers and polymer layers in specially designed tanks inside the splint [24]. Such a combined approach is used in the Yukon stent (Translumina GmbH). The stent is based on the application of a polymer layer of polylactide PLA (with drug application), on a microporous stainless-steel stent platform with Shellac resin coating. The analysis [25] found that the biodegradable DES polymer-coated stent improved safety and efficacy compared to the original generations of durable polymers in DES. Less well known is how much the biodegradable polymer in DES has improved the second generation of permanent DES.

Release of polymer-free drugs

DES polymer-free stents must include other mechanisms to control the release of drugs from the stent surface. The introduction of surface porosity on macro- and micro- or nano-structures has proven to be a popular approach to controlling drug release. It was proven clinically that the most useful structures were macro and microporous. The Jonus Tacrolimus-eluting carbostent (Sorin Group) have such stents, with pores or holes or grooves, with slots at the macro level, and a stent system filled with Medtronic [26].

The first stent in use with a microporous surface was the Yukon stent (Translumina GmbH) [27]. The usual stent plate was made of stainless steel, sandblasted, in order to create a rough surface treatment having microporous holes 1-2 μm in size, which were filled with spray-coated drugs to ensure the controlled release of the drug. The advantage of this stent was that it reduced the rate of restenosis and accelerated endothelialisation [28].

Newer microporous stents, DES BioFreedom (Biosensors International), create a rough surface using their micro-abrasion procedure. This gives a treated surface (like Yukon's). This stent allows for more targeted drug delivery to a lesion. The development of alternative approaches with the coating of polymer-free drugs continues, which is also reflected in the emergence of patents for various technologies [29]. An important role in further development will be played by the biocompatible surface and, thus, also by such stents, which inhibit neointima and accelerate the regeneration of a healthy endothelium.

3.3 Bio-resorbable stents (BRS)

The desire for ever better results and the reduction of problems, and, thus, the complete recovery of blood vessels, led to the concept of complete decomposition of the device, and thus developed bio-resorbable stents. BRS can be made of bio-resorbable polymers or metals. BRS made of polymers have emerged from materials such as PLLA (Poly-L-Lactic Acid). PLLA is a thermoplastic polymer, namely, aliphatic polyester. It consists of the L-enantiomer of lactic acid (2-hydroxy propionic acid). PLLA has a high solidity. At 55 °C, it has a reversible transition from a relatively hard state to a state like that of rubber. At 175 °C, it has a melting point, and the temperature required for processing is 185-190 °C. However, a problem arises, because, at 185 °C, it begins to lose molecular weight, due to chain reactions and thermal decomposition. PLLA is degraded by hydrolysis of the ester bond and metabolised to water and carbon dioxide. Decomposition takes place in five steps. It begins with the absorption of water from the surrounding tissue and continues with depolymerisation, resulting in loss of molecular weight. The third step is the crushing of the polymer, which causes a loss of mass resulting in loss of radial solidity. This is where the chain breakage occurs, and the shorter chains are excised from the polymer stent. Cells process small polymer chains by phagocytosis (a process in which a cell devours and digests solid particles), then metabolises them to L-lactate and converts them to pyruvate. Pyruvate is eventually broken down into carbon dioxide and water. The first stent made from PLLA that could be absorbed in humans was the Igaki-Tamai stent (Igaki Medical Planning Co., Ltd.). It had a helical structure of a zigzag spiral coil. The length of the stent was 12 mm and the thickness of the splint was 0.17 mm [30]. The mentioned stent was a self-expanding, mounted on a standard balloon for angioplasty. The study showed that, after the expansion, the stent did not cause any significant inflammatory response in patients. Self-expansion occurred within 20 to 30 minutes after installation. The stent provided radial support for 6 months and was absorbed completely in 2-3 years. This stent required heat for the self-expanding process; therefore, it has not been used in the coronary arteries since. A more advanced form of a stent is the BRS, like a small mesh tube whose base is made of Poly-L-lactide (PLLA) covered with a surface layer of Poly-D-lactide (PDLLA) that releases an antiproliferative drug. They are comparable to DES. However, lower efficiency and a higher risk of thrombosis appeared. It provided mechanical support to the coronary artery, and its degradation time was two years [31-33] (Fig. 3).

The crucial advantage of a biodegradable polymer stent is in the slower and longer release of drugs. Their disadvantage is lower mechanical strength, and, consequently, the splint must be thicker. Biological problems, such as inflammatory reactions and increased neointima, are caused mainly by their decomposing products. Due to these problems, biodegradable metal stents with alloys based on iron (Fe) and magnesium (Mg), and later based on zinc (Zn), have started to develop in the last ten years [34]. In studies [35, 36], they were establishing characteristics and biocompatibility, and they determined that a biodegradable Fe-based stent is biocompatible and has proper mechanical properties. Their degradation is slow and causes poor regeneration with iron oxide residues [37, 38].

Another group of biodegradable stents are magnesium-based stents (Mg). Mg-alloys are well biocompatible and have good mechanical properties; on the other hand, their decomposition time is slightly too fast. Therefore, stents were made from a Mg-alloy with an optimised extrusion process and, they were treated with heat. This way a more even degradation and minimal inflammation in vivo was achieved. This is how the WE43 alloy was formed [39].

The newer generation of the bio-resorbable stents was based on zinc (Zn). It has a better in vivo degradation rate than its predecessor. Zinc-based BVS is a new generation that has many advantages over other materials: An ideal rate of in vivo degradation, overall biocompatibility and less proliferation of smooth muscle cells, and a good antibacterial effect. The response to inflammation is like that of BVS in Fe in vivo [40-44].

A review of the current state of BRS shows that the most commonly used biodegradable material is poly-1-lactic acid, followed by magnesium. Other investigated materials are tyrosine polycarbonate, polymer salicylic acid and iron. Fig. 4 shows BRSs also demonstrated by optical coherence tomography (OCT) [15].

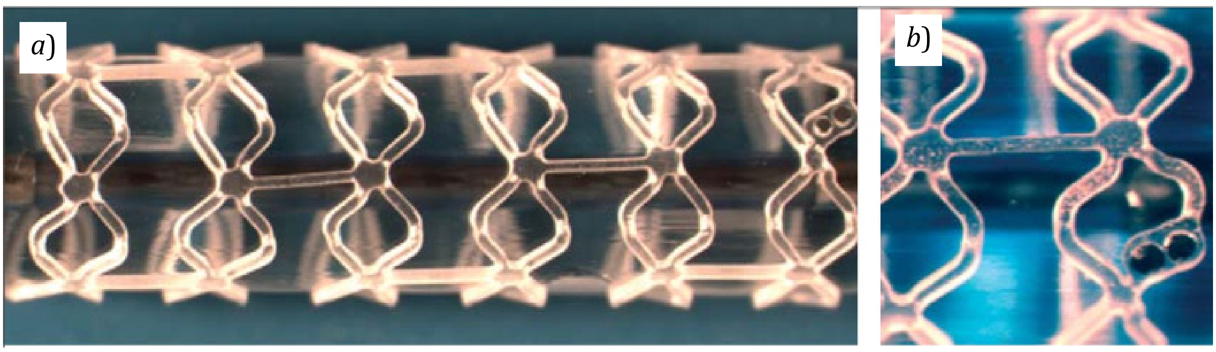

Fig. 3 a) PLLA bio-resorbable stent, b) Magnified image of the stent [31]

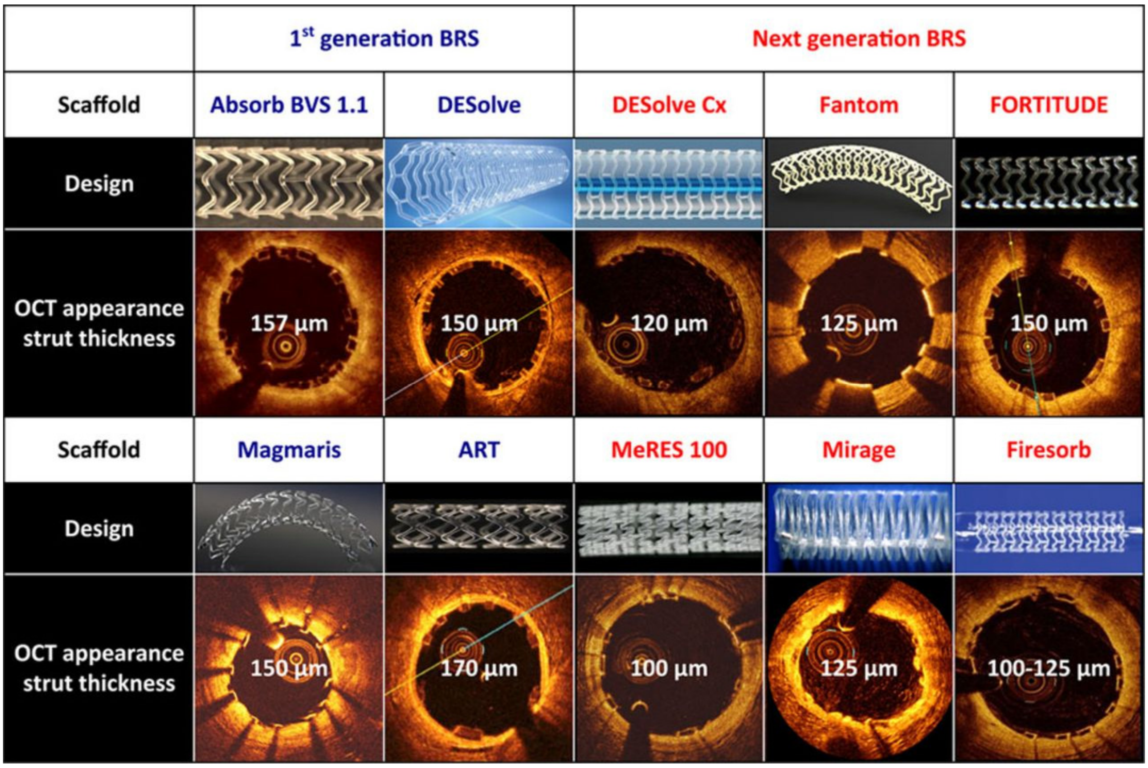

Fig. 4 Design and OCT appearance of BRSs [15]

Table 1 An overview of stent materials

	BMS	DES	BRS
Advantages	• Good mechanical properties, durability, good processing, biocompatibility, corrosion resistance	• Reduction of neointima due to drug release	• Slow and prolonged drug release • Reduction of adverse clinical events due to complete stent degradation • Possibility of restoring vascular function and performing MRI examination after stent degradation
Disadvantages	• Thick splints • Poor degradability	• Occurrence of late thrombosis	• Lower mechanical strength
Limitations	• Occurrence of late restenosis	• Design of DES is a multidisciplinary process	• The material must be a biodegradable polymer or metal • Thicker splints
Prospects	• Development stents from metal alloys, smart memory alloys and polymers • Development drug-eluting stents	• Development of several generations of DES • It leads to the development of BRS stents	• Development of BRS metal stent with Fe, Mg, and Zn based alloys • Good mechanical properties • Good degradation and biocompatibility

4. Production technologies for manufacturing of stents

A review through various literature shows that, in the manufacture of a stent, a distinction must be made between the manufacture of a stent and a stent-graft (see Table 2). This can be divided into nitinol stent and polymer film fabrication. Nitinol stents are made by laser cutting, weaving, or suturing processes, hence, the same as bare-metal stents. The stent-graft also contains a polymer film for which mouldings are used as for textiles. Looms are used, the material is extruded, an electrostatic base is used, and it has a micro to nano composition [46]. For the manufacture of stents, the following production processes are mentioned in the literature: The filament winding phase, micro-EDM using electro-erosion, stent injection, laser cutting and additive manufacturing technology, which also includes Selective laser melting.

4.1 The manufacture of a stent-graft

The existing methods for integrating metal and film moulds include sewing and application. The sewing method performs easy penetration of the film, which often results in tearing. Another bad attribute is that this method takes a lot of time to make. In the application method, the outer film is applied to the surface of the inner film of the stent-graft. When the solution evaporates, the inner and outer film wrap tightly around the metal stent. This method avoids possible tearing caused by hand sewing and has greater efficiency [45]. Therefore, the metal stent is combined with the film by the deposition method. However, it is difficult to use 3D printing for direct integration and to design composite materials containing a cover film and metal stent. To solve this problem, the Rapid Prototyping Sacrificial Core-Coating Technique (RPSC CF) can be used, first proposed by Huang *et al.* [47]. A vascular stent was designed using a patient's Computed Tomography (CT) scan. A water-soluble sacrificial core was fabricated using FDM (Fused Deposition Modelling). With the application process, biopolymer material was applied layer by layer. In the next step, a Nitinol alloy was woven into the stent and coated again with the biopolymer. This integrates the alloy and polymer film into the stent. The wall structure of the multilayer tube can also be formed layer by layer using coating, injection moulding or other material application procedures, and finally, the inner core is dissolved to obtain a stent.

4.2 Stent fabrication technologies

Wire winding with the help of laser local welding

This procedure was used mostly in the initial stages of stent fabrication when stents were made of stainless steel. Each unit related to the laser local welding. Difficulties in such stent manufacture arise in locating the weld, due to the small size and complexity of the vascular stent structure [46].

Micro-EDM

A micro-electrical discharge machining (micro-EDM) is a process where the material removal occurs by electro-erosion due to electric discharge generated between closely spaced electrodes in the presence of a dielectric medium. The shape of a stent's cells is the mirror image of the electrode [48].

Injection moulding

We distinguish between low-pressure reaction injection moulding (RIM) and high-speed injection (HSI). HSI is the injection into a mould with a significantly higher speed (more than 500 mm/s) at lower temperatures, which reduces polymer degradation. HSI was used for stents of arbitrary geometries with high radial length, small offset, and shape stability. This avoided the negative effects of laser cutting. RIM is a technical process for making polymer products. The molten polymer is injected at high pressure into a mould, which can be made of metal (steel or aluminium). Products are formed directly in the mould. The products can be solid or have a foam structure. Stents made in this way have low tolerance, the possibility of coating different materials, no visual defects, are durable, and offer flexibility. The additional advantage is that this kind of production offers low tool costs. However, the disadvantages of this process to produce stents are mainly in the uneven design, slow fabrication and high requirements for injection moulds, and the associated higher costs [45, 46].

Laser cutting

It is a commonly widely used manufacturing technique for industrial applications, mainly producing bare-metal and polymer stents. Laser cutting is a technology where a high energy density laser beam focuses on a raw tube surface. The stent is made of a nano or microtube by laser cutting to produce the desired structural elements. Different types of lasers have been used in stent manufacture, including CO2 lasers, Nd:YAG lasers, fiber lasers, excimer lasers, and ultra-short pulse lasers. The disadvantage of laser cutting is that this process can cause thermal damage such as heat-affected zone (HAZ), striation, recast layer, microcracks, tensile residual stress, and dross. The splints may have sharp edges due to such construction, damaging the vessel or cause un-stable blood flow after implantation. However, the supporting component is rectangular, causing local eddy blood flows, followed by leukocyte aggregation leading to restenosis. Some post-processing techniques are used, like annealing and electropolishing to overcome the thermal da-mages. Due to introducing these post-processing techniques, the manufacturing cost are raised. Over the last decade, ultra-short pulse lasers (picosecond and femtosecond) have been available for high precision processing, which are an alternative to the longer pulse lasers for machining thin materials for stent applications. Although the thermal effect is reduced, debris and recast formation still have to be removed by other methods [47, 48].

Additive manufacturing technology

In the case of metal stents, this technology does not work due to oxidation problems. Additive production is suitable for biodegradable polymer stents. In 2013, Flege at al. [49] used PLLA and PCL material for the first time for processing selective laser melting (SLM). SLM is an additive technique in which a laser beam melts and joins the material layer by layer selectively [50]. The disadvantages of this process are reflected in poor surface accuracy and a long manufacturing process. Due to the poor properties of SLM, Park *et al*. [51] used bio cutting technology in 2015. The disadvantages of this technology have been demonstrated in the difficulty of stent personalisation and the lengthy stent fabrication process. The procedure takes more than 10 hours. Tumblestone *et al*. [52] developed the continuous liquid interface production (CLIP) technology. This is a process where UV projection hardens a photosensitive resin. The liquid resin maintains a stable area of the liquid, and ensures continuous solidification due to contact with oxygen. The good features of this process are the higher speed of 3D printing, namely by 25 to 100 times, and in the high precision of the product surface. In 2016, degradable citrate-based polymer material was synthesised using the micro CLIP process [53]. This process gave the stent very good properties, such as good elasticity, good strength, oxidation resistance and biodegradability. The manufacturing time is short, and, after 180 days, the stent degrades by 25%. The procedure also has negative properties which were shown during clinical tests. The mechanical properties of the stent do not match the BRS, the materials are not FDA approved and the biocompatibility is questionable. In 2017, Ware *et al*. [54] used photopolymerisable materials that can be embedded using the micro CLIP method to print flexible BRS, meeting the requirements for precision biomedical devices. According to research [56], the Micro CLIP process has quite a few advantages over SLM. The stent fabrication time is reduced (it is possible to fabricate a stent of length 2 cm, with 4,000 layers in 26.5 minutes), the surface treatment is of better quality, the mechanical properties are unified and match Ni stents. In 2017, Cabrera *et al*. [55] printed a stent with Fused Deposition Modelling (FDM) as shown in Fig. 5. The printing device used was the Baker Bot by Replicator, the material was Thermo-Plastic Copolyester (TPC). The stent made in this way fused with the vessel wall in 8-16 weeks. Guerra *et al*. [56, 57] used the same technology the following year and used PCL for the material. The disadvantage of this stent was in the poor resolution, and many experiments performed. With this procedure, the process of 3D stent printing was researched thoroughly. Lei *et al*. [44] mentioned a combination of bio 3D printing and electro-bonding technology to form a poly (p-dioxanone) sliding stent (PPDO) for the inner layer with 3D printing and prepared a mixture of chitosan and poly- (vinyl alcohol) (PVA) for the outer layer with electrospinning and in this way planted the cells on the stent. Due to the natural biological material on the outer layer, cell adhesion and proliferation were good. In [44] the authors also described the development of a 4-axis 3D printing platform with FDM technology. An additional axle is added to the platform, namely a rotating spindle structure, so that it is possible to avoid the supporting structure and develop a set of mini screw extrusion nozzles. This nozzle uses granular biological material, and the diameter of the extruded wire is 100 μm. PCL and PLLA material were used to study the effects of rapid rate quenching and centrifugation on the mechanical properties of the stent and to optimise them.

The lumen diameter of an organ and stent length are two parameters defined, among many others. The design optimization of a stent and using the 3D printing technique allows a patient-specific personalization of the device.

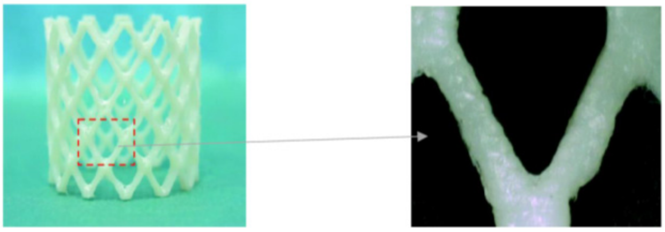

Fig. 5 3D printed FDM-stent [53]

Table 2 An overview of fabrication techniques for stent

	Wire winding	Injection and compression moulding process	Laser cutting	Additive manufacturing
Advantages	Widespread use of stents made in this way	• No visual defects, durable, offer flexibility • Fast production	• Fast processing • High accuracy	• Development of many different additive production techniques • High efficiency
Disadvantages	Difficulties in locating the weld	• Design restriction • Slow fabrication	• Thermal damage • Sharp edges • Incompatible for all material	• Poor surface accuracy • Long manufacturing process
Limitations	Only for stainless steel	• High requirements for moulds	• Heat load of the material	• Unsuitable for metal stent because of the oxidation problems • Nozzle diameter limitation
Prospects	For stainless steel	• Possibility of coating different material	• For all types of materials	• Possibility of individualization • Rapid prototyping
Economic aspect		• Low cost for tools	• High investment and operating costs	• Low cost

5. Conclusion

This research paper contains an overview of the development of the stents and the technology for their production. Different stent systems, new materials, metallic and polymeric, and bioresorbable stents can be traced in various studies. It will be challenging to discover an ideal stent suitable for all patients and their health problems. The lesion characteristics of individual patients, their age, their proneness to restenosis and thrombosis differ so much that it is difficult to produce a single device that would eliminate such a diverse spectrum of problems. The desire for the most qualified and useful stent, however, offers broad areas for further research.

Finding the stents' best manufacturing process has to be considered besides the stents' mechanical and medical properties. The stent industry needs to make continuous advances towards improving mechanical properties and reducing this medical device's costs by developing new production technologies. In this context, Additive Manufacturing techniques could be more economical than traditional laser micro-cutting used for manufacturing stents based on metallic materials. Nowadays, 3D printing could be an exciting manufacturing method to produce polymeric biomaterials, suitable for the latest generation of biodegradable stents applications. Further understanding and actualisation of those manufacturing methods are required in the field of Stent Technology.

Computational modelling is a valuable tool when evaluating stent mechanics and optimizing stent design. Finite element analysis (FEA) and computational fluid dynamics (CFD) are efficient methods to investigate and optimize a stent's mechanical behaviour virtually. FEA can help understand the role of the different geometrical and mechanical behaviour of the stents. Besides analysing stents' mechanical behaviour during the development process, these methods can be combined with special patient images to plan a surgery procedure.

The challenges associated with stents are numerous, like material, geometry, manufacturing process, biocompatibility, etc. Among the traditional design and manufacture, the most challenging is the development of a new generation of biodegradable materials, where medical devices function only during a specific period and then degrade.

Acknowledgements

The authors acknowledge the financial support of the Research Core Funding (No. P2-0063) from the Slovenian Research Agency and of the Research Program OP20-04332 which is co-financed by the Republic of Slovenia and the European Union under the European Structural and Investment Funds.

References

[1] Fogarotto, F. (2010). *Finite element analysis of coronary artery stenting*, Università degli Studi di Pavia Facoltà di Ingegneria, Pavia, Italy, from *http://www-2.unipv.it/compmech/dissertations/fogarotto.pdf*, accessed July 2020.

[2] McCormic, C. (2018). 1 – Overview of cardiovascular stent designs, In: Wall, J.G., Podbielska, H., Wawrzyńska, M. (eds.), *Finite element analysis of coronary artery stenting*, Elsevier, Duxford, UK, 3-26, doi: 10.1016/B978-0-08-100496-8.00001-9.

[3] Sigwart, U., Puel, J., Mirkovitch, V., Joffre, F., Kappenberger, L. (1987). *Intravascular stents to prevent occlusion and re-stenosis after transluminal angioplasty*, *The New England Journal of Medicine*, Vol. 316, No. 12, 701-706, doi: 10.1056/NEJM198703193161201.

[4] Rogers, C., Edelman, E.R. (1995). Endovascular stent design dictates experimental restenosis and thrombosis, *Circulation*, Vol. 91, No. 12, 2995-3001, doi:10.1161/01.CIR.91.12.2995.

[5] Schwartz, R.S., Chronos, N.A., Virmani, R. (2004). Preclinical restenosis models and drug-eluting stents: still important, still much to learn*, Journal of the American College of Cardiology,* Vol. 44, No. 7, 1373-1385, doi: 10.1016/j.jacc.2004.04.060.

[6] Morton, A.C., Crossman, D., Gunn, J. (2004). The influence of physical stent parameters upon restenosis, *Pathologie Biologie*, Vol. 52, No. 4, 196-205, doi: 10.1016/j.patbio.2004.03.013.

[7] Pache, J., Kastrati, A., Mehilli, J., Schühlen, H., Dotzer, F., Hausleiter, J., Fleckenstein, M., Neumann F.-J., Sattelberger, U., Schmitt, C., Müller, M., Dirschinger, J., Schömig, A. (2003). Intracoronary stenting and angiographic results. Strut thickness effect on restenosis outcome (ISAR-STEREO-2) trial, *Journal of the American College of Cardiology,* Vol. 41, No. 8, 1283-1288, doi: 10.1016/S0735-1097(03)00119-0.

[8] Jayendiran, R., Nour, B., Ruimi, A. (2018). Fluid-structure interaction (FSI) analysis of stent-graft for aortic endovascular aneurysm repair (EVAR): Material and structural considerations, *Material and structural considerations,* Vol. 87, 95-110, doi: 10.1016/j.jmbbm. 2018.07.020.

[9] O'Brien, B., Carroll, W. (2009). The evolution of cardiovascular stent materials and surfaces in response to clinical drivers: A review, *Acta Biomaterialia*, Vol. 5, No. 4, 945-958, doi: 10.1016/j.actbio.2008.11.012.

[10] Bertrand, O.F., Sipehia, R., Mongrain, R., Rodés, J., Tardif, J.-C., Bilodeau, L., Côté, G., Bourassa, M.G. (1998). Biocompatibility aspects of new stent technology, *Journal of the American College of Cardiology*, Vol. 32, No. 3, 562-571, doi: 10.1016/S0735-1097(98)00289-7.

[11] Mani, G., Feldman, M.D., Patel, D., Agrawal, C.M. (2007). Coronary stents: A materials perspective, *Biomaterials*, Vol. 28, No. 9, 1689-1710, doi: 10.1016/j.biomaterials.2006.11.042.

[12] Pache, J., Dibra, A., Mehilli, J., Dirschinger, J., Schömig, A., Kastrati, A. (2005). Drug-eluting stents compared with thin-strut bare stents for the reduction of restenosis: A prospective, randomized trial, *European Heart Journal,* Vol. 26, No. 13, 1262-1268, doi: 10.1093/eurheartj/ehi098.

[13] Htay, T., Liu, M.W. (2005). Drug-eluting stent: A review and update, *Vascular Health and Risk Management*, Vol. 1, No. 4, 263-276, doi: 10.2147/vhrm.2005.1.4.263.

[14] Yang, C., Burt, H.M. (2006). Drug-eluting stents: factors governing local pharmacokinetics, *Advanced Drug Delivery Reviews,* Vol. 58, No. 3, 402-411, doi: 10.1016/j.addr.2006.01.017.

[15] Sotomi, Y., Onuma, Y., Collet, C., Tenekecioglu, E., Virmani, R., Kleiman, N.S., Serruys, P.W. (2017). Bioresorbable scaffold: the emerging reality and future directions, *Circulation Research,* Vol. 120, No. 8, 1341-1352, doi: 10.1161/CIRCRESAHA.117.310275.

[16] Venkatraman, S., Boey, F. (2007). Release profiles in drug-eluting stents: Issues and uncertainties, *Journal of Controlled Release,* Vol. 120, No. 3, 149-160, doi: 10.1016/j.jconrel.2007.04.022.

[17] Commandeur, S., van Beusekom, H.M.M., van der Giessen, W.J. (2006). Polymers, drug release, and drug-eluting stents, *Journal of Interventional Cardiology,* Vol.19, No. 6, 500-506, doi: 10.1111/j.1540-8183.2006.00198.x.

[18] Joner, M., Finn, A.V., Farb, A., Mont, E.K., Kolodgie, F.D., Ladich, E., Kutys, R., Skorija, K., Gold, H.K., Virmani, R. (2006). Pathology of drug-eluting stents in humans: Delayed healing and late thrombotic risk*, Journal of the American College of Cardiology*, Vol. 48, No. 1, 193-202, doi: 10.1016/j.jacc.2006.03.042.

[19] Garcia-Touchard, A., Burke, S.E., Toner, J.L., Cromack, K., Schwartz, R.S. (2006). Zotarolimus-eluting stents reduce experimental coronary artery neointimal hyperplasia after 4 weeks, *European Heart Journal,* Vol. 27, No. 8, 988-993, doi: 10.1093/eurheartj/ehi752.

[20] Brugaletta, S., Burzotta, F., Sabaté, M. (2009). Zotarolimus for the treatment of coronary artery disease: Pathophysiology, DES design, clinical evaluation and future perspective, *Expert Opinion on Pharmacotherapy,* Vol. 10, No. 6, 1047-1058, doi: 10.1517/14656560902837998.

[21] Byrne, R.A., Joner, M., Kastrati, A. (2009). Polymer coatings and delayed arterial healing following drug-eluting stent implantation, *Minerva Cardioangiologica*, Vol. 57, No. 5, 567-584.

[22] Finkelstein, A., McClean, D., Kar, S., Takizawa, K., Varghese, K., Baek, N., Park, K., Fishbein, M.C., Makkar, R., Litvack, F., Eigler, N.L. (2003). Local drug delivery via a coronary stent with programmable release pharmacokinetics, *Circulation*, Vol. 107 No. 5, 777-784, doi: 10.1161/01.CIR.0000050367.65079.71.

[23] Alexis, F., Venkatraman, S.S., Rath, S.K., Boey, F. (2004). In vitro study of release mechanisms of paclitaxel and rapamycin from drug-incorporated biodegradable stent matrices*, Journal of Controlled Release,* Vol. 98, No. 1, 67-74, doi: 10.1016/j.jconrel.2004.04.011.

[24] Falotico, R., Parker, T., Grishaber, R., Price, S., Cohen, S.A., Rogers, C. (2009). NEVO™: A new generation of sirolimus-eluting coronary stent, *EuroIntervention*, Vol. 5 (Supplement F), F88-F93.

[25] Stefanini, G.G., Byrne, R.A., Serruys, P.W., de Waha, A., Meier, B., Massberg, S., Jüni, P., Schömig, A., Windecker, S., Kastrati, A. (2012). Biodegradable polymer drug-eluting stents reduce the risk of stent thrombosis at 4 years in patients undergoing percutaneous coronary intervention: A pooled analysis of individual patient data from the ISAR-TEST 3, ISAR-TEST 4, and LEADERS randomized trials, *European Heart Journal*, Vol. 33, No. 10, 1214-1222, doi: 10.1093/eurheartj/ehs086.

[26] O'Brien, B., Zafar, H., Ibrahim, A., Zafar, J., Sharif, F. (2016). Coronary stent materials and coatings: A technology and performance update, *Annals of Biomedical Engineering*, Vol. 44, No. 2, 523-535, doi: 10.1007/s10439-015-1380-x.

[27] Wessely, R., Hausleiter, J., Michaelis, C., Jaschke, B., Vogeser, M., Milz, S., Behnisch, B., Schratzenstaller, T., Renke-Gluszko, M., Stöver, E., Wintermantel, E., Kastrati, A., Schömig, A. (2005). Inhibition of neointima formation by a novel drug-eluting stent system that allows for dose-adjustable, multiple, and on-site stent coating, *Arteriosclerosis, Thrombosis, and Vascular Biology*, Vol. 25, No. 4, 748-753, doi: 10.1161/01.ATV.0000157579.52566.ee.

[28] Dibra, A., Kastrati, A., Mehilli, J., Pache, J., von Oepen, R., Dirschinger, J., Schömig, A. (2005). Influence of stent surface topography on the outcomes of patients undergoing coronary stenting: A randomized double-blind controlled trial, *Catheterization & Cardiovascular Interventions,* Vol. 65, No. 3, 374-380, doi: 10.1002/ccd.20400.

[29] Demidov, V., Currie, D., Wen, J. (2017). Patent watch: Patent insight into polymer-free drug-eluting stents, *Nature Reviews Drug Discovery*, Vol. 16, No. 4, 230-231, doi: 10.1038/nrd.2017.32.

[30] Schwartz, R.S., Chronos, N.A., Virmani, R. (2004). Preclinical restenosis models and drug-eluting stents: Still important, still much to learn, *Journal of the American College of Cardiology*, Vol. 44, No. 7, 1373-1385, doi: 10.1016/j.jacc.2004.04.060.

[31] Ormiston, J.A., Serruys, P.W., Regar E., Dudek, D., Thuesen, L., Webster, M.W.I., Onuma, Y., Garcia-Garcia, H.M., McGreevy, R. (2008). A bioabsorbable everolimus-eluting coronary stent system for patients with single de-novo coronary artery lesions (ABSORB): A prospective open-label trial, *The Lancet*, Vol. 371, No. 9616, 899-907, doi: 10.1016/S0140-6736(08)60415-8.

[32] Onuma, Y., Serruys, P.W., Perkins, L.E.L., Okamura, T., Gonzalo, N., García-García, H.M., Regar, E., Kamberi, M., Powers, J.C., Rapoza, R., van Beusekom, H., van der Giessen, W., Virmani, R. (2010). Intracoronary optical coherence tomography and histology at 1 month and 2, 3, and 4 years after implantation of everolimus-eluting bioresorbable vascular scaffolds in a porcine coronary artery model: An attempt to decipher the human optical coherence tomography images in the ABSORB trial, *Circulation*, Vol. 122, No. 22, 2288-2300, doi: 10.1161/ CIRCULATIONAHA.109.921528.

[33] Alexy, R.D., Levi, D.S. (2013). Materials and manufacturing technologies available for production of a pediatric bioabsorbable stent, *BioMed Research International*, Vol. 2013, Article ID 137985, doi: 10.1155/2013/137985.

[34] Beshchasna, N., Saqib, M., Kraskiewicz, H., Wasyluk, Ł., Kuzmin, O., Duta, O.C., Ficai, D., Ghizdavet, Z., Marin, A., Ficai, A., Sun, Z., Pichugin, V.F., Opitz, J., Andronescu, E. (2020). Recent advances in manufacturing innovative stents, *Pharmaceutics*, Vol. 12, No. 4, 349, doi: /10.3390/pharmaceutics12040349.

[35] Peuster, M., Wohlsein, P., Brügmann, M., Ehlerding, M., Seidler, K., Fink, C., Brauer, H., Fischer, A., Hausdorf, G. (2001). A novel approach to temporary stenting: Degradable cardiovascular stents produced from corrodible metal – results 6-18 months after implantation into New Zealand white rabbits*, Heart*, Vol. 86, No. 5, 563-569, doi: 10.1136/heart.86.5.563.

[36] Huang, T., Cheng, J., Zheng, Y.F. (2014). In vitro degradation and biocompatibility of Fe-Pd and Fe-Pt composites fabricated by spark plasma sintering, *Material Science and Engineering: C*, Vol. 35, 43-53, doi: 10.1016/j.msec. 2013.10.023.

[37] Bowen, P.K., Drelich, J., Goldman, J. (2013). Zinc exhibits ideal physiological corrosion behavior for bioabsorbable stents, *Advanced Materials*, Vol. 25. No. 18, 2577-2582, doi: 10.1002/adma.201300226.

[38] Pierson, D., Edick, J., Tauscher, A., Pokorney, E., Bowen, P., Gelbaugh, J., Stinson, J., Getty, H., Lee, C.H., Drelich, J., Goldman, J. (2012). A simplified *in vivo* approach for evaluating the bioabsorbable behavior of candidate stent materials, *Journal Biomedicine Materials and Research*, Vol. 100B, No. 1, 58-67, doi: 10.1002/jbm.b.31922.

[39] Erbel, R., Di Mario, C., Bartunek, J., Bonnier, J., de Bruyne, B., Eberli, F., Erne, P., Haude, M., Heublein, B., Horrigan, M., Ilsley, C., Böse D., Koolen, J., Lüscher, T.F., Weissman, N., Waksman, R. (2007). Temporary scaffolding of coronary arteries with bioabsorbable magnesium stents: a prospective, non-randomised multicentre trial, *The Lancet*, Vol. 369, No. 9576, 1869-1875, doi: 10.1016/S0140-6736(07)60853-8.

[40] Su, Y., Cockerill, I., Wang, Y., Qin, Y.-X., Chang, L., Zheng, Y., Zhu, D. (2019). Zinc-based biomaterials for regeneration and therapy, *Trends in Biotechnology*, Vol. 37, No. 4, 428-441, doi: 10.1016/j.tibtech.2018.10.009.

[41] Yang, H., Wang, C., Liu, C., Chen, H., Wu, Y., Han, J., Jia, Z., Lin, W., Zhang, D., Li, W., Yuan, W., Guo, H., Li, H., Yang, G., Kong, D., Zhu, D., Takashima, K., Ruan, L., Nie, J., Li, X., Zheng, Y. (2017). Evolution of the degradation mechanism of pure zinc stent in the one-year study of rabbit abdominal aorta model, *Biomaterials*, Vol. 145, 92-105, doi: 10.1016/j.biomaterials.2017.08.022.

[42] Bowen, P.K., Shearier, E.R., Zhao, S., Guillory 2nd, R.J., Zhao, F., Goldman, J., Drelich, J.W. (2016). Biodegradable metals for cardiovascular stents: From clinical concerns to recent Zn-alloys, *Advanced Healthare Materials*, Vol. 5, No. 10, 1121-1140, doi: 10.1002/adhm.201501019.

[43] Zhu, D., Su, Y., Zheng, Y., Fu, B., Tang, L., Qin, Y.-X. (2018). Zinc regulates vascular endothelial cell activity through zinc-sensing receptor ZnR/GPR39, *American Journal of Physiology – Cell Physiology,* Vol. 314, No. 4, C404-C414, doi: 10.1152/ajpcell.00279.2017.

[44] Lei, Y., Chen, X., Li, Z., Zhang, L., Sun, W., Li, L., Tang, F. (2020). A new process for customized patient-specific aortic stent graft using 3D printing technique, *Medical Engineering and Physics*, Vol. 77, 80-87, doi: 10.1016/j.medengphy.2019.12.002.

[45] Yang, L., Chen, X., Zhang, L., Li, L., Kang, S., Wang, C., Sun, W. (2019). Additive manufacturing in vascular stent fabrication, *MATEC Web of Conf., 2018 International Conference on Materials Science and Manufacturing Engineering*, Vol. 253, Article number 03003, doi: 10.1051/matecconf/201925303003.

[46] Zhang, L., Chen, X., Liu, M. (2017). Research of customized aortic stent graft manufacture, *IOP Conference Series: Materials Science and Engineering*, Vol. 187, 012027, doi: 10.1088/1757-899x/187/1/012027.

[47] Huang, B., Gale, D.C., Gale, Hossainy, S.F.A. (2011). Fabricating polymer stents with injection molding, Patent Application Publication, No. US 2011/0169197 A1.

[48] Guerra, A.J., Ciurana, J. (2018). Stent's manufacturing field: Past, present, and future prospects, In: *Angiography*, Amukçu, B. (ed.), IntechOpen, 41-60, doi: 10.5772/intechopen.81668.

[49] Flege, C., Vogt, F., Höges, S., Jauer, L., Borinski, M., Schulte, V.A., Hoffmann, R., Poprawe, R., Meiners, W., Jobmann, M., Wissenbach, K., Blindt, R. (2013). Development and characterization of a coronary polylactic acid stent prototype generated by selective laser melting, *Journal of Materials Science: Materials in Medicine*, Vol. 24, No. 1, 241-255, doi: 10.1007/s10856-012-4779-z.

[50] Finazzi, V., Demir, A.G., Biffi, C.A., Chiastra, C., Migliavacca, F., Petrini, L., Previtali, B. (2019). Design rules for producing cardiovascular stents by selective laser melting: Geometrical constraints and opportunities*, Procedia Structural Integrity.* Vol. 15, 16-23, doi: 10.1016/j.prostr.2019.07.004.

[51] Park, S.A., Lee, S.J., Lim, K.S., Bae, I.H., Lee, J.H., Kim, W.D., Jeon, M.H., Park, J.-K. (2015). *In vivo* evaluation and characterization of a bio-absorbable drug-coated stent fabricated using a 3D-printing system, *Materials Letters*, Vol. 141, 355-358, doi: 10.1016/j.matlet.2014.11.119.

[52] Tumbleston, J.R., Shirvanyants, D., Ermoshkin, N., Janusziewicz, R., Johnson, A.R., Kelly, D., Chen, K., Pinschmidt, R., Rolland, J.P., Ermoshkin, A., Samulski, E.T., DeSimone, J.M. (2015). Additive manufacturing. Continuous liquid interface production of 3D objects, *Science,* Vol. 347, No. 6228, 1349-1352, doi: 10.1126/science.aaa2397.

[53] van Lith, R., Baker, E., Ware, H., Yang, J., Farsheed, A.C., Sun, C., Ameer, G. (2017). 3D-printing strong high-resolution antioxidant bioresorbable vascular stents, *Advanced Materials Technologies*, Vol. 1, No. 9, doi: 10.1002/admt.201600138.

[54] Ware, H.O.T., Farsheed, A.C., van Lith, R., Baker, E., Ameer, G., Sun. C. (2017). Process development for high-resolution 3D-printing of bioresorbable vascular stents, In: *Proceedings Volume 10115, Advanced Fabrication Technologies for Micro/Nano Optics and Photonics X*, SPIE OPTO, 2017, San Francisco, California, USA, doi: 10.1117/12.2252856.

[55] Cabrera, M.S., Sanders, B., Goor, O.J.G.M., Driessen-Mol, A., Oomens, C.W.J., Baaijens, F.P.T. (2017). Computationally designed 3D printed self-expandable polymer stents with biodegradation capacity for minimally invasive heart valve implantation: A proof-of-concept study, *3D Printing and Additive Manufacturing*, Vol. 4, No. 1, 19-29, doi: 10.1089/3dp.2016.0052.

[56] Guerra, A.J., Ciurana, J. (2017). 3D-printed bioabsordable polycaprolactone stent: The effect of process parameters on its physical features, *Materials & Design*, Vol. 137, 430-437, doi: 10.1016/j.matdes.2017.10.045.

[57] Guerra, A., Roca, A., de Ciurana, J. (2017). A novel 3D additive manufacturing machine to biodegradable stents, Procedia Manufacturing, Vol. 13, 718-723, doi: 10.1016/j.promfg.2017.09.118.

APEM journal

Advances in Production Engineering & Management
Volume 15 | Number 4 | December 2020 | pp 403–415
https://doi.org/10.14743/apem2020.4.374

ISSN 1854-6250
Journal home: apem-journal.org
Original scientific paper

High-speed machining parametric optimization of 15CDV6 HSLA steel under minimum quantity and flood lubrication

Khawaja, A.H.[a,*]**, Jahanzaib, M.**[b]**, Cheema, T.A.**[c]

[a]Department of Mechanical Engineering, University of Engineering and Technology, Taxila, Pakistan
[b]Department of Industrial Engineering, University of Engineering and Technology, Taxila, Pakistan
[c]Department of Mechanical Engineering, GIK Institute of Engineering Sciences, Topi, Pakistan

A B S T R A C T

High-speed machining (HSM) maintains a high interest in the preparation of metal parts for optimum results, but with the application of HSM, the sustainability issue becomes important. To overcome the problem, minimum quantity lubrication (MQL) during HSM is one of the innovative and challenging tasks during conventional cutting (milling) to improve quality, productivity, and strength under the umbrella of sustainability. The objective of this research is to achieve sustainable machining by simultaneously optimizing sustainable machining drivers during the HSM of 15CDV6 HSLA steel under MQL and flood lubrication. The response surface methodology has been applied for the development of mathematical models and selecting the best combination of process parameters to optimized responses, i.e. surface roughness, material removal rate, and strength. Optimization associated with sustainability produced compromising optimal results (Min. *Ra* 0.131 µm, Max. *MRR* 0.64 cm^3/min, and Max. *ST* 1132 MPa) at the highest cutting speed 270 m/min and the lowest feed rate 0.09 mm/rev and depth of cut 0.15 mm under MQL. The comparative investigation exposed that significant improvement in *Ra* (1.1-16.6 %) and *ST* (1.3-2.3 %) of the material using MQL has been witnessed and gives a strong indication that MQL is the best substitute than the flood lubrication. The scientific contribution of the approach is to develop mathematical models under MQL and flood lubrication that will aid practitioners to choose input parameters for desired responses without experimentations. The work would be beneficial in the field of aviation, defense, and aeronautical applications due to the excellent mechanical properties of 15CDV6 HSLA steel.

A R T I C L E   I N F O

Keywords:
High-speed machining;
Milling;
HSLA steel;
Chromium-molybdenum-vanadium steel (15CDV6);
Minimum quantity lubrication;
Optimization;
Sustainability

**Corresponding author:*
amar.khawaja@students.uettaxila.edu.pk
(Khawaja, A.H.)

Article history:
Received 3 August 2020
Revised 28 November 2020
Accepted 3 December 2020

1. Introduction

The minimization of surface roughness and maximization of material removal rate may not be possible through non-conventional techniques, due to these limitations conventional machining (HSM) is preferred and has been used to improve the quality and productivity. High-speed machining is known in the advanced and emerging machining process increasingly used for innovative materials such as high strength low alloys to produce complex parts with improved quality (minimum surface roughness), high productivity (maximum material removal rate), sustainability, and economy [1]. High-speed machining (HSM) is defined as machining at higher cutting speed than conventional machining to enhance productivity without compromising quality. The range of HSM depends on the properties of material, i.e. thermal conductivity, material strength, alloying composition, microstructure, and cutting conditions [2, 3].

The influence of cutting conditions during high-speed machining has a great impact on heat generation that causes surface variation and early failure of the tool. Cutting fluids in the form of MQL and flood are used to reduce the generated heat and friction between the tool and chip through lubricating effect. The cutting fluid has a significant influence on material surface roughness, productivity, strength, tool life, and dimensional accuracies. The use of cutting fluid can be ineffective in reducing generated heat during HSM because of high spatial stress and high temperatures, it is difficult to obtain cutting fluid from the secondary contact zone. Furthermore, dry machining may not always be economically feasible due to its limited ability to withstand tools at high temperatures and perform effectively. As such, bridging technology is essential so that the cutting fluid requirements can be partially met without negotiating the environment. The most reliable and promising bridging technology between flood and dry is minimum quantity lubrication that minimizes the use of cutting fluid and improves sustainability.

The objective of this research is to achieve sustainable machining by simultaneously optimizing sustainable machining drivers during high-speed machining of 15CDV6 HSLA steel under MQL and flood lubrication.

2. Literature review

Sustainability achievement during high-speed machining is a key interest nowadays. Industrial trends are moving from conventional to sustainable manufacturing paradigms. Such reforms are a result of sicknesses found in laborers at the shop floor, a prerequisite of manufacturing cost reduction, and government policies for ecological safety [4]. Cutting fluids are dangerous to health and the environment. The environmental effects of cutting fluid contain waste disposal, the release of hazardous ingredients into the atmosphere and harmful working circumstances for the workers usually causes inhalation and skin disease. To overcome these problems scholars, have annoyed machining without using cutting fluid (dry machining). Wherever the whole exclusion of cutting fluid is not likely, a very minute quantity of lubrication is used, called minimum quantity lubrication (sustainable approach) [5].

Various researchers studied the effect of lubrication modes and process parameters like cutting speed (C_S), feed rate (F_R), depth of cut (D_C) on surface roughness (*Ra*), material removal rate (*MRR*), and strength (*ST*) of the material during high-speed machining using minimum quantity lubrication. Gunda *et al.* [6] studied the sustainability aspects during machining of stainless steel using MQL, dry, and flood lubrication modes and found that MQL gives a better surface finish as compared to dry and flood. Yildirim *et al.* [7, 8] investigated the effect of machining factors and cooling methods (dry, wet, and MQL) on *Ra*, tool life, and wear during HSM of nickel-based alloys. The results showed that MQL machining provided improvement in *Ra* and tool wear when compared to dry and wet machining. The MQL system is recommended during the milling of nickel-based alloys by considering economics, environment, and worker health. Mia *et al.* [9] studied the milling process of AISI 4140 hardened steel to optimize the parameters and fluid flow rate for minimum Ra and cutting force. Response surface methodology has been applied for experimental design and ANOVA was utilized for analysis of results. It was concluded that *Ra* was significantly affected by fluid flow rate and 150ml/h is the optimum value for minimum *Ra*. Khan *et al.* [10] examined the influence of process parameters and MQL on *Ra*, *MRR*, and energy consumption during milling of AISI 1045 steel. It was shown that lower C_S and higher width of cut were appropriate for energy efficiency with nano MQL. Nguyen *et al.* [11] optimized the machining parameters and tool geometry for minimum *Ra*, specific cutting energy, and higher *MRR*. The archive-based micro GA was employed for the determination of optimal parameters combination. The results showed that *Ra* and cutting energy is substantially affected by D_C. Further, it recommended that higher parametric values produced lower cutting energy and improved *MRR*.

Borojevic *et al.* [12] examined the influence of process parameters during milling of Al 7075 thin-walled structures. Central composite design technique in RSM was employed for the optimization of parameters. The experimental results were verified by calculated optimal values and demonstrate a satisfactory fitting. Songmei *et al*. [13] explored the effect of nano-enhanced lubricants and machining parameters (C_S, F_R, and D_C) during the milling of titanium alloy using Taguchi method. The findings confirmed that milling force was significantly influenced by type and concentration of nanoparticles, D_C, and F_R as compared to surface roughness. Liao and Lin [14] investigated HSM of hardened steel (NAK80) under MQL and dry environment. The aim was to explore the process of MQL in HSM of hardened steel and to obtain the optimal parameters combination for optimal *Ra*, cutting force, and tool life. It was found that MQL gives better results than dry cutting during HSM. Hamdan *et al*. [15] investigated the HSM of AISI 304 steel to optimize process parameters for minimum *Ra* and cutting force as well as high *MRR* during dry, MQL, and flood lubrication modes. For experimental design, RSM was applied to optimize the parameters combination and ANOVA was used to investigate the results. It was concluded that an improvement of 41.3 % *Ra* with a 25.5 % reduction in cutting force was produced with MQL lubrication mode, also revealed that D_C is the utmost substantial factor for getting the anticipated *MRR* while reducing the value of *Ra*. Zhenchao *et al*. [16] experimentally studied the HSM of 16Co14Ni10Cr2Mo HSLA steel to establish the impact of milling parameters on surface integrity using the MQL technique. It was concluded that with the increase of C_S and F_R *Ra* value increases and residual stresses increase with C_S, D_C, and F_R. Feed was the most substantial factor that affects the stresses. Begic-Hajdarevic *et al*. [17] studied HSM of hardened X37CrMoV5-1 tool steel to govern the impact of operational parameters on *Ra* using 20mm and 40mm diameter tools. It was established that the increase of C_S, *Ra* decreases and increases by the increase of F_R, and the improved surface is achieved at a larger diameter tool. Motorcu *et al*. [18] investigated the impacts of C_S, number of inserts, milling direction and coating layer on surface layer and tool life of Inconel 718 during milling process using Taguchi method. The results showed that *Ra* significantly affected by cutting tool coating.

Cutting fluids are used to reduce the generated heat during HSM, and friction between the tool and chip through lubricating effect. The cutting fluid has a significant impact on material *Ra*, productivity, strength, residual stress, tool life, and dimensional accuracies. The expense of cutting fluids and their administration framework can go up to 16-20 % of the absolute expense of the machined part [19]. Cutting fluids are applied in the machining process in many ways such as flood and minimum quantity. In the flood lubrication large volume (10-100 liters per minute) of fluid continuously applied during machining while in minimum quantity lubrication (2-15 ml/min) CF is applied in the form of mist or fog [5]. The advantages of using MQL improves surface quality, better safety characteristics, eco-friendly, and reduces machining cost [5, 20-22]. E. Benedicto *et al*. [23] analyzed the use of cutting fluids and main alternatives (dry, MQL, cryogenic, nanofluids) during machining. Especially, the examination was done concentrating on technical, economic, and environmental points. The best ecological option is dry machining since it totally expels the cutting fluid and guarantees a clean atmosphere and laborers security, however, it has numerous application impediments. To actualize this option is important to have thorough control of the cutting parameters and a reasonable tool choice. MQL framework lessens the utilization of the liquid and is a progressively feasible option considering the environmental, social, and economic effects as well as the performance.

The main pillars of sustainability are technical, environment, society, and economy [5, 20, 21, 23, 24]. The sustainable machining model of the current research is shown in Fig. 7. The key drivers that sustain these pillars are resource efficiency, a clean and green environment that incorporates effective waste reduction and management, and cost-effective production. In the domain of high-speed machining, resource efficiency can be incorporated by minimum surface roughness, a clean and green environment by reducing lubrication amounts by employing minimum quantity lubrication, and cost-effectiveness using machining productivity (material removal rate). The main limitation to achieve sustainability in machining is to simultaneously address these drivers. For instance, by increasing cost-effectiveness (*MRR*), resource efficiency (surface roughness) decreases. This problem of sustainability achievement becomes more challenging in the case of machining at higher speeds (also called high-speed machining).

The detailed review of the literature highlighted that various studies have been carried out to optimize individual performance measures including surface roughness, material removal rate, and strength. However, little or no research work has been reported to simultaneously optimize performance measures affecting key sustainable machining drivers during high-speed machining. Hence, this research aims to achieve sustainable machining by simultaneously optimizing sustainable machining drivers during high-speed machining of 15CDV6 HSLA steel under MQL and flood lubrication. 15CDV6 HSLA steel has been considered as a research candidate as it possesses excellent mechanical and heat resistant properties which make it suitable for making rocket booster, rocket motor casing, and suspension components. The response surface methodology was applied for the development of mathematical models and selecting the best combination of process parameters to optimized responses, i.e. surface roughness, material removal rate, and strength. Besides, sustainability has been achieved keeping desirability function-based multi-objective optimization.

3. Materials, methods, and experimental procedure

This section briefly explains the description of predictors, the experimental setup including CNC machining, and response measurements.

3.1 Material selection

Due to excellent mechanical properties like high strength to weight ratio, toughness, yield strength, and weldability 15CDV6 HSLA steel is selected as a research candidate mostly used in the aeronautical, defense, and aviation industry with applications in rocket motor casing, rocket booster, suspension components, pressure vessels, and many others. The 15CDV6 is a low carbon chromium-molybdenum-vanadium high strength low alloy steel containing the concentration of carbon (0.15 %), chromium (1-5 %), and the concentration of molybdenum and vanadium are less than 1.5 % each and weight proportion of all the alloying elements combined is less than 5 % [25]. The chemical composition of the material was analyzed with the XRF analyzer and wet analysis method as given in table 1.

Table 1 Chemical composition (wt %) of 15CDV6 HSLA steel

C	Si	P	S	Mn	Cr	Mo	V	Fe
0.15	0.15	0.016	0.012	0.87	1.33	0.84	0.24	96.392

3.2 Method selection

Face milling was selected as a machining process under a sustainable environment during high-speed. The experiments were performed under the framework of face milling because it gives a better surface finish as well as high productivity.

A total of 40 experimental runs were performed to collect the experimental data, twenty experiments using MQL through a controlled coolant flow of 15 ml/min, and 6 bars pressure while twenty with flood coolant flow of 100 l/min. The following four predictor variables (C_S, F_R, D_C, Lubrication mode) were controlled in the experiments:

- Process parameters: Cutting speed, feed rate, and depth of cut;
- Lubrication mode: Minimum quantity lubrication (MQL) and flood lubrication (FL).

The 3-controlled variables with cooling mode, central composite design (CCD) technique was used for the design of experiments. The CCD in RSM is a very efficient design for fitting the second-order model. Two parameters in the design must be specified: the distance α of the axial runs from the design center and the number of center points n_c. In this study, twenty ($2^n + 2n + 2n_c$, n is the number of input parameters, including eight factorial points 2^n, six axial points $2n$ and six center points $2n_c$) design points for each MQL and flood were considered for experimentation with six-star points [26]. The complete DOE with experiment runs, input variables, and responses have been presented in table 4 for MQL and flood lubrication.

3.3 Experimental procedure

After the confirmation of composition, the material was cut from a bigger plate of 40 mm thickness to block size 150×120 mm using a bandsaw machine for heat treatment.

The material was heat treated to the required hardness value of 39 ± 2 HRC [27], the procedure given in table 2. The hardness was measured using a Universal hardness tester with a diamond indenter.

Table 2 Heat treatment parameters

Austenzing		Quenching			Tempering		Cooling
Temp (°C)	Time (min)	Medium	Temp (°C)	Time (min)	Temp (°C)	Time (min)	Medium
600 700 960	45 10 60	PSO Oil No. 10	30	30	650	120	Air cool to 39HRC

The input process parameters such as C_S, F_R, and D_C are selected due to their significant impact on responses which are surface roughness, material removal rate, and strength of the material. The objective is to optimize input parameters to achieve the desired value of performance measurements. The levels of input process parameters during HSM of HSLA steel were selected after the detailed literature survey, pilot run, and expert's opinion as given in table 3. The recommended threshold values mostly dependent on C_S, F_R, D_C, and lubrication mode. The range of cutting speed during HSM (210 m/min < cutting speed < 360 m/min) [28] and for steel materials having hardness value 39HRC-48HRC (cutting speed > 150 m/min for rough cutting and cutting speed < 350 m/min for finish cutting) (Sandvik).

Table 3 Levels of input process parameters

Cutting parameters	Levels		
	Low	Middle	High
Cutting speed, C_S (m/min)	200	235	270
Feed rate, F_R (mm/rev)	0.08	0.10	0.12
Depth of cut, D_C (mm)	0.1	0.2	0.3

Before running the actual experimental runs, initially, the material was cut from a bigger plate of 40 mm thickness using a bandsaw machine in a 150×120 mm block. The block was then split into 04 parts of 10 mm thickness each on the wire-cut along with the thickness such that the final size of the blocks was 150×120×10 mm each. Now each block is further split into half from the 150mm length, so the final dimensions of each block become 120×75×10 mm (08 blocks). Now, each of the blocks was held on the CNC Milling machine vice, dialled and faced from one side and then the cavity for the tensile sample is machined out overall 75mm length as per the drawing taking the center of 120 mm length. A similar process was carried out on the other side of the block to give it a proper shape of the tensile sample. The same way all 08 blocks were machined. The sides of each block were faced to 100mm length and the block dimension becomes 75×100×10 mm with a proper sample shape. The blocks were engaged to wire cut again for slicing them into 10×100×10 mm sample sizes (05 from each block). Now, tensile sample preparation is completed in final dimensions according to ASTM E-8M-04 standard except the thickness that is 10mm which gives us a margin for experimentation.

Now, high-speed milling of 15CDV6 HSLA steel was performed during MQL and flood lubrication using a CoroMill 290 Square Shoulder Milling Cutter (R290-040A32-12L) attached multi-layer tungsten carbide inserts (TiCN+Al2O3+TiN) having 0.8 mm nose radius to achieve the high surface finish. The MQL apparatus (Model: LXL-210-2L) was attached outside the machine and the nozzle was adjusted near the tool so that mist can be thrown out on the cutting zone. The following parameters were selected for nozzle position; spray distance from the nozzle to the tool-tip 9 mm, nozzle diameter 3 mm as shown in Fig. 1b [29], fluid flow rate 15 ml/min, a compressor is attached outside the MQL setup which produces air pressure of 6 bars. The flow rate was controlled through an adjustable screw (point A) attached to the MQL pump. The range of MQL setup is 0.03-0.3 ml/s. Finally, at the mist line small quantity of fluid (15 ml/min) mixed with compressed air flow (6 bars) resulting to produce mist or fog that is delivered to the cutting zone. The experimental setup has been shown in Fig. 1. Initially, the MQL setup was calibrated, followed by special care, and after each experiment, it was ensured that proper mist was delivered to the cutting zone. Pakistan state oil (PSO) neat metal cutting oil was used for lubrication in MQL and flood machining because of good thermal stability, environmentally acceptable, rust-free and provides good surface finishes.

Now, each sample was held on a machine vice on the CNC milling machine (DAHLIH MCV-720) and dialled to keep them perpendicular to the tool axis. The sample was firstly faced to provide a good surface for experimental precise depth of cut value (final thickness 6mm). Each experiment was carried out on a separate sample as per the DOE has given in table 4. Twenty experiments were carried out using MQL through a controlled coolant flow of 15 ml/min and 6 bar pressure while twenty were carried out with flood coolant flow of 100 l/min [30, 31]. The machine tool coolant pump (TUAN LU-China) specifications are as under; (Model: YLP-900MFWD, flow rate 180 l/min (maximum).

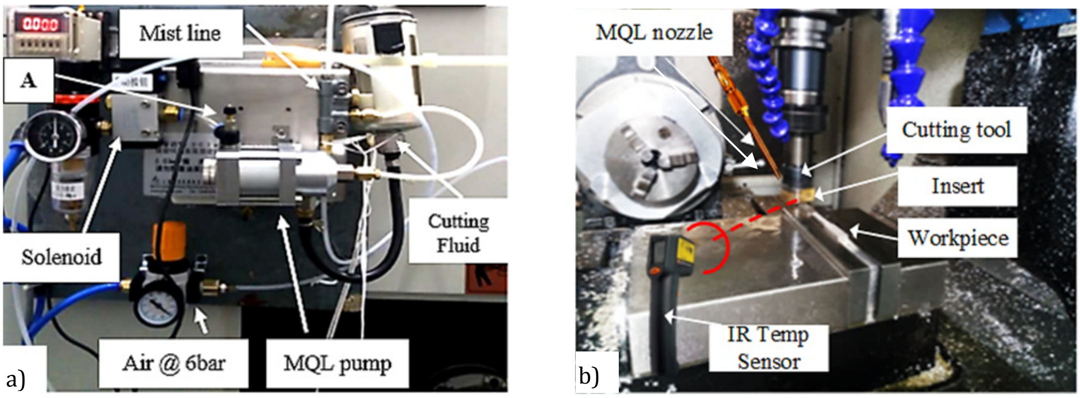

Fig. 1 Experimental setup: a) MQL setup, b) CNC machining

3.4 The responses

During each experimental run following responses were measured:

1. Surface roughness (μm): The *Ra* is a part of the surface texture and measured by the deviation in the direction of the normal surface vector, if the deviation is large, the surface rough otherwise the surface is smooth. The surface roughness of each experimental run during MQL and flood lubrication was measured using Mitutoyo SJ-410 surface roughness measuring apparatus and values recorded.

2. Material removal rate (cm^3/min): The *MRR* was calculated as the volume of material removed per unit time (cm^3/min), which is productivity. It has been measured for each sample using the weight-loss method. Each machined sample was weighed before and after the experimentation using a weight balance machine. The machining time was observed using a stopwatch. Volume removed/Unit time was then calculated using Eq. 1 [32].

$$MRR = \frac{(initial\ weight\ of\ specimen - final\ weight\ of\ specimen)}{density \cdot machining\ time} \tag{1}$$

3. Strength (MPa): Ability to bear loads without failure. The strength of the specimen has been measured after machining at different machining parameter combinations. The strength was measured using the Material Testing System (MTS) and values were recorded. The specimens have been adjusted among the two hydraulic grips of a 21 MPa, having a static force capacity of 120 KN and Dynamic 100 KN MTS load frame by MTS System Corporation with the automatic data acquisition processing.

Table 4 Design matrix with responses for flood and MQL

Exp. No.	Input process parameters			Responses				
	C_S m/min	F_R mm/rev	D_C mm	*Ra* µm		*MRR* cm³/min	Strength (*ST*) MPa	
				Flood	MQL		Flood	MQL
1	200	0.08	0.1	0.145	0.121	0.228	1088	1106
2	270	0.08	0.1	0.112	0.098	0.392	1124	1142
3	200	0.12	0.1	0.168	0.153	0.392	1066	1084
4	270	0.12	0.1	0.148	0.134	0.627	1102	1120
5	200	0.08	0.3	0.205	0.185	0.794	1058	1076
6	270	0.08	0.3	0.185	0.175	1.032	1094	1112
7	200	0.12	0.3	0.219	0.196	1.276	1036	1054
8	270	0.12	0.3	0.208	0.181	1.648	1076	1090
9	176.12	0.1	0.2	0.189	0.173	0.591	1050	1068
10	293.86	0.1	0.2	0.145	0.135	0.932	1110	1128
11	235	0.07	0.2	0.181	0.162	0.542	1096	1114
12	235	0.13	0.2	0.219	0.187	0.973	1062	1082
13	235	0.1	0.032	0.109	0.1	0.157	1110	1128
14	235	0.1	0.37	0.187	0.185	1.476	1054	1072
15	235	0.1	0.2	0.197	0.167	0.847	1083	1108
16	235	0.1	0.2	0.197	0.167	0.748	1083	1105
17	235	0.1	0.2	0.189	0.167	0.821	1086	1107
18	235	0.1	0.2	0.197	0.172	0.785	1087	1108
19	235	0.1	0.2	0.191	0.171	0.832	1085	1108
20	235	0.1	0.2	0.194	0.167	0.769	1084	1103

4. Results and discussion

4.1 Analysis of surface roughness

The integrity of machining surface was systematically characterized by surface roughness, microhardness, and microstructure changes [33]. In this investigation, experimentally the influence of process parameters and lubrication mode during high-speed machining of 15CDV6 HSLA steel on surface roughness has been presented as shown in Fig. 2. A concise vision of the plot indicates the following observations: a) The surface roughness decreases with higher cutting speed, and lower feed rate and depth of cut; b) The trend lines showed that surface roughness has been improved using MQL than flood lubrication and the percentage improvement in *Ra* is ranging from 1.1-16.6 %.

The effects of cutting speed, feed rate, and depth of cut on surface roughness are illustrated in response surface plots shown in Fig. 3a and 3b. The trends highlight that *Ra* is more influenced by D_C followed by F_R and C_S. Further, observed that *Ra* decreased with the increase of cutting speed because C_S increases heat generation and reduces the friction coefficient of tool-chip and cutting force [34]. The *Ra* increases with the increase of F_R due to the reason the contact area between the cutting tool and the workpiece increases, which leads to higher thrust force and vibration and therefore increases the *Ra*. Moreover, *Ra* increases with the increase of D_C because when D_C increases tool-chip contact length also increases which leads to an increase in cutting forces and temperature which in turn affects *Ra* [35]. During HSM minimum value of *Ra* (0.098

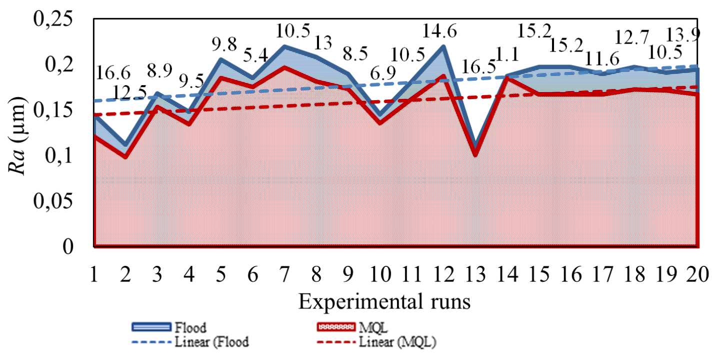

Fig. 2 Experimental results with percentage (%) improvement in surface roughness

μm) at the highest value of C_S (270 m/min) and the lowest value of F_R (0.08 mm/rev) and D_C (0.1 mm) have been achieved using MQL because during MQL high-pressure mist removes the chips which reduce the friction, no thermal shocks and fewer vibrations induced in a rotating tool which minimizes wear and tear leading to improved surface finish as compared to flood lubrication [36]. The minimum quantity lubrication produces a smoother surface, i.e. the difference between peak and valley is less than other conditions (flood lubrication) generated. In flood lubrication, traces of feed are more visible, which increases the average surface roughness [37].

For in-depth analysis, the adequacy of developed models has been checked by ANOVA as a statistical tool. The most significant parameter indicates the highest F-value. The predictor's main and interaction effects on *Ra* are significant where $p < 0.05$. The significant terms for *Ra* are depth of cut; depth of cut squared; feed rate; cutting speed; cutting speed squared for flood while the depth of cut; depth of cut squared; cutting speed; feed rate; cutting speed squared; feed rate × depth of cut for MQL. The regression models for the prediction of *Ra* under flood and MQL system are given in Eq. 2 and 3 respectively.

$$\begin{aligned} Ra_{flood} = \; & -0.1328 + 2.52540\text{E}-003 \cdot C_S - 1.458 \cdot F_R + 0.85137 \cdot D_C \\ & -003 \cdot C_S \cdot F_R + 7.85715\text{E}-004 \cdot C_S \cdot D_C - 1.375 \cdot F_R \cdot D_C \\ & -7.24671\text{E}-006 \cdot C_S^2 + 6.97511 \cdot F_R^2 - 1.55947 D_C^2 \end{aligned} \quad (2)$$

$$\begin{aligned} Ra_{MQL} = \; & -0.13714 + 1.66455\text{E}-003 \cdot C_S + 0.18179 \cdot F_R + 0.82542 \cdot D_C - 1.78571 \\ & -004 \cdot C_S \cdot F_R + 6.07143\text{E}-004 \cdot C_S \cdot D_C - 3.18750 \cdot F_R \cdot D_C \\ & -4.34468\text{E}-006 \cdot C_S^2 + 4.81404 \cdot F_R^2 - 0.93881 \cdot D_C^2 \end{aligned} \quad (3)$$

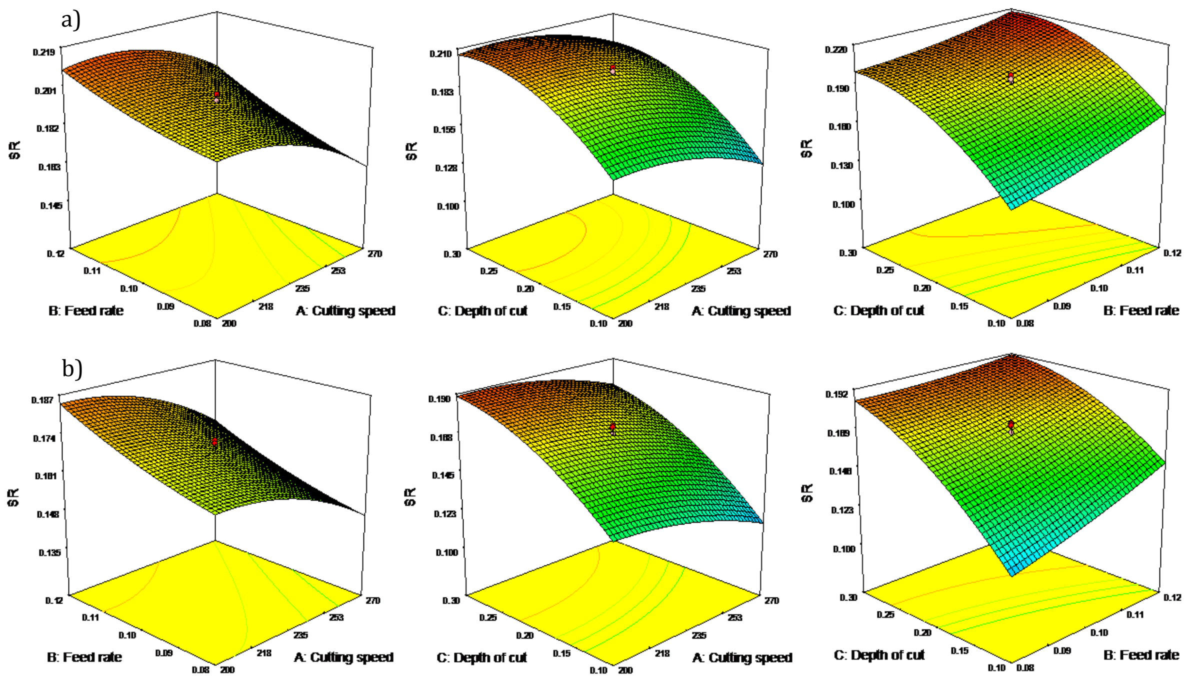

Fig. 3 Effects of process parameters on surface roughness: a) flood, b) MQL

4.2 Analysis of material removal rate

The material removal rate is calculated using Eq. 1 and results are tabulated in table 4. It has been examined that the *MRR* is more influenced by the D_C followed by C_S and F_R. The effects of cutting speed, feed rate, and depth of cut on the material removal rate is shown in Fig. 4. The maximum *MRR* (1.648 cm^3/min) is obtained at the highest value of C_S (270 m/min), F_R (0.12 mm/rev), and D_C (0.3 mm) by experimental investigation as given in table 4. The experimental investigation shows that negligible differences present in *MRR* value for MQL and flood.

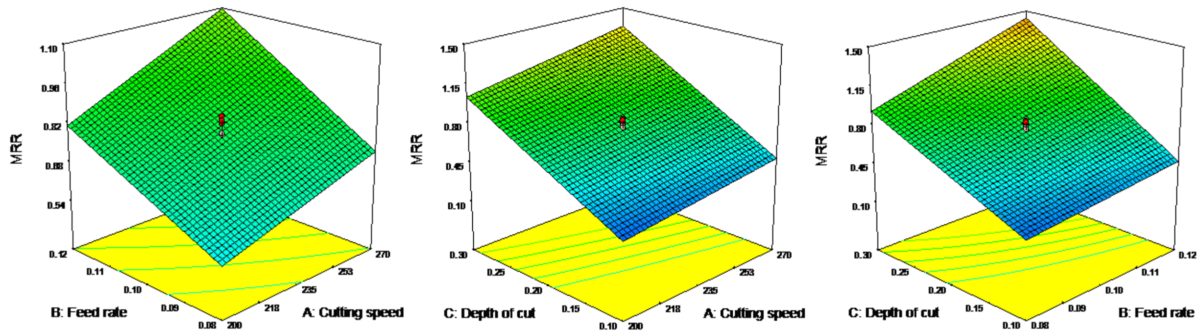

Fig. 4 Effects of process parameters on material removal rate

For more detailed analysis, ANOVA has been carried on the *MRR* data. The F-value indicates that the most significant factor for *MRR* is D_C that boosts production by increasing *MRR*. The significant factors for *MRR* are depth of cut; feed rate; cutting speed; feed rate × depth of cut. The empirical model for the prediction of *MRR* under flood and MQL is given in Eq. 4.

$$
\begin{aligned}
MRR_{flood=MQL} = {} & +0.50936 - 1.85714\text{E}-003 \cdot C_S - 9.20561 \cdot F_R - 2.23736 \cdot D_C \\
& +0.036607 \cdot C_S \cdot F_R + 7.53571\text{E}-003 \cdot C_S \cdot D_C + 43.68750 \cdot F_R \cdot D_C
\end{aligned} \tag{4}
$$

4.3 Analysis of strength

Fig. 5 illustrates experimentally the effects of process parameters and lubrication mode on the strength of material. The maximum value of *ST* has been achieved at the highest C_S and the lowest F_R and D_C. The strength has been improved using MQL and percentage improvement is ranging from 1.3-2.3 %. The most prominent observation of the data is less heat is attained at the lowest value of F_R and D_C, which produces a better surface finish and further improves the strength of the material.

The response surface plots describe the effects of C_S, F_R, and D_C on strength of the material as shown in Fig. 6. The strength of the material is more influenced by C_S as compared to D_C and F_R. The strength of the material is increased with the increase of C_S and decreased by increasing D_C and F_R. The maximum strength has been achieved at the highest C_S with the lowest F_R and D_C. Moreover, a greater value of strength is observed using MQL than flood lubrication. The maximum value of *ST* (1142MPa) at C_S (270 m/min), F_R (0.08 mm/rev) and D_C (0.1 mm) is attained using MQL. Further, it has been investigated that surface is finer at the lowest value of D_C and F_R, which produces less heat generation and greater strength.

The F-value suggests that C_S is the most important factor for strength followed by D_C and F_R. The significant terms are cutting speed; depth of cut; feed rate; feed rate squared; cutting speed squared for flood while cutting speed; depth of cut; feed rate; cutting speed squared; feed rate squared; depth of cut squared for MQL. The regression models for the prediction of *ST* under flood and MQL are given in Eq. 5 and Eq. 6, respectively.

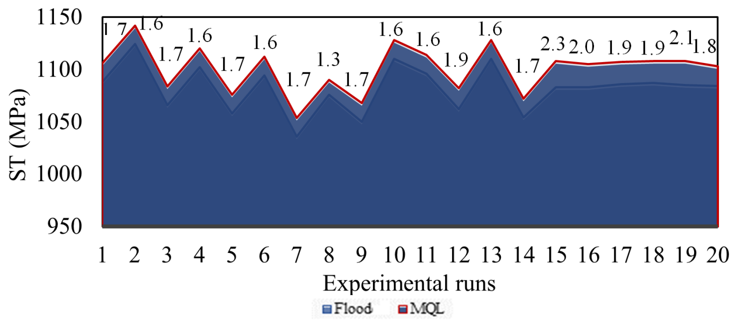

Fig. 5 Experimental results with percentage (%) improvement in strength

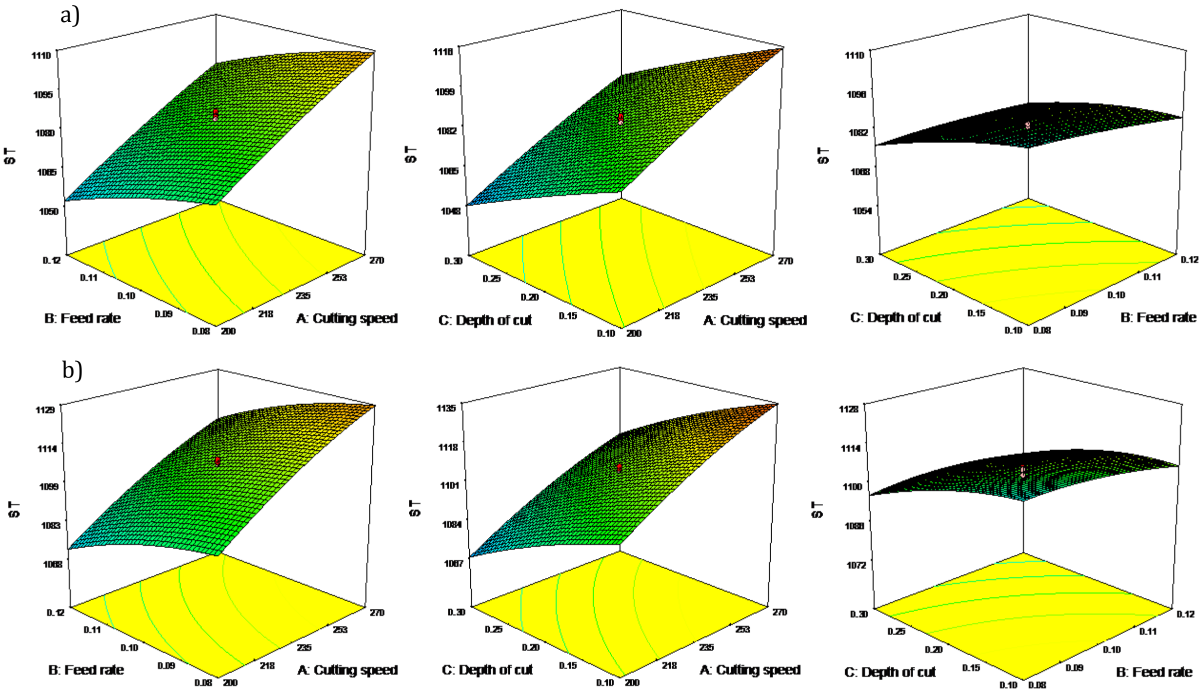

Fig. 6 Effects of process parameters on strength: a) flood, b) MQL

$$ST_{flood} = +951.72416 + 1.01899 \cdot C_S + 221.67035 \cdot F_R - 178.38573 \cdot D_C + 0.71429 \cdot C_S \cdot F_R + 0.14286 \cdot C_S \cdot D_C + 250.00 \cdot F_R \cdot D_C - 1.27288\text{E} - 003 \cdot C_S^2 - 4782.07149 \cdot F_R^2 - 85.21684 \cdot D_C^2 \quad (5)$$

$$ST_{MQL} = +846.59134 + 1.68089 \cdot C_S + 1003.59014 \cdot F_R - 63.28968 \cdot D_C - 2.48622\text{E} - 003 \cdot C_S^2 - 7614.03485 \cdot F_R^2 - 233.85072 \cdot D_C^2 \quad (6)$$

4.4 Sustainable machining model

The sustainable machining model is shown in Fig. 7. It has been found that as a technical aspect *Ra* is improved up to 17 %, and *ST* improved up to 2.3 % using minimum quantity lubrication as a sustainable approach. It is also examined that using MQL reduces cutting fluid (CF) consumption that minimizes waste disposal, saves the environment, and reduces machining costs up to 17 %. It has been further noticed that using MQL reducing health hazards and improve worker's safety.

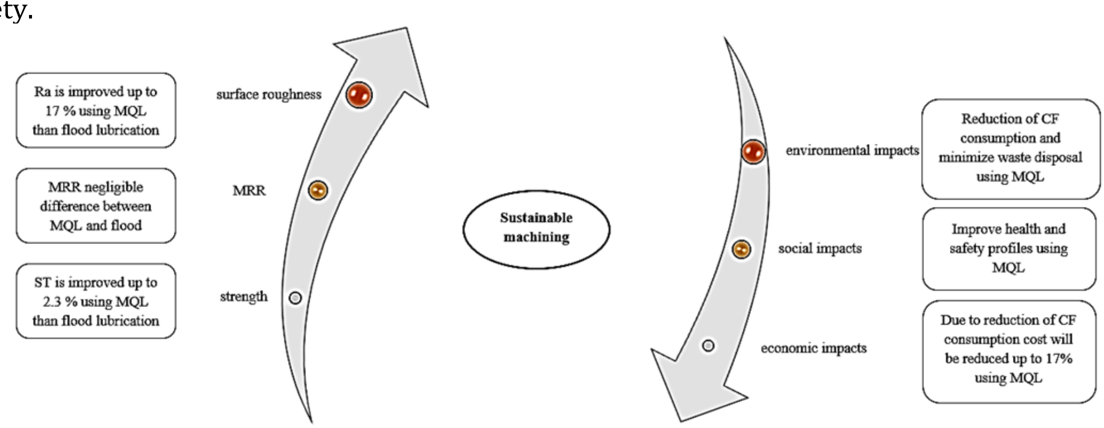

Fig. 7 Sustainable machining model

4.5 Multi-objective optimization associated with sustainability

Sustainable machining aims to achieve a better surface finish, high productivity, and strength of the material. Simultaneous optimizations of these objective functions lead to minimizing environmental damage with worker's safety and thus ensures sustainable production. The performance measures for the current research include *Ra*, *MRR*, and *ST*. To achieve a compromise between performance measures, this research proposed a desirability function-based multi optimization solution. The sustainability function is the combination of these objective functions and is given by relation 7.

$$Sustainability = \begin{Bmatrix} Minimize\ Ra \\ Maximize\ MRR \\ Maximize\ ST \end{Bmatrix} \tag{7}$$

Mostly, multi-response optimization techniques are used to produce a set of optimal solutions instead of a single solution. In this research, surface roughness, material removal rate, and strength have been designated as responses and optimized simultaneously. The responses are conflicting with each other due to which optimal solutions have been obtained through a numerical technique called the desirability approach in RSM established by Derringer and Suich [38] and mostly used for multi-response optimization problems [39, 40]. The desirability functions are smooth piecewise objective functions. In desirability profiling, a desirability function for each response is specified. The desirability values switch between the maximize (*higher is better*), target (*nominal/the best*), and minimize (*smaller is better*) values. Desirability function-based approach comprise of transforming the estimated quadratic response models into individual desirability functions that are then cluster into combined function. This function is generally a geometric or an arithmetic mean, which will be maximized or minimized, respectively. The processing and execution steps of desirability function method for calculating the desirability value and calculating the overall desirability function value and its optimization is taken care by the response surface methodology approach. Finally, it gives the optimum process parametric setting and minimizes *Ra*, maximize *MRR* and *ST* at optimum combinations. In this research, the combined desirability of 57.5 % for MQL and 56.6 % for flood lubrication has been achieved, which provides optimal solutions for minimum *Ra*, and maximum *MRR* and *ST* simultaneously. The optimization results are summarized in Table 5 which shows MQL is more desirable than flood lubrication.

Table 5 Optimization results are tabulated against the respective objectives

Response variable being optimized		Optimum process parameters			Optimum response values		
		C_S (m/min)	F_R (mm/rev)	D_C (mm)	*Ra* (μm)	*MRR* (cm³/min)	*ST* (MPa)
Min. *Ra*	MQL	270	0.08	0.1	0.098	0.392	1142
	Flood	270	0.08	0.1	0.112		1124
Max. *MRR*	MQL	270	0.12	0.3	0.181	1.648	1090
	Flood	270	0.12	0.3	0.206		1076
Max. *ST*	MQL	270	0.08	0.1	0.098	0.575	1142
	Flood	270	0.08	0.1	0.112		1124
Min. *Ra*, Max. *MRR*, and Max. *ST*	MQL	270	0.09	0.15	0.131	0.64	1132
	Flood	270	0.09	0.14	0.144	0.609	1113

5. Conclusion

This research aimed to achieve sustainable machining by simultaneously optimizing sustainable machining drivers during high-speed machining of 15CDV6 HSLA steel under MQL and flood lubrication. The following conclusions are drawn from the research:

- It is concluded that minimum surface roughness and maximum strength have been achieved at the highest C_S and the lowest F_R and D_C with compromising *MRR*. Also, the maximum material removal rate is attained at the highest C_S, F_R, and D_C with negotiating surface roughness, and strength of the material. The optimal parameter combinations for best responses under MQL and flood lubrication are given in table 5.
- Optimization associated with sustainability produced compromising optimal results (Min. *Ra* (0.131μm), Max. *MRR* (0.64cm³/min), and Max. *ST* (1132MPa) at the highest cutting speed 270m/min and the lowest feed rate 0.09mm/rev and depth of cut 0.15 mm for minimum quantity lubrication and confirmed that MQL is an alternative of a flood to enhance

the quality, productivity and strength of the material. The combined desirability for MQL (57.5 %) and flood (56.6 %) showed that MQL is more desirable than the flood.

- The results from experimental runs showed that an improvement in surface roughness (1.1-16.6 %), and strength (1.3-2.3 %) of the material using minimum quantity lubrication has been witnessed.

The research confirmed that minimum quantity lubrication has a potential for practitioners to improve the quality and strength of the material during high-speed machining under the umbrella of sustainability. The work would be beneficial in the field of aviation, defense, and aeronautical applications under the principles of sustainable manufacturing paradigms. The developed models will help the shop floor technician to predict the responses before experimenting. The evolutionary techniques can be explored to further investigate 15CDV6 HSLA steel.

References

[1] Jain, A., Bajpai, V. (2020). Chapter 1 – Introduction to high-speed machining (HSM), In: Gupta, K., Davim, J.P. (eds.), *High Speed Machining*, Academic Press, Elsevier, Cambridge, United Kingdom, 1-25, doi: 10.1016/B978-0-12-815020-7.00001-1.

[2] Kar, T., Mandal, N.K., Singh, N.K. (2020). Multi-response optimization and surface texture characterization for CNC milling of inconel 718 alloy, *Arabian Journal for Science and Engineering*, Vol. 45, No. 2, 1265-1277, doi: 10.1007/s13369-019-04324-5.

[3] Raja, V.P., Moorthy, R.S. (2019). Prediction of temperature distribution of the spindle system by proposed finite volume and element method, *Arabian Journal for Science and Engineering*, Vol. 44, No. 6, 5779-5785, doi: 10.1007/s13369-019-03732-x.

[4] Jayal, A.D., Badurdeen, F., Dillon Jr., O.W., Jawahir, I.S. (2010). Sustainable manufacturing: Modeling and optimization challenges at the product, process and system levels, *CIRP Journal of Manufacturing Science and Technology,* Vol. 2, No. 3, 144-152, doi: 10.1016/j.cirpj.2010.03.006.

[5] Goindi, G.S., Sarkar, P. (2017). Dry machining: A step towards sustainable machining – Challenges and future directions, *Journal of Cleaner Production*, Vol. 165, 1557-1571, doi: 10.1016/j.jclepro.2017.07.235.

[6] Gunda, R.K., Reddy, N.S.K., Kishawy, H. (2016). A novel technique to achieve sustainable machining system, *Procedia CIRP,* Vol. 40, 30-34, doi: 10.1016/j.procir.2016.01.045.

[7] Yıldırım, Ç.V., Kivak, T., Erzincanlı, F. (2019). Influence of different cooling methods on tool life, Wear mechanisms and surface roughness in the milling of nickel-based waspaloy with WC tools, *Arabian Journal for Science and Engineering,* Vol. 44, No. 9, 7979-7995, doi: 10.1007/s13369-019-03963-y.

[8] Yıldırım, Ç.V., Kivak, T., Erzincanlı, F. (2019). Tool wear and surface roughness analysis in milling with ceramic tools of Waspaloy: A comparison of machining performance with different cooling methods, *Journal of the Brazilian Society of Mechanical Sciences and Engineering*, Vol. 41, No. 2, Article No. 83, doi: 10.1007/s40430-019-1582-5.

[9] Mia, M., Al Bashir, M., Khan, M.A., Dhar, N.R. (2017). Optimization of MQL flow rate for minimum cutting force and surface roughness in end milling of hardened steel (HRC 40), *The International Journal of Advanced Manufacturing Technology,* Vol. 89, No. 1-4, 675-690, doi: 10.1007/s00170-016-9080-8.

[10] Khan, A.M., Jamil, M., Salonitis, K., Sarfraz, S., Zhao, W., He, N., Mia, M., Zhao, G. (2019). Multi-objective optimization of energy consumption and surface quality in nanofluid SQCL assisted face milling, *Energies*, Vol. 12, No. 4, Article No. 710, doi: 10.3390/en12040710.

[11] Nguyen, T.-T. (2019). Prediction and optimization of machining energy, surface roughness, and production rate in SKD61 milling, *Measurement,* Vol. 136, 525-544, doi: 10.1016/j.measurement.2019.01.009.

[12] Borojević, S., Lukić, D., Milošević, M., Vukman, J., Kramar, D. (2018). Optimization of process parameters for machining of Al 7075 thin-walled structures, *Advances in Production Engineering & Management,* Vol. 13, No. 2, 125-135, doi: 10.14743/apem2018.2.278.

[13] Songmei, Y., Xuebo, H., Guangyuan, Z., Amin, M. (2017). A novel approach of applying copper nanoparticles in minimum quantity lubrication for milling of Ti-6Al-4V, *Advances in Production Engineering & Management,* Vol. 12, No. 2, 139-150, doi: 10.14743/apem2017.2.246.

[14] Liao, Y.S., Lin, H.M. (2007). Mechanism of minimum quantity lubrication in high-speed milling of hardened steel, *International Journal of Machine Tools and Manufacture,* Vol. 47, No. 11, 1660-1666, doi: 10.1016/j.ijmachtools.2007.01.007.

[15] Hamdan, A., Sarhan, A.A.D., Hamdi, M. (2012). An optimization method of the machining parameters in high-speed machining of stainless steel using coated carbide tool for best surface finish, *The International Journal of Advanced Manufacturing Technology*, Vol. 58, 81-91, doi: 10.1007/s00170-011-3392-5.

[16] Yang, Z., Xue, Y., Li, Y., Xu, J., Wang, Q. (2018). The effect of milling parameters on surface integrity in high-speed milling of ultrahigh strength steel, *Procedia CIRP*, Vol. 71, 83-88, doi: 10.1016/j.procir.2018.05.076.

[17] Begic-Hajdarevic, D., Cekic, A., Kulenovic, M. (2014). Experimental study on the high speed machining of hardened steel, *Procedia Engineering,* Vol. 69, 291-295, doi: 10.1016/j.proeng.2014.02.234.

[18] Motorcu, A.R., Kuş, A., Arslan, R., Tekin, Y., Ezentaş, R. (2013). Evaluation of tool life – Tool wear in milling of Inconel 718 superalloy and the investigation of effects of cutting parameters on surface roughness with Taguchi method, *Tehnički Vjesnik – Technical Gazette,*Vol. 20, No. 5, 765-774.
[19] Krolczyk, G.M., Nieslony, P., Maruda, R.W., Wojciechowski, S. (2017). Dry cutting effect in turning of a duplex stainless steel as a key factor in clean production, *Journal of Cleaner Production,* Vol. 142, Part 4, 3343-3354, doi: 10.1016/j.jclepro.2016.10.136.
[20] Masood, I., Jahanzaib, M., Haider, A. (2016). Tool wear and cost evaluation of face milling grade 5 titanium alloy for sustainable machining, *Advances in Production Engineering & Management,* Vol. 11, No. 3, 239-250, doi: 10.14743/apem2016.3.224.
[21] Martínez-Lage, I., Vázquez-Burgo, P., Velay-Lizancos, M. (2020). Sustainability evaluation of concretes with mixed recycled aggregate based on holistic approach: Technical, economic and environmental analysis, *Waste Management,* Vol. 104, 9-19, doi: 10.1016/j.wasman.2019.12.044.
[22] Maruda, R.W., Legutko, S., Krolczyk, G.M., Raos, P. (2015). Influence of cooling conditions on the machining process under MQCL and MQL conditions, *Tehnički Vjesnik – Technical Gazette,* Vol. 22, No. 4, 965-970, doi: 10.17559/TV-20140919143415.
[23] Benedicto, E., Carou, D., Rubio, E.M. (2017). Technical, economic and environmental review of the lubrication/cooling systems used in machining processes, *Procedia Engineering,* Vol. 184, 99-116, doi: 10.1016/j.proeng.2017.04.075.
[24] Niamat, M., Sarfraz, S., Ahmad, W., Shehab, E., Salonitis, K. (2020). Parametric modelling and multi-objective optimization of electro discharge machining process parameters for sustainable production, *Energies,* Vol. 13, No. 1, Article No. 38, doi: 10.3390/en13010038.
[25] Kumar, P.N., Bhaskar, Y., Mastanaiah, P., Murthy, C.V.S. (2014). Study on dissimilar metals welding of 15CDV6 and SAE 4130 steels by inter pulse gas tungsten arc welding, *Procedia Materials Science,* Vol. 5, 2382-2391, doi: 10.1016/j.mspro.2014.07.483.
[26] Azam, M., Jahanzaib, M., Wasim, A., Hussain, S. (2015). Surface roughness modeling using RSM for HSLA steel by coated carbide tools, *The International Journal of Advanced Manufacturing Technology,* Vol. 78, No. 5-8, 1031-1041, doi: 10.1007/s00170-014-6707-5.
[27] Srinivasan, L., Kannan, T.D.B., Sathiya, P., Biju, S. (2017). Effect of heat input, heat treatment on microstructure and mechanical properties of GTA welded aerospace material 15CDV6, *Journal of Materials Research,* Vol. 32, No. 7, 1361-1366, doi: 10.1557/jmr.2017.70.
[28] Groover, M.P. (2010). *Fundamentals of modern manufacturing: Materials processes, and systems,* 4th edition, John Wiley & Sons, New York, USA.
[29] Abd Rahim, E., Dorairaju, H. (2018). Evaluation of mist flow characteristic and performance in minimum quantity lubrication (MQL) machining, *Measurement,* Vol. 123, 213-225, doi: 10.1016/j.measurement.2018.03.015.
[30] Mishra, S.K., Ghosh, S., Aravindan, S. (2020). Machining performance evaluation of Ti6Al4V alloy with laser textured tools under MQL and nano-MQL environments, *Journal of Manufacturing Processes,* Vol. 53, 174-189, doi: 10.1016/j.jmapro.2020.02.014.
[31] Keerthana, B., Kumar, G.V., Babu, K,A. (2019). Effect of minimum quantity lubrication on surface roughness and temperature in milling of EN31 steel for die making, *Strojnícky Časopis – Journal of Mechanical Engineering,* Vol. 69, No. 1, 61-68, doi: 10.2478/scjme-2019-0005.
[32] Zahoor, S., Ameen, F., Abdul-Kader, W., Stagner, J. (2020). Environmentally conscious machining of Inconel 718: Surface roughness, tool wear, and material removal rate assessment, *The International Journal of Advanced Manufacturing Technology,* Vol. 106, No. 1-2, 303-313, doi: 10.1007/s00170-019-04550-z.
[33] Jin, D., Liu, Z. (2012). Effect of cutting speed on surface integrity and chip morphology in high-speed machining of PM nickel-based superalloy FGH95, *The International Journal of Advanced Manufacturing Technology*, Vol. 60, No. 9-12, 893-899, doi: 10.1007/s00170-011-3679-6.
[34] Wang, G., Liu, Z., Huang, W., Wang, B., Niu, J. (2019). Influence of cutting parameters on surface roughness and strain hardening during milling NiTi shape memory alloy, *The International Journal of Advanced Manufacturing Technology,* Vol. 102, No. 5-8, 2211-2221, doi: 10.1007/s00170-019-03342-9.
[35] Gaitonde, V.N., Karnik, S.R., Maciel, C.H.A., Rubio, J.C.C., Arbao, A.M. (2016). Machinability evaluation in hard milling of AISI D2 steel, *Materials Research,* Vol. 19, No. 2, 360-369, doi: 10.1590/1980-5373-MR-2015-0263.
[36] Khan, A.M., Jamil, M., Ul Haq, A., Hussain, S., Meng, L., He, N. (2019). Sustainable machining. Modeling and optimization of temperature and surface roughness in the milling of AISI D2 steel, *Industrial Lubrication and Tribology,* Vol. 71, No. 2, 267-277, doi: 10.1108/ILT-11-2017-0322.
[37] Kaynak, Y., Gharibi, A., Yılmaz, U., Köklü, U., Aslantaş, K. (2018). A comparison of flood cooling, minimum quantity lubrication and high pressure coolant on machining and surface integrity of titanium Ti-5553 alloy, *Journal of Manufacturing Processes*, Vol. 34, Part A, 503-512, doi: 10.1016/j.jmapro.2018.06.003.
[38] Derringer, G., Suich, R. (1980). Simultaneous optimization of several response variables, *Journal of Quality Technology,* Vol. 12, No. 4, 214-219, doi: 10.1080/00224065.1980.11980968.
[39] Sachin, B., Narendranath, S., Chakradhar, D. (2020). Application of desirability approach to optimize the control factors in cryogenic diamond burnishing, *Arabian Journal for Science and Engineering*, Vol. 45, No. 2, 1305-1317, doi: 10.1007/s13369-019-04326-3.
[40] Liman, M.M., Abou-El-Hossein, K. (2019). Modeling and multiresponse optimization of cutting parameters in SPDT of a rigid contact lens polymer using RSM and desirability function, *The International Journal of Advanced Manufacturing Technology*, Vol. 102, No. 5-8, 1443-1465, doi: 10.1007/s00170-018-3169-1.

Advances in Production Engineering & Management ISSN 1854-6250
Volume 15 | Number 4 | December 2020 | pp 416–430 Journal home: apem-journal.org
https://doi.org/10.14743/apem2020.4.375 Original scientific paper

Evolutionary game of green manufacturing mode of enterprises under the influence of government reward and punishment

Awaga, A.L.[a], Xu, W.[a], Liu, L.[a], Zhang, Y.[b,*]

[a]School of Management, Shenyang University of Technology, Shenyang, P.R. China
[b]School of Public Health, Dalian Medical University, Dalian, P.R. China

ABSTRACT

Green production mode is an advanced manufacturing mode. However, due to the environmental externality of green production, it is different for a pure market mechanism to promote the evolution of green operation mode of manufacturing enterprises. Government regulation is very important. This paper establishes an evolutionary game model of whether manufacturing enterprises choose to implement green production mode when the government implements two different mechanisms of reward and punishment. Considering the complexity of strategy selection of enterprises' green production behaviour under market competition, the method constructs the simulation analysis model of enterprises' green product production behaviour with multi-subject participation. We can simulate the influence of these factors on the strategic choice of both parties (enterprises and governments) by changing the different influence factors, and studying the evolutionary law of different government guidance and regulation strategies on the production behaviour of green products. These factors include government incentives, penalties, reputations, costs, differences in the cost of implementing green production on the corporate side, corporate reputation, and false rewards or penalties. By the computer implementation of multi-subject modelling, the results show that enterprises' green product production behaviour needs the government's guidance and regulation. When formulating relevant policies, the government should combine various guidance and regulation strategies and fully consider the influence of market competition.

ARTICLE INFO

Keywords:
Evolutionary game;
Green manufacturing;
Smart manufacturing;
Reward and punishment;
Multi-objective decision making (MODM);
Evolutionary stabilization strategy

**Corresponding author:*
zhangyuan7981@126.com
(Zhang, Y.)

Article history:
Received 12 October 2020
Revised 6 December 2020
Accepted 9 December 2020

1. Introduction

The green operation of enterprises is an important way to realize social sustainable development. Green operation mode refers to the operation mode in which the production and operation activities of an enterprise can be harmonious with the environment. In the process of green manufacturing, manufacturing enterprises not only pursue profit but also bear social and environmental responsibility [1]. The government should not only supervise and manage enterprises to implement green manufacturing, but also promote the development and popularization of green manufacturing mode and application. Green manufacturing involves complex game subjects with different goals, dynamic complex environments, and many uncertain factors, therefore the stability of the economic and political environment in the game process can't be guaranteed. Manufacturing enterprises have insufficient power and the ability to carry out green manufacturing. Only through the guidance of penalty policy or direct subsidy and reward can this advanced manufacturing mode be gradually promoted among manufacturing enterprises [2]. Evolutionary Game Theory will no longer be modelled into a completely rational game party, but humans usually achieve the game equilibrium by trial and error method. The choice of equilibrium is the function whose balanced process has been achieved, thus historical, institutional factors and balanced process details will have an influence on the multiple equilibrium choices in a game.

Zhu and He [3] analysed the influence of government subsidy on the choice of enterprise innovation mode. They point out that increasing innovation subsidy and establishing a long-term subsidy mechanism can make innovation subsidy become an effective incentive measure. Govindan *et al*. established the reward and punishment mechanism supply chain, and point out that the reward and punishment mechanism can not only improve the recovery rate, reduce the price of new products, but also benefit the whole social welfare [4-5]. Tseng *et al*. constructed a game model which considers green consumption subsidy and non-green consumption tax, analyses and discusses the influence of government financial strategy on the optimal decision of supply chain members under decentralized decision and centralized decision [6]. A game model of a green supply chain is built under a single channel, and different subsidy strategies are compared under the same government subsidy expenditure [7]. Micheli *et al*. established a green supply chain model with reward and punishment mechanism under different government target decisions. They discuss the influence of product market size, sensitivity coefficient of energy-saving level, and cost coefficient of energy-saving input on the reward and punishment intensity [8]. This paper constructs a green supply chain model considering government subsidies and risk aversion of supply chain members, and studies the risk aversion behaviours of manufacturers and retailers under centralized and decentralized decisions.

2. Model building

2.1 Evolutionary game analysis of green manufacturing

The formation mechanism of green manufacturing is due to the different social division of labour. Hence, the government supervision decision and the enterprise production decision have different responsibilities in the final production mode selection, and the relationship between the two is an evolutionary game, jointly promoting the sustainable development of green manufacturing [9-10]. However, in reality, due to the different divisions of functions between government and enterprises, their decision focus is different. Governments mainly focus on social and environmental benefits, while enterprises pay more attention to their economic benefits [11]. There is somehow a competitive relationship in profit distribution between them. Therefore, the government and enterprises are in a game state of cooperation and competition as to whether to carry out green manufacturing or not. The main manifestations are as follows: First, there is an asymmetric partnership between the government and enterprises. From the perspective of environmental and social sustainable development, both the government and enterprises need green manufacturing mode. Green manufacturing can improve government performance and regional social reputation, which includes both government reputation and corporate reputation [12]. The green production of enterprises in the region is conducive to the formation of a green industrial chain and a green manufacturing industrial cluster in the region. This forms an agglomeration effect and attracts more enterprises to adopt the green manufacturing production mode. Thus, the virtuous circles of the government tax increase and enterprise green manufacturing cost reduction are realized.

For any specific green manufacturing mode, the reason it can gain market share in the market is that the manufacturing mode satisfies the supervision and management of government market access departments, safety supervision departments, environmental supervision departments, industrial and commercial administration departments, and taxation departments outside the enterprise [13]. At the same time, it is also the result of internal and external cooperation between product design departments, the processing industrial arts department, the marketing department, the comprehensive management department, and the internal planning department which is needed for production [14].

The manufacturing industry chain is reflected in the cooperation between raw material suppliers, parts suppliers, manufacturers, service providers, capital operators, terminal equipment suppliers, and relevant government departments.

The formation mechanism of the region where the industrial cluster is located is based on the existence of the social division of labour [15]. The main approach adopted is the construction of the assistance of the upstream and downstream of the manufacturing, with the support of government policies to form a close relationship between them.

As a public policy service provider, the government carries out policy planning on environmental rewards and punishment and provides manufacturing enterprises with the environment for the development of the guaranteed green manufacturing mode. As the provider of specific green manufacturing mode, manufacturing enterprises put the environmentally friendly production mode into practice through advanced technological innovation to produce green industrial products, which can be directly used by consumers. Therefore, they are interdependent and have a cooperative relationship [16].

2.2 Model assumption

The basic assumptions of the evolutionary game model between the government and manufacturers in the green manufacturing industry chain are:

- A is the government's reward for enterprises to implement green production. $-A$ is the government's reward for the implementation of green production enterprises. B is the government's punishment for not implementing green production enterprises. $-B$ is the fine submitted by the enterprises for not implementing green production.
- R_1 symbolises that the government gives incentives to the green production enterprises to gain social reputation; R_2 symbolises that the government wrongly penalizes the enterprises that implement green production resulting in the loss of social reputation; R_3 is the social reputation loss caused by the government's false reward to enterprises that fail to implement green production; R_4 is the social reputation gained by the government for punishing enterprises that fail to implement green production.
- π_0 is the income obtained by the enterprises; G_0 is the office income obtained by the government.
- r_1 and r_2 are the enterprises gains of the social reputation by implementing green production; r_3 and r_4 are the losses of the social reputation of the enterprises for not implementing green production; The social reputation that enterprises gain or lose only depends on whether they have implemented green production or not, and has nothing to do with whether the government has carried out the right incentives and penalties or not.
- θ is the probability that the enterprise is rewarded for not implementing green production; ϕ is the probability that the enterprise is punished for green production, $0 \leq \theta \leq 1$, $0 \leq \phi \leq 1$.
- Suppose that the proportion of the government choosing incentive strategy is x, the proportion of the punishment strategy is $1 - x$, the proportion of the enterprise choosing to implement green production is y, the proportion of choosing not to implementing green production is $1 - y$, where $0 \leq x \leq 1, 0 \leq y \leq 1$.
- Based on the above assumptions, their payment matrix can be obtained, as shown in Table 1.

Table 1 Payment matrix of government and enterprises

Government \ Enterprise	Green manufacturing	Non-green manufacturing
Reward	$G_0 - C_1 - A + R_1$, $\pi_0 - c_1 + A + r_1$	$G_0 - C_1 - \theta A - R_3$, $\pi_0 - c_2 + \theta A - r_3$
Punishment	$G_0 - C_2 + \varphi B - R_2$, $\pi_0 - c_1 - \varphi B + \mathrm{r}_2$	$G_0 - C_2 + B + R_4$, $\pi_0 - c_2 - B - r_4$

3. Game analysis of government rewards, punishments, and green production evolution of manufacturing enterprises

3.1 Game pay-off matrix

Based on the above assumptions, the evolutionary game analysis of the government presented is as follows:

(1) ***The payment when the government chooses the reward strategy***

$$W_1 = y(G_0 - C_1 - A + R_1) + (1-y)(G_0 - C_1 - \theta A - R_3) \quad (1)$$

The payment when the government carries out the penalty policy:

$$W_2 = y(G_0 - C_2 + \varphi B - R_2) + (1-y)(G_0 - C_2 - B + R_4) \quad (2)$$

The average payment from the government:

$$\overline{W} = xW_1 + (1-x)W_2 \quad (3)$$

Therefore, the dynamic differential equation for the government is shown as follows:

$$\frac{dx(t)}{dt} = x(W_1 - \overline{W}) \quad (4)$$

$$= x(1-x)\ \{[(1-\varphi)B + (\theta-1)A + R_1 + R_2 + R_3 + R_4]y + C_2 - C_1 - A\theta - B - R - R_4\}$$

$$F(x) = x(1-x)\{[(1-\varphi)B + (\theta-1)A + R_1 + R_2 + R_3 + R_4]y + C_2 - C_1 - A\theta - B - R_3 - R_4\} \quad (5)$$

and so,

$$F'(x) = (1-2x)\{[(1-\varphi)B + (\theta-1)A + R_1 + R_2 + R_3 + R_4]y + C_2 - C_1 - A\theta - B - R_3 - R_4\} \quad (6)$$

According to the stability principle: If $F'(x^*) < 0$, x^* will be in a stable state.

$\frac{dx(t)}{dt} = 0 \Rightarrow x_1 = 0\ ,\ x_2 = 1\ ,\ y = \frac{\theta A + B + R_3 + R_4 + C_1 - C_2}{(1-\phi)B + (\theta-1)A + R_1 + R_2 + R_3 + R_4}$

Next, the evolutionary stable state analysis is carried out for the three points:

a) When $y = \frac{\theta A + B + R_3 + R_4 + C_1 - C_2}{(1-\varphi)B + (\theta-1)A + R_1 + R_2 + R_3 + R_4}$, $\frac{dx(t)}{dt}$ is always zero (0), this means that x does not change over time;

b) When $y > \frac{\theta A + B + R_3 + R_4 + C_1 - C_2}{(1-\varphi)B + (\theta-1)A + R_1 + R_2 + R_3 + R_4}$, $F'(x) < 0\ ,\ x = 1$. This is an evolutionary stable state. It means that through continuous imitation and learning, the proportion of reward chosen by the government tends to be 100 %.

c) When $y < \frac{\theta A + B + R_3 + R_4 + C_1 - C_2}{(1-\varphi)B + (\theta-1)A + R_1 + R_2 + R_3 + R_4}$, $F'(x) < 0\ ,\ x = 0$. This is an evolutionary stable state. It means that through continuous imitation and learning, the proportion of punishment chosen by the government tends to be 100 %.

(2) ***The payment when the manufacturer chooses to implement the green production strategy***

$$U_1 = x[\pi_0 - c_1 + A + r_1] + (1-x)(\pi_0 - c_1 - \varphi B + r_2) \quad (7)$$

The payment when the manufacturer chooses not to implement the green production strategy:

$$U_2 = x[\pi_0 - c_2 + \theta A - r_3] + (1-x)(\pi_0 - c_2 - B - r_4) \quad (8)$$

The average payment of the manufacturer:

$$\overline{U} = yU_1 + (1-y)U_2 \quad (9)$$

$$\frac{dx(t)}{dt} = y(U_1 - \overline{U}) \quad (10)$$

$$= y(1-y)\{[(1-\theta)A + (\varphi-1)B + r1 - r_2 + r_3 - r_4]x + (1-\varphi)B - c_1 + c_2 + r_2 + r_4\}$$

Therefore, the dynamic differential equation of the production enterprise is shown as follows:

$$F(y) = y(1-y)\{[(1-\theta)A + (\varphi - 1)B + r_1 - r_2 + r_3 - r_4]x + (1-\varphi)B - c_1 + c_2 + r_2 + r_4\} \quad (11)$$

and so,

$$F'(y) = (1-2y)\{[(1-\theta)A + (\varphi - 1)B + r_1 - r_2 + r_3 - r_4]x + (1-\varphi)B - c_1 + c_2 + r_2 + r_4\} \quad (12)$$

According to the stability principle: If $F'(y^*) < 0$, y^* is a stable state.

$\frac{dy(t)}{dt} = 0 \Rightarrow y_1 = 0$, $y_2 = 1$, $x = \frac{(\varphi-1)B+c_1-c_2-r_2-r_4}{(1-\theta)A+(\varphi-1)B+r_1-r_2+r_3-r_4}$

Next, the evolutionary stable state analysis is carried out for the three points:

a) When $x = \frac{(\varphi-1)B+c_1-c_2-r_2-r_4}{(1-\theta)A+(\varphi-1)B+r_1-r_2+r_3-r_4}$, $\frac{dx(t)}{dt}$ always is 0. This means that y doesn't change over time.

b) When $x > \frac{(\varphi-1)B+c_1-c_2-r_2-r_4}{(1-\theta)A+(\varphi-1)B+r_1-r_2+r_3-r_4}$, $F'(x) < 0$, $y = 1$. This is a revolutionary stable state. It means that through continuous imitation and learning, the proportion of production enterprises choosing to implement green production tends to be 100 %.

c) When $x < \frac{(\varphi-1)B+c_1-c_2-r_2-r_4}{(1-\theta)A+(\varphi-1)B+r_1-r_2+r_3-r_4}$, $F'(x) < 0$, $y = 0$. This is a revolutionary stable state. It means that through continuous imitation and learning, the proportion of production enterprises choosing not to implement green production tends to be 100 %.

(3) ***System evolution game stability strategy***

Eq. 4 and Eq. 10 can be combined to obtain a system of differential Eq. 13, which can represent the game evolution process of the whole system:

$$\begin{cases} \frac{dx(t)}{dt} = x(1-x)\begin{Bmatrix}[(1-\varphi)B + (\theta-1)A + R_1 + R_2 + R_3 + R_4]y \\ +C_2 - C_1 - A\theta - B - R_3 - R_4\end{Bmatrix} \\ \frac{dy(t)}{dt} = y(1-y)\begin{Bmatrix}[(1-\theta)A + (\varphi-1)B + r_1 - r_2 + r_3 - r_4]x \\ +(1-\varphi)B - c_1 + c_2 + r_2 + r_4\end{Bmatrix}\end{cases} \quad (13)$$

Make $\begin{cases}\frac{dx(t)}{dt} = 0 \\ \frac{dy(t)}{dt} = 0\end{cases}$ to get the possible equilibrium point of the system A (0, 0), B (0, 1), C (1, 0), D (1, 1), E $\left(\frac{(\varphi-1)B+c_1-c_2-r_2-r_4}{(1-\theta)A+(\varphi-1)B+r_1-r_2+r_3-r_4}, \frac{\theta A+B+R_3+R_4+C_1-C_2}{(1-\varphi)B+(\theta-1)A+R_1+R_2+R_3+R_4}\right)$, which is the point of the Evolutionary Stable Strategy (ESS). In this paper, according to the method of calculating the local stability of the system created by Friedman in 1991, the Jacobi matrix of the equations of evolutionary systems can be analysed [17].

From Eq. 13, partial derivatives of the two equations can be obtained as shown in Eq. 14.

$$J = \begin{vmatrix} \frac{\partial F(x)}{\partial x} & \frac{\partial F(x)}{\partial y} \\ \frac{\partial F(y)}{\partial x} & \frac{\partial F(y)}{\partial y} \end{vmatrix} \quad (14)$$

$$\frac{\partial \mathrm{F}(x)}{\partial x} = (1-2x)\{[(1-\varphi)\mathrm{B} + (\theta-1)A + R_1 + R_2 + R_3 + R_4]y + C_2 - C_1 - A\theta - B - R_3 - R_4\} \quad (15)$$

$$\frac{\partial \mathrm{F}(x)}{\partial y} = x(1-x)[(1-\varphi)\mathrm{B} + (\theta-1)A + R_1 + R_2 + R_3 + R_4] \quad (16)$$

$$\frac{\partial \mathrm{F}(y)}{\partial x} = y(1-y)[(1-\theta)\mathrm{A} + (\varphi-1)B + r_1 - r_2 + r_3 - r_4] \quad (17)$$

$$\frac{\partial \mathrm{F}(y)}{\partial y} = (1-2y)\{[(1-\theta)\mathrm{A} + (\varphi-1)B + r_1 - r_2 + r_3 - r_4]x + (1-\varphi)B - c_1 + c_2 + r_2 + r_4\} \quad (18)$$

The local equilibrium points A, B, C, D, and E are put into the Jacobi matrix and $\det J$ and $\operatorname{tr} J$ can be obtained to find the Evolutionary Stable Strategy (ESS) of the system. The determinant of the matrix is:

$$\det J = \left(\frac{\partial F(x)}{\partial x} \times \frac{\partial F(y)}{\partial y} - \frac{\partial F(y)}{\partial x} \times \frac{\partial F(x)}{\partial y}\right) > 0 \quad (19)$$

The trace of the matrix is:

$$\operatorname{tr} J = \left(\frac{\partial F(x)}{\partial x} + \frac{\partial F(y)}{\partial y}\right) < 0 \quad (20)$$

3.2 Phase diagram of evolutionary game

Put the above five points (A, B, C, D, and E) into the trace and determinant of the matrix respectively, and further analyse the strategy behaviour trend and system stability state of the evolutionary game system according to the symbol of sum:

1. When $x = 0, y = 0$, as shown in Fig. 1, the determinant and trace of matrix J is:

$$\begin{cases} \det J = (C_2 - C_1 - A - \varphi B + R_1 + R_2)(-1)[(1-\varphi)B - c_1 + c_2 + r_2 + r_4] \\ \operatorname{tr} J = (C_2 - C_1 - A - \varphi B + R_1 + R_2) - [(1-\varphi)B - c_1 + c_2 + r_2 + r_4] \end{cases} \quad (21)$$

and the result is as shown in Table 2.

When the model parameters take the following values respectively: $C_1 = 10$, $C_2 = 1$, $c_1 = 10$, $c_2 = 1$, $s = 0.5$, $f = 0.3$, $B = 1$, $A = 1$, $r_1 = 1$, $r_2 = 1.5$, $r_3 = 1.7$, $r_4 = 2$, $R_1 = 2$, $R_2 = 1.5$, $R_3 = 3$, $R_4 = 1$, the cost of government supervision and management is high, and this tends to impose penalties on enterprises to reduce operating costs. Enterprises with high cost of green manufacturing tend to choose non-green manufacturing to reduce costs. The ESS point is at this time (penalty, non-green manufacturing).

Table 2 The result of (0, 0)

$(C_2 - C_1 - A\theta - B - R_3 - R_4) > 0$, $[(1-\varphi)B - c_1 + c_2 + r_2 + r_4] > 0$	$\det J > 0$, $\operatorname{tr} J > 0$	Instability
$(C_2 - C_1 - A\theta - B - R_3 - R_4) > 0$, $[(1-\varphi)B - c_1 + c_2 + r_2 + r_4] < 0$	$\det J < 0$, $\operatorname{tr} J$ Not sure	Saddle point
$(C_2 - C_1 - A\theta - B - R_3 - R_4) < 0$, $[(1-\varphi)B - c_1 + c_2 + r_2 + r_4] > 0$	$\det J < 0$, $\operatorname{tr} J$ Not sure	Saddle point
$(C_2 - C_1 - A\theta - B - R_3 - R_4) < 0$, $[(1-\varphi)B - c_1 + c_2 + r_2 + r_4] < 0$	$\det J > 0$, $\operatorname{tr} J < 0$	Stability

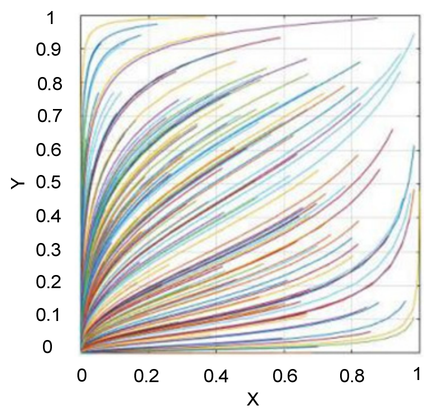

Fig. 1 (0, 0) evolutionary equilibrium

2. When $x = 0, y = 1$, as shown in Fig. 2, the determinant and trace of matrix J is:

$$\begin{cases} \det J = (-1)(C_2 - C_1 - A - \varphi B + R_1 + R_2)[(1-\varphi)B - c_1 + c_2 + r_2 + r_4] \\ \operatorname{tr} J = [(1-\varphi)B - c_1 + c_2 + r_2 + r_4] - (C_2 - C_1 - A - \varphi B + R_1 + R_2) \end{cases} \quad (22)$$

and the result is as shown in Table 3.

When the model parameters take the following values, respectively: $C_1 = 10$, $C_2 = 1$, $c_1 = 1$, $c_2 = 8$, $s = 0.5$, $f = 0.3$, $B = 2$, $A = 1$, $r_1 = 1$, $r_2 = 3.5$, $r_3 = 1.7$, $r_4 = 4$, $R_1 = 2$, $R_2 = 1$, $R_3 = 3$, $R_4 = 1$, the cost of government supervision and management is high, which tends to impose penalties on enterprises to reduce operating costs. Enterprises with high cost of green manufacturing tend to choose non-green manufacturing to reduce costs. The ESS point is at this time (i.e. penalty and non-green manufacturing).

Table 3 The result of (0, 1)

$(C_2 - C_1 - A - \varphi B + R_1 + R_2) > 0$, $[(1-\varphi)B - c_1 + c_2 + r_2 + r_4] > 0$	tr J Instability	Saddle point
$(C_2 - C_1 - A - \varphi B + R_1 + R_2) > 0$, $[(1-\varphi)B - c_1 + c_2 + r_2 + r_4] < 0$	det J > 0, tr J > 0	Instability
$(C_2 - C_1 - A - \varphi B + R_1 + R_2) < 0$, $[(1-\varphi)B - c_1 + c_2 + r_2 + r_4] > 0$	det J < 0, tr J < 0 Not sure	Stability
$(C_2 - C_1 - A - \varphi B + R_1 + R_2) < 0$, $[(1-\varphi)B - c_1 + c_2 + r_2 + r_4] < 0$	det J > 0, tr J Instability	Saddle point

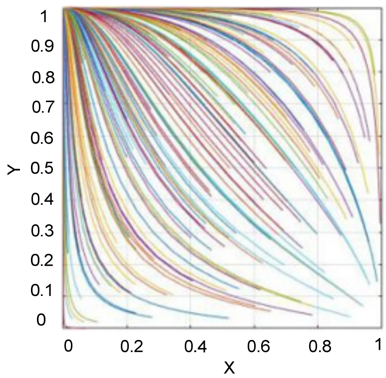

Fig. 2 (0, 1) evolutionary equilibrium

3. When $x = 1$, $y = 0$, as shown in Fig. 3, the determinant and trace of matrix J is:

$$\begin{cases} \det J = (-1)(C_2 - C_1 - A\theta - B - R_3 - R_4)[(1-\theta)A + r_1 + r_3 - c_1 + c_2] \\ \operatorname{tr} J = [(1-\theta)A + r_1 + r_3 - c_1 + c_2] - (C_2 - C_1 - A\theta - B - R_3 - R_4) \end{cases} \tag{23}$$

and the result is as shown in Table 4.

When the model parameters take the following values, respectively: $C_1 = 2$, $C_2 = 10$, $c_1 = 15$, $c_2 = 1$, $s = 0.5$, $f = 0.3$, $B = 2$, $A = 1$, $r_1 = 6.5$, $r_2 = 5$, $r_3 = 1.7$, $r_4 = 4$, $R_1 = 2$, $R_2 = 1$, $R_3 = 3$, $R_4 = 1$, the government rewards management cost is low, and tends to implement rewards to enterprises to reduce the operation cost. Enterprises with high cost of green manufacturing tend to choose non-green manufacturing to reduce costs. This time (reward, non-green production) has the ESS point.

Table 4 The result of (1, 0)

$(C_2 - C_1 - A\theta - B - R_3 - R_4) > 0$, $[(1-\theta)A + r_1 + r_3 - c_1 + c_2] > 0$	det J < 0, tr J Not sure	Saddle point
$(C_2 - C_1 - A\theta - B - R_3 - R_4) > 0$, $[(1-\theta)A + r_1 + r_3 - c_1 + c_2] < 0$	det J > 0, tr J < 0	Stability
$(C_2 - C_1 - A\theta - B - R_3 - R_4) < 0$, $[(1-\theta)A + r_1 + r_3 - c_1 + c_2] > 0$	det J > 0, tr J > 0	Instability
$(C_2 - C_1 - A\theta - B - R_3 - R_4) < 0$, $[(1-\theta)A + r_1 + r_3 - c_1 + c_2] < 0$	det J < 0, tr J Not sure	Saddle point

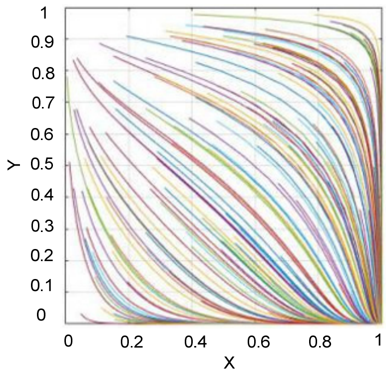

Fig. 3 (1, 0) evolutionary equilibrium

4. When $x = 1, y = 1$, as shown in Fig. 4, the determinant and trace of matrix J is:

$$\begin{cases} \det J = (C_2 - C_1 - A - \varphi B + R_1 + R_2)[(1-\theta)A + r_1 + r_3 - c_1 + c_2] \\ \operatorname{tr} J = (-1)(C_2 - C_1 - A - \varphi B + R_1 + R_2) + (-1)[(1-\theta)A + r_1 + r_3 - c_1 + c_2] \end{cases} \quad (24)$$

and the result is as shown in Table 5.

When the model parameters take the following values, respectively: $C_1 = 2$, $C_2 = 10$, $c_1 = 1$, $c_2 = 5$, $s = 0.5$, $f = 0.3$, $B = 2$, $A = 1$, $r_1 = 6.5$, $r_2 = 5$, $r_3 = 1.7$, $r_4 = 4$, $R_1 = 5$, $R_2 = 6$, $R_3 = 3$, $R_4 = 1$; the government rewards management cost is low, and tends to implement rewards to enterprises to reduce the operation cost. The cost of green manufacturing is not significantly higher than that of non-green manufacturing, so enterprises tend to choose green manufacturing to improve their social image and win government awards. The ESS point is recorded at this time (reward, non-green production).

Table 5 The result of (1, 1)

$(C_2 - C_1 - A - \varphi B + R_1 + R_2) > 0$, $[(1-\theta)A + r_1 + r_3 - c_1 + c_2] > 0$	$\det J > 0$, $\operatorname{tr} J < 0$	Stability
$(C_2 - C_1 - A - \varphi B + R_1 + R_2) > 0$, $[(1-\theta)A + r_1 + r_3 - c_1 + c_2] < 0$	$\det J < 0$, $\operatorname{tr} J$ Not sure	Saddle point
$(C_2 - C_1 - A - \varphi B + R_1 + R_2) < 0$, $[(1-\theta)A + r_1 + r_3 - c_1 + c_2] > 0$	$\det J < 0$, $\operatorname{tr} J$ Not sure	Saddle point
$(C_2 - C_1 - A - \varphi B + R_1 + R_2) < 0$, $[(1-\theta)A + r_1 + r_3 - c_1 + c_2] < 0$	$\det J > 0$, $\operatorname{tr} J > 0$	Instability

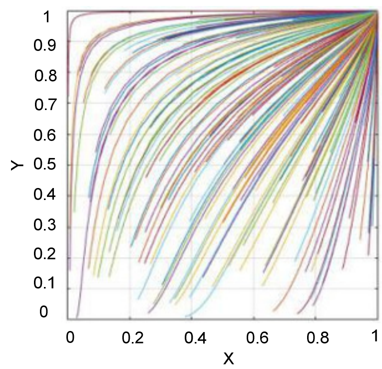

Fig. 4 (1, 1) evolutionary equilibrium

5. Then, at E, because $\operatorname{tr} J = 0$, there is no stable point.

4. Simulation analysis of the evolutionary game

(1) The influence of government reward on the evolutionary game between the two sides is as shown in Fig. 5.

The graph in Fig. 5 shows that compared with enterprises, the incentive value has a greater impact on the government. With the increase of the incentive value, the government's governance cost increases, and the incentive value can stimulate enterprises to maintain the status quo. However, due to the existence of a speculative effect, the government tends to reduce the incentive value, enterprises are stimulated by the incentive value, and non-green manufacturing tends to slow down.

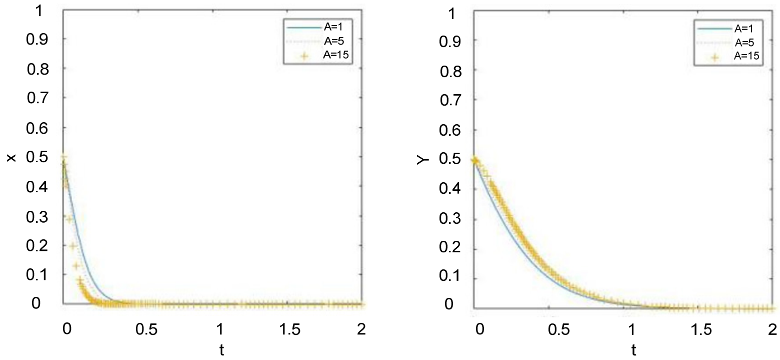

Fig. 5 Different government incentive intensities

(2) The influence of government punishment on the evolutionary game between the two sides is as shown in Fig. 6.

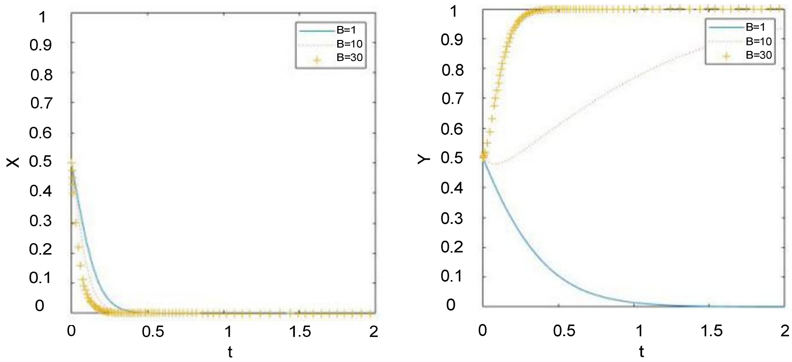

Fig. 6 Different government penalty intensities

The graph in Fig. 6 shows that with the increase of the punishment intensity, the government will quickly implement green manufacturing with the increase of the punishment, reducing the chances of being punished.

(3) The influence of government operating costs on the evolutionary game between the two sides is as shown in Fig. 7.

It can be seen from Fig. 7 that the government is more inclined to adopt a penalty strategy with the increase of operating cost of incentive strategy. Since the increase in government operating costs cannot directly affect enterprises, it has little impact on their green manufacturing strategies. With the increase of operating cost of punishment strategy, the government is more inclined to adopt an incentive strategy.

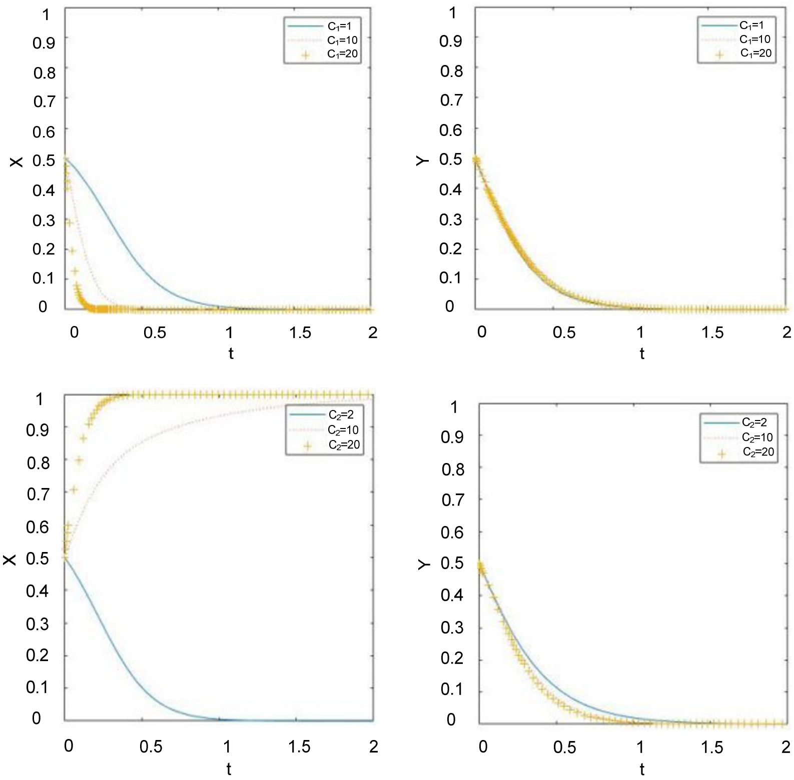

Fig. 7 Different government operating costs

(4) The influence of the change in government social reputation on the evolution game between the two sides is as shown in Fig. 8.

It can be seen from Fig. 8 that the increase of R_1 and R_2 in the social credibility of the government will slow down the government's punishment strategy, while the increase of R_3 and R_4 will lead to the government's tendency to adopt punishment strategy.

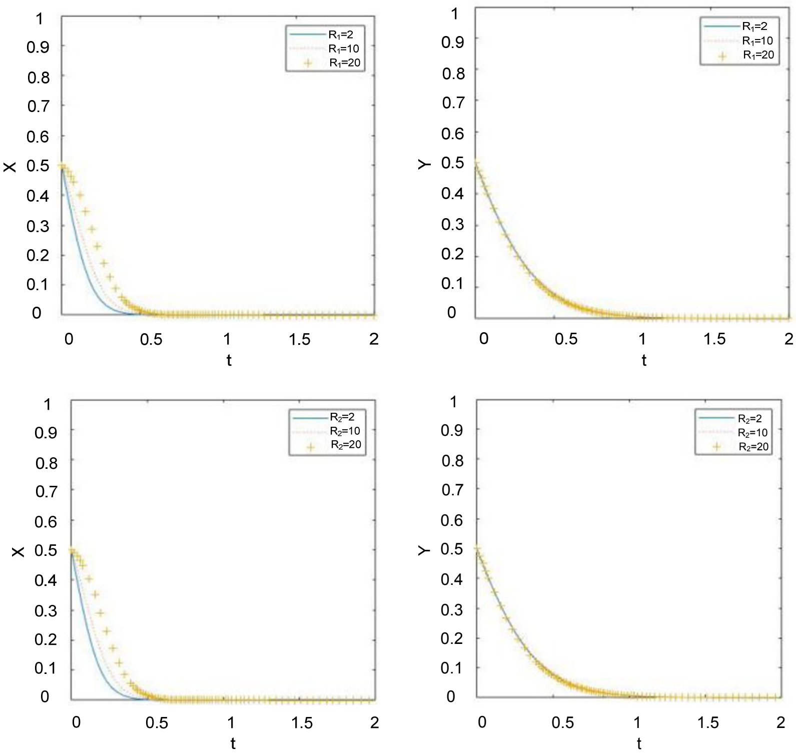

Fig. 8 Different social credibility of the government

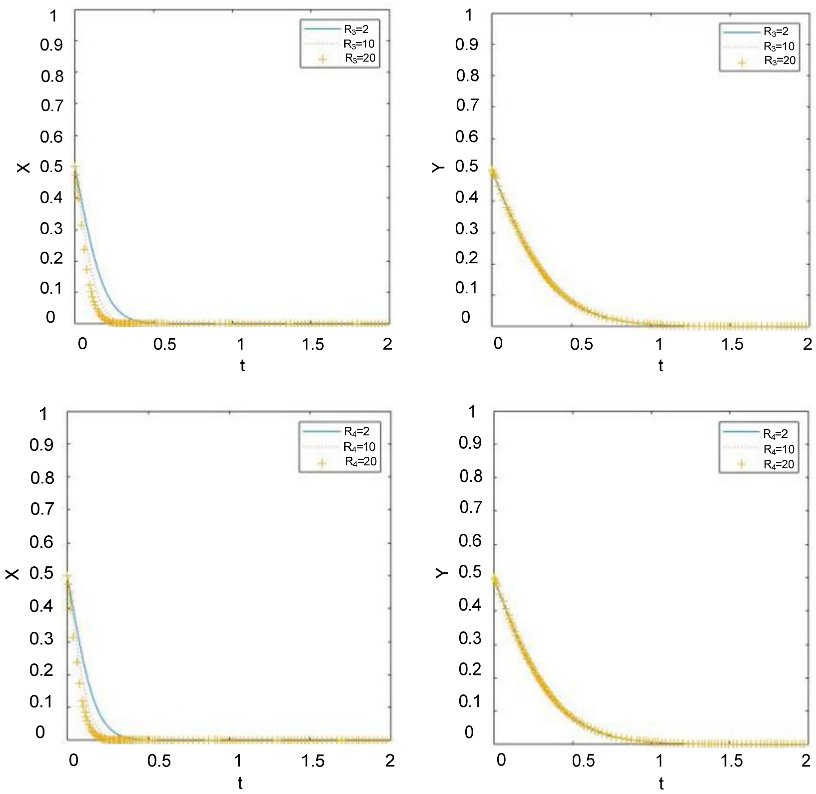

Fig. 8 Different social credibility of the government (continuation)

(5) The influence of the change in corporate social reputation on the evolutionary game between the two sides is as shown in Fig. 9.

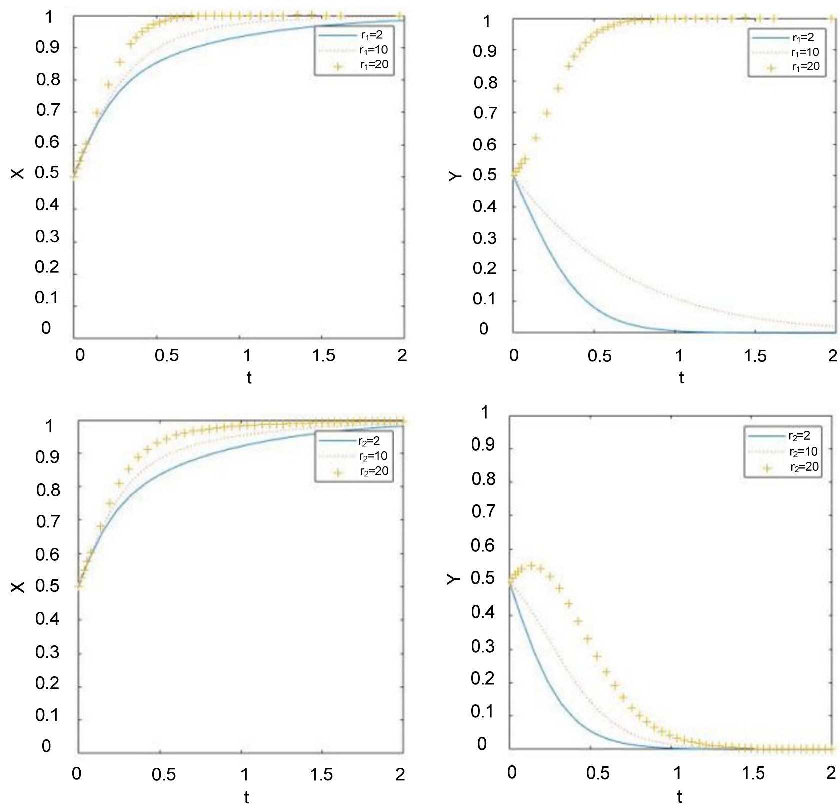

Fig. 9 Different social credibility of enterprises

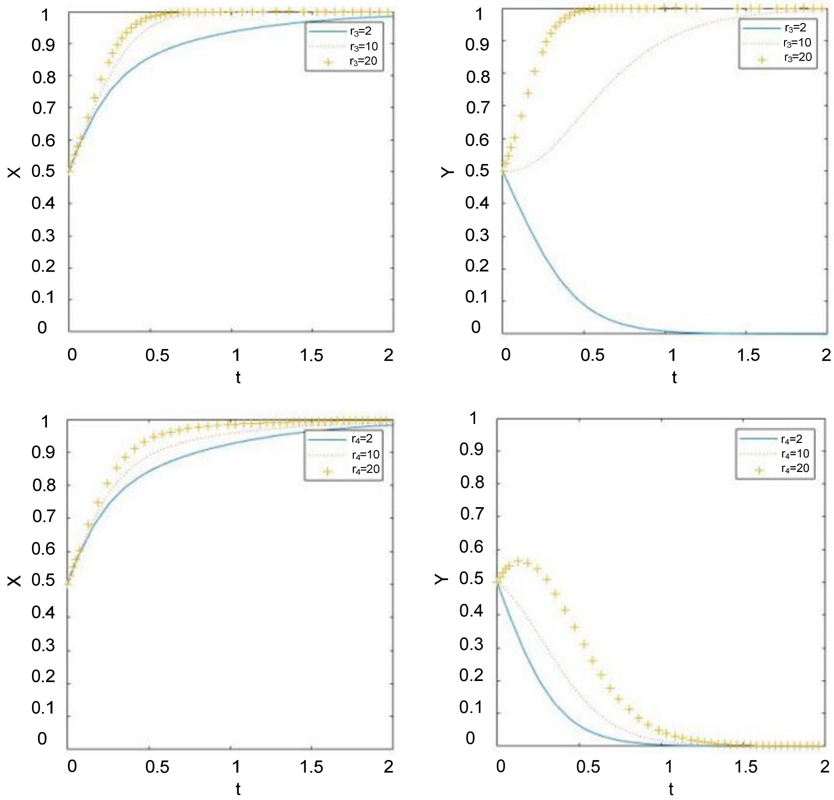

Fig. 9 Different social credibility of enterprises (continuation)

From Fig. 9, it shows that the increase of r_1, r_2, r_3, and r_4 in the social reputation of enterprises will stimulate the government to adopt incentive strategies for enterprises. r_3 is the fastest way to stimulate enterprises to adopt green manufacturing mode. Although r_1 is slower than r_3, it can still stimulate enterprises to adopt green manufacturing mode. The increase of r_2 and r_4 will lead enterprises to adopt green manufacturing mode, but after a long time, they will revert to non-green manufacturing mode.

(6) The influence of the cost of enterprises' green production cost on the evolutionary game between the two sides is as shown in Fig. 10.

As can be seen from the figure, with the increase of c_1 in green manufacturing operation cost, the government is inclined to take punitive measures to strengthen green production, but the change in the intensity of this measure is not obvious. With the improvement of c_1, enterprises will largely choose non-green manufacturing mode for production. With the increase of c_2 of non-green operating cost of enterprises, the government tends to choose incentive measures, but the change of the intensity of this measure is not obvious. With the improvement of c_2, enterprises will largely choose green manufacturing mode for production.

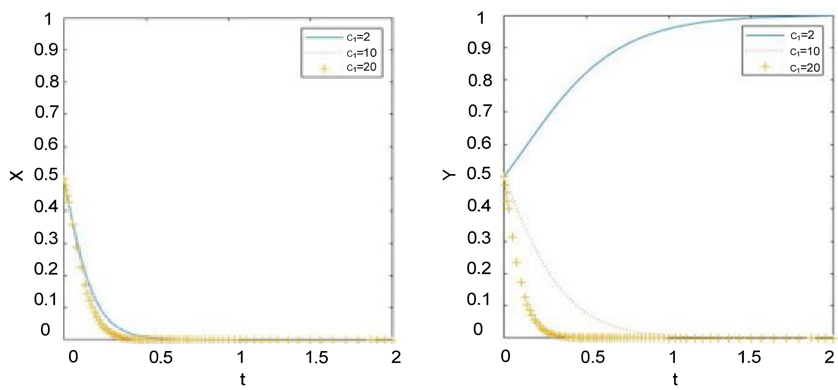

Fig. 10 Different manufacturing costs of enterprises

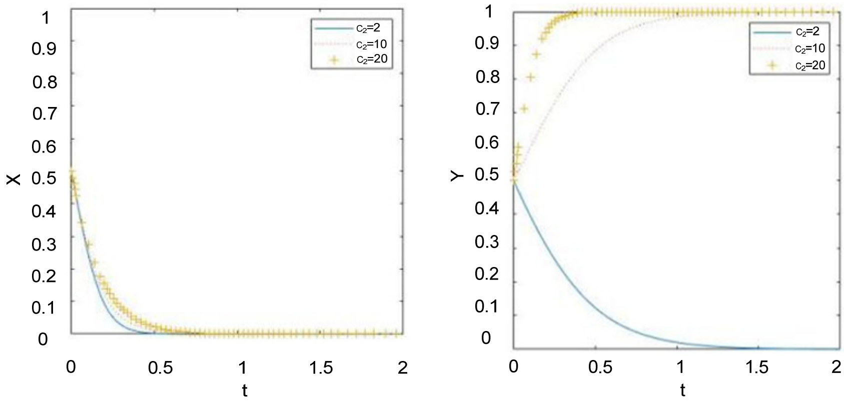

Fig. 10 Different manufacturing costs of enterprises (continuation)

(7) The influence of the false reward on the evolutionary game between the two sides is as shown in Fig. 11.

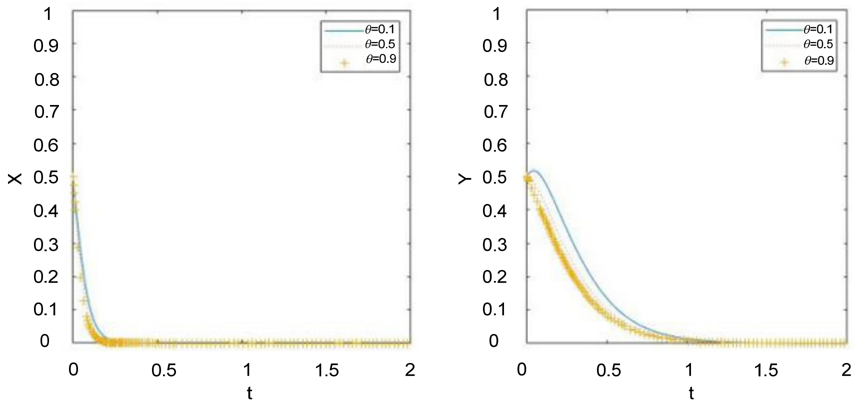

Fig. 11 Different error reward probabilities

From Fig. 11, it shows that, with the increase of possibility θ of the government's false reward, the government tends to choose punishment measures to avoid the waste of rewards, but the change of the intensity of this measure is not obvious. With the improvement of θ, enterprises will choose non-green manufacturing mode for production more quickly, so that they may get more government error rewards.

(8) The influence of the wrong punishment on the evolutionary game between the two sides is as shown in Fig. 12.

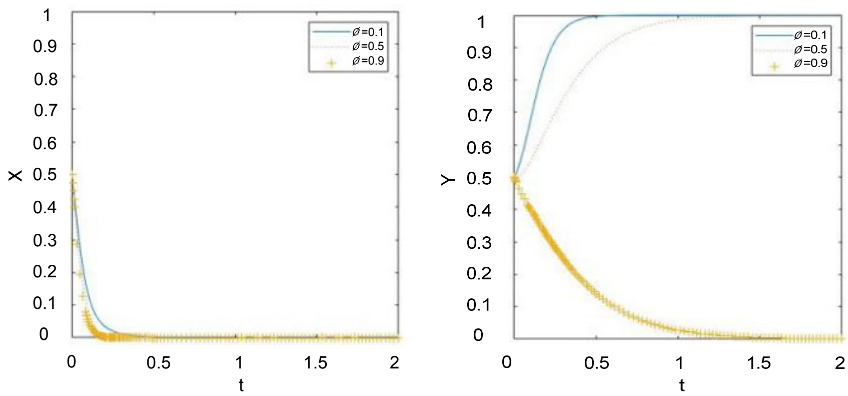

Fig. 12 Different error punishment probabilities

It can be seen from Fig. 12 that with the increase of possibility ϕ of government error punishment, the intensity of government punishment measures will increase, but the intensity of this measure also does not change significantly. With the improvement of ϕ, enterprises will choose non-green manufacturing mode for production more quickly, so as to reduce the possible government error penalty.

5. Conclusion

Through the simulation solution, it can be seen that the two evolutionary equilibrium points (0, 0) and (1, 1) passed through the parameter adjustment. It can be concluded that: the expansion of government incentives or penalties indicates the government's determination to recommend the development of green manufacturing mode. For enterprises, the increase of incentive value would increase the willingness to implement green manufacturing to a certain extent, but the increase of government penalty value would significantly increase their decision willingness to choose the green manufacturing mode. The change in government operating cost would seriously affect the decision of reward and punishment, however, it has little influence on the decision of enterprises. The change in social reputation plays a certain role in accelerating or decelerating the government's decision, however, it has a great influence on the decision of whether enterprises implement green manufacturing or not. Enterprises are most sensitive to the cost difference between green manufacturing mode and non-green manufacturing mode. The government's false reward has little influence on itself and enterprises, but the wrong punishment has a great influence on the enterprise and limited influence on the government. Therefore, from the perspective of the government, it is the best decision plan to strengthen the government that increase the punishment intensity of enterprises that violate the rules, increase the frequency of enterprise supervision, explore various forms of social reputation evaluation value of enterprises, and reduce the wrong punishment of enterprises by the government. From the perspective of enterprises, it is the best decision plan for enterprises that reduce the operating costs of green manufacturing mode by science and technology innovation, expand the popularity of green manufacturing mode, to improve the social reputation of enterprises.

The main contributions of this paper are as follows:

- Combination of reward and punishment into a model, which expands the previous model to measure the evolutionary game between government departments and enterprises only from one aspect of reward or punishment;
- Introduction of the error judging factor θ and ϕ of reward and punishment, making the model assumption closer to the actual situation;
- Through the simulation analysis of different parameters, this paper gives the government reward and punishment strategy, changes the value of influencing factors of enterprises' green manufacturing selection strategy, and influences the result of evolutionary game.

Acknowledgement

This study was financially supported by Liaoning Province Planning Office of Philosophy and Social Science (L18BJY029), the Liaoning Province Department of Education Project (WFGD2019001, WGD2016002), and Liaoning Provincial Federation Social Science Circles (2020lslktyb-069). The authors acknowledge the contribution of Liaoning Key Lab of Equipment Manufacturing Engineering Management, Liaoning Research Base of Equipment Manufacturing Development, Liaoning Key Research Base of Humanities and Social Sciences, Research Centre of Micromanagement Theory, and Shenyang Association for Science and Technology.

References

[1] Madani, S.R., Rasti-Barzoki, M. (2017). Sustainable supply chain management with pricing, greening and governmental tariffs determining strategies: A game-theoretic approach, *Computers & Industrial Engineering*, Vol. 105, 287-298, doi: 10.1016/j.cie.2017.01.017.

[2] Swami, S., Shah, J. (2013). Channel coordination in green supply chain management, *Journal of the Operational Research Society*, Vol. 64, No. 3, 336-351, doi: 10.1057/jors.2012.44.

[3] Zhu, W., He, Y. (2016). Green product design in supply chains under competition, *European Journal of Operational Research*, Vol. 258, No. 1, 165-180, doi: 10.1016/j.ejor.2016.08.053.

[4] Govindan, K., Azevedo, S.G., Carvalho, H., Cruz-Machado, V. (2015). Lean, green and resilient practices influence on supply chain performance: Interpretive structural modelling approach, *International Journal of Environmental Science and Technology,* Vol. 12, 15-34, doi: 10.1007/s13762-013-0409-7.

[5] Govindan, K., Khodaverdi, R., Vafadarnikjoo, A. (2015). Intuitionistic fuzzy based DEMATEL method for developing green practices and performances in a green supply chain, *Expert Systems with Applications*, Vol. 42, No. 20, 7207-7220, doi: 10.1016/j.eswa.2015.04.030.

[6] Tseng, M.-L., Islam, M.S., Karia, N., Fauzi, F.A., Afrin, S. (2019). A literature review on green supply chain management: Trends and future challenges, *Resources Conservation and Recycling*, Vol. 141, 145-162, doi: 10.1016/j.resconrec.2018.10.009.

[7] Kazancoglu, Y., Kazancoglu, I., Sagnak, M. (2019). A new holistic conceptual framework for green supply chain management performance assessment based on circular economy, *Journal of Cleaner Production*, Vol. 195, 1282-1299, doi: 10.1016/j.jclepro.2018.06.015.

[8] Micheli, G.J.L., Cagno, E., Mustillo, G., Trianni, A. (2020). Green supply chain management drivers, practices and performance: A comprehensive study on the moderators, *Journal of Cleaner Production*, Vol. 259, Article No. 121024, doi: 10.1016/j.jclepro.2020.121024.

[9] Rezaei, S., Maihami, R. (2020). Optimizing the sustainable decisions in a multi-echelon closed-loop supply chain of the manufacturing/remanufacturing products with a competitive environment, *Environment Development and Sustainability*, Vol. 22, No. 7, 6445-6471, doi: 10.1007/s10668-019-00491-5.

[10] Comăniţă, E.-D., Cozma, P., Simion, I.M., Roșca, M., Gavrilescu, M. (2018). Evaluation of eco-efficiency by multicriteria decision analysis. Case study of eco-innovated and eco-designed products from recyclable waste, *Environmental Engineering and Management Journal*, Vol. 17, No. 8, 1791-1804, doi: 10.30638/eemj.2018.178.

[11] González-Zapatero, C., González-Benito, J., Lannelongue, G. (2019). Effect of purchasing and marketing integration on new product development speed: The moderating role of environmental dynamism, *Advances in Production Engineering & Management*, Vol. 14, No. 2, 213-224, doi: 10.14743/apem2019.2.323.

[12] Ma, C., Liu, X., Zhang, H., Wu, Y. (2016). A green production strategies for carbon-sensitive products with a carbon cap policy, *Advances in Production Engineering & Management*, Vol. 11, No. 3, 216-226, doi: 10.14743/apem2016.3.222.

[13] Burinskiene, A., Lorenc, A., Lerher, T. (2018). A simulation study for the sustainability and reduction of waste in warehouse logistics, *International Journal of Simulation Modelling*, Vol. 17, No. 3, 485-497, doi: 10.2507/IJSIMM17(3)446.

[14] Hussain, S., Jahanzaib, M. (2018). Sustainable manufacturing – An overview and a conceptual framework for continuous transformation and competitiveness, *Advances in Production Engineering & Management*, Vol. 13, No. 3, 237-253, doi: 10.14743/apem2018.3.287.

[15] Mustata, I.C., Alexe, C.G., Alexe, C.M. (2017). Developing competencies with the general management II business simulation game, *International Journal of Simulation Modelling,* Vol. 16, No. 3, 412-421, doi: 10.2507/IJSIMM16(3)4.383.

[16] Huang, J.-H., He, S., Chen, Y., Yang, C.-H. (2017). Modelling of special equipment supervision game considering risk expectation, *International Journal of Simulation Modelling,* Vol. 16, No. 4, 670-681, doi: 10.2507/IJSIMM16(4)9.404.

[17] Friedman, D. (1991). Evolutionary games in economics, *Econometrica*, Vol. 59, No. 3, 637-666, doi: 10.2307/2938222.

APEM journal
Advances in Production Engineering & Management
Volume 15 | Number 4 | December 2020 | pp 431–440
https://doi.org/10.14743/apem2020.4.376
ISSN 1854-6250
Journal home: apem-journal.org
Original scientific paper

Using a discrete event simulation as an effective method applied in the production of recycled material

Knapčíková, L.[a,*], **Behúnová, A.**[b], **Behún, M.**[c]

[a]Technical University of Košice, Faculty of Manufacturing Technologies with a seat in Prešov, Department of Industrial Engineering and Informatics, Prešov, Slovak Republic
[b]Technical University of Košice, Faculty of Mining, Ecology, Process Control and Geotechnology, Institut of earth sources, Košice, Slovak Republic
[c]Technical University of Košice, Faculty of Mining, Ecology, Process Control and Geotechnology, Institut of earth sources, Košice, Slovak Republic

ABSTRACT

Technological processes play an essential task in the enterprise's production system. The behaviour and functioning of these systems cannot be predicted with certainty as they belong to a group of probable determinate structures. Generally, if we wanted to know precisely the behaviour of this condition in advance, we would have to be able to describe them mathematically or observe the action of the system on a real object. By applying discrete event simulation software, we realize the development of environmentally friendly products and using the simulation, we gain the certainty that the planned tasks can be implemented in a given time frame, while the simulation of the production process can help to clearly clarify and better understand the processes. To choose the optimal manufacturing ways of cleaning the fabrics component from waste tyres, we used the Witness discrete event simulation software to determine the usability and time occupancy of individual machines in the production of new fabric-based material. We simulated the ultrasonic method of cleaning the fabrics component from waste tyres and the subsequent creation of the test specimen. After the simulation, the obtained data can be used by a selection of type and number of machines and auxiliary equipment, by numbers of tools and fixtures, and by numbers of transport equipment. Obtained results bring the best layout of the workplace, the optimal dose of input materials and resources used in production. We have identified bottlenecks in the machines with long waiting times. The research priority was to reduce bottlenecks and increase the effectiveness of the entire of production line.

ARTICLE INFO

Keywords:
Green manufacturing;
Recycling;
Waste tyres;
Discrete event simulation;
Witness simulation software;
Economic impact;
Efficiency;
Ultrasonic separation

**Corresponding author:*
lucia.knapcikova@tuke.sk
(Knapčíková, L.)

Article history:
Received 12 August 2020
Revised 1 December 2020
Accepted 3 December 2020

1. Introduction

As a result of crucial cost following within each manufacturing process and logistics management, it is required to validate the feasible solutions of scheduled and innovation systems. Important is to look for successful and economical solutions during whole production monitoring [1]. It should be emphasized that the demands for changes in the enterprise still involve some risks. Many problems and dangers arise in the design and operation of complex logistics and production systems. A large number of variants and the complexity of their evaluation do not allow the manager to choose the optimal solution with classic tools [2].

It is through simulation software that it is possible to limit, reduce and limit these risks, by the fact that the simulation software can design the work environment and simulate the results of various conclusions within manufacturing processes [3, 4]. The advantages founded from using of application of the simulation have to be higher than the costs necessary to implement the simulation and improve the system; this is the priority of each simulation used in the manufacturing processes. Industry 4.0 focuses on the complete digitization of all physical assets and their integration into digital ecosystems [5] that communicate with each other, including partners throughout the value chain [6] as can be seen on Fig. 1. Nowadays, the priority is to transform the enterprise with the traditional point of view to a new type, which uses all the knowledge in the field of Industry 4.0, comprehensively in terms of enterprise's digitization, IoT, robotics and connecting the manufacturing enterprise with educational institutions into the one [7].

The certain standard for the simulation to be used in practice introduces a high impact of its use. When deciding whether or not to use simulation support, a simple rule applies – simulation is applicable if the direct benefits of simulation outweigh the simulation costs themselves [8]. It is known that in most cases, the aim of the simulation is not an immediate economic effect. Currently, the use of simulation is focused on increasing a specific market position [2, 8]. This applies to various areas, such as business logistics and supply chain management. This demonstrates functionality, performance or reliability [9]. The effect of simulation is greatly influenced by the time when simulation performed [10]. It is known that optimization by simulation is used at the beginning of the problem. Only in this way will we achieve positive results for the entire company, which will be reflected in the costs themselves, which are the lowest at this stage [11]. In the next step, specifically the introduction of the simulation itself, we have at our disposal the variability of the decision-making process that the simulation brings with it [4]. Quick and correct decisions at the beginning of the decision-making process have a significant impact on the overall result of the examined object [8]. Businesses also use green production strategies that apply, for example, to the principles of lean production, the development of new products that are more environmentally friendly or the use of recyclable, degradable or renewable materials [9, 12]. If green activities are introduced, savings or returns will be proven often in another area and over a more extended period of time [13-15]. If an enterprise invests in these activities, it will achieve efficient use of available resources, a rapid return on investment, increase sales, improve the corporate image and, last but not least, make it easier for new businesses to find new potential customers.

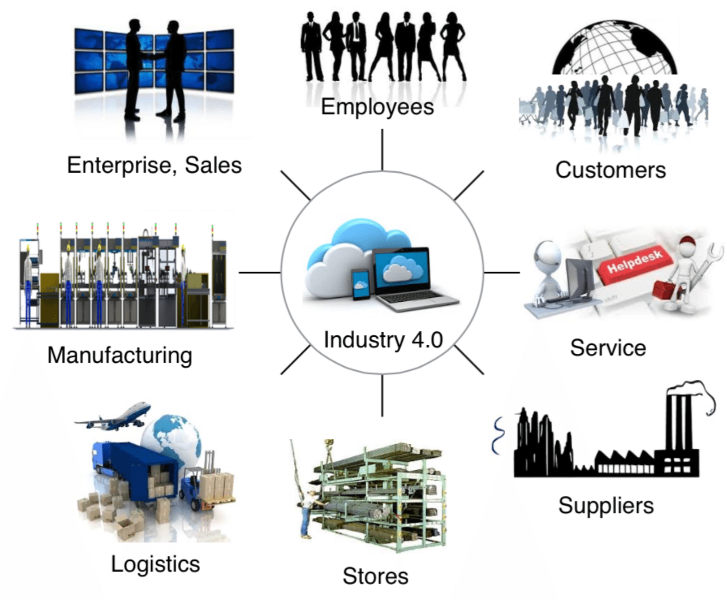

Fig. 1 Industry 4.0 concept [4]

2. Problem definition

Nowadays, the situation in Europe points to increased activity in the field of waste management of waste tyres. At present, waste treatment plants are motivated by the recycling system to recover in terms of environmental solutions [16, 17]. The research enterprises are trying to develop new, more suitable methods for processing waste tyres, as well as using well-known recovery methods and continually updating them. There is no point in using waste tyres philosophy for recycling only. At the beginning of the recycling process, we have to look for and find application possibilities for waste material in the industry. Recycling of waste tyres introduces several technical and technological challenges for recycling companies in all European Union Member States. In each Member State, enterprises involved in the collection and processing of information on the recovery or disposal of used tyres create a critical database [15]. Equally important is ETRA (European Tyre Recycling Association), which collects and elaborates information, processes it and ultimately evaluates and informs the population and other related companies about new opportunities [18, 19]. Simulation significantly helps in planning, management and continuous improvement of production processes. It is an essential help in increasing their productivity, efficiency and flexibility; especially flexibility as a response to the ever-changing requirements of customers in the conditions of global markets that becomes an advantage for companies using advanced technologies, like simulation software. Using discrete event simulation software [20] which we will use in the initial phase of the research, will focus on finding answers to questions presented in Fig. 2. The decision for using a discrete event simulation as a solving method we can see in the uncertainty of future production requirements, time pressure, limited financial resources and the unavailability of modern design tools [21]. Very often, it is challenging to talk about the overall optimization of system parameters. It often happens that there are already shortcomings in the project of the system, which will not allow the full use of all its possibilities [8, 22]. During the real-time monitoring operation presented in the following sections, it is necessary to solve the problems of additional system modifications, which is usually associated with a further increase in costs [9, 23]. The use of discrete event simulation is very suitable for solving the above-presented problems [12]. According to statistics, the area of transport, storage and handling employs up to 25 % of workers, occupies 55 % of the area and accounts for up to 87 % of the time the material spends in the company [15, 18]. These activities sometimes build up 15 % to 70 % of the total cost of the product and also significantly affect the quality of the products (up 3 % to 5 % of the material is degraded by improper transport, handling and storage) [18].

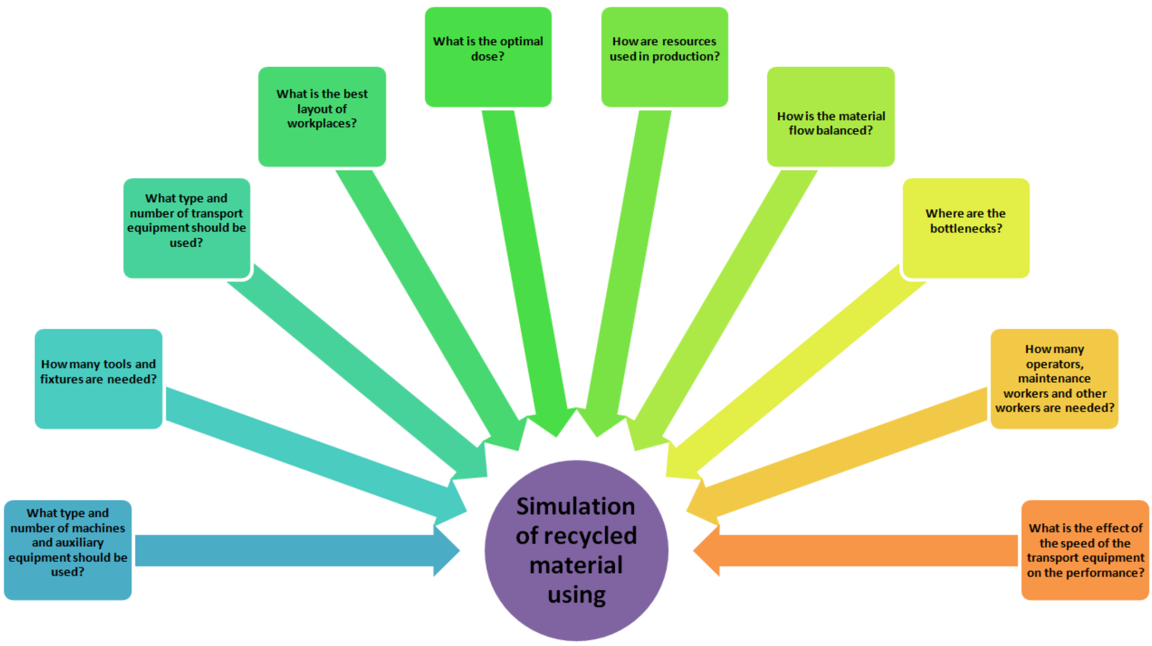

Fig. 2 Main questions about simulation possibilities by the research (Authors own processing)

Waste tyre as a key material

Every vehicle needs a complete replacement of all four tyres every 8 to 10 years. Of course, their wear depends mainly on several kilometre's rides and way of driving. Currently, industrial technologies are dedicated to improving and innovating technologies that deal with the processing of used tyres at the end of their lifetime [19]. In the traditional technological process, separation of three essential components is achieved:

- rubber (Fig. 3),
- steel (Fig. 3),
- fabrics fraction (Fig. 4).

The rubber accounts for about 56 % of the total volume of the separated parts of this commodity. Its other components are steel of about 10 %, fabrics which make up 34 % of the total amount of separated parts of waste tyres [24].

Fig. 3 Waste tyres components: left – rubber; right – steel (Authors own processing)

Fig. 4 Fabrics from waste tyres (Authors own processing)

3. Materials and methods

We used the Witness simulation software, which is the most successful simulation program for the simulation of manufacturing, service and logistics processes offered by the British company Lanner Group Ltd. (UK). The software is suitable for the simulation of discrete systems [25]. The Witness software allows not only the modelling of processes and procedures, it is helpful by visualization of the processes in the 3D view [4]. Still, we used software to select the optimum method for cleaning the fabrics component busyness of individual machines, in the manufacture of moulded test samples, using selected technologies of fabrics component and cleaning analysis of waste tyres (Table 1). Our priority was to use discrete event simulation software [23], in which it is possible to carry out experiments outside the real object and based on the obtained results to propose possible solutions applicable in practice. We can say that simulation is experimenting with a computer model of an entire production system that aims to optimize the production process [19, 26]. The cleaning process [27] of the fabrics component was carried out by the ultrasonic method. The search for optimal solutions by model-based methods is referred to as simulation-based optimization [20].

Table 1 Input parameters of simulation process (Authors own processing)

Name of Process	Fabric from waste tyres	Matrix	Mixtures (fabrics + matrix)	Composites
No. of entered materials	1	1	1	1
No. of assemble	1	1	1	0
Work in process	0	0	0	1
Average work in process	0.98	0.98	0.01	0.00
Average time [s]	1495.00	1495.00	20.00	3.00

Simulation software support used by fabric's cleaning process

The input materials by the investigation are fabrics from waste tyres. Using the ultrasonic separation (Fig. 5), we cleaned the impurities into structures. This separation method is based on the action of the ceramic oscillator. The ceramic oscillator oscillates on the underside of the bath (the bath is filled with liquid) and causing the energy. The result is cavitation effect [27-29]. Material manufactured in this way from the fabrics itself is polyvinyl butyral (PVB) as a thermoplastic matrix to the final product as a composite material [28, 29].

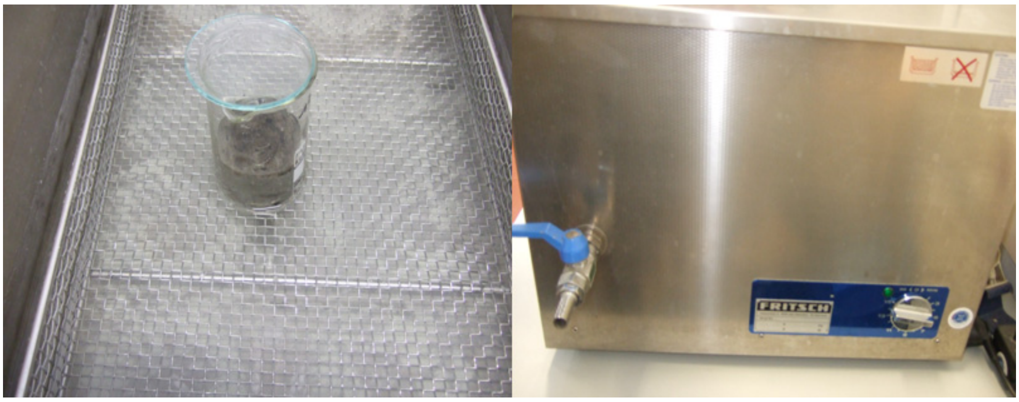

Fig. 5 Ultrasound cleaning process of fabrics from waste tyres: left – sample of fabrics inside equipment; right – ultrasound equipment Fritsch, Germany (Authors own processing)

4. Results and discussion

Using simulation software, which we used in the initial phase of research, we focused on finding answers to questions about material flow and type and number of machines and auxiliary equipment, type and amount of transport equipment (Table 2). The input data from Table 2 is based on a 50:50 material ratio (50 % of fabrics and 50 % PVB matrix). The average work activity for a specific technological process for fabrics and PVB is 98 %. The average technological process times for these commodities are 1495.00 seconds. Table 2 shows the input parameters for operators' work that are transformed into a graphical representation, during their work.

Graphical representation of labour statistics is shown in Fig. 6. From the graph, it can see average job time for each operator. Operator 1 is a crucial employer, deals with the separation process of waste fabrics by 1440.00 seconds. Operators 2 and 3 are excluded from the statistical report because are numbered as a help force (non-full-time employers). Operator 4 works with homogenization equipment. Operator 5 has 0.00 seconds average job time, it is meant only for equipment services. By manipulations with the final product (including all necessary logistics work), our operator spent an average job time of 20.00 seconds.

Table 2 Input parameters of simulation process (Authors own processing)

Name	Operator 1	Operator 4	Operator 5	Operator 6
%Busy	94.86	3.62	0.00	1.32
%Idle	5.14	96.38	100.00	98.80
Quantity	1	1	1	1
Jobs started	1	1	0	1
Jobs ended	1	1	0	1
Average job time (s)	1440.00	55.00	0.00	20.00

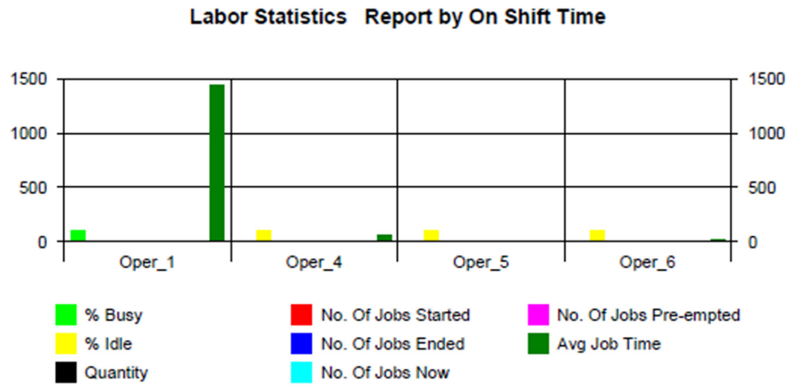

Fig. 6 Statistics evaluation of operators by the ultrasound cleaning method (Authors own processing). Legend: Oper_1 – separation process of waste fabrics; Oper_4 – empty of homogenization's equipment; Oper_5 – moulding process of composites; Oper_6 – manipulation with the final product

Table 3 Part statistics by used conveyors (Authors own processing)

Name	Conveyor 1	Conveyor 2	Warehouse
Total in	1	1	1
Total out	1	1	0
Now in work	0	0	1
Avg. size	0.00	0.95	0.00
Avg. time [s]	2.00	1440.00	20.00

The utilization of conveyors in the simulation of this production process is assumed only at the end of the whole process, it is mean after pressing the board and its transport to the warehouse [26]. However, it is the manual activity of the worker. Table 3 shows the processing of conveyor data used in the individual manufacturing operations, which are preceded by separation by the ultrasonic method.

In the ultrasonic method, the containers were used mainly for material handling for individual operations. The part "Total in" means the total amount of unique components entering the process, also the other items in Table 4 have a value of 1, which represents a value for one particular material, mixture, i.e. for one specific product. The values of 1440.00 seconds belong to fabric's cleaning process. The values 20.00 seconds are by Conveyor 1 and by transporting of product to the warehouse before final control [27]. The cleaning process provided on the one technology equipment located directly on the simulated workplace.

Fig. 7 presents a simulation of material flow in the work environment of Witness software. One of the main advantages of using computer simulation in our research was the ability to simulate the processes mentioned above at the required time [26, 27]. The simulation of the real time necessary in a computer simulation only takes a few minutes [28]. After performing the simulation process, we kept the possibility of reports, based on which it is possible to verify the validity of the required main goal of the simulation, which was defined in Section 2. Through advanced models, it is possible to find the optimal solution under specified limiting conditions in a short time.

Table 4 Part statistics by used buffers (Authors own processing)

Name	Buffer 1	Buffer 2	Warehouse
Total in	1	1	1
Total out	1	1	0
Now in work	0	0	1
Average size	0.00	0.95	0.00
Average time (s)	0.00	1440.00	0.00

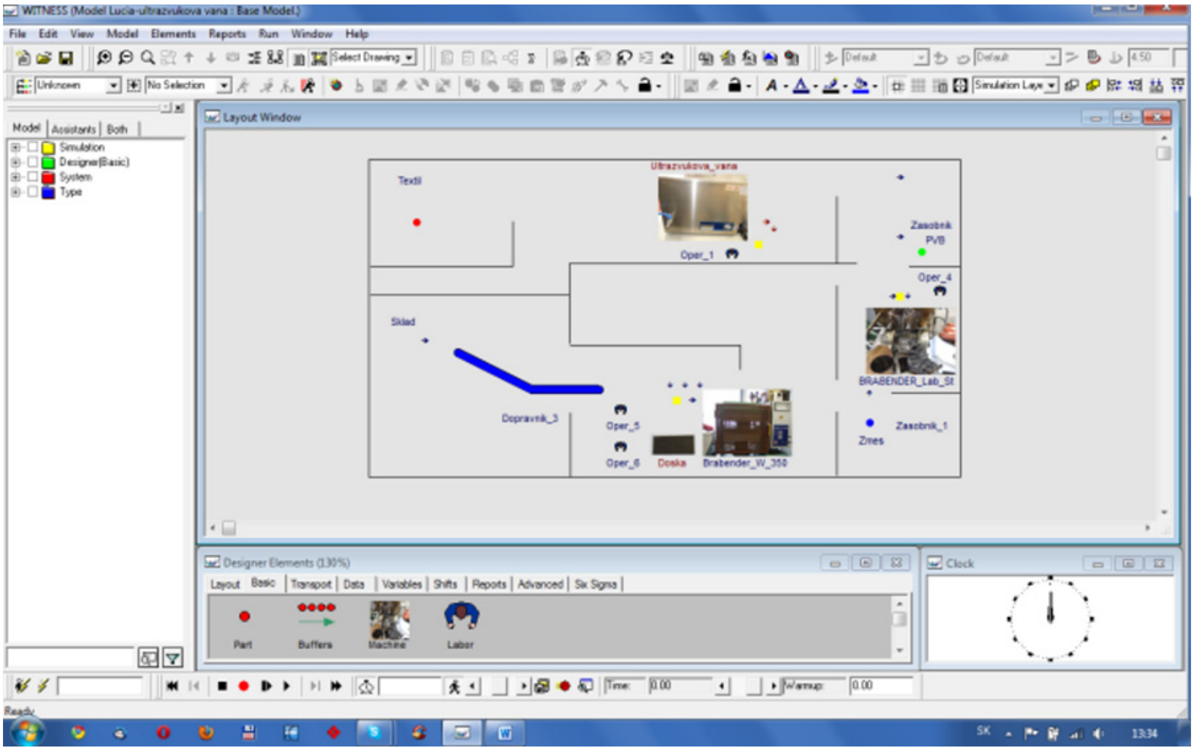

Fig. 7 Ultrasound cleaning process used simulation software Witness – simulated manufacturing process (Authors own processing)

Optimization of the production system requires constant attributes of production requirements, which do not lead to the overall optimization of the system in times of uncertainty of future production requirements, time pressure and lack of financial capital for design tools [30]. Problems arising during operation need to be solved by additional system modifications, which result in increased costs [29]. We can avoid this problem by using Witness discrete event simulation, which will allow a more in-depth examination to occur and significantly reduce the risk [31, 32].

The presented paper used the Witness discrete event software, which can effectively model the critical elements present in the new modern enterprise and industrial systems, as follows:

- manufacturing systems (fabrics separation from waste tyres/cleaning process),
- their internal processes (separation, mixture process of two main components and moulding technology),
- logistics operations (material flow, operators activities, buffers, warehouse logistics),
- available material flow analysis.

After realised investigation, we can answer the question mentioned in the problem definition stage, by the beginning of the research (Table 5). Economic point of view is visible in every step of simulation creation [33]. The modelling itself takes place in a discrete-time. It can be used to design various scenarios of production processes, from which the simulation outputs choose the most suitable in terms of overall optimization of material consumption and operating costs [34].

Intelligent manufacturing systems [31, 33, 35] are at the forefront in which knowledgeable information agents form a network of decentralized and distributed intelligence [36]. Decentralization and distribution of control are equally significant in the case of intra-logistics processes of manufacturing enterprises.

Table 5 Summary results after simulation (Authors own processing)

Summary results	
Problem definition	After the simulation process
What type and number of machines and auxiliary equipment should be used?	• 2 × Conveyor belts • 2 × Buffers • 1 × Ultrasound equipment • 1 × Homogenization equipment • 1 × Moulding equipment
How many tools and fixtures are needed?	• Cleaning • Homogenization • Press moulding
What type and number of transport equipment should be used?	• Band conveyors
What is the best layout of workplaces?	• Best layout of the workplace is presented in Fig. 6, after the simulation process
What is the optimal dose?	• The optimal dose for cleaned material is, according to input data: 1 for fabric-filler, 1 PVB-matrix, 1 mixture, 1 final product-test sample
How are resources used in production?	• Use of recycled material by the production of new material • Waste tyres fabrics • Recycled PVB
How is the material flow balanced?	• Product and by-product (relevant only for organizations that produce a physical product) • Non-product Outputs (Waste and Emissions/Pollutants).
Where are the bottlenecks?	• For production lines, we monitored the percentage utilization of each production unit. The machine that uses the highest percentage of its capacity is an obstacle. • The machine operates at full capacity while working as a bottleneck and limits other production units to a lower capacity utilization rate. • Machine with long waiting times. • We need to increase the capacity of the bottleneck and thus increase the size of the entire production line.
How many operators, maintenance workers and other workers are needed?	• 1x Operator by input materials and manipulation works • 1x Operator by ultrasound cleaning process • 1x Operator by homogenization • 1x Operator by press moulding
What is the effect of the speed of the transport equipment on the performance?	• Conveyor belts provide a speed that can be calculated as the linear distance travelled by a point on the conveyor belt in one minute.

5. Conclusion

Intelligent manufacturing system provides the necessary information infrastructure for the proper functioning of used technologies. In addition to automation and subsequent autonomization of activities, these solutions increase the agility of individual operations [36].

Our proposed production process of cleaning fabrics from waste tyres becomes more flexible and better respond to external stimuli (customers, markets) with the possibility of more significant variability of the resulting product or service. The summary of the most essential inputs and outputs of used simulation software is presented in Table 6.

Advantages of our research we see in minimizing of productions times by homogenization of the mixture and pressing samples and less human intervention in the whole production process in comparison with work without simulation of material flow. Regarding this issue, we can expect less spoilages, optimized distribution ways, better energy and money flow. Last but not least is the environmental impact.

Using Witness discrete event simulation software, we used Icons to create a production system model. The icons formed our "Menu" from which we selected icons that corresponded to the required element of cleaning the fabric from waste tyres. The simulation model created by us can visually precisely communicate to what is required from practice. In the future, we plan to expand our research by adding a third dimension to virtual memory using a simulation model that is created in two-dimensional space. The display of the production line using virtual reality will thus expand the possibility of a visual approach to the simulation model of reality.

Table 6 Evaluation of the use of simulation in the cleaning process of fabrics from waste tyres (Authors own processing)

Strengths of simulation	Weaknesses of simulation
• Fast verification of the simulation process without the need for real time • Detection of restrictions • Enough reports to verify the simulation target • Ease of simulation, with no programming required	• The need to know the researched object and the relationships between entities • Simplification of the model • Failure to anticipate employee behaviour • Higher start-up costs • Methodological complexity
The simulation allows	**The simulation does not allow**
• Solving analytically unsolvable tasks • Examine system dynamics • Temporal and spatial comparison • Disclosure of new facts • Decision support at different levels of decision making • System improvements • Cost savings in various areas of the enterprise	• Replacing a person in the decision-making process • Complete production management • Accuracy of data with incorrect parameters • Automatic system optimization • Result if the goal is not defined

References

[1] Lambert, D.M., Stock, J.R., Ellram, L.M. (2000). *Logistika*, Computer Press, Prague, Czech Republic.

[2] Drastich, A. (2017). Optimization of material flow by simulation methods, *Acta Logistica,* Vol. 4, No. 4, 23-26, doi: 10.22306/al.v4i4.76.

[3] Fabricators & Manufacturers Association, International. For Bridgestone's sustainability, zero landfill is where the rubber meets the road, from *https://www.fmamfg.org/blog/bridgestones-sustainability-zero-landfill-rubber-meets-road*, accessed February 14, 2020.

[4] Industry 4.0. From *http://www.emyras.com/industry-4-0/*, accessed July 28, 2020.

[5] Lalinská, J., Kremeňová, I. (2011). Green logistics, In: *Proceedings of 12th International Scientific Conference LOGI 2011*, Košice, Czech Republic, 252-257, from *https://journals.vstecb.cz/wp-content/uploads/2017/02/2011-1.pdf*, accessed July 24, 2020.

[6] Zhang, Y.M., Huang, G.H., He, L. (2011). An inexact reverse logistics model for municipal solid waste management systems, *Journal of Environmental Management,* Vol. 92, No. 3, 522-530, doi: 10.1016/j.jenvman.2010.09.011.

[7] Sidora, J. (2019). Green logistics, from *https://www.ipaslovakia.sk/clanok/green-logistika*, accessed November 25, 2019.

[8] Tavakoli, M.M., Haleh, H., Mohammadi, M. (2018). A mathematical model for scheduling of production process and allocation of an automatic guided vehicle in a flexible manufacturing system, *International Journal of Engineering Systems Modelling and Simulation,* Vol. 10, No. 2, 125-131, doi: 10.1504/IJESMS.2018.091937.

[9] Trebuna, P., Pekarcikova, M., Edl, M. (2019). Digital value stream mapping using the Tecnomatix plant simulation software, *International Journal of Simulation Modelling,* Vol. 18, No. 1, 19-32, doi: 10.2507/IJSIMM18(1)455.

[10] Rosova, A. (2010). Indices system design of distribution logistics, transport logistics and materials flow as parts of controlling in enterprise's logistics, *Acta Montanistica Slovaca,* Vol. 15, No. 1, 67-72.

[11] Bai, C., Sarkis, J. (2010). Integrating sustainability into supplier selection with grey system and rough set methodologies, *International Journal of Production Economics,* Vol. 124, No. 1, 252-264, doi: 10.1016/j.ijpe.2009.11.023.

[12] Erol, I., Sencer, S., Sari, R. (2011). A new fuzzy multi-criteria framework for measuring sustainability performance of a supply chain, *Ecological Economics,* Vol. 70, No. 6, 1088-1100, doi: 10.1016/j.ecolecon.2011.01.001.

[13] Crawford, R.J. (1987). *Plastics engineering,* 2nd edition, Pergamon Press, Oxford, England, doi: 10.1002/zamm.19890691016.

[14] Harper, C.A. (2000). *Modern plastics handbook,* 1st edition, McGraw-Hill Professional, New York, USA.

[15] Abdallah, T., Farhat, A., Diabat, A., Kennedy, S. (2011). Green supply chains with carbon trading and environmental sourcing: Formulation and life cycle assessment, *Applied Mathematical Modelling,* Vol. 36, No. 9, 4271-4285, doi: 10.1016/j.apm.2011.11.056.

[16] Straka, M., Rosová, A., Lenort, R., Besta, P., Šaderová, J. (2018). Principles of computer simulation design for the needs of improvement of the raw materials combined transport system, *Acta Montanistica Slovaca*, Vol. 23, No. 2, 163-174.
[17] Wang, F., Lai, X., Shi, N. (2011). A multi-objective optimization for green supply chain network design, *Decision Support Systems,* Vol. 51, No. 2, 262-269, doi: 10.1016/j.dss.2010.11.020.
[18] Straka, M., Khouri, S., Rosova, A., Caganova, D., Culkova, K. (2018). Utilization of computer simulation for waste separation design as a logistics system, *International Journal of Simulation Modelling,* Vol. 17, No. 4, 583-596, doi: 10.2507/IJSIMM17(4)444.
[19] Vasiliev, V.V., Morozov, E.V. (2001). *Mechanics and analysis of composite materials,* 1st edition, Elsevier Science, Oxford, United Kingdom.
[20] Knapčíková, L. (2011). *Optimizing of technological processes by plastics recovery,* Doctoral thesis, Faculty of Manufacturing Technologies of the Technical University of Košice with the seat in Prešov Prešov, Slovakia.
[21] Ivanov, V.A., Feshchenko, A.A. (2019). Simulation of parts manufacturing in the enterprise mechanical-repair department, *Journal of Physics: Conference Series,* Vol. 1333, No. 9, Article No. 072007, doi: 10.1088/1742-6596/1333/7/072007.
[22] Okoro, E.E., Iwuajoku, S., Sanni, S.E. (2020). Performance evaluation of biodiesel produced from waste tire pyrolytic oil as a lubricant additive in oil drilling systems, *Recycling,* Vol. 5, No. 4, Article No. 29, doi: 10.3390/ recycling5040029.
[23] Rupnik, B., Nardin, R., Kramberger, T. (2019). Discrete event simulation of hospital sterilization logistics, *Tehnički Vjesnik – Technical Gazette*, Vol. 26, No. 5, 1486-1491, doi: 10.17559/TV-20180614102011.
[24] Knapčíková, L., Herzog, M., Oravec, P. (2010). Material characterization of composite materials from used tires, *Manufacturing Engineering,* Vol. 2010, No. 4, 31-34.
[25] Václavík, V., Daxner, J. (2020). Recovery material use by building insulation (Recyklát slouží při zateplení staveb), from *http://www.enviweb.cz/*, accessed January 10, 2020.
[26] Taranu, N., Banu, D., Oprisan, G., Budescu, M., Bejan, L. (2013). Strengthening of thin reinforced concrete slabs with composite strips, *Romanian Journal of Materials*, Vol. 43, No. 1, 3-13.
[27] Schürmann, H. (2001). *Konstruieren mit faser-kunststoff-verbunden,* Springer, Berlin, Germany.
[28] Dupláková, D., Hatala, M., Duplák, J., Radchenko, S., Steranka, J. (2018). Direct metal laser sintering – Possibility of application in production process, *SAR Journal,* Vol. 1, No. 4, 123-127, doi: 10.18421/SAR14-01.
[29] Telišková, M., Török, J., Dupláková, D., Kaščák, J., Mezencevová, V., Birčák, J. (2018). Non-destructive diagnostics of hard-to-reach places by spatial digitization, *TEM Journal*, Vol. 7, No. 3, 612-616, doi: 10.18421/TEM73-18.
[30] Sandin, G., Peters, G.M. (2017). Environmental impact of textile reuse and recycling – A review, *Journal of Cleaner Production,* Vol. 184, 353-365, doi: 10.1016/j.jclepro.2018.02.266.
[31] Chryssolouris, G. (2006). *Manufacturing systems: Theory and practice,* 2nd edition, Springer-Verlag, New York, USA.
[32] Müller, M. (2015). Hybrid composite materials on basis of reactoplastic matrix reinforced with textile fibres from process of tyres recyclation, *Agronomy Research,* Vol. 13, No. 3, 700-708.
[33] Zajac, J., Dupláková, D., Hatala, M., Goldyniak, D., Poklemba, R., Šoltés, P. (2019). The effect of used fillers on the strength characteristics of polymer concrete test bodies, *TEM Journal,* Vol. 8, No. 3, 795-800, doi: 10.18421/TEM83-14.
[34] Mohajerani, A., Burnett, L. Smith, J.V., Markovski, S., Rodwell, G., Rahman, M.T., Kurmus, H., Mirzababaei, M., Arulrajah, A., Horpibulsuk, S., Maghool, F. (2020). Recycling waste rubber tyres in construction materials and associated environmental considerations: A review, *Resources Conservation and Recycling,* Vol. 155, Article No. 104679, doi: 10.1016/j.resconrec.2020.104679.
[35] Liu, J., Teng, Y., Wang, D., Gong, E. (2019). System dynamic analysis of construction waste recycling industry chain in China, *Environmental Science and Pollution Research,* Vol. 27, No. 30, 37260-37277, doi: 10.1007/s11356-019-06739-x.
[36] Kuo, Y.-H., Kusiak, A. (2019). From data to big data in production research: The past and future trends, *International Journal of Production Research,* Vol. 57, No. 15-16, 4828-4853, doi: 10.1080/00207543.2018.1443230.

APEM journal

Advances in Production Engineering & Management **ISSN 1854-6250**
Volume 15 | Number 4 | December 2020 | pp 441–452 Journal home: apem-journal.org
https://doi.org/10.14743/apem2020.4.377 Original scientific paper

Effect of glass and carbon fibres on the compressive and flexural strength of the polymer concrete composite

Petruška, O.[a], Zajac, J.[a], Dupláková, D.[a,*], Simkulet, V.[a], Duplák, J.[a], Botko, F.[a]

[a]Technical University of Košice, Faculty of Manufacturing Technologies with a seat in Prešov, Institue of Advanced Technologies, Prešov, Slovak Republic

A B S T R A C T

This article is focused on testing the mechanical properties of polymer concrete testing samples. After a thorough literature search, the basic conditions of the research were determined and under the standards, three types of samples of special new concrete mixtures were created as a building element for special CNC machines. The samples were subjected to the research of the influence of used fillers, binders and additives on their properties. Testing was carried out in a certified laboratory and included checking the dimensions of the test bodies, weighing on the calibrated weight, determining the volumetric weight, determining the maximum load of the testing samples using special devices and then determining the compressive strength, or flexural tensile strength according to the relevant formulas. The final part of the testing also examined the morphology and mapping of the chemical composition with a focus on carbon, oxygen and aluminum using an electron microscope. The obtained results clearly show an increase in tensile and compressive strength using dispersed carbon fibre reinforcement of approximately 4 MPa. The conclusion of the article provides an overall summary of the results obtained and a summary of the features.

A R T I C L E I N F O

Keywords:
Concrete composite;
Polymer concrete;
Compressive strength;
Flexural strength;
Glass fibres;
Carbon fibres

**Corresponding author:*
darina.duplakova@tuke.sk
(Dupláková, D.)

Article history:
Received 21 January 2019
Revised 30 November 2020
Accepted 3 December 2020

1. Introduction

The structures of machines used for machining have to correspond to the increasing performance and dynamic parameters, namely the stiffness and damping parameter. At present, materials such as steels and cast irons are conventionally used in these constructions to meet the rigidity requirements, but they are characterized by low damping [1-3]. If the machine has a high dynamic, these conventionally used materials are not able to adequately absorb the impact from the drive. The impacts make the machine vibrations, which are perceived as a negative impact throughout the production process. One option to eliminate the vibrations of machines made of steel or cast iron is to replace the construction materials [4-5]. One of the possible materials that the existing problem could eliminate is polymer concrete. This material is essentially a composite material [6-7] and it is characterized by the synergistic effect, which means that the value of the properties of the resulting composite material is higher than the sum of the properties for each component separately. This special material is a combination of binder, filler and other suitable admixtures. The particular ingredients achieve the desired properties for a particular use. Since polymer concrete is composed of natural materials which can be recycled at the end of the casting life, this material becomes a modern non-conventional material [8-10].

Many experts are dedicated to the research of polymer concrete mixtures. The study of microstructure and mechanical properties with the creation of the quantitative characterization methodology for concrete containing polymeric fibres was discussed by a team of authors Trofimov *et al.* [11]. Authors Tanyilizi and Asilturk in their research paid attention to the strength properties of polymers containing phosphazene during the exposure to high temperatures. This study utilized the Taguchi L-25 method (5 (5)), which reduced the number of experiments to find parameters influencing the experimental results. Research has shown that polymer concrete can favourably effect on the structure of buildings that are exposed to high temperatures under determined conditions [12]. Strength analysis and determination of deformation characteristics of methyl methacrylate modified vinyl ester were studied in 2018. In this study, attention was paid to curing temperatures as the test variable. After the research, it was found that the increased modulus of MMA decreases the modulus of elasticity and the heat of solidification [13]. The research by Simsek and Uygunoglu was focused on mechanical properties, workability and thermal properties of polymers, namely polycarbonate, thermoplastic polyurethane and polybutylene terephthalate mixed concrete. During the research, they were selected and optimized special properties by using full factorial design through Minitab software [14]. In the current research, attention was also paid to the analysis of the increase in elasticity of epoxy polymer concrete with short natural fibres, namely sisal fibres and ramie fibres [15]. In the field of civil engineering, it was researched flexural efficiency in the polymer concrete with the basalt fibre. The testing evaluated the compression and flexural properties, cracks, stresses and disturbances. Based on the experiments carried out, it was developed the guidelines for sea-sand concrete beams with basalt fibre bar-reinforced [16]. In the Materials Journal, there was presented research focused on the creation and evaluation of microstructure, mechanical and physical properties of recycled glass aggregate additive implemented in polymer concrete. Recycled glass fractions were added to the individual mixtures, with the most appropriate physical and mechanical properties being achieved by applying a 50 % recycle deposit to the polymer concrete mixture [17]. The thermal and mechanical properties of the glass-fibre polymer concrete composite were also described by Schmitt *et al*. This paper was focused on the experimental investigation of sandwich panels made of polymer-fibre material with glass fibre adhesion and polystyrene insulation layer. The panels were subjected to extreme experimental conditions, with a significant change in the insulation layer resulting in a reduction in total stiffness and load capacity [18]. The issue of the influence of the basalt, ash and silica sand on the mechanical properties of the polymer-concrete material was also addressed in the paper published in the Bulletin of Materials Science. The paper describes the study of the production of these polymers and the optimization of the weight percent of the epoxide resin, silicon sand, ultra-fine ash and basalt [19]. A team of authors Burlacu *et al*. in their research focused on testing the polymer concrete made from polystyrene granules. During the study, the impact of the granules on the mixture density, compressive strength, bending strength and tensile strength was analysed. The results obtained showed a decrease in mechanical properties by increasing the substitution dose of polystyrene granules [20]. Research of the production and assessment of physical, mechanical and thermal properties of various mixtures were discussed by many authors such as [21-31].

As can be seen in the previous survey of the research, the research of the properties of polymer concrete is currently carried out by a large number of experts. However, as can be seen from the above-mentioned survey, these studies are rather focused on building engineering and not on the field of research into the construction of machinery and equipment. The present paper provides a preview of the mechanical properties of the mixtures with a focus on the field of engineering - specifically on the field of construction of machines. The main contribution of the article lies in the determination and presentation of the obtained properties of newly created materials, which will serve as an elementary building element in the design solution for special CNC machines used for machining parts using DMLS technology.

2. Material and methods

Twelve test samples were produced, representing 3 types of the composition of the mixture. These test samples were tested for compressive strength and flexural tensile strength. According to STN EN 12390-3, at least 3 test bodies of the same composition have to be tested to make the measurement (experiment) statistically significant. For this reason, 3 test bodies of each type of composition were produced. This is a total of 9 test samples that have been tested for compressive strength. Three further test samples, one of each kind, were tested for flexural tensile strength. The test samples according to STN EN 12390-1 have the shape of a cube, cylinder and prism. This standard includes standardized dimensions, tolerances and types of moulds. For the compression strength tests, they have produced test cubes with 150×150×150 mm dimensions. For tensile strength tests, prism-shaped test pieces of 100×100×500 mm were produced.

Both organic (natural) and inorganic (artificial) fillers were used as testing samples. The organic fillers included silicate sand and gravel with the parameters shown in Table 1.

The 6 mm glass and 3 mm carbon fibres in the form of dispersed reinforcement were used. The matrix was the epoxy resin CHS-EPOXY 324 and hardener TELATIT 0492. The properties of the resin and hardener used are described in Table 2.

The advantages of the binder system (matrix) are excellent adhesion, high thermal and chemical resistance and high strength. Tables 3 and 4 illustrate the properties of the binder system used during the production and / cured system properties measured after 7 days hardening at 23 °C and hardening for 2 hours at 120 °C.

The system resists diluting mineral acids (hydrochloric acid 10 %, nitric 10 %, sulfur 30 %), an alkaline solution (sodium hydroxide 40 %, ammonia 10 %), water, gasoline, oil and diesel oil. It does not resist organic acids (acetic acid 5 %, milk 10 %).

Table 1 Organic fillers

Name	Type	Fraction size (mm)
STJ 25	Silica powder	0.06-0.31
ST06/12	Silica Sand	0.63-1.2
ST PBT 4	Silica grit	2-4

Table 2 Properties of CHS-EPOXY 324 resin and TELATIT 0492 hardener

Name	Property	Value	Unit
CHS-EPOXY 324	Viscosity – at temperature 25 °C	20-60	Pa·s
	Epoxy index	3-3.4	$mol·kg^{-1}$
	Epoxy mass equivalent	294-333	$g·mol^{-1}$
	Colour	maximum 300	j·Hazen
TELATIT 0492	Viscosity at temperature 23 °C	15-30	mPa·s
	Density at temperature 23 °C	0.93-0.96	$g·cm^{-3}$
	Aminic equivalent	550-600	mg $KOH·g^{-1}$
	Hydrogen equivalent	minimum 49	$g·mol^{-1}$
	Colour	maximum 3	Gardner

Table 3 Properties of bending and hardening system during the production

Bending system	Max. exotherm	Jellify time	Processability time
	(°C)	(hod)	(min)
CHS-EPOXY 324/TELATIT 0492	118	3	50-70
Hardening system	Modulus of rigidity	Strength in flaking	Tensibility
	(MPa)	$(N·cm^{-1})$	(%)
CHS-EPOXY 324/TELATIT 0492	25	14	3

Table 4 The ratios of the ingredients in the test samples

Testing samples No. 0623-0001, No. 0623-0002, No. 0623-0003 and No. 0623-0010		
Filler 70 %	48 %	ST PBT 4
	28 %	06/12
	18 %	STJ 25
	6 %	Carbon fibre (3 mm)
Binder 30 %	100 portions	CHS-EPOXY 324
	16 portions	TELATIT 0492
Testing samples No. 0623-0004, No. 0623-0005, No. 0623-0006 and No. 0623-0011		
Filler 70 %	48 %	ST PBT 4
	28 %	06/12
	18 %	STJ 25
	6 %	Glass fibre (6 mm)
Binder 30 %	100 portions	CHS-EPOXY 324
	16 portions	TELATIT 0492
Testing samples No. 0623-0007, No. 0623-0008, No. 0623-0009 and 0623-0012		
Filler 70 %	50 %	ST PBT 4
	30 %	06/12
	20 %	STJ 25
Binder 30 %	100 portions	CHS-EPOXY 324
	16 portions	TELATIT 0492

3. Experimental setup, results and discussion

Plastic moulds of standardized dimensions were used for casting, and each type of composition was cast from a single production batch to ensure complete compliance of the individual components in all test samples. First, the batch processing and mixing of the fillings was performed to ensure that the components were evenly distributed throughout the volume. Thereafter, batch processing and mixing of CHS-EPOXY 324 epoxy resin and TELATIT 0492 hardener were performed using a hand-held electric blender for 3 minutes. Subsequently, the filler was added to the binder (the matrix) under constant mixing. This process lasted for another 5 minutes to completely lubricate the filler and ensure the best adhesion. Then, casting into plastic moulds and vibrating the moulds on the vibration table was done to optimize compaction and removal of air bubbles. It took 2 minutes. Subsequently, the moulds were filled onto the work table and after 24 hours the polymers were cast from these moulds. Test assemblies were then stored in a curing room at 23 ± 1 °C with relative humidity 65 ± 5 % for 20 days.

Testing samples were tested by the Technical and Testing Institute in the accredited testing laboratory. The test samples were tested 20 days after the date of manufacture to have a hardening time of 15 days from the casting process. During the experiment, there were performed 9 compression strength tests and 3 flexural tensile tests. The room temperature was 19 ° C and the relative humidity was 60 %. Testing of test samples was carried out according to STN EN 12390-1. This standard defines, in particular, the possible shapes of the test samples, their standardized sizes and allowed variations in the length of the walls, perpendicularity and planarity. All test samples have passed shape and dimension control. Fig. 1 shows dimension measurement using a Mitutoyo ABSOLUTE AOS 500 calibrated digital scroll gauge. The device provides the measurement accuracy up to a measured length of a maximum 200 mm within ± 0.02 mm. The Mitutoyo ABSOLUTE AOS 500 was also used to measure the length of the prism, but a large measuring range, namely 0 mm to 600 mm, with a precision of ± 0.05 mm.

Fig. 1 Dimension inspection of the test sample

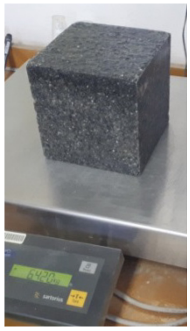

Fig. 2 Weighing of testing samples

Additionally, weighing the test samples (Fig. 2) and determining the volumetric weight – this part of the experiment was done according to the standard STN EN 12390-7. In the experiment, the method was realized by calculating the measured dimensions due to that dimension measurement was necessary for the previous part to check the test samples. From the measured dimensions, the volume of the test samples was calculated and then the weights were taken. This was done on a Sartorius®-EA150-FEG-l high-resolution digital calibrated scale. This device can weigh samples with a maximum weight of 150 kg, accuracy of weighing is within ± 5 g and has a weighing area made of galvanized steel measuring 500×400 mm.

Based on the determined volume of testing samples and measured weigh, the volumetric weight was calculated according to the formula:

$$D = \frac{m}{V} \tag{1}$$

where: D – the volumetric weight of testing sample (kg/m^3), m – weight of testing sample (kg), V – the volume of the testing sample (m^3).

The obtained results of volumetric weight are round of 10 according to standard STN EN 12390-7. In Table 5, there is presented the measured sizes, weight and volumetric weight of testing samples.

Table 5 Specification of testing samples

Sample	Sample number	Dimension			Weight	Volumetric
		Push area (mm)		Height (mm)	(kg)	weight (kg/m^3)
Cube	0623-0001	150.8	150.1	150	6.420	1890
	0623-0002	152.1	150.1	150	6.630	1940
	0623-0003	151.9	150.0	150.0	6.470	1890
	0623-0004	151.5	150.0	150.1	6.320	1850
	0623-0005	150.1	150.7	150.6	6.380	1860
	0623-0006	152.7	150.1	150.0	6.355	1850
	0623-0007	151.6	149.8	149.9	6.560	1930
	0623-0008	152.0	150.1	150.2	6.570	1920
	0623-0009	151.9	150.2	150.0	6.625	1940
Prism		Width	Height	Length		
	0623-0010	101.2	100.3	499.6	9.430	1860
	0623-0011	102.5	100.4	499.8	9.435	1840
	0623-0012	102.6	100.2	500.0	9.985	1940

3.1 Execution of compression strength test, and obtained results

Then the compression strength was measured according to STN EN 12390-3. Testing was carried out on the CONTROLS, model: 50-C0050/HRD7 with a maximum load of 3000 kN, and machine weight 1140 kg which is shown in Fig. 3.

The testing sample was positioned on the lower pressing plate of the press machine so that the deviation from the centre was not more than ± 1 % of the length of the edge of the cube. The test sample was turned in such a way that the compressive force applied perpendicularly to the direction in which the polymer was placed into the mould, i.e. the top surface of the casting on the side. A constant test load rate of 0.6 MPa/s was then set. After the initial load, the sample was loaded according to a set speed until the maximum load was reached. According to the

Fig. 3 Compressive strength testing

standard, the movable upper pushing surface stops after reaching it, then rises to a zero position, and assesses whether the type of failure of the test piece complies with the standard. The standard image contains both satisfactory and unsatisfactory types of test sample breaks. The tested samples did not have a visible break as the test press automatically recorded the maximum load possible and returned to the initial position. Subsequently, the compressive strength of the test samples was determined according to the equation:

$$f_c = \frac{F}{A_C} \tag{2}$$

where: f_c – Compressive strength (MPa), F – total force at break (N), A_C – section of a testing sample (mm^2).

In Table 6, there is presented the results of compressive strength testing.

Table 6 Compressive strength for testing samples

Testing sample	Maximum pushing force (kN)	Compressive strength (MPa)		
		Calculated value	Round value ± U ($k = 2$)	Average value
0623-0001	1775.4	78.45	78.5 ± 0.9	
0623-0002	1829.0	80.10	80.1 ± 1.0	79.00
0623-0003	1787.8	78.44	78.4 ± 0.9	
0623-0004	1657.6	72.96	73.0 ± 0.9	
0623-0005	1705.3	74.68	74.7 ± 0.9	70.23
0623-0006	1442.7	62.97	63.0 ± 0.8	
0623-0007	1751.2	77.12	77.1 ± 0.9	
0623-0008	1719.7	75.37	75.4 ± 0.9	75.26
0623-0009	1673.1	73.35	73.3 ± 0.9	

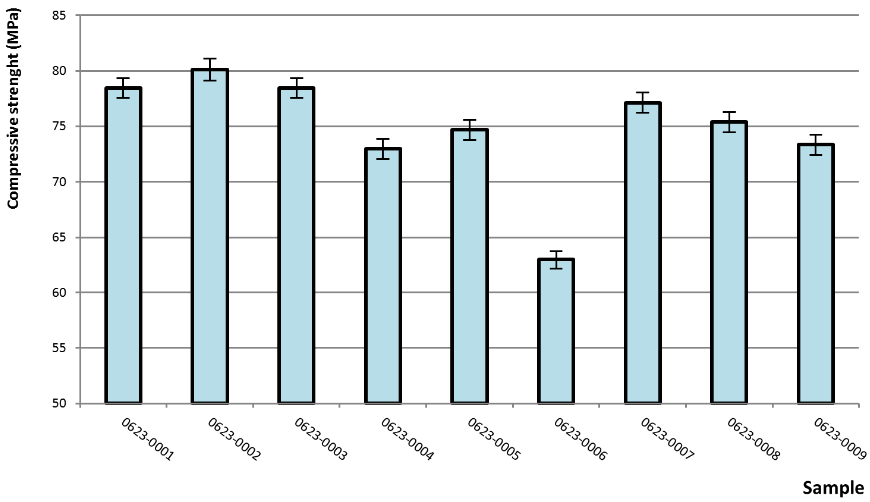

Fig. 4 Graphical representation of compressive strength for individual samples of polymer concrete mixture

Fig. 4 shows individual values of compressive strength of polymer concrete samples. As can be observed from figure values of compressive strength are in the range from 63 MPa to 85 MPa. Different types of reinforcement influence polymer concrete mechanical properties.

Fig. 5 shows comparison compressive strength for different mixtures of polymer concrete. As can be observed from the figure above the compressive strength of polymer concrete samples for the same reinforcement is in a very small interval. Highest compressive strength was measured for samples with short carbon fibre reinforcement. Also, good results for compressive strength testing were obtained for samples without fibre reinforcement. Values were slightly lower compared to carbon fibre reinforced samples. Samples prepared using glass fibre shows higher dispersity of compressive strength values. In this case, it can be stated that this type of reinforcement negatively influences the compressive strength of polymer concrete mixture.

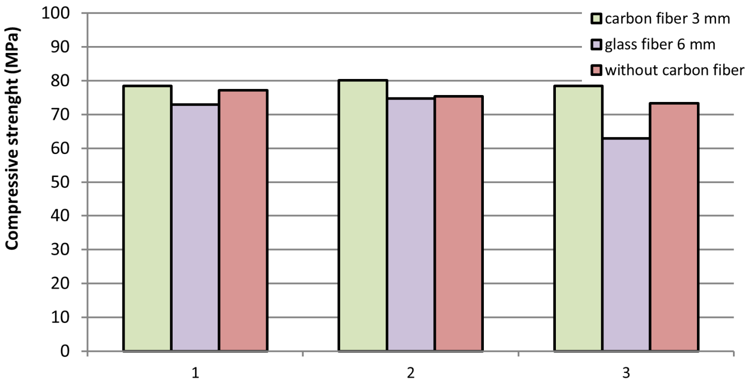

Fig. 5 Comparison of compressive strength of polymer concrete mixtures

3.2 Execution of flexural tensile test, and obtained results

In the second experiment, there was realised flexural strength according to EN 12390-5. Testing was executed by CONTROLS 50-C1201 machine which is shown in Fig. 6. This test machine has a special frame designed to minimize deformation at maximum pressure, resulting in high measurement accuracy. Technical parameters of the machine: maximum load 100 kN, maximum vertical distance 182 mm, maximum horizontal distance 720 mm, the distance between upper rollers 100 mm, 150 mm or 200 mm, the distance between bottom rollers adjustable from 50 mm to 900 mm, machine dimensions 950×1000×981 mm, and weight 175 kg.

Before the experiment, the spacing of the upper load rollers and the lower support rollers of steel with circular cross-sections and a diameter of 40 mm was set. The length of the rollers was 300 mm, so they met the test condition that they must protrude from the test sample at least 5 mm on both sides of the print area. They also met the requirements that they freely rotate around their axes and were moved in a perpendicular area to the longitudinal axis of the test sample. Roller surround was set according to the scheme presented in Fig. 7.

Fig. 6 Flexural strength testing

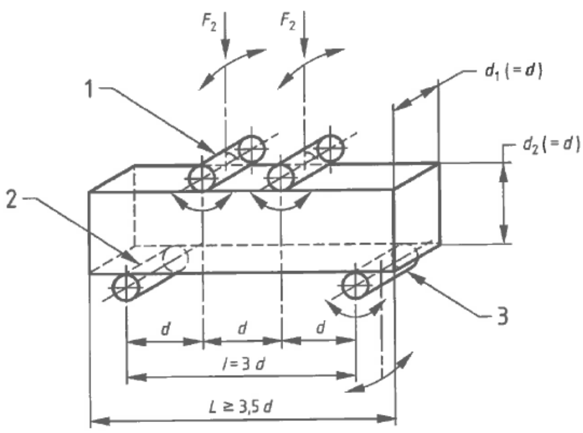

Fig. 7 Load layout scheme of testing sample

Fig. 8 Load layout scheme

Then, the sample was centrally positioned in the press machine by a longitudinal axis perpendicular to the longitudinal axes of the upper and lower rollers. The test body has been rotated so that the reference direction of loading is perpendicular to the direction in which the polymer was placed into the mould, i.e. the top surface of the casting on the side. A constant load rate of 0.05 MPa/s was then set. After the initial load, the sample was loaded at a set speed until the maximum load was reached. Achieving this boundary caused a transversal break of the test body, Fig. 8.

After the experiment, it was determined by the tensile strength at the bending of the test bodies according to the equation:

$$f_{cf} = \frac{F \cdot l}{d_1 \cdot d_2^2} \tag{3}$$

where: f_{cf} – flexural strength (MPa/s), F – maximum load (N), l – distance between supporting rollers (mm), d_1, d_2 – cross-section dimension of testing sample (mm).

In Table 7, there are presented the results of flexural strength testing.

Fig. 9 shows a comparison of flexural strength for samples prepared using carbon fibre reinforcement, glass fibre reinforcement and without fibre reinforcement. Highest flexural strength was observed for the sample prepared using carbon fibre reinforcement. Difference between the sample with glass fibre reinforcement and without reinforcement was 1 MPa.

Table 7 Flexural strength for testing samples

Testing sample	Maximum pushing force (kN)	Flexural strength (MPa) Round value ± U (k = 2)
0623-0010	83.99	24.8 ± 0.4
0623-0011	76.67	22.3 ± 0.4
0623-0012	72.18	21.0 ± 0.4

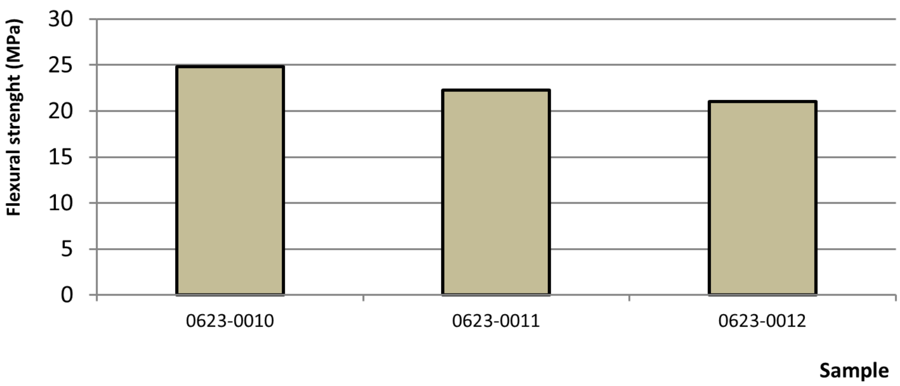

Fig. 9 Comparison of flexural strength of polymer concrete mixtures

3.3 Morphology of fracture area

The Tescan Mira 3 electron microscope observed for determination of the morphology of the fracture area. Samples for observation were carbon-cured to maintain the conductivity of the electron beam transition. Figs. 10, 11, and 12 show the observed samples of the polymer-composite composite at magnifications of 80×, 400×, and 2000×.

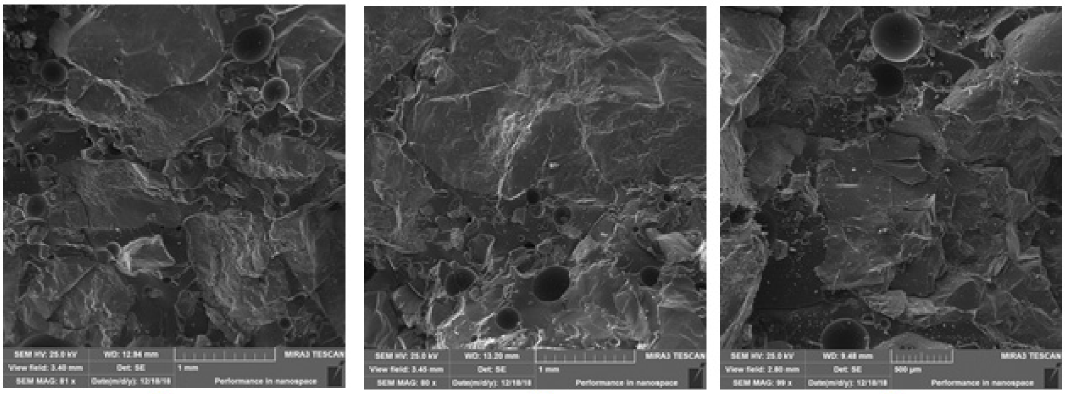

a) b) c)

Fig. 10 Polymer concrete composite with: a) sand, b) carbon fibres, c) glass fibers (magnification 80×)

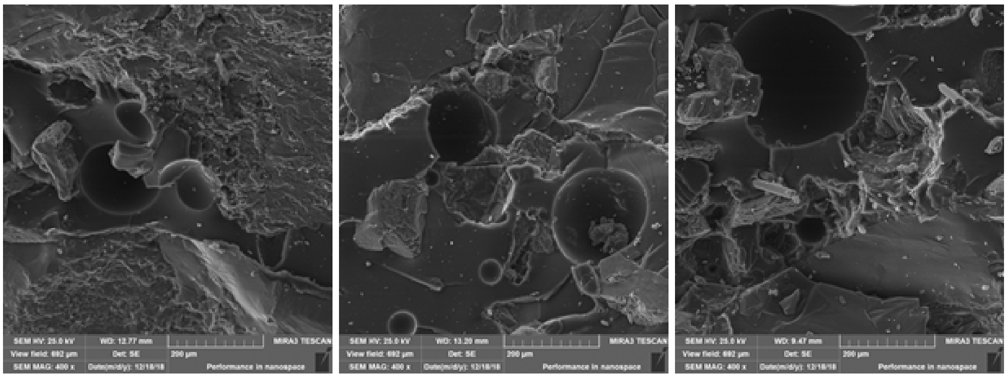

a) b) c)

Fig. 11 Polymer concrete composite with: a) sand, b) carbon fibres, c) glass fibers (magnification 400×)

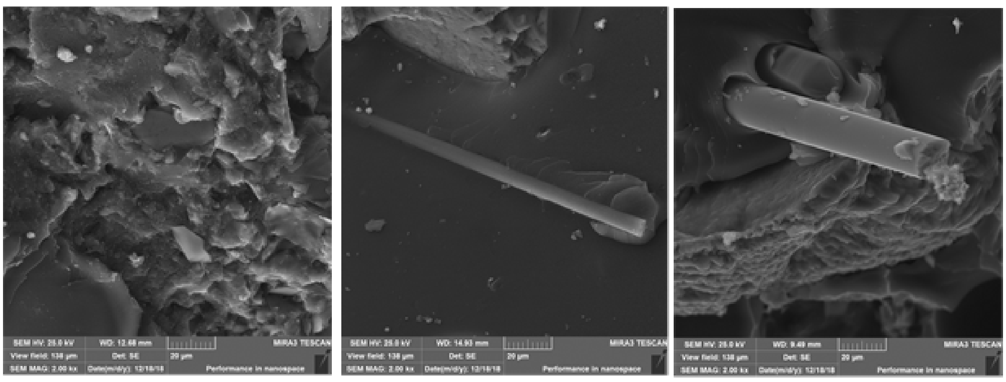

a) b) c)

Fig. 12 Polymer concrete composite with: a) sand, b) carbon fibres, c) glass fibers (magnification 2000×)

In the case of the second and third type samples, the reinforcing fibre used is visible at higher magnification. In both cases, the fracture area is visible; it is here to see the places of aggregate in various shapes (spherical and sponge-shaped). At a magnification of 400×, a hole in the resin is also visible, indicating the presence of air cavities in the polymerization process or by tearing of particles of aggregate. The reinforcing carbon fibres used are sufficiently coated with resin. In the case of the use of glass fibres, they were partly touching aggregates (Fig. 12c).

Observations also revealed the distribution of the material by mapping the chemical composition – carbon, oxygen, and aluminium. In the sample of the first type, silicon also showed us, suggesting the use of sand. With the same magnification observed, Fig. 13 shows a visible distribution of filler and binder. The binder of the resinous form is represented by a red colour containing the carbon component. The aggregate as filler contains oxygen, aluminium, and silicon, shown in blue and green below. Oxygen has a lower presence, suggesting an associated silicon and aluminium component in the form of SiO_2 and Al_2O_3.

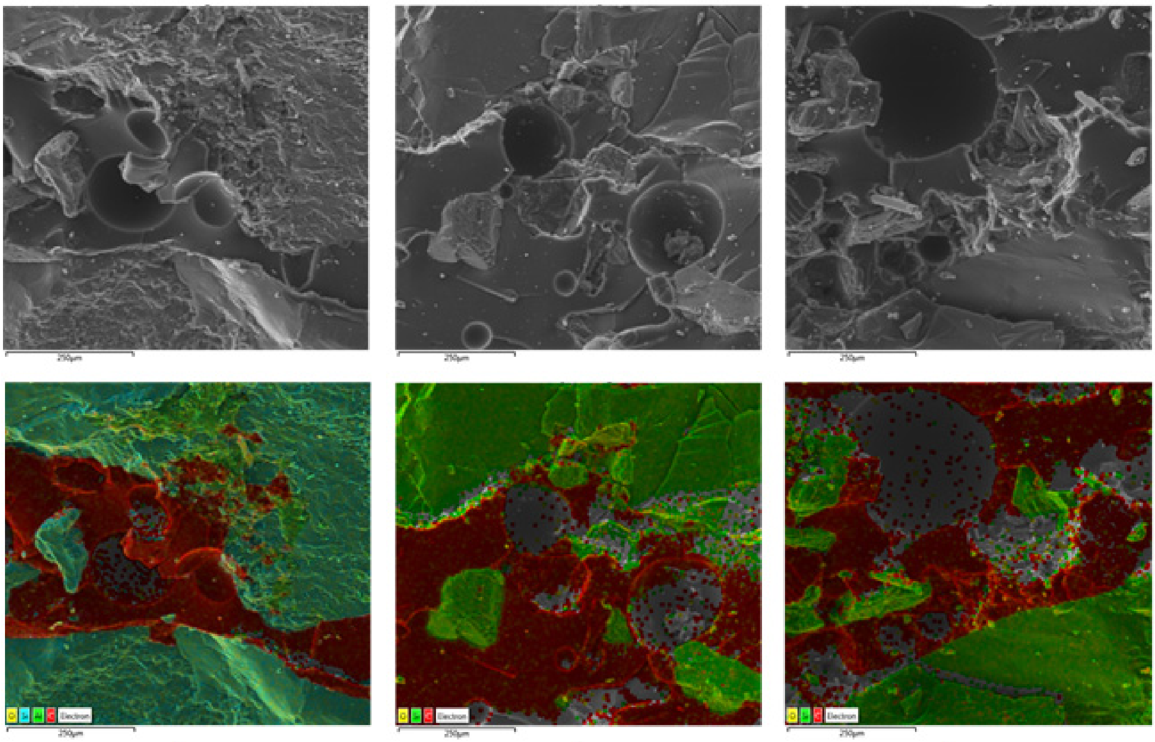

a) b) c)

Fig. 13 Polymer concrete composite with: a) sand, b) carbon fibres, c) glass fibres

4. Conclusion

The use of polymer concrete as a composite material in various areas of the industry brings several advantages. However, for the maximum utilization of its positive properties in specific application cases, it is necessary to know the effect of individual components on the resulting properties of the casting. This article focused on the effect of diffused reinforcement in the form of glass and carbon fibres on compressive strength and tensile strength at bending. From the above-presented results, the use of carbon fibres in a particular polymer concrete mixture increased the compressive strength on average by about 4 MPa compared to the mixture that did not contain a diffuse reinforcement. On the other hand, the use of glass fibres causes a reduction in compressive strength compared to a non-reinforcement mixture, on average by 5 MPa. For bending tensile strength, the use of carbon fibres also has a positive effect, namely an increase in strength of about 4 MPa compared to a non-fibre reinforced blend. Glass fibres increased the tensile strength of the samples by more than 1 MPa. The hole extractions in resin indicate the presence of air bubbles in castings that have a negative effect on mechanical properties. Bubbles may be caused by insufficient vibration (compaction) of the mixture on the vibration table, or the use of too heavy a bit of resin, which was not able to run into all the cavities and fill empty spaces. The achieved results have also a practical use in industry, in the production of special CNC equipment using the created materials with the described properties.

Acknowledgement

This work was supported by the Slovak Research and Development Agency under the contract No. APVV-15-0700. This research was also supported by research grant VEGA 1/0080/20.

References

[1] Knapčíková, L. (2018). Surface topography of composite reinforced with fibres from used tyres, *Acta Tecnología,* Vol. 4, No. 2, 29-32, doi: 10.22306/atec.v4i2.36.

[2] Krolczyk, J., Legutko, S. (2014). Innovation as a key factor for entrepreneurial activity, *Applied Mechanics and Materials,* Vol. 657, 1046-1050, doi: 10.4028/www.scientific.net/AMM.657.1046.

[3] Neslušan, M., Turek, S., Brychta, J., Čep, R., Tabaček, M. (2007). *Experimental methods in splinter machining*, EDIS Žilina, Slovak Republic.

[4] Adamczak, S., Stępień, K., Wrzochal, M. (2017). Comparative study of measurement systems used to evaluate vibrations of rolling bearings, *Procedia Engineering,* Vol. 192, 971-975, doi: 10.1016/j.proeng.2017.06.167.

[5] Harničárová, M., Mitaľová, Z., Kušnerová, M., Valíček, J., Mitaľ, D., Kopal, I., Václavík, V. (2016). Analysis of physical-mechanical and surface properties of wood plastic composite materials to determine the energy balance, Defect and diffusion forum, Vol. 370, 78-89, doi: 10.4028/www.scientific.net/DDF.370.78.

[6] Krolczyk, J.B., Legutko, S. (2015). Devices and equipment for mixing granular materials in industry, *Applied Mechanics and Materials,* Vol. 809-810, 742-747, doi: 10.4028/www.scientific.net/AMM.809-810.742.

[7] Knapcíková, L., Dupláková, D., Radchenko, S., Hatala, M. (2017). Rheological behavior modelling of composite materials used in engineering industry, *TEM Journal,* Vol. 6, No. 2, 242-245, doi: 10.18421/TEM62-07.

[8] Foldyna, V., Foldyna, J., Klichova, D., Klich, J., Hlaváček, P., Bodnarova, L., Jarolim, T., Mamulová Kutláková, K. (2017). Effects of continuous and pulsating water jet on CNT/concrete composite, *Tehnički Vjesnik – Technical Gazette,* Vol. 63, No. 10, 583-589, doi: 10.5545/sv-jme.2017.4357.

[9] Agunsoye, J.O., Bello, S.A., Bello, L., Idehenre, M.M. (2016). Assessment of mechanical and wear properties of epoxy based hybrid composites, *Advances in Production Engineering & Management,* Vol. 11, No. 1, 5-14, doi: 10.14743/apem2016.1.205.

[10] Dupláková, D., Hatala, M., Duplák, J., Radchenko, S., Steranka, J. (2018). Direct metal laser sintering – Possibility of application in production process, *SAR Journal,* Vol. 1, No. 4, 123-127, doi: 10.18421/SAR14-01.

[11] Trofimov, A., Mishurova, T., Lanzoni, L., Radi, E., Bruno, G., Sevostianov, I. (2018). Microstructural analysis and mechanical properties of concrete reinforced with polymer short fibers, *International Journal of Engineering Science,* Vol. 133, 210-218, doi: 10.1016/j.ijengsci.2018.09.009.

[12] Tanyildizi, H., Asilturk, E. (2018). Performance of phosphazene-containing polymer-strengthened concrete after exposure to high temperatures, *Journal of Materials in Civil Engineering,* Vol. 30, No. 12, Article ID 04018329, doi: 10.1061/(ASCE)MT.1943-5533.0002505.

[13] Jin, N.J., Yeon, J., Min, S.-H., Yeon, K.-S. (2018). Strength developments and deformation characteristics of MMA-modified vinyl ester polymer concrete, *International Journal of Concrete Structures and Materials,* Vol. 12, Article No. 4, doi: 10.1186/s40069-018-0232-0.

[14] Şimşek, B., Uygunoğlu, T. (2018). A full factorial-based desirability function approach to investigate optimal mixture ratio of polymer concrete, *Polymer Composites,* Vol. 39, No. 9, 3199-3211, doi: 10.1002/pc.24330.

[15] Hu, B., Zhang, N.-L., Liao, Y.-T., Pan, Z.-W., Liu, Y.-P., Zhou, L.-C., Liu, Z.-J., Jiang, Z.-Y. (2018). Enhanced flexural performance of epoxy polymer concrete with short natural fibers, *Science China Technological Sciences*, Vol. 61, No. 8, 1107-1113, doi: 10.1007/s11431-017-9272-4.

[16] Li, L., Lu, J., Fang, S., Liu, F., Li, S. (2018). Flexural study of concrete beams with basalt fibre polymer bars, *Proceedings of the Institution of Civil Engineers – Structures and Buildings,* Vol. 171, No. 7, 505-516, doi: 10.1680/jstbu.16.00204.

[17] Zegardło, B., Szeląg, M., Ogrodnik, P., Bombik, A. (2018). Physico-mechanical properties and microstructure of polymer concrete with recycled glass aggregate, *Materials,* Vol. 11, No. 7, Article No. 1213, doi: 10.3390/ma11071213.

[18] Schmitt, A., Carvelli, V., Haffke, M.M., Pahn, M. (2018). Thermo-mechanical response of concrete sandwich panels reinforced with glass fiber reinforced polymer bars, *Structural Concrete,* Vol. 19, No. 3, 839-850, doi: 10.1002/suco.201700048.

[19] Niaki, M.H., Fereidoon, A., Ahangari, M.G. (2018). Effect of basalt, silica sand and fly ash on the mechanical properties of quaternary polymer concretes, *Bulletin of Materials Science,* Vol. 41, No. 3, Article No. 69, doi: 10.1007/s12034-018-1582-6.

[20] Burlacu, A., Ciocan, V., Şerbănoiu, A.A., Barbuţă, M., Verdeş, M., Cojocaru, A. (2018). Study on polymer concretes with waste of polystyrene granules, *Environmental Engineering & Management Journal*, Vol. 17, No. 5, 1229-1235, doi: 10.30638/eemj.2018.122.

[21] Niaki, M.H., Fereidoon, A., Ahangari, M.G. (2018). Experimental study on the mechanical and thermal properties of basalt fiber and nanoclay reinforced polymer concrete, *Composite Structures,* Vol. 191, 231-238, doi: 10.1016/j.compstruct.2018.02.063.

[22] Jafari, K., Tabatabaeian, M., Joshaghani, A., Ozbakkaloglu, T. (2018). Optimizing the mixture design of polymer concrete: An experimental investigation, *Construction and Building Materials,* Vol. 167, 185-196, doi: 10.1016/j.conbuildmat.2018.01.191.

[23] Niaki, M.H., Fereidoon, A., Ahangari, M.G. (2018). Mechanical properties of epoxy/basalt polymer concrete: Experimental and analytical study, *Structural Concrete,* Vol. 19, No. 2, 366-373, doi: 10.1002/suco.201700003.
[24] Hashemi, M.J., Jamshidi, M., Aghdam, J.H. (2018). Investigating fracture mechanics and flexural properties of unsaturated polyester polymer concrete (UP-PC), *Construction and Building Materials,* Vol. 163, 767-775, doi: 10.1016/j.conbuildmat.2017.12.115.
[25] Lu, Y., Zhu, T., Li, S., Liu, Z. (2018). Bond behavior of wet-bonded carbon fiber-reinforced polymer-concrete interface subjected to moisture, *International Journal of Polymer Science,* Vol. 2018, Article ID 3120545, doi: 10.1155/2018/3120545.
[26] Şimşek, B., Uygunoğlu, T. (2017). A design of experiment application to improve raw materials utilization ratio of polymer concrete composites, *Journal of Engineering Research,* Vol. 5, No. 4., 1-18.
[27] Jafari, K., Toufigh, V. (2017). Experimental and analytical evaluation of rubberized polymer concrete, *Construction and Building Materials,* Vol. 155, 495-510, doi: 10.1016/j.conbuildmat.2017.08.097.
[28] Shokrieh, M.M., Rezvani, S., Mosalmani, R. (2017). Mechanical behavior of polyester polymer concrete under low strain rate loading conditions, *Polymer Testing,* Vol. 63, 596-604, doi: 10.1016/j.polymertesting.2017.09.015.
[29] Hwang, E.-H., Kim, Y.-Y., Song, M.-K. (2017). Durability of high performance polymer concrete composites (focusing on chemical resistance and hot water resistance), *Applied Chemistry for Engineering*, Vol. 28, No. 3, 360-368, doi: 10.14478/ACE.2017.1040.
[30] Yue, Q., Liu, Z., Li, R., Chen, X. (2017). Experimental investigation into the development length of carbon-fiber-reinforced polymer grids in concrete, *Advances in Structural Engineering,* Vol. 20, No. 6, 953-962, doi: 10.1177/1369433216668360.
[31] Agunsoye, J.O., Bello, S.A., Bello, L., Idehenre, M.M. (2016). Assessment of mechanical and wear properties of epoxy-based hybrid composites, *Advances in Production Engineering & Management,* Vol. 11, No. 1, 5-14, doi: 10.14743/apem2016.1.205.

APEM journal
Advances in Production Engineering & Management
Volume 15 | Number 4 | December 2020 | pp 453–466
https://doi.org/10.14743/apem2020.4.378
ISSN 1854-6250
Journal home: apem-journal.org
Original scientific paper

Optimal channel decision of retailers in the dual-channel supply chain considering consumer preference for delivery lead time

Hu, Y.S.[a,b], **Zeng, L.H.**[a], **Huang, Z.L.**[c], **Cheng, Q.**[c,*]

[a]School of Transportation, Fujian University of Technology, Fuzhou, P.R. China
[b]School of Business, Maynooth University, Maynooth, County Kildare, Republic of Ireland
[c]Research Center of Logistics, Fuzhou University, Fuzhou, P.R. China

A B S T R A C T

Facing competition from manufacturers' online direct channels, how retailers make sales channel decisions to increase consumer stickiness has become the core concern of the industry and academia. Empirical research showed that delivery lead time is a key factor that affects consumers' preference for online channels. To analyze the impact of consumer delivery time preference on channel selection and pricing strategy of retailers, consumer delivery lead time preference function was improved from a linear function to an exponential function and consumer demand under the mixed dual-channel supply chain of manufacturer and retailer was derived. Then, the Stackelberg game models under different channel strategies of retailer were established and solved. Results show that consumer preference for delivery lead time has four implications on the channel decision of retailers under manufacturer encroachment in the dual-channel supply chain. First, the dual retail channels strategy is the optimal choice for retailers, and the profit margins that a retailer obtains from dual retail channels supply chain and single online retail channel supply chain will increase as consumers' delivery lead time preference coefficient increases. Second, the optimal pricing of online retail channel and offline retail channel is positively related to consumers' delivery lead time preference coefficient. By contrast, the optimal pricing of online direct channel is negatively related to consumers' delivery lead time preference coefficient. Third, the optimal pricing of online retail channel is higher than that of offline retail and online direct channels. Fourth, a retailer and a manufacturer can adopt a compensation-based whole price contract to address the conflict brought about by the optimal channel choice of the retailer. This study introduces consumer delivery lead time preference into retailer channel decision making and provides a theoretical reference for retailer's mixed channel construction in practice.

A R T I C L E I N F O

Keywords:
Supply chain;
Dual-channel;
Consumer preference;
Delivery lead time preference;
Channel selection;
Channel coordination

**Corresponding author:*
chengquan@fzu.edu.cn
(Cheng, Q.)

Article history:
Received 20 September 2020
Revised 6 December 2020
Accepted 9 December 2020

1. Introduction

The advent of the Internet has made consumers accustomed to purchasing products online. To expand market coverage, control sales prices, and increase profits, a growing number of manufacturers who traditionally distribute their products through retail stores are engaging in online direct sales [1-2]. For example, Nike increased its consumer penetration and achieved success via the online direct channel [3]. According to the financial report released by Nike on June 27, 2019, Nike Direct generated a revenue of US$ 11.8 billion in the fiscal year 2018-2019, which increased by 16 % year-on-year on a constant exchange rate basis. In particular, online direct channel sales increased by 35 %, whereas the growth of offline channel sales was only 6 %. The online direct channel established by manufacturers has complicated the relationships among supply chain members. Here, manufacturers are not only the suppliers but also the competitors of retailers, which may result in manufacturer encroachment. As a result, manufacturer encroachment will reduce the revenue of online retailers. Some traditional online retailers believe that the online direct channel of manufacturers will cannibalize their market share, and they need to take measures to cope with such manufacturer encroachment.

Listening to the voice of consumers is an important way of retailer to improve the market competitiveness [4]. In a supply chain, customers have heterogeneity preferences [5], which is an important factor that affects the decision-making strategies of enterprises [6]. Empirical results have shown that delivery service is a more important factor than product prices in the preference of consumers for the online channel [7-9]. Some consumers are willing to pay high prices for fast delivery. Therefore, an increasing number of online retailers are beginning to shorten delivery lead time to cope with the competition from the online direct channel of manufacturers. Delivery lead time refers to the duration between the order time and the time of receiving the products, which mainly includes order handling time, collecting time, binding time, and delivery time from the warehouse to consumers [1]. In practice, online retailers take two measures to shorten delivery lead time. One is increasing the construction of smart warehouses and innovative distribution models [10-11], such as Alibaba and JD. These online retailers have vigorously built pre-warehouses in recent years on the basis of predicting consumer demand via data mining [12]. Pre-warehouses, which are warehouses that are closest to consumers, are where retailers deliver goods in anticipation of future consumer demand. As long as consumers place orders on the e-platform, the products will be delivered to consumers in the shortest time, even within 24 hours. The other measure is building physical stores and using them as distribution centers. Amazon has opened a variety of physical retail stores worldwide, such as Whole Foods, Amazon Go, Amazon Go Grocery, Amazon Books, Amazon 4-star, and Amazon Pop-up. These physical stores improve consumers' shopping experience and the timeliness of delivery. However, shortening delivery lead time will lead to increased service cost no matter what online retailers takes. Retailers should balance delivery lead time and service cost under manufacturer encroachment, which increases the difficulties of retailers in choosing between single online retail channel or dual retail channel supply chain.

The aforementioned phenomenon is the key motivation of our research, which seeks to answer the following questions. How do retailers choose between single online retail channel or dual retail channels to cope with manufacturer encroachment in consideration of consumer preference for delivery lead time? What are the optimal pricing strategies for retailers and manufacturers? How does consumer preference of delivery lead time influence the optimal equilibrium strategies?

The remainder of this study is organized as follows. Section 2 briefly reviews the related literature. Section 3 develops two game models based on the different channel selection decisions of the online retailer. Section 4 presents a comparison of the optimal equilibrium strategies and the corresponding profits under different channel selection decisions. Section 5 concludes the study with managerial implications and future extensions.

2. State-of-the-art

The research is closely related to two streams of literature, that is, channel decision for retailers and the impact of consumer time preference on supply chain decision.

Different from the traditional supply chain, manufacturers can sell products to consumers through online direct channel besides traditional retail channel in the e-commerce environment. In this set-up, manufactures are not only a partner but also a competitor of retailers. Facing competition from manufacturers, retailers need to consider the impact of dual-channel operation on their own profits. If retailers choose dual channel, then they need to address the problems of cooperation and competition between their offline channel and online channel besides the competition and cooperation with the manufacturer. Additionally, Zhou *et al*. [13] found that channel decisions can be used by retailers to weaken the information advantage of service providers. Therefore, the channel decision of retailers is an important issue worthy of discussion in dual-channel supply chain.

Is the opening of online retail channels necessary for offline retailers? Should online retailers open offline retail channels? Karray and Sigue [14] believed that retailers should not dive into the online market when the online market is not yet large enough. Otherwise the expansion of online retail would erode the sales of offline retail channels. Shi *et al*. [15] explored online retailers with an existing resale channel that are introducing an additional market channel and found that the strategy of introducing a new market does not always improve the realization of cost–to-value ratio. Nie *et al*. [16] investigated the influence of cross-channel effects on the distribution channel strategies of two competing traditional retailers and found that retailers may abandon the online-and-offline channel strategy when the cross-channel effects are significantly negative. Wang and Goldfarb [17] used evidence from store openings by a dual-channel retailer to examine the drivers of substitution and complementarity between online and offline retail channels. They found that opening of an offline store is related to a decrease in online sales in the place where the retailer has a strong influence, whereas opening offline store is related to an increase in online sales in places where the retailer is not strong.

A large number of studies have shown that dual retail channels are important channel structures. If retailers choose dual channel, then how can they organize and coordinate the operations of the two channels? Huang *et al*. [18] explored how a large retailer combined its online and offline department by using Suning as a case study and found that an online–offline hybrid organization is hybridized through three multiple and conflicting boundary penetration paths, namely complete, partial, and preventive penetration paths.

The time preference of consumers reflects the importance that consumers place on near-term benefits over long-term benefits. At present, a lot of literature on supply chain decision-making considered the delivery lead time of goods. After studying a duopoly market in which customers are heterogeneous, Jayaswal and Jewkes [19] found that the firm with a larger market base and the firm with capacity cost advantage should always maintain a large price and lead time differentiation between different market segments. Considering two companies competing based on price and delivery decisions in the common market, Pekgun *et al*. [20] found that decentralized operations may not lead to low prices or long lead times if the production department chooses capacity along with lead time.

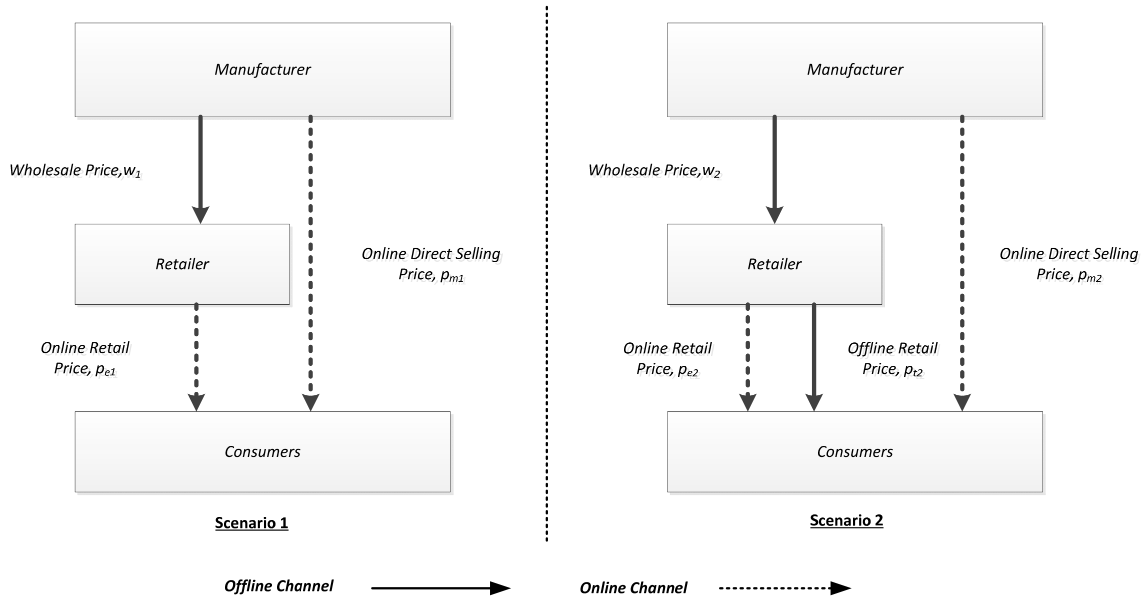

Fig. 1 Supply chain structure of Scenario 1 and Scenario 2

Other researchers transferred the research on consumer time preference from manufacturing to retail. Li *et al*. [21] found that the optimal price of a retailer's online/offline channel has a linear relationship with the delivery lead time of the online channel. In addition, the profit of the manufacturer would not be affected by retailer decisions if consumers in online and offline channels show consistent time preferences in a retailer-led dual-channel supply chain. Zhao *et al*. [22] studied price and promised delivery lead time competition between two online retailers considering product returns and found that the retailer with lower basic return rates or lower return rate sensitivities always quote higher prices and shorter promised delivery lead times. Considering the impact of promised delivery time into the choice of sales channel, Ye *et al*. [23] found that the logistics capability of the third-party logistics providers has a significant impact on the optimal sales channel. In addition, the introduction of an online channel would hurt the retailer's profit when the logistics capability coefficient is sufficiently small or large because logistics capability has a significant impact on the promised delivery time and demand. Aiming at the inventory competition of perishable products in dual-channel supply chain, Yang et al. [24] explored the manufacturer's optimal delivery lead time decision in the online direct channel and found that consumers in online direct channel enjoy shorter delivery lead time and the service in decentralized scheme is better compared with the centralized scheme.

The above-mentioned literature explored the channel selection decisions under different conditions. However, the impacts of consumer preference for delivery lead time on retailer channel selection decision under the mixed dual-channel structure of manufacturers and retailers are not considered. Moreover, most research on the influence of preferences on supply chain decision-making focuses on the preferences of decision makers, and research from the perspective of consumer preferences is still relatively limited [25]. Due to the complexity of model construction, most literature used linear functions to describe consumer preference for delivery lead time in the dual-channel supply chain, which may affect the accuracy of decisions. Therefore, we analyze the impact of consumers' preference of delivery lead time on retailers' channel decision in the mixed dual-channel supply chain under manufacturer encroachment. Game models under single online retail channel supply chain and dual retail channels supply chain are developed to obtain the optimal retail channel selection for retailers and the according optimal pricing strategy.

3. Methodology

3.1 Problem description

We consider a retailer-led dual-channel supply chain with a single manufacturer and a single retailer. The manufacturer wholesales products to the retailer at price w and to end consumers through an online direct channel at price p_m. Facing competition from the online direct channel of the manufacturer, the retailer can adopt two different channel strategies, namely single online retail channel strategy or dual retail channel strategy. Accordingly, two types of supply chain structures are studied in this paper, as shown in Fig. 1. In Scenario 1, the retailer sells products exclusively through an online retail channel, whereas in Scenario 2, the retailer sells products through an online retail channel as well as an offline retail channel. Both the manufacturer and the retailer are risk-neutral and maximize their profits.

In the retailer-led dual-channel supply chain, the game sequence is summarized as follows. In stage 1, the retailer determines the online retail price and offline retail price. In stage 2, the manufacturer determines the wholesale price and online direct selling price.

Furthermore, we use U_e to represent the utility that customers gain from per unit product in the online retail channel, U_t in the offline retail channel, and U_m in the online direct channel. We use q_e to represent the demand in the online retail channel, q_t in the offline retail channel, and q_m in the online direct channel. The online retail price and offline retail price offered by the retailer to customers is denoted by p_e and p_t, respectively. Assume that consumers are heterogeneous in the valuation of the product. Following Chiang *et al*. [26], we denote the consumption value (alternatively called "willingness to pay") by v, where $0 \leq v \leq 1$. In addition, assume that

v is uniformly distributed within the consumer population from 0 to 1, with a density of 1. The profits earned by the retailer from selling per unit product through the online retail channel and the offline retail channel are denoted by λ_e and λ_t, respectively. The profits earned by the retailer and the manufacturer are denoted by Π_r and Π_m, respectively. The delivery lead time in the online retail channel and online direct channel is denoted by t_e and t_m, respectively. We use β to represent consumers' delivery lead time preference coefficient, where $\beta > 0$. Table 1 summarizes the notations used in this paper.

Let $g(t_i) = e^{-\beta t_i}(t_i \geq 0, i = e, m)$ represent the consumer preference for delivery lead time. Previous studies mentioned that the delivery lead time in the online channel (no matter online retail channel or online direct channel) affects the perceived value of a product, thus influencing the utility of customers [3-5]. The utility that consumers obtain in the online channel is not only negatively related to its delivery lead time, but positively related to the delivery lead time of its competing online channels. Hence, the utilities of the customers purchasing products from the online retail channel and online direct channel are represented as follows, respectively: $U_e = [g(t_e)/g(t_m)]v - p_e = e^{-\beta(t_e - t_m)}v - p_e$, and $U_m = [g(t_m)/g(t_e)]v - p_m = e^{-\beta(t_m - t_e)}v - p_m$.

Let $\Delta t = t_m - t_e$, and we obtain $U_e = e^{\beta \Delta t}v - p_e$ and $U_m = e^{-\beta \Delta t}v - p_m$. In general, the retailer is closer to the consumers than the manufacturer, we have $t_m > t_e$. It implies that $e^{\beta \Delta t} > 1$ and $0 < e^{-\beta \Delta t} < 1$.

Next, we discuss the demand functions of the retailer and the manufacturer under the two different channel strategies.

Table 1 Summary of notations

Notation	Description
U_m	The utility of consumers buying per unit product from the online direct channel
U_e	The utility of consumers buying per unit product from the online retail channel
U_t	The utility of consumers buying per unit product from the offline retail channel
Π_r	The profit of a retailer
Π_m	The profit of a manufacturer
p_m	The online direct selling price offered by a manufacturer to a consumer
p_e	The online retail price offered by a retailer to a consumer
p_t	The offline retail price offered by a retailer to a consumer
λ_e	The profits earned by a retailer from selling per unit product through the online retail channel
λ_t	The profits earned by a retailer from selling per unit product through the offline retail channel
q_m	The quantity demanded of a product in the online direct channel
q_e	The quantity demanded of a product in the online retail channel
q_t	The quantity demanded of a product in the offline retail channel
t_m	The delivery lead time in the online direct channel
t_e	The delivery lead time in the online retail channel
w	The wholesale price charged by a manufacturer to a retailer
v	The consumption value of per unit product
β	Consumers' delivery lead time preference coefficient

3.2 Model formulation

Scenario 1: Retailer adopts the single online retail channel strategy

We assume that the utilities of the consumers purchasing products from the online retail channel and the online direct channel are $U_{e1} = e^{\beta \Delta t}v - p_{e1}$ and $U_{m1} = e^{-\beta \Delta t}v - p_{m1}$, respectively, where subscript 1 represents the Scenario 1.

When $U_{m1} > 0$ and $U_{e1} \geq U_{m1}$, the consumers will choose online retail channel, i.e. $v \geq e^{-\beta \Delta t}p_{e1}$ and $v \geq \frac{p_{e1} - p_{m1}}{e^{\beta \Delta t} - e^{-\beta \Delta t}}$. Similarly, when $U_{m1} \geq 0$ and $U_{m1} > U_{e1}$, the consumers will choose online direct channel, i.e. $v \geq e^{\beta \Delta t}p_{m1}$ and $v \leq \frac{p_{e1} - p_{m1}}{e^{\beta \Delta t} - e^{-\beta \Delta t}}$. Here, the condition $\frac{p_{e1} - p_{m1}}{e^{\beta \Delta t} - e^{-\beta \Delta t}} \geq e^{\beta \Delta t}p_{m1}$ should be satisfied. In summary, the demand functions of the online retail channel and the online direct channel can be written as follow:

$$q_{e1} = 1 - \frac{p_{e1} - p_{m1}}{e^{\beta\Delta t} - e^{-\beta\Delta t}} \tag{1}$$

$$q_{m1} = \frac{p_{e1} - p_{m1}}{e^{\beta\Delta t} - e^{-\beta\Delta t}} - e^{\beta\Delta t} p_{m1} \tag{2}$$

Scenario 2: Retailer adopts the dual retail channels strategy

The utilities of the consumers purchasing products from the offline retail channel, the online retail channel, and the online direct channel are denoted by $U_{t2} = v - p_{t2}$, $U_{e2} = e^{\beta\Delta t}v - p_{e2}$, and $U_{m2} = e^{-\beta\Delta t}v - p_{m2}$, respectively, where subscript 2 represents the Scenario 2.

When $U_{t2} \geq 0$, $U_{t2} \geq U_{e2}$, and $U_{t2} \geq U_{m2}$, the consumers will choose offline retail channel. Here, we have $v \geq p_{t2}$, $v \leq \frac{p_{t2}-p_{e2}}{1-e^{\beta\Delta t}}$, and $v \geq \frac{p_{t2}-p_{m2}}{1-e^{-\beta\Delta t}}$. Moreover, the condition $\frac{p_{t2}-p_{e2}}{1-e^{\beta\Delta t}} > p_{t2}$ should be satisfied.

When $U_{e2} \geq U_{t2}$, and $U_{e2} \geq U_{m2}$, the consumers will choose online retail channel. It implies that $v \geq e^{-\beta\Delta t}p_{e2}$, $v \geq \frac{p_{t2}-p_{e2}}{1-e^{\beta\Delta t}}$, and $v \geq \frac{p_{e2}-p_{m2}}{e^{\beta\Delta t}-e^{-\beta\Delta t}}$.

When $U_{m2} \geq 0$, $U_{m2} \geq U_{t2}$, and $U_{m2} \geq U_{e2}$, the consumers will choose online direct channel. Here, we have $v \geq e^{\beta\Delta t}p_{m2}$, $v \leq \frac{p_{t2}-p_{m2}}{1-e^{-\beta\Delta t}}$, and $v \leq \frac{p_{e2}-p_{m2}}{e^{\beta\Delta t}-e^{-\beta\Delta t}}$. In addition, the following conditions should be satisfied: $\frac{p_{t2}-p_{m2}}{1-e^{-\beta\Delta t}} \geq e^{\beta\Delta t}p_{m2}$ and $\frac{p_{e2}-p_{m2}}{e^{\beta\Delta t}-e^{-\beta\Delta t}} \geq e^{\beta\Delta t}p_{m2}$.

In summary, the demand function of the offline retail channel, the online retail channel, and the online direct channel can be written as follow:

$$q_{t2} = \frac{p_{t2} - p_{e2}}{1 - e^{\beta\Delta t}} - \frac{p_{t2} - p_{m2}}{1 - e^{-\beta\Delta t}} \tag{3}$$

$$q_{e2} = 1 - \frac{p_{t2} - p_{e2}}{1 - e^{\beta\Delta t}} \tag{4}$$

$$q_{m2} = \frac{p_{t2} - p_{m2}}{1 - e^{-\beta\Delta t}} - e^{\beta\Delta t}p_{m2} \tag{5}$$

3.3 Equilibrium outcomes

Scenario 1: Retailer adopts the single online retail channel strategy

In Scenario 1, the profit of the manufacturer can be written as:

$$\Pi_{m1} = w_1\left(1 - \frac{w_1 + \lambda_{e1} - p_{m1}}{e^{\beta\Delta t} - e^{-\beta\Delta t}}\right) + p_{m1}\left(\frac{w_1 + \lambda_{e1} - p_{m1}}{e^{\beta\Delta t} - e^{-\beta\Delta t}} - e^{\beta\Delta t}p_{m1}\right) \tag{6}$$

According to Eq. 6, the Hesse matrix of Π_{m1} on p_{m1} and w_1 can be obtained as $H(\Pi_{m1}) = \frac{1}{e^{\beta\Delta t}-e^{-\beta\Delta t}}\begin{bmatrix} -2e^{2\beta\Delta t} & 2 \\ 2 & -2 \end{bmatrix}$. Since $\frac{\partial \Pi_{m1}^2}{\partial {p_{m1}}^2} = -\frac{2e^{2\beta\Delta t}}{e^{\beta\Delta t}-e^{-\beta\Delta t}} < 0$ and $|H(\Pi_{m1})| >$, $H(\Pi_{m1})$ is a negative definite matrix. It implies that Π_{m1} has a unique maximum about p_{m1} and w_1.

Let $\partial\Pi_{m1}/\partial p_{m1} = 0$ and $\partial\Pi_{m1}/\partial w_1 = 0$. The reaction function of the manufacturer can be written as $p_{m1} = e^{-\beta\Delta t}/2$ and $w_1 = \left(e^{\beta\Delta t} - \lambda_{e1}\right)/2$.

In Scenario 1, the profit of the retailer can be written as:

$$\Pi_{r1} = \lambda_{e1}(1 - \frac{w_1 + \lambda_{e1} - p_{m1}}{e^{\beta\Delta t} - e^{-\beta\Delta t}}) \tag{7}$$

After substituting the reaction function of the manufacturer into Eq. 7, the second derivative of Π_{r1} on λ_{e1} is given as follows $\partial^2\Pi_{r1}/\partial{\lambda_{e1}}^2 = e^{-\beta\Delta t} - e^{\beta\Delta t} < 0$. It means that Π_{r1} has a unique maximum on λ_{e1}.

Let $\partial\Pi_{r1}/\partial\lambda_{e1} = 0$. The optimal pricing decision for the retailer and the manufacturer can be obtained as follows:

$$p_{e1}^{*}=\frac{3}{4}e^{\beta\Delta t}-\frac{1}{4}e^{-\beta\Delta t} \tag{8}$$

$$p_{m1}^{*}=\frac{e^{-\beta\Delta t}}{2} \tag{9}$$

The according optimal profits for the retailer and the manufacturer can be obtained as follows:

$$\Pi_{r1}^{*}=\frac{1}{8}\left(e^{\beta\Delta t}-e^{-\beta\Delta t}\right) \tag{10}$$

$$\Pi_{m1}^{*}=\frac{1}{16}\left(e^{\beta\Delta t}-3e^{-\beta\Delta t}\right) \tag{11}$$

Scenario 2: Retailer adopts the dual retail channel strategy

In Scenario 2, the profit of the manufacturer can be written as:

$$\Pi_{m2}=w_2\left(1-\frac{\lambda_{t2}+w_2-p_{m2}}{1-e^{-\beta\Delta t}}\right)+p_{m2}\left(\frac{\lambda_{t2}+w_2-p_{m2}}{1-e^{-\beta\Delta t}}-e^{\beta\Delta t}p_{m2}\right) \tag{12}$$

According to Eq. 12, the Hesse matrix of Π_{m2} on p_{m2} and w_2 can be obtained as $H(\Pi_{m2})=\frac{1}{1-e^{-\beta\Delta t}}\begin{bmatrix}-2e^{\beta\Delta t} & 2\\ 2 & -2\end{bmatrix}$.

Since $\partial^2\Pi_{m2}/\partial {p_{m2}}^2=-2e^{\beta\Delta t}/\left(1-e^{-\beta\Delta t}\right)<0$ and $|H(\Pi_{m2})|>0$, $H(\Pi_{m2})$ is a negative definite matrix, which means Π_{m2} has a unique maximum on p_{m2} and w_2.

Let $\partial\Pi_{m2}/\partial p_{m2}=0$ and $\partial\Pi_{m2}/\partial w_2=0$; hence, the reaction function of the manufacturer can be denoted as $p_{m2}=e^{-\beta\Delta t}/2$ and $w_2=(1-\lambda_{t2})/2$.

In Scenario 2, the profit of the retailer can be written as:

$$\Pi_{r2}=\lambda_{t2}\left(\frac{\lambda_{t2}-\lambda_{e2}}{1-e^{\beta\Delta t}}-\frac{\lambda_{t2}+w_2-p_{m2}}{1-e^{-\beta\Delta t}}\right)+\lambda_{e2}\left(1-\frac{\lambda_{t2}-\lambda_{e2}}{1-e^{\beta\Delta t}}\right) \tag{13}$$

After substituting the reaction function of the manufacturer into Eq. 13, the Hessian matrix of Π_{r2} on λ_{t2} and λ_{e2} can be obtained as $H(\Pi_{r2})=-\frac{1}{1-e^{\beta\Delta t}}\begin{bmatrix}-\left(e^{\beta\Delta t}+2\right) & 2\\ 2 & -2\end{bmatrix}$.

Since $\partial^2\Pi_{r2}/\partial{\lambda_{t2}}^2=\left(e^{\beta\Delta t}+2\right)/\left(1-e^{\beta\Delta t}\right)<0$ and $|H(\Pi_{r2})|>0$, $H(\Pi_{r2})$ is a negative definite matrix, which means Π_{r2} has a unique maximum about λ_{t2} and λ_{e2} . Let $\partial\Pi_{r2}/\partial\lambda_{t2}=0$ and $\partial\Pi_{r2}/\partial\lambda_{e2}=0$, we can get $\lambda_{t2}^{*}=\frac{e^{-\beta\Delta t}\left(-1+e^{\beta\Delta t}\right)}{2}$ and $\lambda_{e2}^{*}=\frac{-e^{-\beta\Delta t}+e^{\beta\Delta t}}{2}$.

Therefore, the optimal pricing strategies for the retailer and the manufacturer can be represented as follows, respectively:

$$p_{t2}^{*}=\frac{3}{4}-\frac{e^{-\beta\Delta t}}{4} \tag{14}$$

$$p_{e2}^{*}=\frac{1}{4}\left(1-e^{-\beta\Delta t}+2e^{\beta\Delta t}\right) \tag{15}$$

$$p_{m2}^{*}=\frac{e^{-\beta\Delta t}}{2} \tag{16}$$

Accordingly, the optimal profit for the retailer and the manufacturer can be obtained as follows:

$$\Pi_{r2}^{*}=\frac{1}{8}\left(2e^{\beta\Delta t}-e^{-\beta\Delta t}-1\right) \tag{17}$$

$$\Pi_{m2}^{*}=\frac{1}{16}\left(1+3e^{-\beta\Delta t}\right) \tag{18}$$

4. Analysis and discussion of results

In this section, we firstly investigate the impact of consumer delivery time preferences on the profit and optimal pricing strategies of the retailers and manufacturers under the two channel structures. Then, we explore the retailer's optimal channel strategy and its impact on the manufacturer, and try to coordinate the conflict between the retailer and the manufacturer in the retailer's channel selection.

Proposition 1: When the retailer adopts the single online retail channel strategy (Scenario 1), we have:

(1) The optimal pricing in the online retail channel is positively related to consumer preference for delivery lead time;
(2) The optimal pricing in the online direct channel is negatively related to consumer preference for delivery lead time;
(3) The optimal profit of the retailer is positively related to consumer preference for delivery lead time;
(4) The optimal profit of the manufacturer is positively related to consumer preference for delivery lead time.

Proof of Proposition 1:

(1) From Eq. 8, we can get $\frac{\partial p_{e1}^*}{\partial \beta} = \frac{1}{4}(3e^{\beta \Delta t} + e^{-\beta \Delta t})\Delta t > 0$. Hence, p_{e1}^* is the monotonically increasing function of β.
(2) Similarly, due to $\frac{\partial p_{m1}^*}{\partial \beta} = -\frac{e^{-\beta \Delta t}\Delta t}{2} < 0$, p_{m1}^* decreases monotonically with β.
(3) From Eq. 10, we can get $\frac{\partial \Pi_{r1}^*}{\partial \beta} = \frac{1}{8}(e^{\beta \Delta t} + e^{-\beta \Delta t})\Delta t > 0$. Hence, Π_{r1}^* is the monotonically increasing function of β.
(4) Similarly, due to $\frac{\partial \Pi_{m1}^*}{\partial \beta} = \frac{1}{16}(e^{\beta \Delta t} + 3e^{-\beta \Delta t})\Delta t > 0$, Π_{m1}^*increases monotonically with β.

Proposition 1(1) indicates that the optimal pricing in the online retail channel increases as β increases. The higher the value of β, the shorter the delivery lead time of products required by consumers, which leads to an increase in deliver costs. Therefore, the online retail price increases accordingly. Moreover, Proposition 1(3) shows that with the increase of online channel price, the profit of the retailer will increase correspondingly. In contrast, Proposition 1(2) indicates that the optimal pricing of online direct channel decreases as β increases. Considering that manufacturers are at a disadvantage compared with the retailers in terms of spatial distance to consumers, manufacturers need to lower the online direct selling price to improve their market competitiveness. This price adjustment may lead to a decline in the profit of the manufacturer as shown in Proposition 1(4).

Proposition 2: When the retailer adopts the dual retail channels strategy (Scenario 2), we have:

(1) The optimal pricing in the offline retail channel is positively related to consumer preference for delivery lead time.
(2) The optimal pricing in the online retail channel is positively related to consumer preference for delivery lead time.
(3) The optimal pricing in the online direct channel is negatively related to consumer preference for delivery lead time.
(4) The optimal profit of the retailer is positively related to consumer preference for delivery lead time.
(5) The optimal profit of the manufacturer is negatively related to consumer preference for delivery lead time.

Proof of Proposition 2:

(1) From Eq. 14, we can get $\frac{\partial p_{t2}^*}{\partial \beta} = \frac{1}{4}e^{-\beta \Delta t}\Delta t > 0$. Hence, p_{t2}^* is the monotonically increasing function of β.

(2) Similarly, due to $\frac{\partial p_{e2}^*}{\partial \beta} = \frac{1}{4}(e^{-\beta \Delta t} + 2e^{\beta \Delta t})\Delta t > 0$, p_{e2}^* increases monotonically with β.

(3) Due to $\frac{\partial p_{m2}^*}{\partial \beta} = -\frac{1}{2}e^{-\beta \Delta t}\Delta t < 0$, p_{m2}^* decreases monotonically with β.

(4) From Eq. 17, we can get $\frac{\partial \Pi_{r2}^*}{\partial \beta} = \frac{1}{8}(2e^{\beta \Delta t} + e^{-\beta \Delta t})\Delta t > 0$. Hence, Π_{r2}^* is the monotonically increasing function of β.

(5) Similarly, due to $\frac{\partial \Pi_{m2}^*}{\partial \beta} = -\frac{3}{16}e^{-\beta \Delta t}\Delta t < 0$, Π_{m2}^* decreases monotonically with β.

Propositions 2(1) and 2(2) indicate that the optimal pricing in the offline retail channel and the online retail channel increases as β increases. Considering that retailers have an inherent advantage in the delivery lead time of products compared with manufacturers, Proposition 2(4) shows that retailers can increase profits by increasing offline retail prices and online retail prices with the increase of β. In contrast, Proposition 2(3) shows that the optimal pricing in the online direct channel decreases with the increase of β. Although manufacturers may obtain more profits from retailers as β increases, Proposition 2(5) shows that the additional profits are not enough to offset the decline in profits from theirs online direct channel.

Proposition 3: The optimal pricing in the online retail channel is higher than that in the offline retail channel and online direct channel under manufacturer encroachment considering consumer preference for delivery lead time.

Proof of Proposition 3:

When the retailer adopts the single online retail channel strategy, we have $p_{e1}^* - p_{m1}^* = \frac{3}{4}e^{\beta \Delta t} - \frac{1}{4}e^{-\beta \Delta t} - \frac{1}{2}e^{-\beta \Delta t} = \frac{3}{4}(e^{\beta \Delta t} - e^{-\beta \Delta t}) > 0$. When the retailer adopts the dual retail channels strategy, we have $p_{e2}^* - p_{t2}^* = \frac{1}{4}\left(1 - e^{-\beta \Delta t} + 2e^{\beta \Delta t}\right) - \frac{1}{4}\left(3 - e^{-\beta \Delta t}\right) = \frac{1}{2}(e^{\beta \Delta t} - 1) > 0$, and $p_{e2}^* - p_{m2}^* = \frac{1}{4}\left(1 - e^{-\beta \Delta t} + 2e^{\beta \Delta t}\right) - \frac{1}{2}e^{-\beta \Delta t} = \frac{1}{4}\left(1 + 2e^{\beta \Delta t} - 3e^{-\beta \Delta t}\right) > 0$. To sum up, Proposition 3 Q.E.D.

Proposition 3 shows that retailers can set online retail price higher than offline retail prices and online direct selling price considering consumer preference for delivery lead time under manufacturer encroachment. This finding is contrary to previous findings that online retail price should be lower than offline retail price to improve market competitiveness.

Proposition 4: Considering consumer preference for delivery lead time under manufacturer encroachment, we have:

(1) The profit of the retailer from adopting the dual retail channels strategy is greater than its profit from adopting the single online retail channel strategy.
(2) The profit margin of the retailer from adopting the dual retail channels strategy and the single online retail channel strategy is positively related to β.

Proof of Proposition 4:

(1) From Eq. 10 and Eq. 17, we can get
$\Pi_{r2}^* - \Pi_{r1}^* = \frac{1}{8}(2e^{\beta \Delta t} - e^{-\beta \Delta t} - 1) - \frac{1}{8}(e^{\beta \Delta t} - e^{-\beta \Delta t}) = \frac{1}{8}(e^{\beta \Delta t} - 1) > 0$.

(2) From Eq. 10 and Eq. 17, we can get $\frac{\partial(\Pi_{r2}^* - \Pi_{r1}^*)}{\partial \beta} = \frac{1}{8}e^{\beta \Delta t}\Delta t > 0$. Hence, $\Pi_{r2}^* - \Pi_{r1}^*$ is the monotonically increasing function of β.

Proposition 5: Considering consumer preference for delivery lead time under manufacturer encroachment, we have:

(1) When $\beta \in \{0 < \beta < \frac{\ln 3}{\Delta t}\}$, the profit of the manufacturer when the retailer adopts the dual retail channels strategy is higher than its profit when the retailer adopts the single online retail channel strategy.

(2) When $\beta \in \{\frac{ln\,3}{\Delta t} < \beta < 1\}$, the profit of the manufacturer when the retailer adopts the dual retail channels strategy is lower than its profit when the retailer adopts the single online retail channel strategy.

Proof of Proposition 5:

(1) From Eq. 11 and Eq. 18, we can get
$\Pi_{m2}^* - \Pi_{m1}^* = \frac{1}{16}(3e^{-\beta\Delta t} + 1) - \frac{1}{16}(e^{\beta\Delta t} - 3e^{-\beta\Delta t}) = \frac{1}{16}(1 + 6e^{-\beta\Delta t} - e^{\beta\Delta t})$
Let $\Pi_{m2}^* - \Pi_{m1}^* > 0$, we have $0 < \beta < \frac{ln\,3}{\Delta t}$.

(2) Similarly, let $\Pi_{m2}^* - \Pi_{m1}^* < 0$, we have $\frac{ln\,3}{\Delta t} < \beta < 1$.

Proposition 4 shows that the retailer can gain more profits from dual retail channels strategy than the single online retail channel strategy considering consumer preference for delivery lead time. Therefore, the dual retail channels strategy is the better choice for the retailer than the single online retail channel strategy. The higher the value of β, the larger the profit margin of the retailer between the two channel strategies. However, Proposition 5 shows that the optimal retail channel selection for the manufacturer is uncertain. When the value of β is greater than some threshold $\frac{ln\,3}{\Delta t}$, the single online retail channel strategy is the best choice for the manufacturer. Conversely, when the value of β is less than some threshold $\frac{ln\,3}{\Delta t}$, the dual retail channels strategy is the best choice for the manufacturer.

Numerical simulation

The following numerical simulations are used to analyze the impact of β on the optimal pricing and profits of the retailer and the manufacturer. For the convenience of discussion, we assume $\Delta t = 2$.

Firstly, we analyze the impact of β on the optimal pricing of the retailer and the manufacturer. As shown in Fig. 2a, when the retailer adopts a single online retail channel strategy, the optimal pricing in the online retail channel supply chain is positively related to β, whereas the optimal pricing in the online direct channel supply chain is negatively related to β. As shown in Fig. 2b, when the retailer adopts the dual retail channels strategy, the optimal pricing in the offline retail channel and online retail channel have a positive correlation with β, whereas the optimal pricing in the online direct channel shows a negative correlation with β. It is worth noting that β has a significant impact on the optimal pricing in the online retail channel when the retailer adopts the dual retail channels strategy. As shown in Fig. 2b, the retailer can set higher online retail prices than offline retail prices and online direct selling prices with the increase of β in the dual retail channels supply chain.

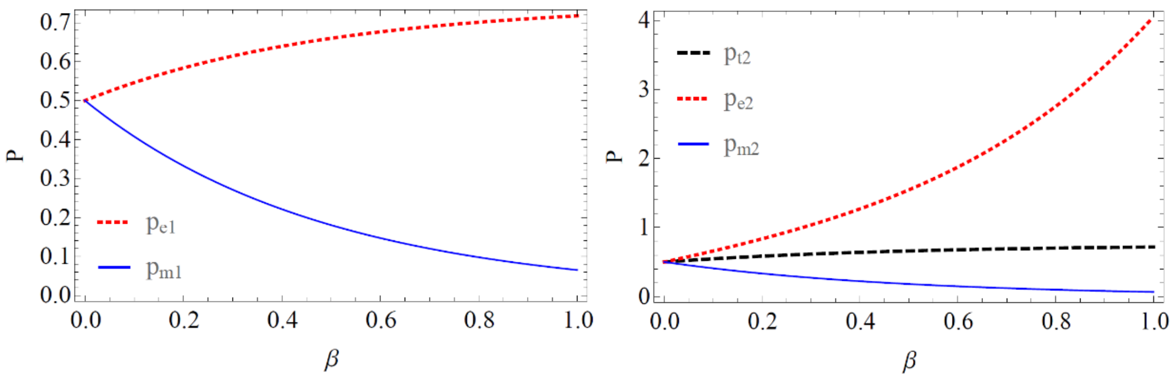

a) Single online retail channel supply chain   b) Dual retail channels supply chain

Fig. 2 Impact of β on optimal pricing ($\Delta t = 2$)

Secondly, we analyze the impact of β on the profit of the retailer and the manufacturer. It can be seen from Fig. 3a that retailer's profit in the dual retail channels supply chain and the single online retail channel supply chain is positively related to β, and that the retailer's profit in the dual retail channels supply chain is always higher than that of the single online retail channel supply chain, which means that dual retail channels strategy is the optimal channel choice for the retailer. Meanwhile, it can be seen from Fig. 3b that manufacturer's profit in the single online retail channel supply chain is positively related to β, whereas manufacturer's profit in the dual retail channels supply chain is negatively related to β, and that the dual retail channels strategy is the optimal choice for the manufacturer only when β is less than $\frac{ln\,3}{2}$. Additionally, it can be seen from Fig. 3 that there is a conflict between the retailer and the manufacturer in the optimal channel choice of the retailer when β is greater than $\frac{ln\,3}{2}$.

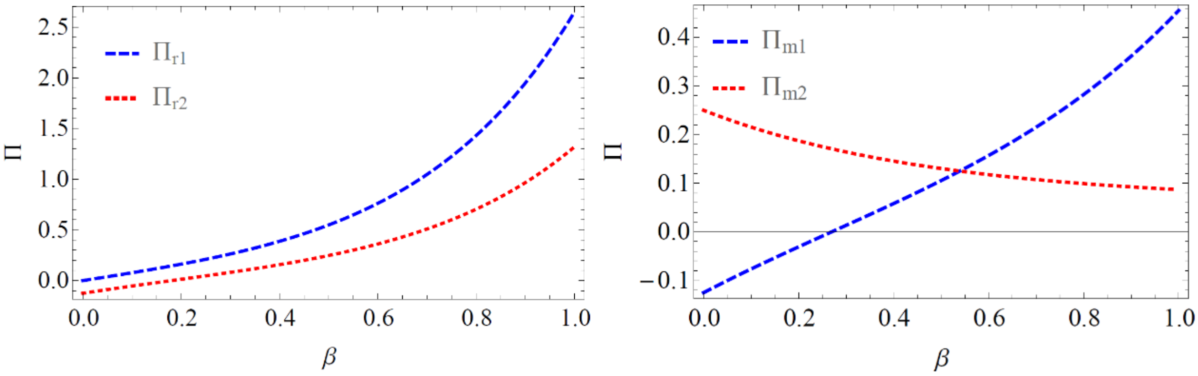

a) Impact on the profit of the retailer b) Impact on the profit of the manufacturer

Fig. 3 Impact of β on profit ($\Delta t = 2$)

Supply chain coordination

A comparative analysis of Proposition 4 and Proposition 5 reveals that a conflict exists between the retailer and the manufacturer as regards to the optimal channel choice of the retailer when β is greater than $\frac{ln\,3}{\Delta t}$. A large number of studies show that supply chain members can resolve the conflict of channel selection through coordination at different stages of supply chain decision [27]. In this section, we attempt to coordinate the conflict by using a compensation-based whole price contract and examine whether the retailer and the manufacturer can reach an agreement on the optimal channel choice of the retailer.

We assume that the coordination strategy is feasible if the two conditions are satisfied: 1) the retailer's profit from adopting the dual retail channels is greater than the profit from the single offline retail channel; 2) when the retailer adopts the dual retail channels, the profit of the manufacturer is not less than its profit when the retailer adopts the single online retail channel.

<u>Proposition 6:</u> In a retailer-led dual-channel supply chain, retailers and manufacturers can use a compensation-based whole price contract to coordinate the conflict regarding the optimal channel choice of the retailer to achieve a win–win scenario.

Proof of Proposition 6:

Assume that the contract (w, ρ) stipulates that the retailer shares the proportion of profit $\rho(0 < \rho < 1)$ with the manufacturer after sales. The decision-making problems of the retailer and the manufacturer under this contract can be written as:

$$\begin{cases} \max\limits_{\lambda_{t2},\lambda_{e2}}(\Pi_{r2}) = (1-\rho)[\lambda_{t2}(\frac{\lambda_{t2}-\lambda_{e2}}{1-e^{\beta\Delta t}} - \frac{\lambda_{t2}+w_2-p_{m2}}{1-e^{-\beta\Delta t}}) + \lambda_{e2}(1-\frac{\lambda_{t2}-\lambda_{e2}}{1-e^{\beta\Delta t}})] \\ s.t.\ \Pi_{r2}^{*} > \Pi_{r1}^{*} \end{cases} \tag{19}$$

and

$$\begin{cases} \max\limits_{p_{m2},w_2}(\Pi_{m2}) = w_2(1-\frac{\lambda_{t2}+w_2-p_{m2}}{1-e^{-\beta\Delta t}}) + p_{m2}(\frac{\lambda_{t2}+w_2-p_{m2}}{1-e^{-\beta\Delta t}} - e^{\beta\Delta t}p_{m2}) \\ \qquad + \rho[\lambda_{t2}(\frac{\lambda_{t2}-\lambda_{e2}}{1-e^{\beta\Delta t}} - \frac{\lambda_{t2}+w_2-p_{m2}}{1-e^{-\beta\Delta t}}) + \lambda_{e2}(1-\frac{\lambda_{t2}-\lambda_{e2}}{1-e^{\beta\Delta t}})] \\ \qquad s.t.\ \Pi_{m2}^* > \Pi_{m1}^* \end{cases} \tag{20}$$

The solution of Eq. 19 and Eq. 20 can be obtained by using the backyard induction.

$$p_{t2}^* = \frac{3}{4} - \frac{1}{4e^{\beta\Delta t}} \tag{21}$$

$$p_{e2}^* = \frac{1+2e^{\beta\Delta t}-e^{-\beta\Delta t}}{4} \tag{22}$$

$$p_{m2}^* = \frac{e^{-\beta\Delta t}}{2} \tag{23}$$

$$w_2^* = \frac{1+e^{-\beta\Delta t}+\rho(e^{-\beta\Delta t}-3)}{4(1-\rho)} \tag{24}$$

$$\Pi_{r2}^* = \frac{2(1-\rho)(1-e^{-\beta\Delta t})+e^{\beta\Delta t}-1}{8} \tag{25}$$

$$\Pi_{m2}^* = \frac{4\rho(e^{\beta\Delta t}-1)+3e^{-\beta\Delta t}+1}{16} \tag{26}$$

We can obtain $\rho \in \{\frac{1}{4} \leq \rho < \frac{1}{2}\}$ by solving the inequalities $\begin{cases} \Pi_{r2}^* > \Pi_{r1}^* \\ \Pi_{m2}^* > \Pi_{m1}^* \end{cases}$, i.e. the inequalities have at least one solution, which means that in contract (w, ρ), the retailer and the manufacturer agree on the optimal channel choice of the retailer. Therefore, the supply chain coordination can be reached by using a compensation-based whole price contract.

Proposition 6 shows that the retailer who chooses dual retail channels strategy can reach a consensus with the manufacturer by sharing part of the profit with the manufacturer after sales. The profit of the retailer is reduced after sharing, but they remain higher than those from the single retail channel strategy. Moreover, dual retail channels strategy becomes the optimal retail channel choice for the manufacturer after it obtains profit sharing.

5. Conclusion

The following conclusions were obtained considering consumer preference for delivery lead time under manufacturer encroachment in the retailer-led dual-channel supply chain:

- The dual retail channels strategy is the optimal channel choice for the retailers. Our numerical studies show that the profit margins that the retailer obtains from dual retail channels supply chain and single online retail channel supply chain will increase as consumers' delivery lead time preference coefficient increases.
- The optimal pricing of online retail channel and offline retail channel are positively related to consumers' delivery lead time preference coefficient, whereas the optimal pricing of online direct channel is negatively related to consumers' delivery lead time preference coefficient. Our numerical studies show that consumers' delivery lead time preference coefficient has a particularly significant impact on the optimal pricing of single online retail channel.
- The optimal pricing in the online retail channel is higher than that in the offline retail channel and online direct channel. Thus, a retailer can set online retail prices higher than its offline retail prices and the manufacturer's online direct selling price.

- Although the optimal channel selection of the retailer may reduce the profit of the manufacturer, the retailer and the manufacturer can adopt a compensation-based whole price contract to coordinate the conflict brought by the optimal channel choice of the retailer.

Several interesting topics can be explored for further research. In this study, we assumed that consumer preference for delivery lead time is determined. In practice, consumer preference for delivery lead time is heterogeneous and varies greatly due to different products purchased. For example, consumers may have a stronger delivery lead time preference for fresh and perishable products and a weaker preference for durable goods. In the future, studying the pricing and channel choice of the retailer in the dual-channel supply chain will be sensible in the case of uncertain consumer preference for delivery lead time.

Acknowledgement

This study was supported in part by Humanities and Social Science Foundation of Ministry of Education of China (16YJC790032), Major projects of Fujian Social Sciences Research Base (FJ2018JDZ023), The Nature Science Foundation of Fujian Provincial (2018J01809), New Century Training Program Foundation for the Talents of Fujian Province and Training Plan for Outstanding Young Researchers of Fujian Province.

References

[1] Chiang, W.Y.K., Monahan, G.E. (2005). Managing inventories in a two-echelon dual-channel supply chain, *European Journal of Operational Research*, Vol. 162, No. 2, 325-341, doi: 10.1016/j.ejor.2003.08.062.

[2] Hu, H., Wu, Q., Han, S., Zhang, Z. (2020). Coordination of dual-channel supply chain with perfect product considering sales effort, *Advances in Production Engineering & Management*, Vol. 15, No. 2, 192-203, doi: 10.14743/apem2020.2.358.

[3] Tsay, A.A., Agrawal, N. (2004). Channel conflict and coordination in the E-commerce age, *Production and Operations Management*, Vol. 13, No. 1, 93-110, doi: 10.1111/j.1937-5956.2004.tb00147.x.

[4] Edinger-Schons, L.M., Lengler-Graiff, L., Scheidler, S., Mende, G., Wieseke, J. (2020). Listen to the voice of the customer – First steps towards stakeholder democracy, *Business Ethics: A European Review*, Vol. 29, No. 3, 510-527, doi:10.1111/beer.12252.

[5] Hu, Y.S., Lin, J., Su, X.-L. (2020). Channel selection decision in a dual-channel supply chain: A consumer driven perspective, *IEEE Access*, Vol. 8, 145634 -145648, doi: 10.1109/ACCESS.2020.3014396.

[6] Jian, M., Wang, Y.L. (2018). Decision-making strategies in supply chain management with a waste averse and stockout averse manufacturer, *Advances in Production Engineering & Management*, Vol. 13, No. 3, 345-357, doi: 10.14743/apem2018.3.295.

[7] Devaraj, S., Fan, M., Kohli, R. (2002). Antecedents of B2C channel satisfaction and preference: Validating e-commerce metrics, *Information Systems Research*, Vol. 13, No. 3, 316-333, doi: 10.1287/isre.13.3.316.77.

[8] Rohm, A.J., Swaminathan, V. (2004). A typology of online shoppers based on shopping motivations, *Journal of Business Research*, Vol. 57, No. 7, 748-757, doi: 10.1016/S0148-2963(02)00351-X.

[9] Gupta, A., Su, B.-C., Walter, Z. (2004). An empirical study of consumer switching from traditional to electronic channels: A purchase-decision process perspective, *International Journal of Electronic Commerce*, Vol. 8, No. 3, 131-161, doi: 10.1080/10864415.2004.11044302.

[10] Buntak, K., Kovačić, M., Mutavdžija, M. (2019). Internet of things and smart warehouses as the future of logistics, *Tehnicki Glasnik – Technical Journal,* Vol. 13, No. 3, 248-253, doi: 10.31803/tg-20190215200430.

[11] Gallego-Gómez, C., de-Pablos-Heredero, C. (2017). Customer relationship management (CRM) and BIG DATA: A conceptual approach and their impact over the power of data applied to selling strategies, *DYNA*, Vol. 92, No. 3, 274-279, doi:10.6036/8071.

[12] Kaya Keleş, M. (2017). An overview: The impact of data mining applications on various sectors, *Tehnicki Glasnik* – Te*chnical Journal*, Vol. 11, No. 3, 128-132.

[13] Zhou, R., Liao, Y., Shen, W., Yang, S. (2020). Channel selection and fulfillment service contracts in the presence of asymmetric service information, *International journal of production economics*, Vol. 222, 107504, doi: 107504.1-107504.17.

[14] Karraya, S., Siguéb, S.P. (2018). Offline retailers expanding online to compete with manufacturers: Strategies and channel power, *Industrial Marketing Management*, Vol. 71, 203-214, doi: 10.1016/j.indmarman.2018.01.004.

[15] Shi, Y., Zhou, L., Qu, T., Qi, Q. (2019). Introducing the marketplace or not? Risk analysis of channel strategy for online retailers, *Industrial Management & Data Systems*, Vol. 120, No. 2, 366-387, doi: 10.1108/IMDS-03-2019-0183.

[16] Nie, J., Zhong, L., Yan, H., Yang, W. (2019). Retailers' distribution channel strategies with cross-channel effect in a competitive market, *International Journal of Production Economics,* Vol. 213, 32-45, doi: 10.1016/j.ijpe.2018.12.019.

[17] Wang, K., Goldfarb, A. (2017). Can offline stores drive online sales?, *Journal of Marketing Research*, Vol. 54, No. 5, 706-719, doi: 10.1509/jmr.14.0518.

[18] Huang, J.-S., Pan, S.L., Liu, J. (2017). Boundary permeability and online-offline hybrid organization: A case study of Suning, China, *Information & Management*, Vol. 54, No. 3, 304-316, doi: 10.1016/j.im.2016.08.002.

[19] Jayaswal, S., Jewkes, E.M. (2016). Price and lead time differentiation, capacity strategy and market competition, *International Journal of Production Research*, Vol. 54, No. 9, 2791-2806, doi: 10.1080/00207543.2016.1145816.

[20] Pekgün, P., Griffin, P.M., Keskinocak, P. (2016). Centralized vs. decentralized competition for price and lead-time sensitive demand. *Decision Sciences, Forthcoming,* Vol. 48, No. 6, 1198-1227.

[21] Li, Y.-B., Lin, C.-P., Wu, T.-J., Chen, J.-L. (2017). The study on price and lead time decisions in retailer-dominated dual-channel supply chain, *Journal of Interdisciplinary Mathematics*, Vol. 20, No. 3, 805-819, doi: 10.1080/09720502.2017.1358869.

[22] Zhao, S., Wu, F., Jia, T., Shu, L. (2018). The impact of product returns on price and delivery time competition in online retailing, *Computers & Industrial Engineering,* Vol. 125, 658-667, doi:10.1016/j.cie.2018.01.007.

[23] Ye, F., Xie, Z., Tong, Y., Li, Y. (2020). Promised delivery time: Implications for retailer's optimal sales channel strategy, *Computers & Industrial Engineering*, Vol. 144, 106474, doi:10.1016/j.cie.2020.106474.

[24] Yang, J.Q., Zhang, X.M., Fu, H.Y., Liu, C. (2017). Inventory competition in a dual-channel supply chain with delivery lead time consideration, *Applied Mathematical Modelling*, Vol. 42, 675-692, doi:10.1016/j.apm.2016.10.050.

[25] He, L., Zhang, X., Wang, Q.P., Hu, C.L. (2018). Game theoretic analysis of supply chain based on mean-variance approach under cap-and-trade policy, *Advances in Production Engineering & Management*, Vol. 13, No. 3, 333-344, doi: 10.14743/apem2018.3.294.

[26] Chiang, W.K., Chhajed, D., Hess, J.D. (2003). Direct marketing, indirect profits: A strategic analysis of dual-channel supply-chain design, *Management Science*, Vol. 49 , No. 1, 1-20, doi: 10.1287/mnsc.49.1.1.12749.

[27] Balcázar-Camacho, D.A., López-Bello, C.A., Adarme-Jaimes, W. (2016). Strategic guidelines for supply chain coordination in healthcare and a mathematical model as a proposed mechanism for the measurement of coordination effects, *DYNA*, Vol. 83, No.197, 203-211, doi: 10.15446/dyna.v83n197.55596.

APEM journal
Advances in Production Engineering & Management
Volume 15 | Number 4 | December 2020 | pp 467–480
https://doi.org/10.14743/apem2020.4.379
ISSN 1854-6250
Journal home: apem-journal.org
Original scientific paper

A simulation-based approach to study the influence of different production flows on manufacturing of customized products

Żywicki, K.[a,*], **Rewers, P.**[a]

[a]Faculty of Mechanical Engineering, Poznan University of Technology, Poznan, Poland

A B S T R A C T

Manufacturing products tailored to the individual requirements of customers is a must if companies want to compete effectively on the market. The production of customized goods poses new challenges for all areas of functioning of production systems. It is necessary to adopt such rules and methods that will allow a flexible response to product design changes and their demand In the organization of production flow (materials and information). The article presents research carried out in the SmartFactory laboratory of the Poznań University of Technology regarding the impact of the structure of products (customization) on the realization of current production orders. The research was carried out using the FlexSim simulation environment. Based on simulation experiments for three forms of organization of production flow with varying degrees of flexibility of production resources, an analysis was made of the time of execution of various sets of production orders and the level of use of available working time. The results of research indicate that in the production of products with low and high planned labor consumption, the use of universal production station is the most advantageous. For such a solution, the degree of utilization of the available working time of production stations is also the highest. It was also found that the principles of scheduling production orders affect the effectiveness of the production system. The best results were obtained for the production schedule, where the sequence of production orders was established from the lowest planned time of resource loading.

A R T I C L E   I N F O

Keywords:
Smart manufacturing;
Production flow;
Customized products;
Variant products;
Discrete-event simulation (DES);
FlexSim simulation modeling and analysis software

**Corresponding author:*
krzysztof.zywicki@put.poznan.pl
(Żywicki, K.)

Article history:
Received 26 May 2020
Revised 4 December 2020
Accepted 7 December 2020

1. Introduction

Manufacturing companies try to meet growing demands and changing customer demand in various ways. Some of them try to improve production processes by implementing various concepts, e.g. Lean Manufacturing or Six Sigma, so as to be able to produce products of the required quality in a short time and at relatively low costs [1]. Others, however, decide to manufacture products designed for individual customer orders, i.e. mass customization (MC) [2]. The term mass customization was first used by Stan Davis in Future Perfect [3] and then developed by Pine II [4]. In this paradigm it is extremely important to offer products tailored to individual customer needs while maintaining mass production efficiency [5-7]. The purpose of mass customization, however, is not to provide different product variants, but to design the product in accordance with the individual requirements of the recipient [8]. The implementation of mass customization is very attractive from the customer's point of view, but for the company it creates the risk of failure, especially due to the increase in costs of designing and manufacturing products. The MC strategy can give a competitive advantage on the market only if the company is able to quickly respond to changing expectations and requirements of customers, i.e. it is able to combine the MC strategy with the Quick Response (QR) strategy. The combination of both strategies is only possible if the company has a flexible production system (including flexible production resources) and is able to quickly design and implement new products and their manufacturing processes [9-12].

Mass customization is also one of the basic goals of industry 4.0 [13, 14]. Industry 4.0 refers to the Digital Manufacturing System provided by the effective integration of production processes, information technologies and equipment [15, 16]. The main goal of industry 4.0 is to improve the efficiency and reactivity of the production system [16]. In industry 4.0, production processes must also be more flexible, combining high efficiency and diversity of the production range, and intelligent to be able to successfully meet the challenges of dynamically changing demand and individual customer needs [18-20].

A measure of the flexibility of the production process is its ability to perform operations, as well as the "speed" at which it can be prepared to perform a new task. However, a high degree of production flexibility causes problems with organization and production control [21-24]. These problems result primarily from the dynamic conditions of customer demand, the production of various products and the failure to use the available production capacity of production resources. One of the factors affecting the use of the available production capacity of machines and technological devices in flexible production systems is the degree of specialization of workstations [25]. This means that in the case of flexible production processes, the use of special and specialized work stations (i.e. having dedicated equipment for the production of specific types of products and production operations on these products) carries the risk of not using the available production capacity of these stations [26]. Therefore, in the case of mass customization strategies, universal work stations that can carry out different production tasks on different products are more often used. These universal work stations can be assembled into a production line, manufacturing cell or take the form of a workplace organization of production [27].

In turn, dynamic conditions of demand and the production of various, customized products force production companies to look for the best solutions in the field of organization and control of production. To this end, many of them decide to use simulation methods that allow the analysis and evaluation of different variants of the organization of production flow [28, 30, 31]. The term "simulation" means imitating the real situation, real objects and connections that exist between these objects [29, 32]. Simulation is a research method and enables research, analysis and evaluation of introduced changes outside of real processes [33, 34]. In a simplified way, the simulation is carried out in three steps [35]:

- designing the simulation model of the actual process or system,
- conducting experiments using the simulation model,
- using the results obtained to improve the actual system or process.

Simulation models of manufacturing processes are built to reduce the risk of failure when making significant changes to the actual process or when designing a new process to be able to choose the best variant of the organization of production. The simulation allows you to gain insight into complex process structures, test new rules for the organization of production, or flow of materials through the process, analyze production indicators or collect information and knowledge without violating the actual process [33, 36].

This article presents the results of research aimed at determining the impact of the form of the organization of production flow on the efficiency of the set of production orders for customized products (with different construction structure). Three groups of products were adopted, different in terms of labour intensity of performance. A series of simulation experiments were carried out for three samples of production order sets implemented in three variants of forms of organization of production flow: linear, cell and station. In addition, each set of orders was subjected to experiments taking into account different rules for scheduling orders: in any order, from the longest to the shortest and from the shortest to the longest. The obtained results were analyzed in terms of the time of order completion and the degree of use of the available work time of the workstations.

2. Problem presentation and a goal of the research

2.1 SmartFactory laboratory at Poznan University of Technology

The production system at the SmartFactory laboratory of the Poznan University of Technology was built to conduct research works for various technical and organizational solutions in line with the concept of Industry 4.0. The laboratory equipment allows mapping of various processes occurring in the real production system.

Research work carried out in the laboratory focuses on:

- development of systems supporting the design and configuration of customized products,
- additive production of parts and production instrumentation,
- application of virtual reality and augmented reality solutions in production and training processes,
- development and testing of methods and information systems supporting production planning and control,
- implementing technical solutions to supervise and control material flow, e.g. RFID, RTLS.

The main element is the automatic assembly line. It consists of three transport loops at which work stations are located. The loops are equipped with switches that enable the redirection of the pallet being the carrier transporting the product to any transport loop. Each pallet has an RFID tag enabling its identification and directing its movement by the RFID head reading and switches steering. The line is controlled by a control cabinet equipped with power elements, protection systems, power supply, PLC controller, and security system module. The system uses two industrial networks AS-interface and ProfiNet for controlling devices.

Production system management is carried out by an IT system called 4Factory. Communication between system elements takes place via the Internet of Things. The 4Factory system is built of a number of modules whose functionalities enable production planning, supervision of material flow, and control of the production line operation (Fig. 1).

The production process in the SmartFactory laboratory involves the assembly of parts products in the form of lego blocks. They were adopted as a basic element of the construction of finished products so that the flexibility was provided in the field of product construction in accordance with the idea of customization of production. The flow of products on the production line is carried out according to the principle of one piece flow, where a transport pallet is the carrier. Work stations are equipped with flow racks that allow storage of containers with parts and assemblies for assembly of finished products. The shelves were also equipped with RFID reading heads enabling their identification. The basis for starting the production process is the schedule developed in the 4Factory program. It provides information about the order of production of products and their assembly sequence at individual positions. The assembly process is carried out manually by operators who carry out tasks in accordance with the schedule and assembly instructions.

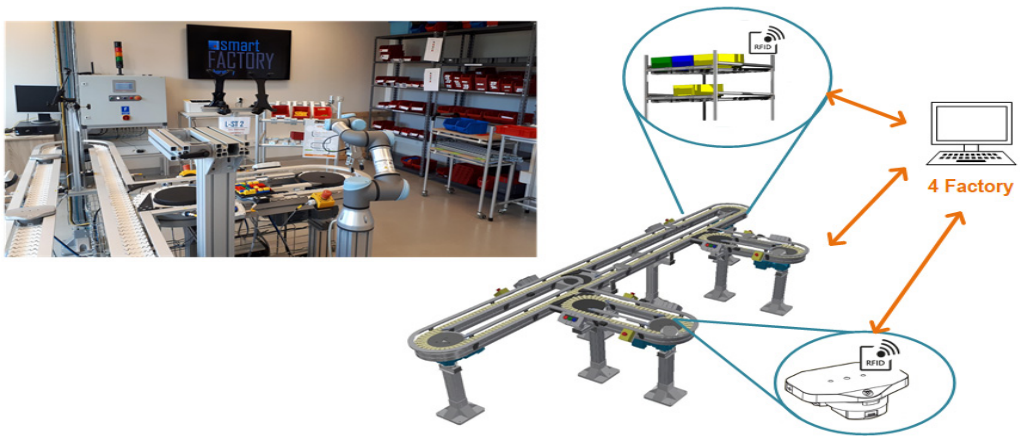

Fig. 1 View and visualization of the SmartFactory laboratory

2.2 The aim of the test

The technical equipment and possibilities in the scope of product construction influence the high flexibility of the production system. Therefore, one of the research directions is the development of a dynamic method of scheduling and controlling production flow for high variability of product variants (customized products). The presented research is one of their stages.

The aim of the research was to determine the impact of the form of the organization of production flow on the efficiency of the realization of a set of production orders for products with different constructional structures.

The study assumed three variants of the production flow form (Fig. 2):

- Variant 1 (variant 1-6): linear form – the production process for each product is carried out at all six subsequent workstations.
- Variant 2 (variant 1-2-2-1): nest form – the production process of a given product is carried out at station 1, manufacturing cell 1 or 2 containing two stations and station 6.
- Variant 3 (variant 1-4-1): workplace form – the process of producing a given product is carried out at station 1, then at one of the universal stations from 2 to 5 and station 6.

18 different parts with different numbers and assembly configuration were the basis for the construction of product variants. In this way, products with different constructional structures and thus different planned load times for work stations are created. The standard assembly time for one part is 4 [s], and the same time to manufacture 1 piece of product is a multiple of this time and the number of pieces of product components.

Variants 1-6 include the assumption that each product with any constructional structure is implemented at all six subsequent work stations. At the given work station, 3 types of parts that are assembled are strictly defined.

Variants 1-2-2-1 assume the occurrence of 2 mutually replaceable manufacturing cells consisting of two stations. In this variant, stations 1 and 6 provide for the assembly of parts as in option 1, while the assembly of other parts is possible in manufacturing cells.

Finally in variant 1-4-1, at stations 1 and 6, the assembly of parts is carried out as in the previous variants. Stations 2 to 5 are replaceable/universal, where it is possible to install other parts.

The presented scope of tests was conducted in the FlexSim simulation environment and the obtained results were the basis for developing the production schedule in the 4Factory program, controlling the assembly line in real conditions.

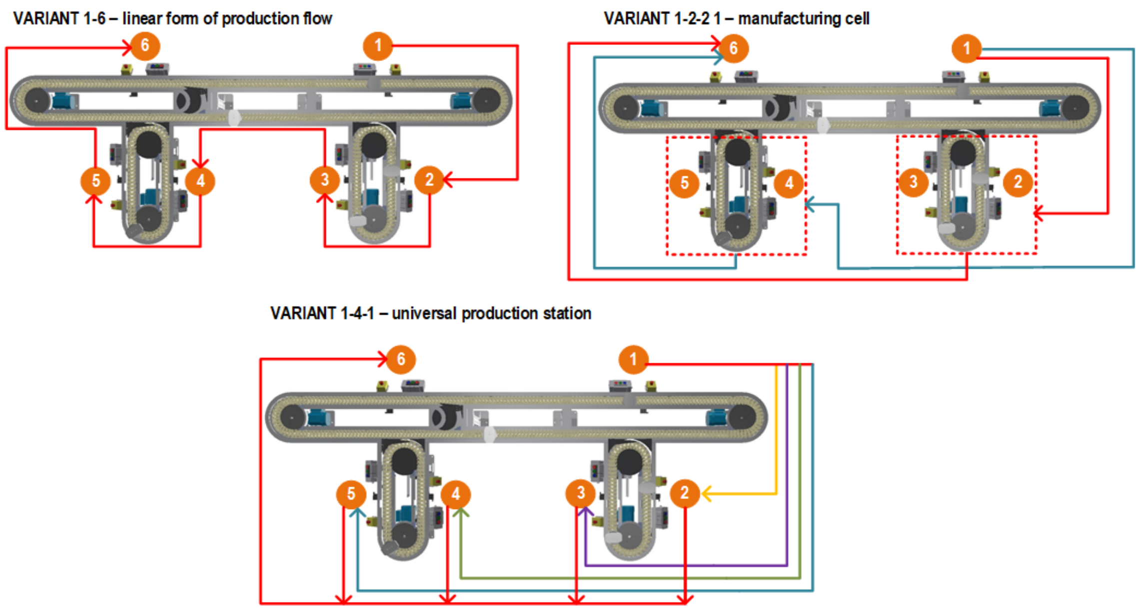

Fig. 2 Schemes of variants of forms of organization of production flow

3. A simulation-based approach

The research involved conducting a number of simulation experiments in the FlexSim environment and included the implementation of production order sets for the assumed three variants of the organizational form of production flow. They were carried out according to the following stages: execution and verification of simulation models of variants of production flow forms, design of products and their technological processes, development of sets of production orders, conducting simulation experiments, and analysis of results.

3.1 Simulation models of different forms of production flow

Simulation models for the SmartFactory laboratory reflected all the necessary technical and functional elements of the production system. Objects representing the necessary elements of the production process (e.g. order list) but also technical elements ensuring the proper operation of the models have been implemented. These elements include tables containing parameters and results of the model's operation as well as objects visualizing its operation. An example of the visualization of the simulation model for one of the variants of the form of organization of the flow is shown in Fig. 3.

The operation of the simulation model is determined by the parameters contained in the "parameters" table. This table contains both general parameters for the model and detailed parameters for each of the products. The list of production orders is represented in the model in the form of an appropriate table of the "orders" object - a single row in this table represents one order and contains the following parameters: product name, order size, and sequence of its execution. The results of the model operation are represented by output tables, messages in the simulator console window, and graphs updated during the model operation.

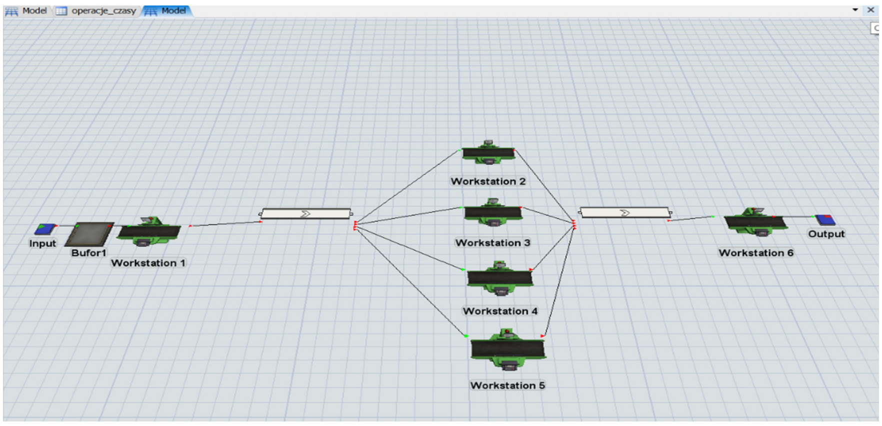

Fig. 3 Schemes of variants of forms of organization of the flow of production

3.2. The aim of the research

The study assumed the existence of three groups of products with different numbers of components forming the constructional structure and thus with different planned load times for work stations. This time is understood as the required standard lead time for assembly tasks at all work stations. Product groups were defined as:

- products with a small planned load time – products containing 10 to 20 parts,
- products with an average planned load time – products with 20 to 40 parts,
- products with a high planned load time – products containing from 40 to 70 parts.

For each product group, 30 structurally different products were designed and technological processes were developed for them, taking into account the assumed variants of production flow.

Product groups were then the basis for generating sets of production orders to be implemented in simulation models. Three sets of production orders were generated for each group of products:

- for products with low labor intensity (designations L 1-3),
- for products with low average labor consumption (designations M 1-3),
- for products with low high labor consumption (designations H 1-3),

which differed in the occurrence of product variants, in their share in the collection and in the number of pieces.

Sets of production orders included restrictions:

- the maximum number of items in the set of production orders: 100 items,
- the number of items in the production order: 5-20 items,
- the number of production orders in the set: 30,
- production orders in the set may refer to a given product many times.

Table 1 presents the general characteristics of production order sets.

Table 1 Characteristics of production order set

Set of orders	Total planned time load workstation	Minimum planned duration of load workstation	Maximum estimated time of load work-station	Minimum number of pieces	Maximum number of pieces
L1	246,67	3.33	17.33	5	20
L2	248.93	3.33	17.07	5	20
L3	238.13	3.33	15.20	5	19
M1	682.07	12.00	47.50	5	20
M2	682.80	13.53	48.00	5	19
M3	674.53	12.00	40.53	5	19
H1	1293.73	41.33	84.00	5	20
H2	1294.93	44.80	88.00	6	20
H3	1290.93	41.67	79.80	5	19

3.3. Simulation experiments

Simulation experiments were carried out for three samples of each of the production order sets with the characteristics described above for each variant of the organization of production flow. Each set of orders was also subjected to experiments taking into account different rules for their ordering (establishing the order of implementation in the production schedule), namely: in random order, from the largest to the smallest and from the smallest to the largest planned load time of work stations. In total, 81 simulation experiments were carried out.

In the research, the production execution time was assumed as the main indicator for the assessment of production flow variants. However, the degree of utilization of the available working time of work stations was also introduced as an additional indicator.

4. Results and discussion

4.1. Production order processing time

The results of the research were the result of simulation tests. The analysis of these results included the time of execution of production orders and the degree of use of the available working time at work stations.

The production order group execution time covers the period from the beginning of the first operation of the first order to the end of the last operation of the last order included in the production schedule.

Based on the analysis of the results, it can be concluded that for products with a small planned load time, the shortest order fulfillment times were obtained for variant 1-4-1 of the form of production flow for three samples and for three rules for order scheduling in the production schedule. The linear form (variants 1-6) turned out to be the worst for all three sets of orders and each of the three variants of the production schedule. Data analysis also showed no significant impact of scheduling on order processing time (Fig. 4).

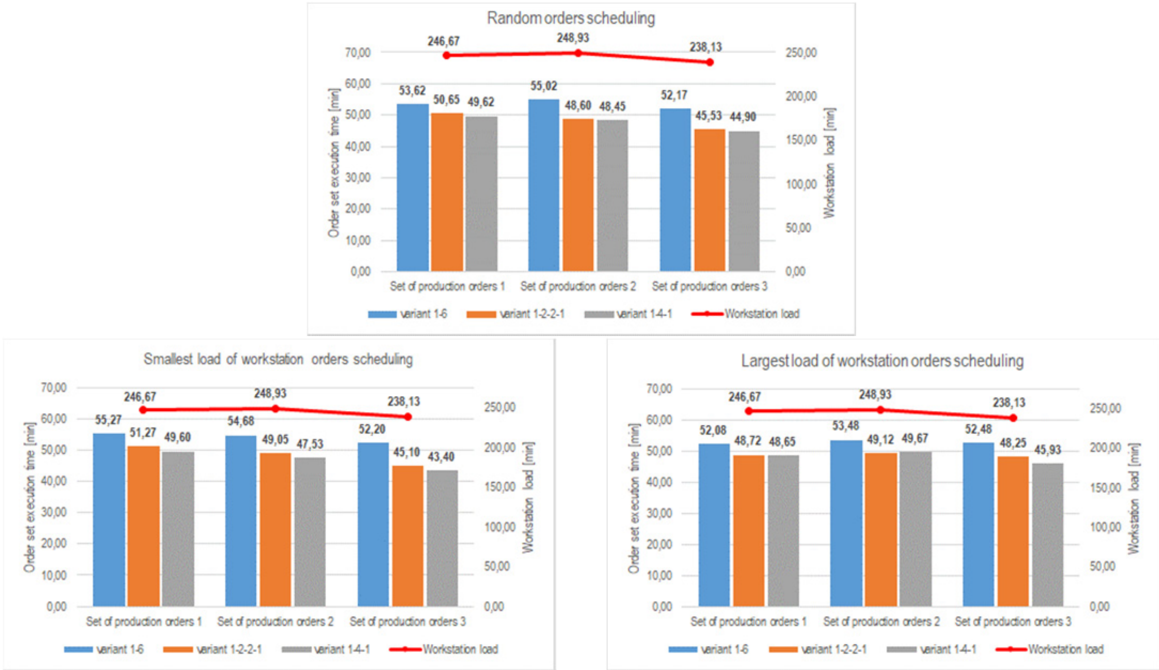

Fig. 4 Comparison of production order fulfillment times for products with low planned resource load

For products with an average planned load of workstation, the time of order sets are comparable for all three variants of organization of production flow. The analysis did not show in this case a significant correlation of the analyzed factors. Only a comparison within a given set of production orders allows to indicate the best variant. For the set of orders 1, the results are comparable with the indication for option 1-4-1. Variant 1-2-2-1 allows the shortest order fulfillment time for the set of orders 2 and 3 (Fig. 5).

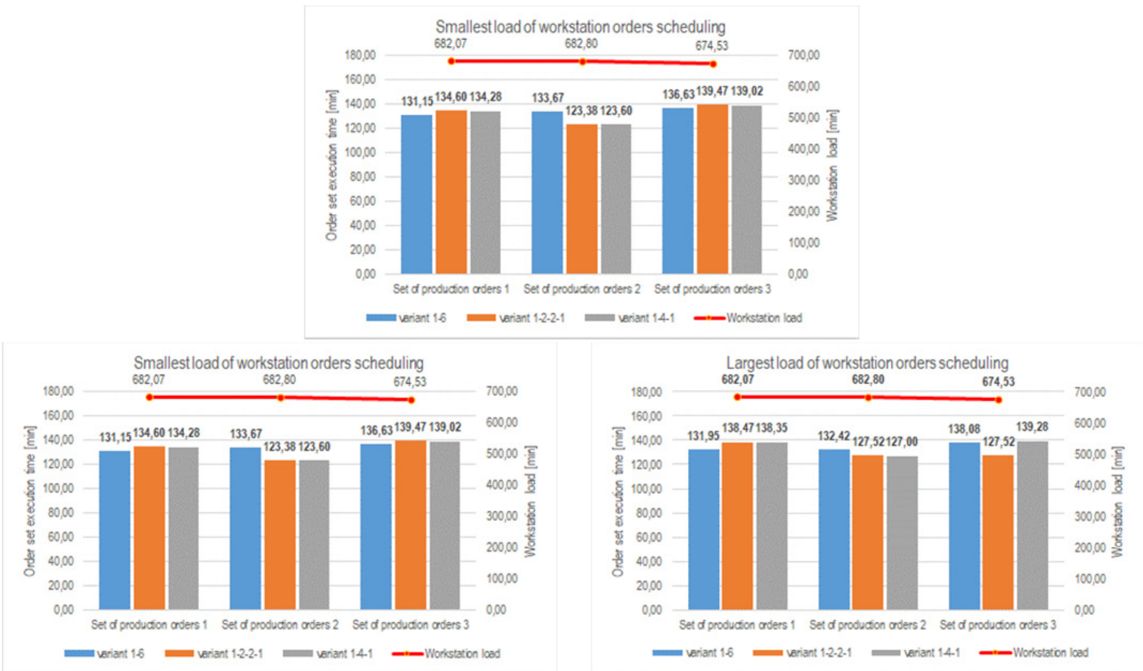

Fig. 5 Comparison of delivery times for production orders for products with average planned resource load

For products with high planned load of stations, the shortest times were obtained in option 1-4-1 forms of production flow for three samples and three rules for order scheduling in the production schedule. The linear form (variants 1-6) turned out to be the worst for all three samples and for each of the three variants of the production schedule. Analysis of the results indicates that for variant 1-6 the shortest times were achieved in the case of order scheduling from the lowest load time for work stations. However, in the case of variants 1-2-2-1 and 1-4-1, the shortest order fulfillment times were obtained for scheduling with the largest planned load of positions (Fig. 6).

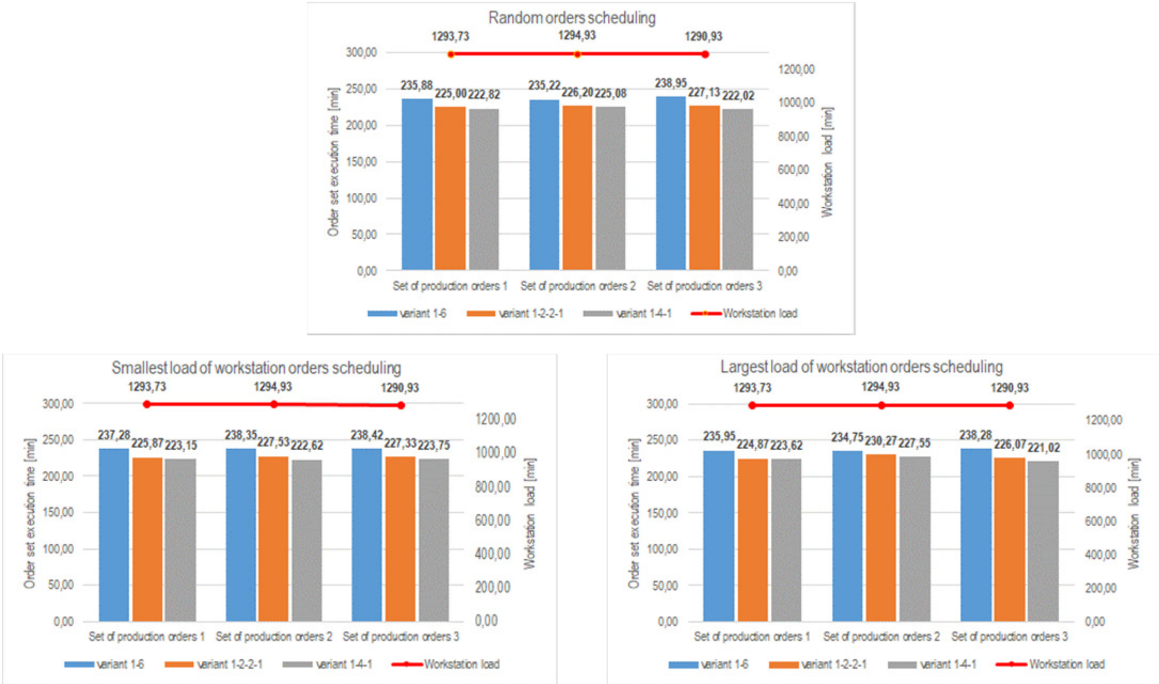

Fig. 6 Comparison of delivery times for production orders for products with high planned resource load

4.2 Use of available working time

The reference value for analyzing the degree of use of the available working time of work stations was the time of implementation of a given set of production orders.

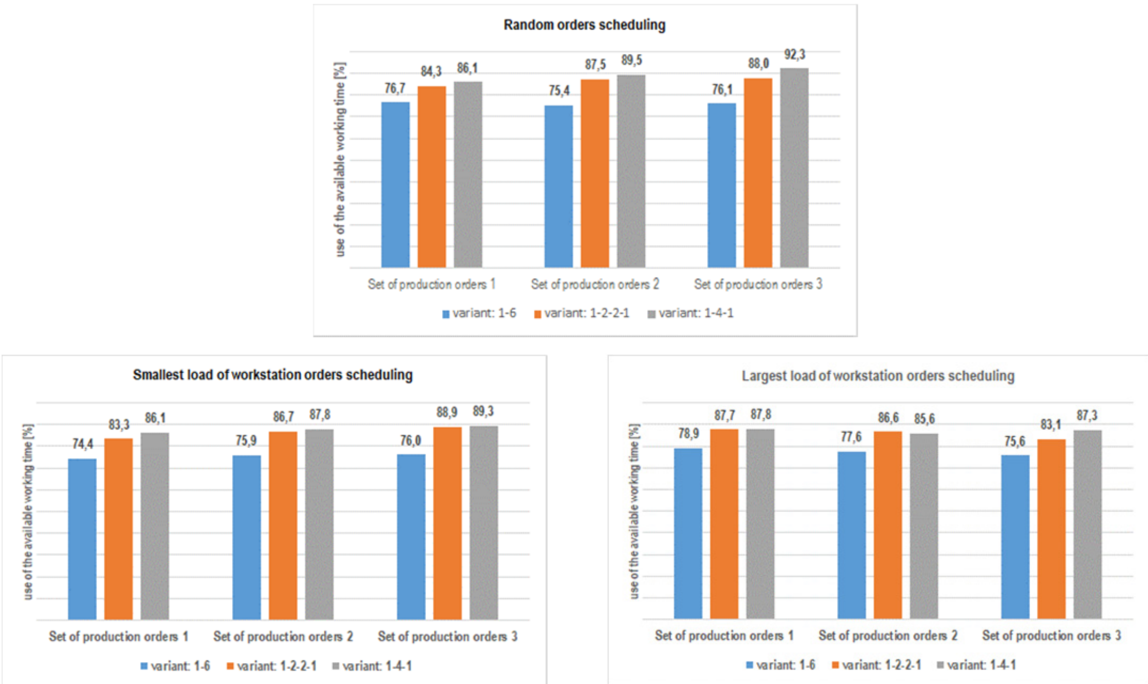

Fig. 7 Comparison of the use of available working time for products with low planned resource load

For orders with a low planned load on work stations, the largest use of available working time was obtained for the variant 1-4-1 of organization of production flow. Similar values were obtained for variant 1-2-2-1, while variant 1-6 has the lowest level of use of available working time. These results apply to all rules for scheduling the implementation of production orders (Fig. 7).

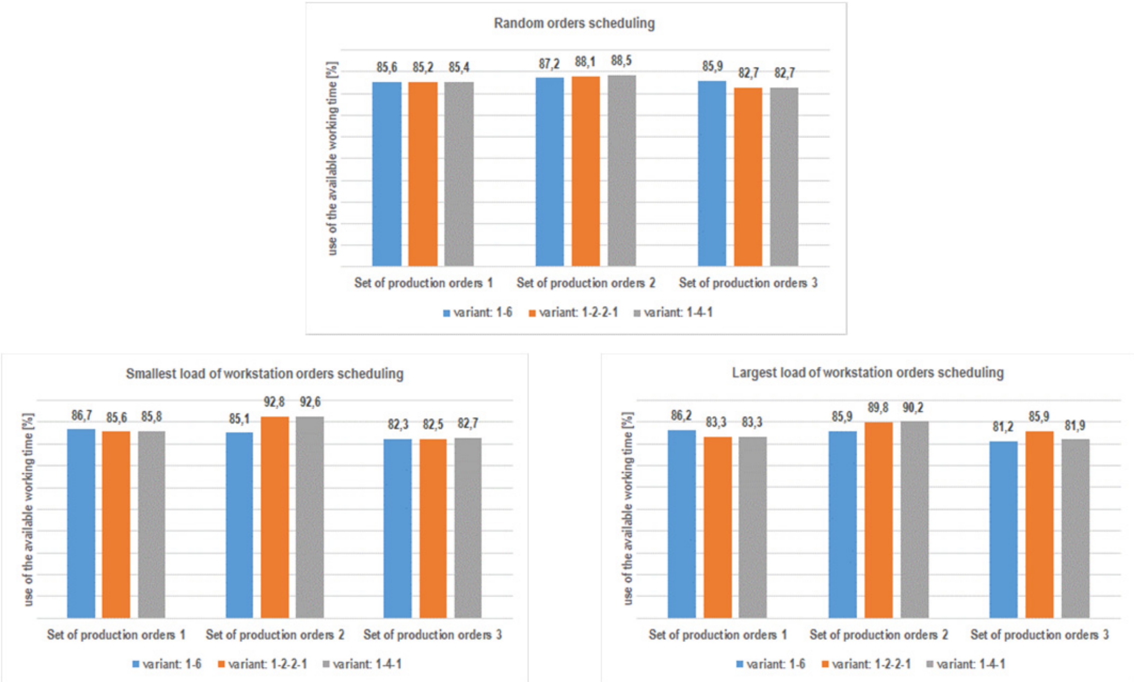

Fig. 8 Comparison of use of available working time for products with average planned resource load

Simulation experiments for sets of orders with an average planned load time of production positions did not indicate clear correlations between the examined factors. In the case of random orders, the results are comparable for each variant of the organization of production flow. Variants 1-2-2-1 and 1-4-1 allow to obtain slightly better results for production schedules set according to the rules from the smallest and the longest planned load time of work stations, Fig. 8.

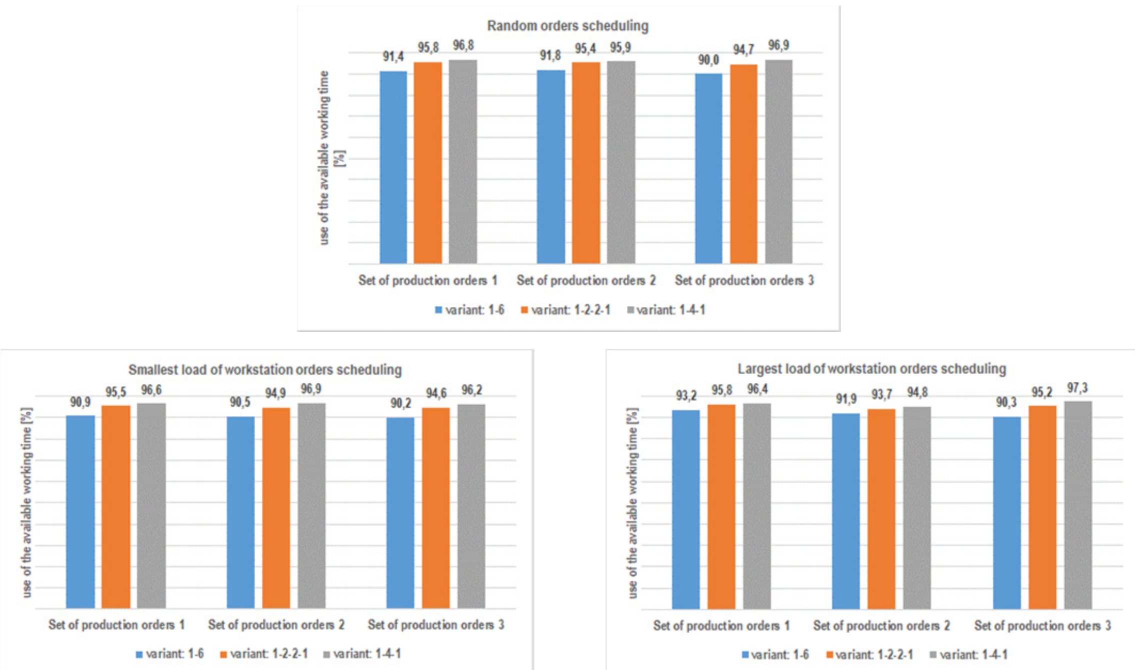

Fig. 9 Comparison of the use of available working time for products with high planned resource load

Analysis of results for order sets with high planned load of stations, the largest use of available working time occurs for variants 1-4-1 of organization of production flow. Similar values were obtained for variant 1-2-2-1, while variant 1-6 has the lowest level of use of available working time. These results apply to all rules for scheduling the implementation of production orders (Fig. 9).

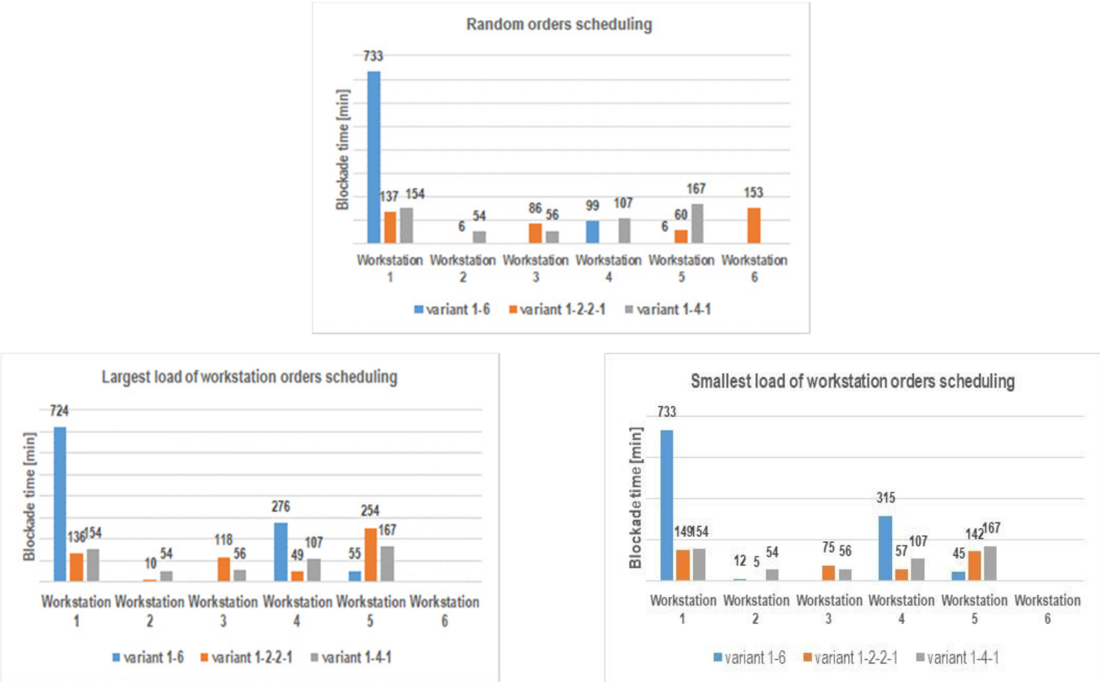

Fig. 10 Production system blockade for products with low planned resource load

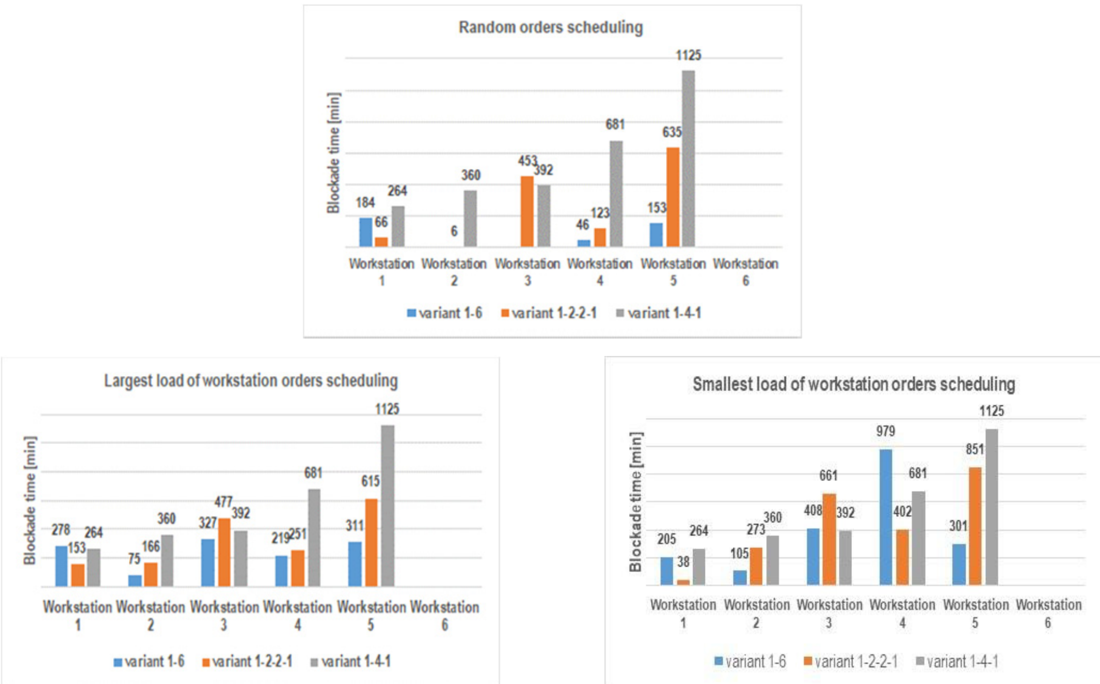

Fig. 11 Production system blockade for products with average planned resource load

The basic factor affecting the degree of use of the available working time of work stations was the so-called "blockade". It refers to the situation in which it is not possible to continue with the production orders for a given position due to the occurrence of the maximum level of inter-operational stock. This is due to the technical limitations of the assembly line, as mentioned earlier, where a maximum of 10 transport pallets (product carrier) can be on a given transport loop between stands.

The results of the simulation experiments carried out indicate that:

- in the case of production orders for products with a low resource load time, station 1 of variants 1-6 most often had downtime caused by blockade for all three types of production schedules (Fig. 10),
- for orders for products with medium load time the longest downtime occurred at stations 4 and 5 for all variants of the organization of production flow (Fig. 11),
- the execution of orders for products with a high resource load time in variants 1-6 and for all variants of their scheduling resulted in stops of positions 2 and 3 (Fig. 12).

The reason for such states of operating of the production system is the lack of load balancing of work stations and synchronization of product flow for the production line.

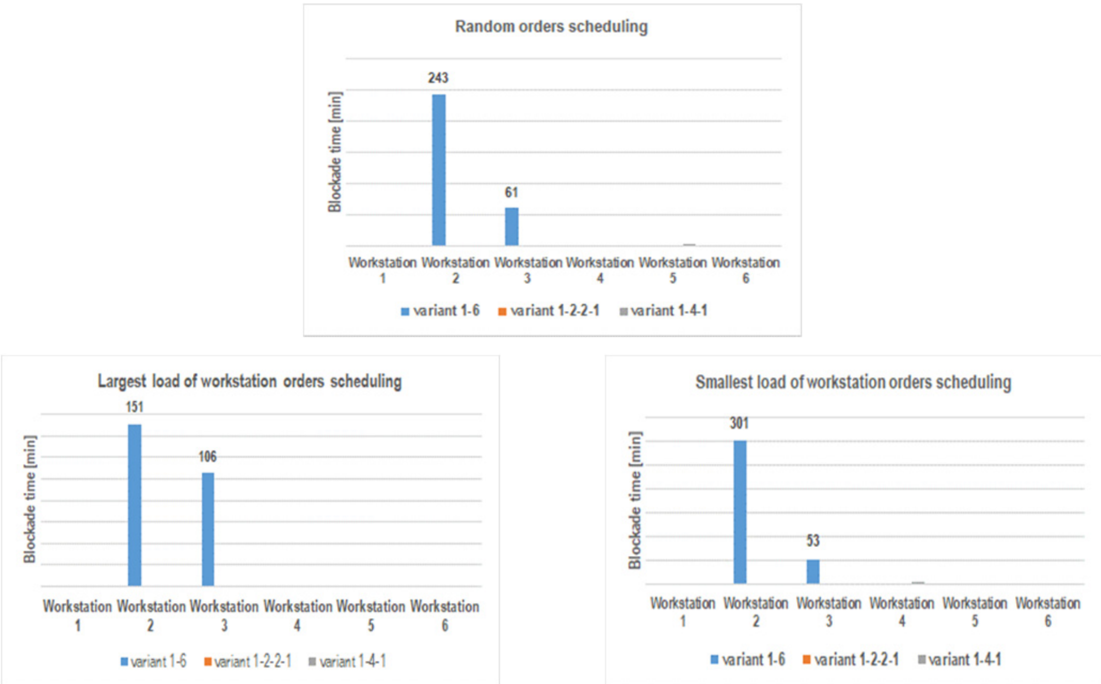

Fig. 12 Production system blockade for products with a high planned resource load

4.3 Comparison of the results

A summary of the results of the tests is presented in Table 2. It contains a summary of average parameter values of assessment for three sets of production orders.

Based on these values it can be concluded that the use of universal positions in the production system (variants 1-4-1 form of organization of production flow) allows to shorten the time of implementation of production orders for products with small and large planned resource load time. For such solution, the degree of utilization of the available working time is also the highest. The obtained results of the effectiveness of functioning of the production system are influenced by the rules for scheduling production orders. The best results can be obtained for the production schedule, where the schedule of work is set starting with the orders with the lowest planned resource load time.

Table 2 Summary of test results

Orders with low planned resource load time									
Assessment parameters	Random order scheduling			Ordering from the shortest resource load time			Ordering from the longest resource load time		
	1-6	1-2-2-1	1-4-1	1-6	1-2-2-1	1-4-1	1-6	1-2-2-1	1-4-1
Order processing time [min]	53.60	48.26	47.66	54.05	48.47	46.84	52.68	48.69	48.08
Utilization of available working time [%]	76.1	86.6	87.7	75.4	86.3	89.3	77.4	85.8	86.9
Orders with average planned resource load									
Order processing time [min]	135.79	134.74	134.47	133.82	132.48	132.30	134.15	131.17	134.88
Utilization of available working time [%]	85.2	85.3	85.5	84.7	87.0	87.1	84.4	86.3	85.1
Orders with high planned resource load									
Order processing time [min]	236.68	226.11	223.31	238.02	226.91	223.17	236.33	227.07	224.06
Utilization of available working time [%]	91.1	95.3	96.5	90.6	95.0	96.6	91.8	94.9	96.2

The variant of organization of production flow based on universal manufacturing cells (variant 1-2-2-1) allows to obtain the best results of order processing time and the degree of use of work stations in the manufacturing of products with medium load time. In this case, it is also beneficial to set the order of execution of orders from those with the largest planned load time. This variant also gives results slightly worse than variant 1-4-1 in the production of products with different characteristics.

The use of a linear form turns out to be the worst solution in the production of this type of products with constructional and quantitative characteristics as adopted in the research. However, for products with an average resource load time, the simulation results obtained do not differ significantly from the other variants of the form of organization of the production flow.

5. Conclusion

Production flexibility is a basic feature of production systems that allows meeting customer requirements in the manufacturing of customized products. The article presents the results of research on determining how the form of organization of production flow affects the implementation of production orders.

The research were carried out in the FlexSim simulation environment and constitute the beginning of research works related to the use of simulation methods in production control. The results of the simulation experiments for the set of production orders, technological processes and evaluation parameters for the analyzed variants of the production system were obtained in a very short time. Nevertheless, it should be borne in mind that the amount of input data and the complexity of the production system will increase the time it takes to obtain simulation results. This is also indicated by the authors' research in research projects commissioned by companies, where the results of simulation experiments were obtained after a few hours. This is undoubtedly a critical factor to consider when applying simulation methods to operational production control.

The indicated results indicate a direct correlation between the flexibility of used production resources and the time of order processing. According to the concept of the Intelligent Factory, production resources constituting a key factor in the manufacturing of products should be based on modularity in order to obtain the possibility of flexible configuration depending on the needs determined by design and technological changes in the manufacturing of products.

Undoubtedly, this flexibility of resources will contribute to increasing the use of their available working time and thus affect their efficiency. Finally, flexible and replaceable production resources will allow for faster and comprehensive execution of customer orders, especially for customized products. And this will have an impact on the increase in the competitiveness of enterprises.

The SmartFactory laboratory is a research facility that allows for testing various technical, IT, and organizational solutions and analyze their impact on the efficiency of the production system. The presented subject and scope of research is related to ongoing works in the field of dynamic production control methods. Research results also indicated directions for further work that will be related to the implementation of production for products with even greater assortment and quantity.

Acknowledgement

The presented results are derived from a scientific statutory research conducted by Faculty of Mechanical Engineering, Poznan University of Technology, Poland, supported by the Polish Ministry of Science and Higher Education from the financial means in 2020.

References

[1] Liker, J.K., Meier, D. (2005). *The Toyota way fieldbook: A practical guide for implementing Toyota's 4Ps*, 1st edition, McGraw-Hill, London, United Kingdom.

[2] Wang, Y., Ma, H.-S., Yang, J.-H., Wang, K.-S. (2017). Industry 4.0: A way from mass customization to mass personalization production, *Advances in Manufacturing,* Vol. 5, 311-320, doi: 10.1007/s40436-017-0204-7.

[3] Davis, S.M. (1987). Future perfect, Addison-Wesley Publishing, Boston, USA.

[4] Pine II, B.J. (1993). *Mass customization: The new frontier in business competition,* Harvard Business School Press, Boston, USA.

[5] Kamble, S., Gunasekaran, A., Dhone, N.C. (2020). Industry 4.0 and lean manufacturing practices for sustainable organisational performance in Indian manufacturing companies, *International Journal of Production Research,* Vol. 58, No. 5, 1319-1337, doi: 10.1080/00207543.2019.1630772.

[6] Tseng, M.M., Jiao, J., Merchant, M.E. (1996). Design for mass customization, *CIRP Annals,* Vol. 45, No. 1, 153-156, doi: 10.1016/S0007-8506(07)63036-4.

[7] Gilmore, J.H, Pine II, B.J. (1997). The four faces of mass customization, *Harvard Business Review,* Vol. 75, No. 1, 91-101.

[8] Tian, X., Huang, L., Jia, X., Zhang, Z. (2008). Exploring parameterised process planning for mass customisation, In: Yan, X.T., Jiang, C., Eynard, B. (eds.), *Advanced Design and Manufacture to Gain a Competitive Edge,* Springer, London, United Kingdom, 643-652, doi: 10.1007/978-1-84800-241-8_65.

[9] Żywicki, K., Zawadzki, P., Hamrol, A. (2017). Preparation and production control in smart factory model, In: Rocha, Á., Correia, A., Adeli, H., Reis, L., Costanzo, S. (eds.), *Recent advances in information systems and technologies, WorldCIST 2017. Advances in Intelligent Systems and Computing,* Vol. 571, Springer, Cham, Switzerland, 519-527, doi: 10.1007/978-3-319-56541-5_53.

[10] Ko, E., Kincade, D., Brown, J.R. (2000). Impact of business type upon the adoption of quick response technologies – The apparel industry experience, *International Journal of Operations & Production Management*, Vol. 20, No. 9, 1093-1111, doi: 10.1108/01443570010339172.

[11] Lebosse, S., Taghipour, A., Canel-Depitre, B. (2017). Quick response to fluctuations in supply chains: A review, *Journal of Advanced Management Science,* Vol. 5, No. 5, 394-400, doi: 10.18178/joams.5.5.394-400.

[12] Tseng, M.M., Wang, Y., Jiao, R.J. (2017). Mass customization, In: Laperrière, L., Reinhart, G. (eds.), *CIRP Encyclopedia of Production Engineering,* Springer, Berlin, Germany, doi: 10.1007/978-3-642-35950-7_16701-3.

[13] Schwab, K. (2017). *The fourth industrial revolution,* World Economic Forum, New York, USA.

[14] Żywicki, K., Zawadzki, P., Górski, F. (2018). Virtual reality production training system in the scope of intelligent factory, In: Burduk, A., Mazurkiewicz, D. (eds.), *Intelligent systems in production engineering and maintenance – ISPEM 2017, Advances in Intelligent Systems and Computing*, Vol. 637, Springer, Cham, Switzerland, 450-458, doi: 10.1007/978-3-319-64465-3_43.

[15] Lasi, H., Fettke, P., Kemper, H.-G., Feld, T., Hoffmann, M. (2014). Industry 4.0, *Business & Information Systems Engineering,* Vol. 6, 239-242, doi: 10.1007/s12599-014-0334-4.

[16] Gajsek, B., Marolt, J., Rupnik, B., Lerher, T., Sternad, M. (2019). Using maturity model and discrete-event simulation for Industry 4.0 implementation, *International Journal of Simulation Modelling,* Vol. 18, No. 3, 488-499, doi: 10.2507/IJSIMM18(3)489.

[17] Ahuett-Garza, H., Kurfess, T. (2018). A brief discussion on the trends of habilitating technologies for Industry 4.0 and smart manufacturing, *Manufacturing Letters,* Vol. 15, Part B, 60-63, doi: 10.1016/j.mfglet.2018.02.011.

[18] Zhong, R.Y., Xu, X., Klotz, E., Newman, S.T. (2017). Intelligent manufacturing in the context of Industry 4.0: A review, *Engineering,* Vol. 3, No. 5, 616-630, doi: 10.1016/J.ENG.2017.05.015.

[19] Shen, W., Norrie, D.H. (1999). Agent-based systems for intelligent manufacturing: A state-of-the-art survey, *Knowledge and Information Systems,* Vol. 1, No. 2, 129-156, doi: 10.1007/BF03325096.

[20] Hermann, M., Pentek, T., Otto, B. (2016). Design principles for Industrie 4.0 scenarios, In: *Proceedings of the 49th Annual Hawaii International Conference on System Sciences HICSS 2016*, Koloa, Hawaii, USA, 3928-3937, doi: 10.1109/HICSS.2016.488.
[21] Ojstersek, R., Lalic, D., Buchmeister, B. (2019). A new method for mathematical and simulation modeling interactivity: A case study in flexible job shop scheduling, *Advances in Production Engineering & Management,* Vol. 14, No. 4, 435-448, doi: 10.14743/apem2019.4.339.
[22] Sethi, A.K., Sethi, S.P. (1990). Flexibility in manufacturing: A survey, *International Journal of Flexible Manufacturing Systems,* Vol. 2, No. 4, 289-328, doi: 10.1007/BF00186471.
[23] Krolczyk, J.B., Krolczyk, G.M., Legutko, S., Napiorkowski, J., Hloch, S., Foltys, J., Tama, E. (2015). Material flow optimization – A case study in automotive industry, *Tehnički Vjesnik – Technical Gazette,* Vol. 22, No. 6, 1447-1456, doi: 10.17559/TV-20141114195649.
[24] Hajduk, M., Sukop, M., Semjon, J., Jánoš, R., Varga, J., Vagaš, M. (2018). Principles of formation of flexible manufacturing systems, *Tehnički Vjesnik – Technical Gazette,* Vol. 25, No. 3, 649-654, doi: 10.17559/TV-20161012132937.
[25] Terkaj, W., Tolio, T., Valente. A. (2009). A review on manufacturing flexibility, In: Tolio, T. (ed.), *Design of Flexible Production Systems,* Springer, Berlin, Heidelberg, Germany, 41-61, doi: 10.1007/978-3-540-85414-2_3.
[26] Terkaj, W., Tolio, T., Valente, A. (2009). Focused flexibility in production systems, In: ElMaraghy, H. (ed.), *Changeable and reconfigurable manufacturing systems,* Springer series in advanced manufacturing, Springer, London, United Kingdom, 47-66, doi: 10.1007/978-1-84882-067-8_3.
[27] Singh, S.P. (2014). *Production and operations management,* Vikas Publishing House, Noida, India.
[28] Zülch, G., Jonsson, U., Fischer, J. (2002). Hierarchical simulation of complex production systems by coupling of models, *International Journal of Production Economics,* Vol. 77, No. 1, 39-51, doi: 10.1016/S0925-5273(01)00198-0.
[29] Brey, P. (2008). Virtual reality and computer simulation, In: Himma, K.E., Tavani, H.T. (eds.), *The handbook of information and computer ethics,* John Wiley & Sons, New York, USA, 361-384, doi: 10.1002/9780470281819.ch15.
[30] Yang, S.L., Xu, Z.G., Li, G.Z., Wang, J.Y. (2020). Assembly transport optimization for a reconfigurable flow shop based on a discrete event simulation, *Advances in Production Engineering & Management,* Vol. 15, No. 1, 69-80, doi: 10.14743/apem2020.1.350.
[31] Saez-Mas, A., Garcia-Sabater, J.P., Morant-Llorca, J. (2018). Using 4-layer architecture to simulate product and information flows in manufacturing systems, *International Journal of Simulation Modelling,* Vol. 17, No. 1, 30-41, doi: 10.2507/IJSIMM17(1)408.
[32] Straka, M., Malindzakova, M., Rosova, A., Trebuna, P. (2016). The simulation model of the material flow of municipal waste recovery, *Przemysl Chemiczny – Chemical Industry*, Vol. 95, No. 4, 773-777, doi: 10.15199/62.2016.4.12.
[33] Mourtzis, D., Doukas, M., Bernidaki, D. (2014). Simulation in manufacturing: Review and challenges, *Procedia CIRP,* Vol. 25, 213-229, doi: 10.1016/j.procir.2014.10.032.
[34] Straka, M., Khouri, S., Lenort, R., Besta, P. (2020). Improvement of logistics in manufacturing system by the use of simulation modelling: A real industrial case study, *Advances in Production Engineering & Management*, Vol. 15, No. 1, 18-30, doi: 10.14743/apem2020.1.346.
[35] Istokovic, D., Perinic, M., Dobovicek, S., Bazina, T. (2019). Simulation framework for determining the order and size of the product batches in the flow shop: A case study, *Advances in Production Engineering & Management*, Vol. 14, No. 2, 166-176, doi: 10.14743/apem2019.2.319.
[36] Pedgen, C.D., Shannon, R.E., Sadowski, R.P. (1995). *Introduction to simulation using SIMAN*, McGraw Hill, New York, USA.

APEM journal

Advances in Production Engineering & Management
Volume 15 | Number 4 | December 2020 | pp 481–492
https://doi.org/10.14743/apem2020.4.380

ISSN 1854-6250
Journal home: apem-journal.org
Original scientific paper

Due date optimization in multi-objective scheduling of flexible job shop production

Ojstersek, R.[a,*], **Tang, M.**[b], **Buchmeister, B.**[a]

[a]University of Maribor, Faculty of Mechanical Engineering, Maribor, Slovenia
[b]Beijing Jiaotong University, International Center for Informatics Research, Beijing, P.R. China

A B S T R A C T

The manuscript presents the importance of integrating mathematical methods for the determination of due date optimization parameter for maturity optimization in evolutionary computation (EC) methods in multi-objective flexible job shop scheduling problem (FJSSP). The use of mathematical modelling methods of due date optimization with slack (SLK) for low and total work content (TWK) for medium and high dimensional problems was presented with the integration into the multi-objective heuristic Kalman algorithm (MOHKA). The multi-objective optimization results of makespan, machine utilization and due date scheduling with the MOHKA algorithm were compared with two comparative multi-objective algorithms. The high capability and dominance of the EC method results in scheduling jobs for FJSSP production was demonstrated by comparing the optimization results with the results of scheduling according to conventional priority rules. The obtained results of randomly generated datasets proved the high level of job scheduling importance with respect to the interdependence of the optimization parameters. The ability to apply the presented method to the real-world environment was demonstrated by using a real-world manufacturing system dataset applied in Simio simulation and scheduling software. The optimization results prove the importance of the due date optimization parameter in highly dynamic FJSSP when it comes to achieving low numbers of tardy jobs, short job tardiness and potentially lower tardy jobs costs in relation to short makespan of orders with highly utilized production capacities. The main findings prove that multi-objective optimization of FJSSP planning and scheduling, taking into account the optimization parameter due date, is the key to achieving a financially and timely sustainable production system that is competitive in the global market.

A R T I C L E   I N F O

Keywords:
Flexible job shop scheduling problem (FJSSP);
Due date;
Makespan;
Capacities utilization;
Multi-objective optimization;
Evolutionary computation;
Multi-objective heuristic Kalman algorithm;
Simio simulation and scheduling software

**Corresponding author:*
robert.ojstersek@um.si
(Ojstersek, R.)

Article history:
Received 15 May 2020
Revised 23 October 2020
Accepted 25 November 2020

1. Introduction

The production planning and scheduling of flexible job shop production (FJSSP) is extremely important if a company wants to ensure global competitiveness and sustainable business [1]. Optimization parameters that define short makespan of orders and enable high utilization of production capacities are meaningless if the expected order due dates are not guaranteed. Adequate planning and scheduling of due dates, which are usually very tight, expresses the need for a detailed discussion of the scheduling orders importance from the point of due dates. The research question presented in the research work refers to the importance of mathematical modelling of the due dates optimization objective in the multi-objective FJSSP optimization problem.

The importance of scheduling FJSSP from the point of the due dates has a significant impact on other optimization parameters that FJSSP deals with.

According to the literature, the problem of scheduling orders in job shop production has long been known, defined and discussed in detail. The initially used scheduling priority rules [2] only allowed the theoretical solution of single-objective optimization problems, which the developers transferred to dynamic job shop production environments by means of simulation modelling approaches [3]. The set of mathematical methods for modelling due date parameter is extensive [4]. Their suitability for individual use is demonstrated by the specificity of the optimization problem and its complexity [5]. The complexity of scheduling is reflected in several supporting parameters that influence the correct assessment of the due date parameter from the average job tardiness, the number of tardy jobs and the total tardy jobs costs leading to time and financial losses of the company [6]. Given the complexity presented, which is defined in FJSSP as NP - hard, the use of evolutionary computation methods (EC) is one of the effective ways of achieving optimal optimization results [7, 8]. The optimization problem of scheduling due dates in flexible manufactured systems [9] has encountered many limitations in the research due to conflicting optimization goals and the use of different mathematical modelling methods [10]. The researchers have limited it to optimization parameters that define the due date of jobs [11], assuming independence from other optimization parameters [12], which significantly influence production flexibility [13]. The dynamic change in FJSSP production due to dynamic customer demand and high-mix low-volume production [14, 15] cites Pareto-based optimization approaches as suitable optimization approaches [16]. The use of fuzzy approaches [17], which satisfactorily solve the optimization problem of FJSSP production, usually treats the problem only on a single-level of primary optimization criteria and limits the multi-level structure of the FJSSP problem [18]. Heuristic methods [19, 20], which allow a detailed devaluation of the optimization approach and the satisfactory optimization method, are usually limited by the transfer of the optimization results to a real-world or simulation environment [21, 22]. The need for an efficient optimization method that allows the planning and scheduling of the FJSSP problem with the optimization parameter of due dates is the key to achieving a comprehensive optimization approach [23]. However, the research results must allow for the devaluation of both test and realistic datasets for appropriate integration of the proposed methods into the real-world production environment [24].

In the presented research work, we want to present the importance of integrating mathematical methods for determining due dates into the existing EC method. The research work tries to overcome the existing limitations of the FJSSP research problem, which does not deal with the optimization parameter of planning and scheduling orders with the due date parameter. The mathematical modelling with known total work content (TWK) and slack (SLK) methods and their integration into the proposed EC algorithm MOHKA allows to evaluate the importance of the FJSSP multi-objective optimization with parameters that ensure short makespan, high utilization of production capacities and the achievement of tight due dates.

2. Problem description

In the optimization problem of planning and scheduling of the flexible job shop production (FJSSP), the three most frequent optimization parameters are shown in Eq. 1, Eq. 2 and Eq. 3:

- Makespan

$$MC = max\{C_j \mid j = 1, \dots, n\}, \tag{1}$$

- Total workload of all machine

$$TW = \sum_{i=1}^{n} \sum_{j=1}^{n_i} \sum_{k=1}^{m} p_{ijk} x_{ijk}, k = 1, 2, \dots, m \tag{2}$$

and

- The workload of the most loaded machine

$$MW = max \sum_{i=1}^{n} \sum_{j=1}^{n_i} p_{ijk} x_{ijk}, k = 1, 2, \dots, m \tag{3}$$

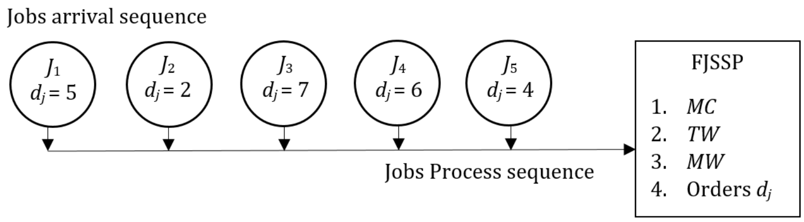

Fig. 1 Jobs arrival sequence with different due dates

Where the C_j is completion time of job j, n represents number of jobs and m the number of machines. These three optimization parameters relate to the time of jobs completion and the achievement of the highest possible utilization of the machines. In the highly dynamic job shop production, a very important parameter is the due date of jobs d_j, which in most cases are very tight. Fig. 1 shows the job arrival sequence of five jobs, where each job must be executed with a different due date in the production system defined as FJSSP. The optimization of the jobs process sequence must be carried out with regard to the multi-objective nature of FJSSP, whereby three parameters must be minimized (MC, MW, d_j) and one parameter must be maximized (TW).

In this case, each job j has a certain number of operations O_i, which must be performed on the available machine m from the given set of machines capable of performing an individual operation. The process time of the operation p_{jk} varies in relation to the assigned machine capable of performing the individual operation O_i. The optimization algorithm must arrange the job process sequence in such a way that it handles all four optimization parameters accordingly. Example: If the conventional priority rule Earliest Due Date (EDD) was used, the job process sequence would be J_2, J_5, J_1, J_4 and J_3. This job process execution sequence deals only with one optimization parameter d_j, which is defined as follows: The due date of job j represents the estimated dispatch date of job j (dispatch date promised to the customer). Completion of job j after the due date (promised to the customer) is allowed, but represents an additional financial penalty for the company. When considering the optimization parameter d_j, important related goals must be specified. The priority objective is to reduce the maximum lateness, which is defined as in Eq. 4:

$$L_{max} = max(L_j, \dots, L_n), \tag{4}$$

where the lateness of an individual job j defined by the Eq. 5

$$L_j = C_j - d_j \tag{5}$$

depends on the completion time of the job j and the assumed delivery time of the job d_j.

The timed L_{max} can be more easily defined with the parameter number of tardy jobs. This optimization parameter only defines whether the individual job j missed the estimated delivery time or not. Tardiness of job j is defined as presented by Eq. 6:

$$T_j = max(C_j - d_j, 0), \tag{6}$$

and the corresponding target function defined by Eq. 7.

$$\sum_{j=1}^{n} T_j \tag{7}$$

Due to the shortcomings of the above optimization function, which refers to some very tardy jobs, it is useful to determine the importance weights of jobs j by w_j. The higher the weight, the more important the job is.

The assumption in the present research work refers to: the given weight w_j refers only to the importance of an individual job j, which can be weighted directly by the planning team of the manufacturing system. However, the importance of the multi-objective decision making between the four optimization parameters (MC, TW, MW and d_j) does not determine the importance of the correlation between them, since this is performed with the evolutionary computation method MOHKA, which presents solutions of the optimization problem with Pareto optimal solutions.

3. Due date modelling

To model due dates of jobs, a random dataset is generated (according to the FJSSP characteristics) and divided into three groups with regard to their complexity dimensions:

- Low dimensional optimization problem, in the present manuscript the dataset J_5, M_{11}, O_{66} has been configured to evaluate MOHKA capabilities in relation to the optimization results of conventional priority rules.
- Middle dimensional optimization problems are represented by two datasets, a theoretical dataset J_{10}, M_{11}, O_{122} and a real-world dataset J_{15}, M_{10}, O_{84}, which was used in the FJSSP case study section.
- High dimensional optimization problems are represented by datasets J_{15}, M_{11}, O_{176} and J_{20}, M_{11}, O_{240}, respectively.

Due date optimization parameter modelling is performed with TWK (Total WorK content) method by the Eq. 8.

$$d_j = at_j + K_x \cdot \sum_{i \in o_j} p_{i,j,k} \tag{8}$$

The tightness coefficient of the order due date K_x (allowance factor) determines the tightness of the delivery times. In the current literature [7] for the TWK method and determination of the tightness coefficient of the permissible deviation of the delivery time for the EC method, values in the range of $3 \le K_x \le 5$ are given. The smaller the value of the tightness coefficient, the narrower the due date of the order j is. The experiments in the manuscript use the value of the coefficient $K_x = 3$. The due date modelled according to the TWK method depends on the arrival time of the order j (at_j), total time of processing of all operations (p_{ijk}) and the described tightness coefficient. The MOHKA algorithm schedules the job orders according to four optimization criteria, including the due date d_j. The adequacy comparison of the proposed MOHKA method is performed with two comparison algorithms: Multi-objective particle swarm optimization (MOPSO) [25] and Bare-bones multi-objective particle swarm optimization (BBMOPSO) [26]. These two algorithms do not use an integrated mathematical decision model to terminate orders according to the due date criterion, this criterion is calculated numerically in the experiment at the end of the optimization results. As stated in the initial research question, the due date parameter in the FJSSP optimization problem is not well researched, especially when it comes to using the EC method to obtain optimal solutions. All algorithms in the experiment use the same initialization parameter: population size (N_s = 300), maximum number of archived nondominated solutions (N_a = 100), and maximum number of algorithm iterations ($MaxIter$ = 300).

The optimization parameter for scheduling jobs by due date is analysed using three criteria: number of tardy jobs, average job tardiness and tardy jobs cost. The tardy jobs costs is modelled as shown in Eq. 9, where the initial job cost (J_{cost}) are multiplied by the constant value of three, divided by the value constant K_s, and multiplied by subtracting the completion time C_j and the due date d_j.

$$L_{cost} = \frac{3 \cdot J_{cost}}{K_S} \cdot (C_j - d_j) \tag{9}$$

A constant value of three determines three times the cost of tardy jobs compared to the cost of in-time completed jobs. The value constant K_S is automatically determined by the orders makespan. The parameter J_{cost} is determined numerically according to the characteristics of the machines performing an individual job operation.

The modelling of the due dates and the achievement of the other three optimization parameters were carried out using conventional methods (priority rules) and the heuristic GSBR method, with the aim of evaluating the efficiency of the conventional scheduling methods compared to the proposed MOHKA EC method. The comparison is performed in the software environment Lekin. As the Lekin software environment only allows the optimization of datasets of up to one hundred operations in the FJSSP optimization problem, the evaluation is performed with a randomly determined dataset classified as low dimensional optimization problem J_5, M_{11}, O_{66}. A randomly generated dataset does not contain data where two or more operations are performed on the same machine within a single order, limitation of Lekin.

In contrast to larger datasets, where in the TWK method is used to model due dates, the SLK (slack) method [4] is recommended for smaller datasets, which can model due dates by the Eq. 10.

$$d_j = at_j + \sum_{i \in o_j} p_{i,j,k} + K_y \tag{10}$$

The time reserve constant K_y determines the looseness-tightness of due dates, in the SLK method the determination of the time reserve constant of the due date is given by the literature values $4 \leq K_y \leq 16$. In the presented research work the value $K_y = 8$ is used. The K_y must be calculated individually for the specific optimization problem.

3.1 Performance testing

To test the performance of the MOHKA algorithm for due date job scheduling, four randomly generated benchmark datasets and one real-world dataset all of which describe a multi-objective FJSSP optimization problem were used. The datasets were created using the interdependency function between different parameters describing the optimization problem. We divided these benchmark datasets into three groups according to the complexity of the optimization problem.

3.2 Using TWK and SLK methods

The division of the datasets used in different groups according to their complexity provided the basis for testing two different due date modelling methods. TWK method for middle and high dimensional optimization problems and SLK method for low dimensional optimization problems. The use of TWK and SLK methods for different datasets is supported by the mathematical formulation of the individual methods. With the presented classification approach, the complexity of the optimization problems can be evaluated more precisely in order to determine the advantages and limitations of the due date methods capabilities. The proposed MOHKA algorithm performed the optimization of datasets with four parameters of a flexible production system: makespan (MC), total workload of all machines (TW), maximum workload of an individual machine (MW) and added due date (d_j) parameter. The obtained optimization results were compared with two multi-objective particle swarm based optimization algorithms MOPSO and BBMOPSO. The experiments were performed on a personal computer with Intel i7 processor and 16 GB internal memory.

3.3 Results for the TWK method

The results in Table 1 show the high reliability of scheduling jobs with the TWK method, taking into account due dates with the MOHKA optimization algorithm. Its success in scheduling jobs with tight due dates, low average job tardiness potentially low tardy jobs cost and short orders makespan.

The middle dimensional dataset J_{10}, M_{11}, O_{122} caused no problems for all three evolutionary computation algorithms in scheduling orders for tight due dates of the TWK method with the tightness coefficient of $K_x = 3$. No job has missed the scheduled due date, which in turn did not result in additional tardy jobs costs in the manufacturing system. Since only the referential MOHKA optimization algorithm takes into account the mathematical architecture of the TWK method, we see that the results of the multi-objective optimization have a positive effect on the achievement of the minimum orders makespan. Makespan is the shortest in the MOHKA algorithm with up to 188 h, in contrast to MOPSO and BBMOPSO, where the makespan is 227 h and 206 h, respectively.

When the dimension of datasets increases from middle dimensional to high dimensional optimization problems, the difference between the optimization results of comparison and reference algorithms is more pronounced, presented on Fig. 2. In dataset J_{15}, M_{11}, O_{176}, the MOHKA algorithm terminates orders in such a way that three orders are late for the expected due date with an average job tardiness of 19 h, resulting in a tardy jobs costs of 2272.2 EUR. The MOPSO algorithm terminates orders so that only two orders miss the expected due date, but with higher average job tardiness of 45.5 h, which means a 139% higher average job tardiness than the MOHKA algorithm. A longer average job tardiness leads to higher tardy jobs costs, which amount to EUR 2966.5 in the MOPSO algorithm. The BBMOPSO algorithm had the most difficulties in scheduling the J_{15}, M_{11}, O_{176} dataset because up to one-third of the orders have missed the scheduled due date, with an average job tardiness of 20.6 h and high tardy jobs costs of 3558.5 EUR. This corresponds to an increase of 56.6% in the costs of tardy jobs compared to the MOHKA algorithm. The results show that the MOHKA algorithm is also most successful with the order makespan parameter of 289 h, which is 2.8% shorter than the BBMOPSO algorithm and 17% shorter than the MOPSO algorithm. Based on the optimization results described above, we can assume how important the scheduling of the dynamic FJSSP with the parameter of due date is, especially if the complexity of the optimization problem increases.

The hypothesis is confirmed for the high-dimensional dataset J_{20}, M_{11}, O_{240}, in which the reference MOHKA algorithm dominates over the results of the two comparison algorithms presented of Fig. 3. The lowest number of tardy jobs with an average job tardiness of 31.1 h compared to 44.4 h and 46.8 h for MOPSO and BBMOPSO, corresponding to 42.8% and 50.5% higher number of tardy jobs. Given the higher number of tardy jobs and the longer average job tardiness, the costs of tardy jobs is also higher for the two comparison algorithms than for the reference MOHKA algorithm, which amounts to 7,318.1 EUR. With the MOPSO algorithm, the tardy jobs costs amount to 13,585.6 EUR, while with BBMOPSO they amount to 33,070.1 EUR, which represents an increase of 85.6% and 351.9%, respectively, in the costs of tardy jobs that have exceeded their scheduled due date. The presented results prove the high importance of mathematical modelling with the parameter of due date optimization, as they have a decisive influence on the makespan and financial justification of a highly dynamic manufacturing. A suitable mathematical model of the multi-objective optimization problem is also reflected in the achievement of short order makespan. For the high dimensional dataset J_{20}, M_{11}, O_{240} the reference MOHKA algorithm achieved a makespan of 341 h and the two comparison algorithms 389 h and 397 h. Appropriate multi-objective decision making allows for an evenly balanced operation of the manufacturing system regarding to the makespan, machine utilization and achievement of tight order due dates.

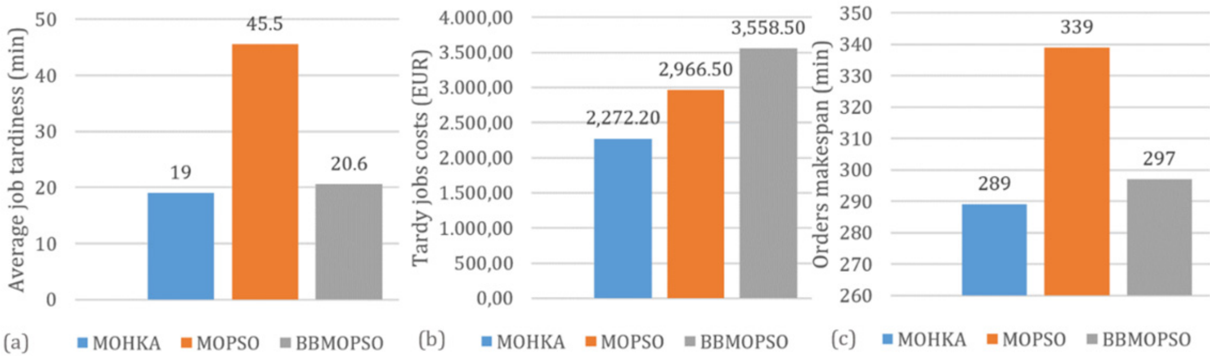

Fig. 2 Optimization results J_{15}, M_{11}, O_{176}: (a) average job tardiness, (b) tardy jobs costs and (c) orders makespan

Table 1 Algorithms optimization results

Algorithm	Dataset	Number of tardy job	Average job tardiness (h)	Tardy jobs costs (EUR)	Orders makespan (h)
MOHKA	J_{10}, M_{11}, O_{122}	0	0	0	188
	J_{15}, M_{11}, O_{176}	3	19	2,272.2	289
	J_{20}, M_{11}, O_{240}	7	31.1	7,318.1	341
MOPSO	J_{10}, M_{11}, O_{122}	0	0	0	227
	J_{15}, M_{11}, O_{176}	2	45.5	2,966.5	339
	J_{20}, M_{11}, O_{240}	10	44.4	13,585.6	389
BBMOPSO	J_{10}, M_{11}, O_{122}	0	0	0	206
	J_{15}, M_{11}, O_{176}	5	20.6	3,558.5	297
	J_{20}, M_{11}, O_{240}	18	46.8	33,070.1	397

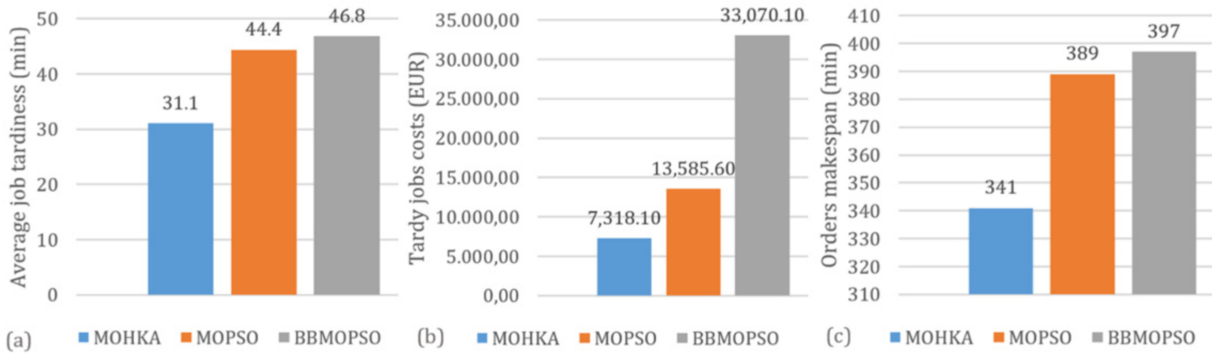

Fig. 3 Optimization results J_{20}, M_{11}, O_{240}: (a) average job tardiness, (b) tardy jobs costs, and (c) orders makespan

3.4 Results for the SLK method

With the aim to compare the solutions of the MOHKA algorithm and the solutions of conventional priority rules, a comparison of the results of the MOHKA optimization with the results of job scheduling in the Lekin software environment was performed for the low dimensional optimization problem of J_5, M_{11}, O_{66}.

Table 2 shows the optimization results of a randomly generated J_5, M_{11}, O_{66} dataset of five jobs with a total of sixty-six operations performed on eleven machines. The optimization was performed with the MOHKA optimization algorithm in the software environment MATLAB and seven optimization approaches in the software environment Lekin. Of the seven optimization approaches, six are conventional priority rules and one is a heuristic algorithm named General Shifting Bottleneck Routine (GSBR). For the optimization of due dates the SLK method with a time reserve constant of K_y = 8 was used.

The results show a high reliability of production jobs scheduling by the optimization algorithm MOHKA. In the considered dataset MOHKA terminates jobs so that two orders miss the scheduled due dates with an average job tardiness of 9.5 h and a tardy jobs costs of 2,651 EUR. With the six priority rules we see that the five priority rules, with the exception of the SPT priority rule, terminate orders in such a way that all five orders miss the scheduled tight due date. The average job tardiness is higher than 309.5% for the CR priority rule to 505.3% for the LPT priority rule than for the MOHKA algorithm. There are also significantly higher tardy jobs costs. The only algorithm that has partially approximated the results of the MOHKA algorithm is the heuristic GSBR algorithm, where four orders are tardy with an average job tardiness of 9.4 h. Due to two additional delayed jobs, the tardy job cost are 39.8% higher than in the MOHKA algorithm. There is also a significant difference in achieving a short makespan of orders, where the MOHKA algorithm terminates work jobs so that they are completed in a makespan of 99 h, and all other algorithms terminate orders with makespan between 208 h (GSBR) and 256 h (CR).

The presented optimization results prove the high ability to terminate production orders with the MOHKA algorithm and to achieve tight due dates from low dimensional optimization cases (with SLK method) to middle and high dimensional optimization cases (with TWK method) compared to optimization solutions according to MOSPO, BBMOPSO and priority rules.

Table 2 MOHKA vs. priority rules optimization results

Algorithm	MOHKA	EDD	MS	FCFS	LPT	SPT	CR	GSBR
Number of tardy job	2	5	5	5	5	4	5	4
Average job tardiness (h)	9.5	34.8	47.6	41.6	48	32.4	29.4	9.4
Tardy jobs costs (EUR)	2,651	11,325.1	14,682.2	13,320	14,436.1	10,570.1	8,905	3,706.2
Orders makespan (h)	99	211	211	215	217	233	256	208

3.5 Real-world case study

With the proposed method for modelling the due date for FJSSP, which was tested on randomly generated benchmark datasets, we proved the high ability to solve multi-objective optimization problems. The initial experiment, which was conducted on randomly generated datasets, was extended to a real-world case study for the FJSSP manufacturing system to evaluate MOHKA efficiency in determining due dates.

The fourth section presents the ability to solve a multi-objective optimization problem of a real-world manufacturing system (the dataset from a real-world environment is called RW_PS). The first part of the section presents the input data of the manufacturing system that has been prepared to describe FJSSP. Working with the company to prepare relevant and credible input data offers the opportunity to achieve reliable optimization results by testing the proposed EC scheduling methods. The RW_PS dataset consists of fifteen job orders that are executed on ten machines with eighty-four operations. The optimization results obtained with the MOHKA algorithm were compared with the optimization results of the MOPSO and BBMOPSO algorithms. The proposed integration approach of transferring the optimization results to the conventional simulation environment was used to transfer the optimization results, the order of the due dates of the job sequence, to the simulation model of the real-world manufacturing system.

Manufacturing system input data

Selected data were obtained from a Central European medium-sized company that manufactures individual orders for different customers. Orders received in the company by the customer must be performed on specific, available machine within the manufacturing system concerning four optimization parameters MC, TW, MW and d_j (FJSSP problem). The orders consist of two types of products with different process times, machine operating costs (O_c), machine idle costs (I_c) and fix location of machine is known by x and y location. Input data are given in Table 3. Compared to the test random generated datasets described in section 3, the additional complexity of the RW_PS optimization problem is added by two different product types, which add one dimensional complexity to the optimization problem.

In a real-world manufacturing system, machines marked M_1 to M_{10} perform the following operations:

- M_1 and M_2 for raw material cutting,
- M_3 to M_5 CNC machining,
- M_6 and M_7 welding,
- M_8 and M_9 assembling and
- M_{10} final control operation.

The main task of the optimization algorithm is to optimally determine the job sequence of operations on the available machine. The algorithm must determine which of the machines is capable of performing the individual operations according to the four optimization criteria. The simulation model was built in the Simio software environment, in which a transfer method for integrating optimization results from the MOHKA method to conventional simulation decision logic was used [18]. Using the MOHKA algorithm, we solved the FJSSP optimization problem, so we decided to extend our existing optimization results with a suitable simulation model. Fig. 4 shows a simulation model of a real-wold manufacturing system running on an order job sequence determined by the MOHKA optimization algorithm.

Table 3 Real-world manufacturing system characteristics

	Machine	M_1	M_2	M_3	M_4	M_5	M_6	M_7	M_8	M_9	M_{10}
	x_{loc} (m)	8	8	12.5	18.5	24.5	30.5	36	36	24.5	19.5
	y_{loc} (m)	9.5	4.5	0	0	0	0	5.5	10.5	16.5	12
Product 1	Processing time (min)	20	24	40	45	38	47	20	25	11	22
	O_c (EUR/h)	45	45	35	35	35	35	52	52	59	43
	I_c [EUR/h]	22.5	22.5	14	14	14	14	31.2	31.2	35.4	21.5
Product 2	Processing time (min)	22	22	43	43	43	43	23	23	12	25
	O_c (EUR/h)	43	43	36	36	36	36	53	53	59	45
	I_c [EUR/h]	21.5	21.5	14.4	14.4	14.4	14.4	31.8	31.8	35.4	22.5

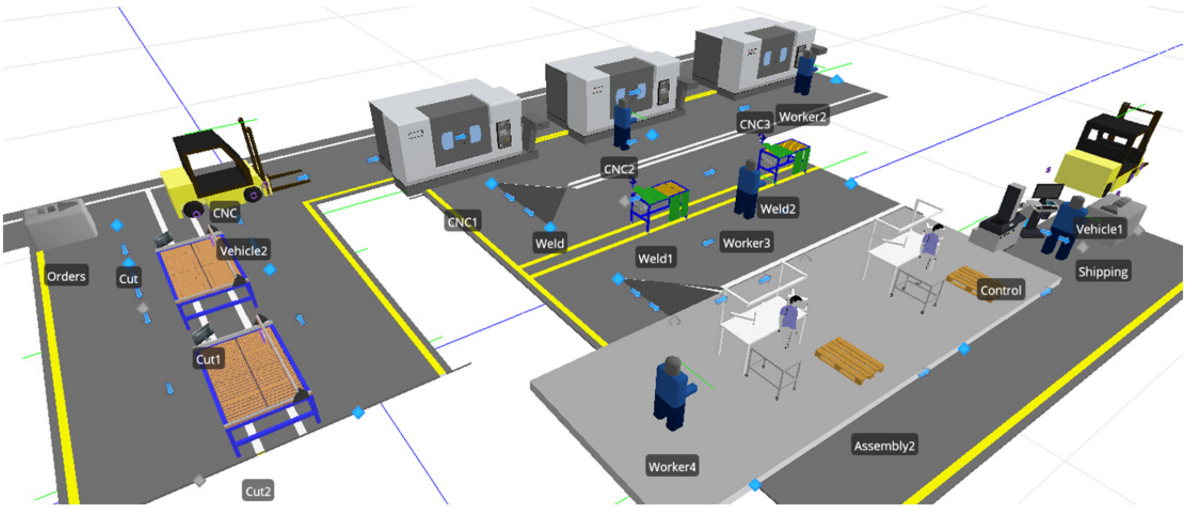

Fig. 4 Simulation model in Simio

Due date scheduling results

Table 4 and Fig. 5 show the results of optimizing the RW_PS dataset according to the order due date parameter. As shown in section 3, the TWK method with a tightness coefficient K_x = 3 was used when evaluating RW_PS dataset. The optimization results show that with the MOHKA optimization algorithm only one job missed a tight due date with an average job tardiness of 46 min. With the BBMOPSO optimization algorithm also, one job missed the due date, but job is tardy by an average job tardiness of 154 min, which corresponds to a 234% longer tardy time of the missed job than the tardy job with the MOHKA algorithm. In the MOPSO algorithm, two jobs are tardy with an average job tardiness of 58 minutes, which is 26.1% longer tardy time than the delay with the MOHKA algorithm. Since the value of tardy jobs costs is low, the percentage difference between them is significant. In this case, the MOHKA algorithm proves to be the most efficient, since it is the only algorithm able to take due dates into account as a decision criterion when determining the job sequence.

The tardy jobs costs in the MOPSO algorithm are 130.2% higher in the MOPSO algorithm than in the MOHKA algorithm. Even if only one job with the BBMOPSO algorithm missed the scheduled due date, this was delayed by a much longer time than the tardy job with the MOHKA algorithm. This is reflected in 230.7% higher tardy job costs. The makespan of orders is shortest with the MOHKA algorithm at 392.45 min, while the makespan of orders is longer by 2.1% longer with MOPSO and 7.6% longer with BBMOPSO. From the perspective of the multi-objective decision making process, we can conclude that the MOHKA algorithm provides a high degree of FJSSP scheduling capabilities even in real-world datasets, considering the ability to achieve a tight job due date.

Table 4 Optimization results of real-world manufacturing system

Algorithm	MOHKA	MOPSO	BBMOPSO
Number of tardy job	1	2	1
Average job tardiness (min)	46	58	154
Tardy jobs costs (EUR)	14.9	34.3	46.3
Orders makespan (min)	392.45	400.48	422.21

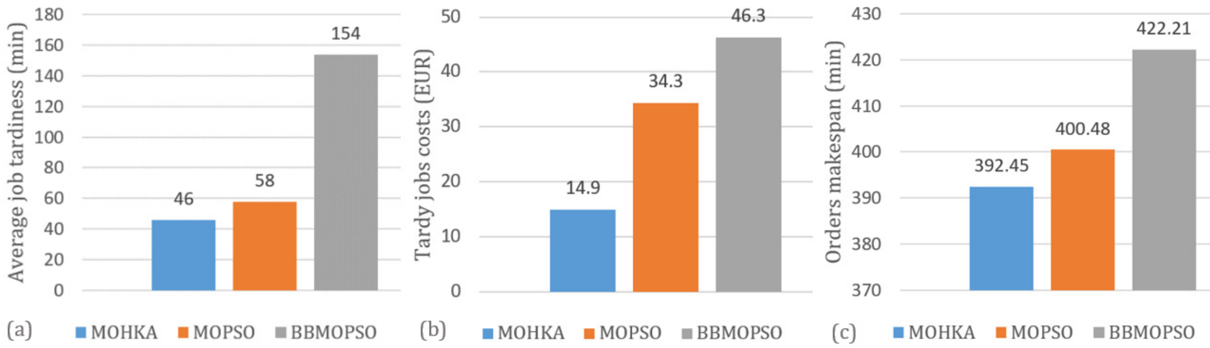

Fig. 5 Optimization results: (a) average job tardiness, (b) tardy jobs costs, and (c) orders makespan

4. Discussion and conclusions

Scheduling multi-objective FJSSP optimization problem is defined as a NP-hard optimization problem. The initial research question of scheduling FJSSP production with the optimization parameter of the due dates importance and taking into account the standard optimization parameters related to the makespan of orders and machine utilization, was evaluated in the presented research with the MOHKA optimization method and the SLK and TWK methods to model due dates. With increasing number of optimization parameters, the computational complexity of the optimization algorithm increases. The presented research work presents the integration of the mathematical structure of the SLK (for low dimensional optimization problems) and TWK methods (for medium and high dimensional optimization problems) into the optimization MOHKA algorithm, which is capable of scheduling FJSSP production. The proposed MOHKA algorithm was used to schedule test datasets with emphasis on achieving a tight due date of the orders. The optimization results were compared with the results of the optimization algorithms MOPSO and BBMOPSO, which terminate orders only at ordinary optimization parameters: *MC, TW and MW*. The disadvantage of the comparative optimization methods becomes apparent when we talk about medium and high dimensional optimization problems in the scheduling of FJSSP. The limited scheduling capabilities of the MOPSO and BBMOPSO algorithms are reflected in the limited mathematical structure of the algorithms, which do not consider the SLK and TWK methods as decision parameters in achieving optimally scheduled orders from the point of due dates. The optimization results of the reference MOHKA algorithm prove the high importance of the due date optimization parameter, since the proposed method optimizes order scheduling with regard to the two comparative algorithms for low, medium and high dimensional optimization problems. Since we are talking about multi-objective decision making and finding compromises between different (even contradictory) optimization parameters, the results of the MOHKA algorithm prove the high ability to reach all four optimization parameters equally and efficiently (*MC*, *TW*, *MW* and d_j). As evidenced the short order makespan, tight due dates, low average order tardiness and the associated low associated job tardiness costs are achieved. The answer to the question about the efficiency of evolutionary methods in multi-objective decision making compared to the conventional optimization approach of priority rules was given by the presented study, in which the optimization results of the MOHKA algorithm are compared with the optimization results of six priority rules and an integrated heuristic method in the Lekin software environment. The obtained results prove the high dominance of the optimization results of the evolutionary method MOHKA, which terminates the FJSSP production according to the used low-dimensional dataset for all optimization parameters most efficiently. Randomly generated datasets were the basis for carrying out the validation of the applicability of the proposed method in real-world manufacturing systems, whereby the satisfactory optimization results were demonstrated in the experiment. The scheduling of the FJSSP production to achieve tight due dates was carried out using the example of a dataset of a real-world manufacturing system. In this case, the TWK method, which is integrated into the decision logic of the MOHKA algorithm, proved the high ability to terminate the significance of real-world datasets importance in relation to the parameter of due date optimization.

Since the presented research work deals only with FJSSP, which is the main part of the research problem of multi-objective optimization job shop production, it is necessary to further investigate the importance of scheduling due dates in dynamic job shop production (DJSSP). Where the main features are dynamic order changes during the execution of the algorithm (at initialization stage the whole order dataset is unknown), machine failures during the execution of operations and the determination of the importance of orders need to be studied. Further research on the research problem of DJSSP would remove the limitations of current research, where the FJSSP optimization problem is based on the assumption of an initially known order dataset, an initially empty production system, a uniform meaning of orders, and known production capacities that do not change during operation.

Acknowledgement

The authors gratefully acknowledge the support of the Slovenian Research Agency (ARRS), Research Core Funding No. P2-0190.

References

[1] Prester, J., Buchmeister, B., Palčič, I. (2018). Effects of advanced manufacturing technologies on manufacturing company performance, *Strojniški Vestnik – Journal of Mechanical Engineering,* Vol. 64, No. 12, 763-771, doi: 10.5545/sv-jme.2018.5476.

[2] Baker, K.R. (1984). Sequencing rules and due-date assignments in a job shop, *Management Science*, Vol. 30, No. 9, 1093-1104, doi: 10.1287/mnsc.30.9.1093.

[3] Udo, G.J. (1994). A simulation study of due-date assignment rules in a dynamic job shop, *Journal of the Operational Research Society*, Vol. 45, No. 12, 1425-1435, doi: 10.1057/jors.1994.219.

[4] Gordon, V.S., Proth, J.-M., Chu, C. (2002). Due date assignment and scheduling: SLK, TWK and other due date assignment models, *Production Planning & Control*, Vol. 13, No. 2, 117-132, doi: 10.1080/09537280110069621.

[5] Modrák, V., Pandian, R.S. (2010). Flow shop scheduling algorithm to minimize completion time for n-jobs m-machines problem, *Tehnički Vjesnik – Technical Gazette,* Vol. 17, No. 3, 273-278.

[6] Demir, H.I., Uygun, O., Cil, I., Ipek, M., Sari, M. (2015). Process planning and scheduling with SLK due-date assignment where earliness, tardiness and due-dates are punished, *Journal of Industrial and Intelligent Information*, Vol. 3, No. 3, 173-180, doi: 10.12720/jiii.3.3.173-180.

[7] Ojstersek, R., Brezocnik, M., Buchmeister, B. (2020). Multi-objective optimization of production scheduling with evolutionary computation: A review, *International Journal of Industrial Engineering Computations*, Vol. 11, No. 3, 359-376, doi: 10.5267/j.ijiec.2020.1.003.

[8] Janes, G., Perinic, M., Jurkovic, Z. (2017). An efficient genetic algorithm for job shop scheduling problems, *Tehnički Vjesnik – Technical Gazette,* Vol. 24, No. 4, 1243-1247, doi: 10.17559/TV-20150527133957.

[9] Scrich, C.R., Armentano, V.A., Laguna, M. (2004). Tardiness minimization in a flexible job shop: A tabu search approach, *Journal of Intelligent Manufacturing*, Vol. 15, No. 1, 103-115, doi: 10.1023/B:JIMS.0000010078.30713.e9.

[10] Simchi-Levi, D., Wu, S.D., Shen, Z.-J.M. (2004). *Handbook of quantitative supply chain analysis: Modeling in the e-business era*, Springer Science & Business Media, New York, USA.

[11] Wu, Z., Weng, M.X. (2005). Multiagent scheduling method with earliness and tardiness objectives in flexible job shops, *IEEE Transactions on Systems, Man, and Cybernetics, Part B (Cybernetics)*, Vol. 35, No. 2, 293-301, doi: 10.1109/TSMCB.2004.842412.

[12] Chen, B., Matis, T.I. (2013). A flexible dispatching rule for minimizing tardiness in job shop scheduling, *International Journal of Production Economics*, Vol. 141, No. 1, 360-365, doi: 10.1016/j.ijpe.2012.08.019.

[13] Ojstersek, R., Buchmeister, B. (2020). The impact of manufacturing flexibility and multi-criteria optimization on the sustainability of manufacturing systems, *Symmetry*, Vol. 12, No. 1, Paper No. 157, doi: 10.3390/sym12010157.

[14] Nie, L., Gao, L., Li, P., Li, X. (2013). A GEP-based reactive scheduling policies constructing approach for dynamic flexible job shop scheduling problem with job release dates, *Journal of Intelligent Manufacturing*, Vol. 24, No. 4, 763-774, doi: 10.1007/s10845-012-0626-9.

[15] Rajabinasab, A., Mansour, S. (2011). Dynamic flexible job shop scheduling with alternative process plans: An agent-based approach, *The International Journal of Advanced Manufacturing Technology*, Vol. 54, No. 9-12, 1091-1107, doi: 10.1007/s00170-010-2986-7.
[16] Gao, K.Z., Suganthan, P.N., Pan, Q.K., Chua, T.J., Cai, T.X., Chong, C.S. (2014). Pareto-based grouping discrete harmony search algorithm for multi-objective flexible job shop scheduling, *Information Sciences*, Vol. 289, 76-90, doi: 10.1016/j.ins.2014.07.039.
[17] Ma, D.Y., He, C.H., Wang, S.Q., Han, X.M., Shi, X.H. (2018). Solving fuzzy flexible job shop scheduling problem based on fuzzy satisfaction rate and differential evolution, *Advances in Production Engineering & Management*, Vol. 13, No. 1, 44-56, doi: 10.14743/apem2018.1.272.
[18] Na, H., Park, J. (2014). Multi-level job scheduling in a flexible job shop environment, *International Journal of Production Research*, Vol. 52, No. 13, 3877-3887, doi: 10.1080/00207543.2013.848487.
[19] Xu, H., Bao, Z.R., Zhang, T. (2017). Solving dual flexible job-shop scheduling problem using a bat algorithm, *Advances in Production Engineering & Management*, Vol. 12, No. 1, 5-16, doi: 10.14743/apem2017.1.235.
[20] Fu, H.C., Liu, P. (2019). A multi-objective optimization model based on non-dominated sorting genetic algorithm, *International Journal of Simulation Modelling*, Vol. 18, No. 3, 510-520, doi: 10.2507/ijsimm18(3)co12.
[21] Getachew, F., Berhan, E. (2015). Simulation and comparison analysis of due date assignment methods using scheduling rules in a job shop production system, *International Journal of Computer Science & Engineering Survey*, Vol. 6, No. 5, 29-40, doi: 10.5121/ijcses.2015.6503.
[22] Ojstersek, R., Lalic, D., Buchmeister, B. (2019). A new method for mathematical and simulation modelling interactivity: A case study in flexible job shop scheduling, *Advances in Production Engineering & Management*, Vol. 14, No. 4, 435-448, doi: 10.14743/apem2019.4.339.
[23] Yin, Y., Wang, D., Cheng, T.C.E. (2020). *Due date-related scheduling with two agents: Models and algorithms*, Springer Nature Singapore, Singapore, doi: 10.1007/978-981-15-2105-8.
[24] Hajduk, M., Sukop, M., Semjon, J., Jánoš, R., Varga, J., Vagaš, M. (2018). Principles of formation of flexible manufacturing systems, *Tehnički Vjesnik – Technical Gazette,* Vol. 25, No. 3, 649-654, doi: 10.17559/TV-20161012132937.
[25] Moslehi, G., Mahnam, M. (2011). A Pareto approach to multi-objective flexible job-shop scheduling problem using particle swarm optimization and local search, *International Journal of Production Economics*, Vol. 129, No. 1, 14-22, doi: 10.1016/j.ijpe.2010.08.004.
[26] Zhang, Y., Gong, D.-W., Ding, Z. (2012). A bare-bones multi-objective particle swarm optimization algorithm for environmental/economic dispatch, *Information Sciences*, Vol. 192, 213-227, doi: 10.1016/j.ins.2011.06.004.

Calendar of events

- International Conference on Manufacturing, Optimization, Industrial and Material Engineering, January 7-8, 2021, Tokyo, Japan.
- International Conference on Green Supply Chain Management Applications, January 18-19, 2021, Rome, Italy.
- International Conference on Industrial Management Technology and Engineering, February 1-2, 2021, Melbourne, Australia.
- International Conference on Modeling and Simulation of Manufacturing Processes, February 25-26, 2021, Buenos Aires, Argentina.
- 12th International Conference on Mechatronics and Manufacturing, February 26-28, 2021, Singapore.
- International Conference on Machine Learning and Deep Learning in Manufacturing, March 15-16, 2021, London, United Kingdom.
- International Summit on Industrial Engineering, March 15-16, 2021, Munich, Germany.
- International Conference on Manufacturing Applications of Artificial Intelligence, March 22-23, 2021, Prague, Czech Republic.
- International Conference on Advanced Materials and Intelligent Manufacturing, March 29-30, 2021, Paris, France.
- 6th International Conference on 3D Printing Technology and Innovations, May 24-25, 2021, Berlin, Germany.
- 38th Global Summit on Nanoscience and Technology, June 21-22, 2021, Osaka, Japan.
- International Conference on Manufacturing Models and Cloud Manufacturing, July 15-16, 2021, Stockholm, Sweden.
- International Conference on Industrial Production Methods and Flow Production, August 5-6, 2021, Montreal, Canada.

This page intentionally left blank.

Notes for contributors

General

Articles submitted to the *APEM journal* should be original and unpublished contributions and should not be under consideration for any other publication at the same time. Manuscript should be written in English. Responsibility for the contents of the paper rests upon the authors and not upon the editors or the publisher. Authors of submitted papers automatically accept a copyright transfer to *Chair of Production Engineering*, *University of Maribor*. For most up-to-date information on publishing procedure please see the *APEM journal* homepage *apem-journal.org*.

Submission of papers

A submission must include the corresponding author's complete name, affiliation, address, phone and fax numbers, and e-mail address. All papers for consideration by *Advances in Production Engineering & Management* should be submitted by e-mail to the journal Editor-in-Chief:

Miran Brezocnik, Editor-in-Chief
UNIVERSITY OF MARIBOR
Faculty of Mechanical Engineering
Chair of Production Engineering
Smetanova ulica 17, SI – 2000 Maribor
Slovenia, European Union
E-mail: editor@apem-journal.org

Manuscript preparation

Manuscript should be prepared in *Microsoft Word 2010* (or higher version) word processor. *Word .docx* format is required. Papers on A4 format, single-spaced, typed in one column, using body text font size of 11 pt, should not exceed 12 pages, including abstract, keywords, body text, figures, tables, acknowledgements (if any), references, and appendices (if any). The title of the paper, authors' names, affiliations and headings of the body text should be in *Calibri* font. Body text, figures and tables captions have to be written in *Cambria* font. Mathematical equations and expressions must be set in *Microsoft Word Equation Editor* and written in *Cambria Math* font. For detail instructions on manuscript preparation please see instruction for authors in the *APEM journal* homepage *apem-journal.org*.

The review process

Every manuscript submitted for possible publication in the *APEM journal* is first briefly reviewed by the editor for general suitability for the journal. Notification of successful submission is sent. After initial screening, and checking by a special plagiarism detection tool, the manuscript is passed on to at least two referees. A double-blind peer review process ensures the content's validity and relevance. Optionally, authors are invited to suggest up to three well-respected experts in the field discussed in the article who might act as reviewers. The review process can take up to eight weeks on average. Based on the comments of the referees, the editor will take a decision about the paper. The following decisions can be made: accepting the paper, reconsidering the paper after changes, or rejecting the paper. Accepted papers may not be offered elsewhere for publication. The editor may, in some circumstances, vary this process at his discretion.

Proofs

Proofs will be sent to the corresponding author and should be returned within 3 days of receipt. Corrections should be restricted to typesetting errors and minor changes.

Offprints

An e-offprint, i.e., a PDF version of the published article, will be sent by e-mail to the corresponding author. Additionally, one complete copy of the journal will be sent free of charge to the corresponding author of the published article.

APEM journal

Advances in Production Engineering & Management

Chair of Production Engineering (CPE)
University of Maribor
APEM homepage: apem-journal.org

Volume 15 | Number 4 | December 2020 | pp 373-496

Contents

ISSN 1854-6250

9 771854 625008

apem-journal.org